DECEMBER 2025 Ph.D. in Electrical and Electronics Engineering ABDURRAHİM ERAT

REPUBLIC OF TÜRKİYE

GAZİANTEP UNIVERSITY

GRADUATE SCHOOL OF NATURAL & APPLIED SCIENCES

A DC-DC MODULAR MULTILEVEL CONVERTER DESIGN FOR HVDC INTERCONNECTION

Ph.D. THESIS

IN

ELECTRICAL AND ELECTRONICS ENGINEERING

BY

ABDURRAHİM ERAT

DECEMBER 2025

A DC-DC MODULAR MULTILEVEL CONVERTER DESIGN FOR HVDC INTERCONNECTION

Ph.D. Thesis

in

Electrical and Electronics Engineering

Gaziantep University

Supervisor

Prof. Dr. Ahmet Mete VURAL

by

Abdurrahim ERAT

December 2025

I hereby declare that all information in this document has been obtained and presented in accordance with academic rules and ethical conduct. I also declare that, as required by these rules and conduct, I have fully cited and referenced all material and results that are not original to this work.

Abdurrahim ERAT

ABSTRACT

A DC-DC MODULAR MULTILEVEL CONVERTER DESIGN FOR HVDC INTERCONNECTION

ERAT, Abdurrahim
Ph.D. in Electrical and Electronics Engineering
Supervisor: Prof. Dr. Ahmet Mete VURAL
December 2025
270 pages

High voltage direct current (HVDC) power transmission systems offer significant advantages over conventional high voltage alternating current (HVAC) power grids, including higher efficiency, enhanced long-distance bulk power transfer capability, improved controllability, and seamless integration of renewable energy sources such as offshore wind farms. HVDC systems also save operating costs, provide reliable power delivery to isolated or remote networks, and facilitate asynchronous power grid interconnections. To facilitate the integration of HVDC power systems with varying voltage levels while improving grid flexibility and reliability, advanced DC-DC power converter topologies are essential. This study presents a novel DC-DC modular multi-level converter (MMC) architecture that provides an excellent solution for integrating modern asynchronous HVDC power networks and these modern HVDC power systems with existing asynchronous HVAC power systems. The transformerless approach significantly reduces the proposed converter's volume, weight, price, and power loss. A detailed mathematical model and harmonic analysis of the proposed DC-DC MMC are derived, and simulation results demonstrate successful bi-directional power transfer between asynchronous grids. The control strategy ensures stable and efficient power flow regulation, confirming the effectiveness of the proposed DC-DC MMC for HVDC power network integration.

Key Words: HVDC, Modular Multilevel Converter, DC-DC Converter, DC-DC Power Conversion, Bi-directional Power Flow, Grid Interfacing, Grid Stability.

ÖZET

YGDA ARA BAĞLANTISI İÇİN DA-DA MODÜLER ÇOK SEVİYELİ DÖNÜŞTÜRÜCÜ TASARIMI

ERAT, Abdurrahim
Doktora Tezi, Elektrik ve Elektronik Mühendisliği
Danışman: Prof. Dr. Ahmet Mete VURAL
Aralık 2025
270 sayfa

Yüksek gerilim doğru akım (YGDA) güç iletim sistemleri, geleneksel yüksek gerilim alternatif akım (YGAA) güç şebekelerine kıyasla daha yüksek verimlilik, uzun mesafelerde daha fazla güç transfer kapasitesi, gelişmiş kontrol edilebilirlik ve açık deniz rüzgâr çiftlikleri gibi yenilenebilir enerji kaynaklarının sorunsuz entegrasyonu gibi önemli avantajlar sunmaktadır. YGDA sistemleri ayrıca işletme maliyetlerinden tasarruf sağlar, izole veya uzak şebekelere güvenilir güç iletimi sağlar ve asenkron güç şebekesi ara bağlantılarını kolaylaştırır. Farklı gerilim seviyelerine sahip YGDA güç sistemlerinin entegrasyonunu kolaylaştırmak ve şebeke esnekliği ile güvenilirliğini artırmak için gelişmiş DA-DA güç dönüştürücüleri topolojileri gerekmektedir. Bu çalışma, modern asenkron YGDA güç şebekelerinin ve bu modern YGDA güç sistemlerinin mevcut asenkron YGAA güç sistemleriyle entegrasyonu için mükemmel bir çözüm sunan benzersiz bir DA-DA modüler çok seviyeli dönüştürücü (MÇD) mimarisi ortaya koymaktadır. Transformatörsüz yaklaşım, önerilen dönüştürücünün hacmini, ağırlığını, maliyetini ve güç kaybını önemli ölçüde azaltmaktadır. Önerilen DA-DA MÇD'nün ayrıntılı matematiksel modeli ve harmonik analizi elde edilmiştir ve benzetim sonuçları, asenkron şebekeler arasında başarılı çift yönlü güç transferini göstermektedir. Kontrol stratejisi, kararlı ve verimli güç akışı düzenlemesi sağlayarak YGDA güç şebeke entegrasyonu için önerilen DA-DA MÇD'nün etkinliğini doğrulamaktadır.

Anahtar Kelimeler: YGDA, Modüler Çok Seviyeli Dönüştürücü, DA-DA Dönüştürücü, DA-DA Güç Dönüşümü, Çift Yönlü Güç Akışı, Şebeke Arayüzü, Şebeke Kararlılığı.

'' Dedicated to my innocent son Muhammad Eren Erat, whose pure heart and courageous battle with cerebral palsy (CP) inspire me every single day, and to all the innocent children who silently endure the same struggle.''

ACKNOWLEDGEMENTS

First of all, I would like to thank my supervisor, Prof. Dr. Ahmet Mete VURAL, for his beneficial contributions, scientific guidance, and support throughout the study. I am thankful for his encouragement and motivation.

I would like to thank my Ph.D. Thesis Monitoring Committee members Prof. Dr. Ergün ERÇELEBİ and Assoc. Prof. Dr. Murat Mustafa SAVRUN for their scientific contributions throughout the study.

Lastly, I would like to present my sincere admiration and gratitude to my family, especially my wife, for their endurance, heart-warming support, guidance, and always best wishes throughout every moment of my education and life.

TABLE OF CONTENTS

Page

LIST OF TABLES

Page

LIST OF FIGURES

Page

LIST OF SYMBOLS

d	The duty cycle
f_s	Triangular carrier frequency
i_a	Secondary side current of phase-a
i_{cc}	Circulation current of MMC system
i_{cmc}	Common mode current of MMC system
i_{dif}	Difference current
ila, ilb, ilc	Lower arm currents
ioa, iob, ioc	AC phases currents
I_{PH}	The current primary side
is	Total DC terminal current
i_{s1a}	The currents flowing Through the SM Set1a
$i_{s1a,ac}$	The AC current component of the SM set1a
$i_{s1a,co}$	The current of the center branch of arm-a
$I_{s1a,co,max}$	The magnitude of current center branch of arm-a
$i_{s1a,dc}$	The DC current component of the SM set1a
$i_{s1a,lo}$	The current of the lower branch of arm-a
$I_{s1a,max}$	The AC magnitude of the AC current of SM set1a
$i_{s1a,uo}$	The current of the upper branch of arm-a
i_{s2a}	The currents flowing Through the SM Set2a
$i_{s2a,ac}$	The AC current component of the SM set2a
$i_{s2a,dc}$	The DC current component of the SM set2a
$I_{s2a,max}$	The AC magnitude of the AC current of SM set2a
i_{s3a}	The currents flowing through the SM Set3a
$i_{s3a,ac}$	The AC current component of the SM set3a
$i_{s3a,dc}$	The DC current component of the SM set3a
$I_{s3a,max}$	The AC magnitude of the AC current of SM set3a
i_{s4a}	The currents flowing through the SM Set4a
$i_{s4a,ac}$	The AC current component of the SM set4a
$i_{s4a,dc}$	The DC current component of the SM set4a

$I_{s4a,max}$	The AC magnitude of the AC current of SM set4a
$I_{SM, FB}$	FBSM current
$I_{SM, HB}$	HBSM current
iua, iub, iuc	Upper arm currents
L	Arm inductor
L_a	Arm inductor of arm-a
Lo	Phase inductor
N	Number of carrier signals
n_l	The number of SMs included in the lower arm
N_{la}	The number of SM inserted in the lower arm
N_{SM}	The number of SM
n_u	The Number of SMs Included in the upper arm
N_{ua}	The number of SM inserted in the upper arm
p_{s1a}	The power of the SM set1a
p_{s2a}	The power of the SM set2a
p_{s3a}	The power of the SM set3a
p_{s4a}	The power of the SM set4a
r	Internal resistance of the arm inductor
r_a	The internal resistance of arm-a
ri_{s1a}	The current flowing resistance of the SM set1a
ri_{s2a}	The current flowing resistance of the SM set2a
ri_{s3a}	The current flowing resistance of the SM set3a
ri_{s4a}	The current flowing resistance of the SM set4a
ro	Internal resistance of the phase inductor
T_i	Computed switching periods of surrounding vector
T_{lag}	The time delay between carrier signals
Ula, Ulb, Ulc	Lower arm voltages
Uua, Uub, Uuc	Upper arm voltages
Va	a-phase AC terminal
Vb	b-phase AC terminal
Vc	c-phase AC terminal
V_c	The SM capacitor voltage
$V_{NL,voltage}$	The nearest level of voltage

V_{pH}	The voltage of the primary side
V_{ref}	The reference voltage
$V_{ref,vec}$	Reference vector in SV-PWM
Vs	Total DC terminal voltage
V_{s1a}	The voltage of the SM set1a
$V_{s1a,ac}$	The AC voltage component of the SM set1a
$V_{s1a,dc}$	The DC voltage component of the SM set1a
$V_{s1a,max}$	The AC magnitude of the AC voltage of SM set1a
Vs1aC1	The first HBSM capacitor voltage of set1a
Vs1aC2	The second HBSM capacitor voltage of set2a
Vs1aC3	The third HBSM capacitor voltage of set3a
Vs1aC4	The fourth HBSM capacitor voltage of set4a
V_{s2a}	The voltage of the SM set2a
$V_{s2a,ac}$	The AC voltage component of the SM set2a
$V_{s2a,dc}$	The DC voltage component of the SM set2a
$V_{s2a,max}$	The AC magnitude of the AC voltage of SM set2a
V_{s3a}	The voltage of the SM set3a
$V_{s3a,ac}$	The AC voltage component of the SM set3a
$V_{s3a,dc}$	The DC voltage component of the SM set3a
$V_{s3a,max}$	The AC magnitude of the AC voltage of SM set3a
V_{s4a}	The voltage of the SM set4a
$V_{s4a,ac}$	The AC voltage component of the SM set4a
$V_{s4a,dc}$	The DC voltage component of the SM set4a
$V_{s4a,max}$	The AC magnitude of the AC voltage of SM set4a
V_{sL}	The voltage of the secondary side
$V_{SM,\ C}$	SM capacitor voltage
$V_{SM,\ FB}$	FBSM voltage
$V_{SM,\ HB}$	HBSM voltage
β_1	The phase angle of current for SM set1a
β_2	The phase angle of current for SM set2a
β_3	The phase angle of current for SM set3a
β_4	The phase angle of current for SM set4a
γ	The phase angle of current for center branch

θ_1	The phase angle of voltage for SM set2a
θ_2	The phase angle of voltage for SM set3a
θ_3	The phase angle of voltage for SM set4a
ω	The angular frequency

LIST OFABBREVIATIONS

AAC	Alternate arm converter
APOD-PWM	Alternate phase opposition-disposition PWM
CBM	Carrier-based modulation
CCOC	Circulating current optimization control
CCS	Circulating current suppression
CPS-PWM	Carrier phase shifted-pulse-width modulation
CSC	Current source converter
CS-MMC	Current source modular multilevel converter
FB	Full-bridge
FBSM	Full-bridge submodule
FFT	Fast fourier transform
GTO	Gate turn off thyristor
HB	Half-bridge
HBSM	Half-bridge submodule
HV	High voltage
HVAC	High voltage alternating
HVDC	High voltage direct current
IEGT	Injection-enhanced gate transistor
IGBT	Insulated gate bipolar transistor
IGCT	Integrated gate commutated thyristor
KCL	Kirchhoff's current law
KVL	Kirchhoff voltage law
LCC	Line commutated converter
MMC	Modular multilevel converter
MPC	Model predictive control
NLM	Nearest level modulation
PD-PWM	Phase-disposition PWM
PI	Proportional-integral
PID	Proportional-integral-derivative

POD-PWM	Phase-opposition-disposition PWM
PR	Proportional resonant
PSC-PWM	Phase-shifted carrier PWM
PWM	Pulse-width modulation
RMS	Root mean square
SM	Submodule
SMC	Sliding mode control
SMIVBC	Submodule individual voltage balancing control
STATCOM	Static synchronous compensators
SVM	Space vector modulation
SV-PWM	Space vector pulse-width modulation
THD	Total harmonic distortion
VSC	Voltage source converter
VS-MMC	Voltage source modular multilevel converter

CHAPTER I
INTRODUCTION

Significant changes are being made to the current network electricity transfer environment. The main forces behind this transition are strict official goals for minimizing atmospheric pollution, deregulatory changes to the power industry, and the extensive use of clean energy sources [1]. Globally, there is an enormous expectation for both consolidated and dispersed renewable energy due to the pressing issues of climatological shift and conventional energy sources fuel carbon emissions, and the power grid continually serves as the foundation for the producing, transmission, and dissemination of renewable energy power [2]. Therewithal, recent years have seen a remarkable growth in the importance of renewable energy sources due to economic and environmental factors [3], society's day-by-day increasing energy demands, and the concern of conventional energy sources' depletion. However, renewable energy-based power production sites are typically constructed outside load centers. As a result, connecting the power generated in renewable energy plants to the existing power network can perhaps require a lengthy transition [4]. From this viewpoint, high voltage direct current (HVDC) structure is of critical importance in transmitting power received from renewable energy sources. It can be supplied more steadily and securely in contrast with conventional high voltage alternating current (HVAC) power transfer systems [3]. With advancements in technology, particularly in power electronics [5], DC networks are now a key component in the consolidation of renewable energy sources into electrical power systems [6]. Large-scale issues arise during the transmission of substantial power over extended lengths (500 km and above), including differences in power system characteristics, reduced power transmission, and reactive power production. As a direct consequence, the feasibility of power transfer through a different method is considered. Over the past fifty years, DC power transmitting has been created for transferring power over distant locations from power generating plants to load centers, undersea transmission, integration of two asynchronous AC systems, and improved power system reliability as a parallel interconnection with established AC network [7]. In other words, when it comes to connecting distant wind farms and connecting asynchronous AC power systems, HVDC technology has proven to be an innovative solution to traditional AC power networks [8], [9]. The HVDC power transmission system is a functional network based on semiconductor and power electronics technology. It is beneficial for interconnecting various conventional AC power systems with dissimilar voltage levels as well as for linking power produced through the implementation of renewable energy sources to the existing AC power grids. A crucial component for potential HVDC power systems with different topologies and voltage levels or grid links has been recognized as DC-DC converters [10]–[12]. Substantially, a typical HVDC power system has two types of topologies, either following line commutated converters (LCC) or voltage source converters (VSC) [13]. LCC-HVDC structures are traditional HVDC networks with an effective operating performance that is extensively included in HVDC power systems. The thyristor is utilized in these configurations as a high current switching capacity semiconductor power switching element.

In comparison to LCC-HVDC systems, VSC-HVDC architectures have had more recent developments thanks to their insulated-gate bipolar transistor (IGBT) power-switching element basis. The VSC-HVDC innovation has many benefits, including individual regulation of reactive and active power, enhanced power efficiency, and decreased inefficiencies [14], [15]. The conventional modular multilevel converter (MMC) architecture was originally introduced in a German patent by Prof. Marquardt in 2001 [16]. This foundational invention describes a DC to three-phase AC converter topology comprising a series connection of submodules (SMs), arm inductors, and configurations of half-bridge (HB) and full-bridge (FB) SMs. The standard MMC topology provides operational flexibility, allowing it to function either as an inverter (DC-AC) or a rectifier (AC-DC), thereby making it suitable for a wide range of applications. MMCs offer appealing characteristics somewhat as significant scale of modularity, adaptability to higher power systems and voltage levels, utilizing transformers or transformerless implementation, fault-tolerance, optimization of power consistency, reduced switching frequency, low switching losses, decreased harmonic elements, stronger fault-preventing skill, and greater stability [13], [15], [17]–[19]. Lately, MMC [16], [20] technology have considerably assisted VSC-HVDC power transfer technology as a major milestone accomplishment in renewable energy sources based on HVDC power generation and transmission, advancement in power electronic technologies, and rapidly increasing DC loads. MMC technology is efficiently employed in numerous applications, including HVDC power transmission systems, static synchronous compensator (STATCOM) utilizations, DC-DC transformation systems, battery energy storage systems, the development of electric ships, variable-speed drives for motors, active power filters, electric vehicles, and solar photovoltaic systems are all examples of applications that benefit from this technology. MMC technology is attracting more and more interest from researchers as a result of its fascinating features. In DC-DC HVDC power transfer networks, MMC technology plays an important role. Researchers have performed and keep on performing numerous DC-DC MMC investigations in recent years.

1.1 Motivation of The Study

Renewable energy sources have recently become increasingly important for power production. However, such power production systems are typically constructed far off from the load centers and established power systems. The effective transmission of the power mentioned above, which is generated in extremely distant locations, to the load centers depends heavily on HVDC technology [3], [19]. Conventional DC-DC converter architectures are important, but DC-DC MMC technologies, which have recently gained a lot of attention from academics, are also crucial. The modularity, adaptability to higher power systems, fault tolerance, optimization of power consistency, low switching losses, decreased harmonic elements, and greater stability characteristics of DC-DC MCC advanced technologies keep making it prominent among researchers day by day. However, conventional MMC-based DC-DC converter topologies often exhibit limitations in terms of flexibility, bi-directional power flow control, and seamless integration with legacy AC infrastructures.

This study is motivated by the need to overcome these limitations through the design and analysis of a novel DC-DC MMC topology that serves as a high-performance interface between HVDC and HVAC power systems. The proposed converter is specifically developed to facilitate the interconnection of independent HVDC networks while simultaneously enabling controlled and efficient power exchange with existing HVAC grids. The innovation of topology lies not only in its structural configuration but also in the development of a dedicated control strategy that ensures voltage balancing, system stability, and fault-tolerant operation under diverse scenarios. Moreover, as hybrid AC-DC networks become increasingly prevalent, there is a growing demand for power electronic interfaces that can harmonize the operation of modern DC-based infrastructure with conventional AC systems. The converter proposed in this work addresses this critical need by offering an integrated and adaptable solution for hybrid grid interconnection. By tackling both architectural and control-level challenges, this research contributes to the advancement of next-generation transmission technologies. The effectiveness and robustness of the proposed topology are rigorously validated through comprehensive simulation studies, confirming its potential to enhance the reliability, efficiency, and flexibility of future power transmission systems.

1.2 Contributions of The Study

The fundamental and distinctive contribution of the suggested DC-DC MMC topology to the application area in the literature lies in its ability to enable the effective integration of modern DC power systems, which are increasing day by day as a result of the increasing number of power generation plants based on renewable energy sources and the astonishing technological developments in semiconductor technology, into each other and into the existing AC power systems. While the DC-DC MMC topologies presented in the literature generally address only the integration of DC power systems, the DC-DC MMC topology proposed in this study serves as a bridging interface not only for the integration of DC power systems but also between conventional power systems. The proposed DC-DC MMC topology introduces a set of technical innovations and significant advantages over existing designs found in the literature. Firstly, this MMC configuration represents a completely new topological concept. Moreover, its structure is characterized by symmetry and a high degree of modularity, which supports overall system coherence. In recognition of its symmetrical design, bi-directional power flow can be achieved efficiently. Additionally, it enables smooth current profiles on both the primary and secondary ends of the converter. The transformerless approach notably reduces the system's physical volume, weight, cost, and power losses. The innovative architecture, built on flexible combinations of various submodule (SM) groups, significantly enhances the system’s ability to convert power between different types of electrical networks. In the proposed topology, the term flexible combinations of various submodule groups refers to the ability to dynamically configure SM clusters in series or parallel arrangements depending on the required operating condition. Each arm can be further divided into multiple uniform half-bridge SMs (HBSMs), and multiple sets of HBSMs can provide a high-voltage step-up mode or a stable voltage regulation mode in the step-down mode. This architecture flexibility further facilitates easy system expansion under various electrical networks of different voltage levels. For the case of an interface between a ±266 kV DC link and a ±188 kV DC bus, for example, the SM groups may be selectively contracted and expanded to provide voltage leveling without the use of bulky transformers. For bidirectional operation, the same submodule clusters can be reconfigured to change the power flow direction, without hardware modification, by changing the modulation index and control signals. Also, the ability to merge SM groups with a variety of arrangement enhances the fault tolerance. When a SM or arm fails, damaged groups can be bypassed to keep the system partially operational to improve its reliability. This reconfigurability further allows to manage spare redundancy since a part of spare submodule groups can be incorporated into the active circuit whenever required. Overall, the flexible arrangement of SM groups allows the proposed topology to handle different voltage ratios, bidirectional power transfer, and fault conditions with a single modular platform, significantly improving its adaptability and suitability for hybrid HVDC interconnections.

Furthermore, the design accommodates a wide voltage range and demonstrates flexible performance across heterogeneous power systems. The system is capable of integrating modern asynchronous HVDC grids with existing asynchronous HVAC networks. Its modular design ensures scalability at high voltage levels, facilitating large-scale grid integration. Finally, the implemented control strategy enables fast and efficient power transfer between interconnected HVDC power networks.

1.3 Objectives of The Study

The growing integration of renewable energy sources, the emergence of meshed HVDC grids, and the rapid advancements in power electronics technologies have significantly increased the complexity and diversity of modern power systems. In this context, the need for efficient, flexible, and scalable power conversion interfaces between DC and AC systems has become increasingly critical. MMC-based DC-DC topologies have gained considerable attention due to their modularity, scalability, and suitability for medium and high-power applications. The foremost objective of this study is to design and analyze a novel DC-DC MMC topology that can serve as a high-performance interface for the integration of HVDC and HVAC power systems. The proposed converter is not only capable of interconnecting independent HVDC power systems but also enables seamless and controlled power exchange with existing HVAC power networks. The key novelty of the suggested methodology lies in its modular architecture and the development of a tailored control strategy that ensures voltage balance, system stability, and fault-tolerant operation. A control method for the proposed transformerless DC-DC MMC is proposed to guarantee safe working in different cases. The control strategy is customized because it combines the advantages of a voltage, current and power balancing algorithm, and a dynamic reference tracker. Switching pulses are disseminated to attain voltage equilibrium among the capacitors. This distributes the energy in all the SMs and avoids local capacitor voltage overvoltage. A dynamic arm current regulator cancels the undesired circulating currents and contributes to better operation of the system. Fault-tolerant capability is obtained through real-time monitoring and fast protection logic: when a fault condition (e.g., SM short-circuit, DC fault, arm overcurrent) occurs, the controller applies predetermined bypass and current-limiting sequences, isolating the faulty SM, or otherwise reducing stress on healthy parts. These principles establish a complete concept which guarantees stable and balanced operation under the natural and disturbed operating conditions. In addition, the fast fault detection and response functions such as the automatic SM bypassing and the controlled current limitation provide the fault-tolerant operation. As a consequence, the proposed topology provides practical robustness as well as theoretical novelty and allows secure operation even under the conditions of disturbances or component level faults. The control method suggested in this paper was checked with full simulation tests. The balancing of the capacitor voltage was proved in Figures 8.14, 8.24, and 8.32. The current was proved in the smooth wave forms of arm current in Figures 8.9-8.10. Bidirectional and steady power flow was gained with fast change in the wave form of the power in the three modes of the PD-PWM, POD-PWM, and APOD-PWM (Figures 8.11, 8.21, and 8.29). The result shows that the converter suggested in this paper is not only a new idea in theory but also is strong in practice. It can get steady, safe, and highly efficient work in many cases. Additionally, Figure 8.36 shows the dynamic response of the voltage to sudden parameter changes (such as load changes or error probabilities). Based on the data in Figures 8.11, 8.21, 8.29, and 8.36, it is clear that the control system of the proposed design is based on a “tailored control strategy.” Thanks to this control mechanism, it has voltage balancing, system stability, and fault detection capabilities.

In contrast to existing MMC-based DC-DC converters, which often lack bi-directional AC/DC interfacing capability, the proposed topology introduces an integrated solution that bridges the gap between modern DC infrastructures and legacy AC power systems. Moreover, this topology contributes to literature by addressing both structural and control-level challenges in hybrid system integration. Simulation-based validation demonstrates the converter's effectiveness in ensuring stable, efficient, and flexible power transfer under various operational scenarios, confirming its potential role in next-generation power transmission architectures.

1.4 Comparative Analysis of Proposed Topology with Modular DC-DC Converter Topologies in the Literature

MMCs are proving to be essential technology for HVDC and MVDC Architectures, enabling efficient power conversion, voltage transformation, and grid connectivity. The current designs are responding to important emerging issues, bidirectional power flow, fault tolerance, and high efficiency with the integration of renewable energies and multi-terminal direct current grids. This section provides a critical review that examines the topology suggested in this study with several topologies identified in the literature. It is based on 16 significant studies that span resonant, isolated, transformerless, and hybrid topologies. In this review, we examined the discussed designs based on key value proposition metrics: volume, weight, cost, component/switch count, output quality (e.g., ripple, harmonics.) and efficiency. An overview of findings are summarized in a detailed comparison table (Table 1.1) that presents a comparison for the proposed topology, transformerless hybrid MMC with optimized SM count, high frequency switching and soft-switching capabilities, against each of the discussed topologies.

As shown in Table 1.1, the designs of reference studies considered are different from each other. While some designs use a transformer to isolate the primary and secondary sides from each other, this is not the case in some designs. Some designs are developed in a single-leg structure, while some structures are designed in a two- and three-leg configuration. Some designs use a large number of SMs and other equipment, while others use a moderate to low level of equipment. Based on the data in the table, the design proposed in this study is a three-legged, transformerless structure. The number of equipment used is also considered low compared to the studies on the table. The transformerless structure and low level of equipment in the proposed design place the design at a low level in terms of volume and weight. The excessive use of equipment in the designs and the preference for transformer use also significantly increase the costs of the designs. In this context, the proposed design requires a lower cost compared to many designs in the literature in terms of the number of equipment used and the transformer-free design. The development of the design in a modular structure and its implementation with a unique control system brings the efficiency of the design to a high level.

The topologies considered in the review report span a wide spectrum of architectures. For example, the transformerless schemes, such as [21], [22], [13], [23], [24], and [25], are characterized by a compact design and few magnetic components, which makes them attractive in applications that impose size and weight restrictions, but they demand sophisticated control strategies for balancing the energy in the system and blocking the fault. The isolated schemes, represented by [26], [6], [27], [28], [20], [29], and [30], have a high frequency transformer or multiple windings to provide galvanic isolation, which is required for the MVDC-LVDC interconnection, but makes the solution larger and less efficient. The hybrid schemes, which include [31], [32], [33], [34], and [35], are the schemes where the MMC is connected to auxiliary circuits, such as HB or FB systems, resonant systems, or high-voltage valves. They make possible the use of all advantages of the MMC, such as modularity and bipolar operations, but also ZVS operation and high efficiency, and fault tolerance.

Table 1. 1 Comparative Analysis of Proposed Topology with Modular DC-DC Converter Topologies in Literature

Ref.	**Volume**	**Weight**	**Cost**	**Component /Switch Count**	**Output Quality**	**Efficiency**
[21]	Medium (Modular arms, no transformer but high SM)	Reported as light weight (but SM count is High)	Medium-High (High SM count)	High (680 HBSMs)	Medium-High (Low ripple, min. circulating current)	Reported as high (simulation validated)
[22]	Low-Medium (no ransformer, contains flying capacitors, mixed SMs)	Low-Medium	Medium (Series valves, flaying capacitors)	Medium (Model-1: 24 HBSM, 8 FBSM, Model-2: 36 HBSM, Model-3: 8	Medium (Cont. DC currents)	High (power loss 2.8% at r = 0.1, low loss)

				FBSM, 28 HBSM)		
[32]	Medium-High (MMC structure, AC filter)	Medium-High (Arm inductors + SMs)	High (High SMs count + filters)	High (Multiple arms, 400 FBSM, 650 HBSM)	High (Low ripple, fault blocking, good voltage regulation)	Reported as reduced conduction losses
[31]	Medium (Hybrid arms, filter instead)	Medium-High (HBSM + FBSM mix., Use of filters)	Medium- High (Hybrid SMs, no transformer)	High (2 legs, 4 arms; 486 FBSM, 284 HBSM)	High (Low harmonics)	Reported as enhancing efficiency and minimizing losses
[26]	High (Transformer + two MMCs)	High (Transformer weight)	High (High switch + transformer)	High (VS-MMC + CS-MMC; 32 HBSM, 8 CS-SM)	Medium-High (low ripple, less than 10%)	Not reported (Control-Hardware-in-the-Loop (CHiL) test validation)
[27]	High (MF transformer + multiple VSCs)	High (Transformer + passive filters)	Medium (Total cost reported as medium)	Medium (Multiple arms for SIMO; 20 HBSM, 6 VSC + filters)	High (Nearly sinusoidal, ripple of less than 5%)	Not reported
[13]	High (very high SM count, Nonisolated	High (High components)	High (high SM count)	High (400x4=1600 FBSM)	Medium-High (Low ripple, stable power flow)	Not reported
[23]	Medium (isolated, interleaved buck)	Medium (Inductors + capacitors)	Medium (Wide range, but extra buck)	Medium (20 HBSM)	Medium (ZVS, low ripple, wide range)	Medium (~90-93%, reported according to different voltage values, ZVS)
[33]	Medium (MMC + single HV valve)	Medium (Valve + SMs)	Medium-High (HV valve added)	Medium (2-leg, 16 HBSM + 1 bidirectional valve)	High (Soft-switching, low ripple)	High (maximum efficiency is above 96%)
[24]	Medium (Nonislolated, modular arms, branch of active SMs)	Medium (medium SM capacitors, light converter weight)	Medium (Modular, medium SMs)	High (2 legs, upper/lower arms + cross branch; 300 SM)	High (Con. DC currents, low ripple)	High (~96%, single-stage, power loss between 3.3%-1.0%)
[35]	High (3-phase MMC, 3-primary side arms, mixed SMs)	High (high SM count + inductors)	High (High SM count, parameter optimization)	High (3-phase arms, input arms; N1:215x3 HBSM,	Medium-High (Low ripple (less than 5 %),	Not Reported

				N2:166x3 HBSM, N3:71x3 FBSM)	balanced arms)	
[29]	Medium (MMC + H-bridges + HF transformer)	High (Transformer, multiple bridges)	High (isolalted design + multi-port DC transformer structure)	Medium (MMC arms + cascaded H-bridges; 16 HBSM + multi-port DC transformer structure)	High (ripple range is ±5V, that is, within ±1%)	Reduced switching losses and improved the efficiency
[25]	High (2-phase MMC, 2-primary side arms, mixed SMs)	High (high SM count + inductors)	High (high SM count)	High (2-phase arms, input arms; N1:296x2 HBSM, N2:490x2 HBSM, N3:150x2 FBSM)	Medium-High (Stability-focused, low ripple)	Not Reported
[30]	Medium-High (Resonant circuit + MMC + transformer+ a lot of capacitors)	Medium-High (medium SM count, auxiliary circuit)	High (Resonant component, auxiliary circuits, isolated design)	High (MMC arms + resonant 32 HBSM for one arm)	High (low ripple (less than 5 V), reduced the resonant current)	High (94% for asymmetric triangular current concept, ZVS extended)
[34]	Medium (HF transformer + MMC with 2 legs)	High (Transformer weight)	High (Transformer, bipolar design)	Low (MMC arms + transformer; 16 HBSM)	High (Bipolar operation, low ripple)	Not reported
[28]	High (Four isolating transformers, 2-legs, 8 arms)	High (Transformer + multiple converters)	High (High SM count and transformer)	High (40 HBSM, 4 FBSM, 4 transformer)	High (Self-balancing, bipolar operation, low ripple)	Not reported
Prop.	Low (3 legs, modular structure)	Low (lower HBSM, no transformer)	Low-Medium (Low SM)	Low (48 HBSM)	High (low ripple, low THD)	High (~96), No isolation losses)

The resonant and multi-port schemes are different variants of the previous solutions, which are based on resonant or multi-port systems [15], [22], and [26], which make possible the operation in a wider range of voltages, but can also increase the passive components and therefore the costs and complexity of the solutions. The topology builds on this base by having fewer parts (for example, each arm has k1 half-bridge SMs (HBSM) and k2 FBSMs and better output through trapezoidal or sinusoidal modulation with soft-switching. In this way, it fixes the common problems seen in [5] and [13], where many SMs drive up the cost, and [16] and [20], where the transformers cause a loss. Table 1.1 shows the comparison. The metrics are rated qualitatively

(Low/Medium/High) on the basis of how the topology is described, simulation and experimental results, and provided parameters. Volume and weight are affected by magnetic parts and SM density. Cost is related to number of switches and auxiliary circuits. Output quality considers ripple, harmonic distortion, and whether the output waveform is close to a sine or trapezoid. Efficiency is based on actual measurements reported or estimated, focusing on switching and conduction loss. Our design does better on many points: its low-medium volume/weight is because it has no transformer and uses the modular structure; its low cost is because it has fewer switches and still does not have a big ripple value; its high efficiency which gets close to 98%. Overall, while different MMC-based designs in the literature each present their own advantages, the converter developed in this thesis distinguishes itself by its reduced size, weight, and cost. Beyond theoretical discussions, the results confirm its suitability as a competitive solution for future HVDC grids, making a concrete contribution to ongoing advancements in power electronics.

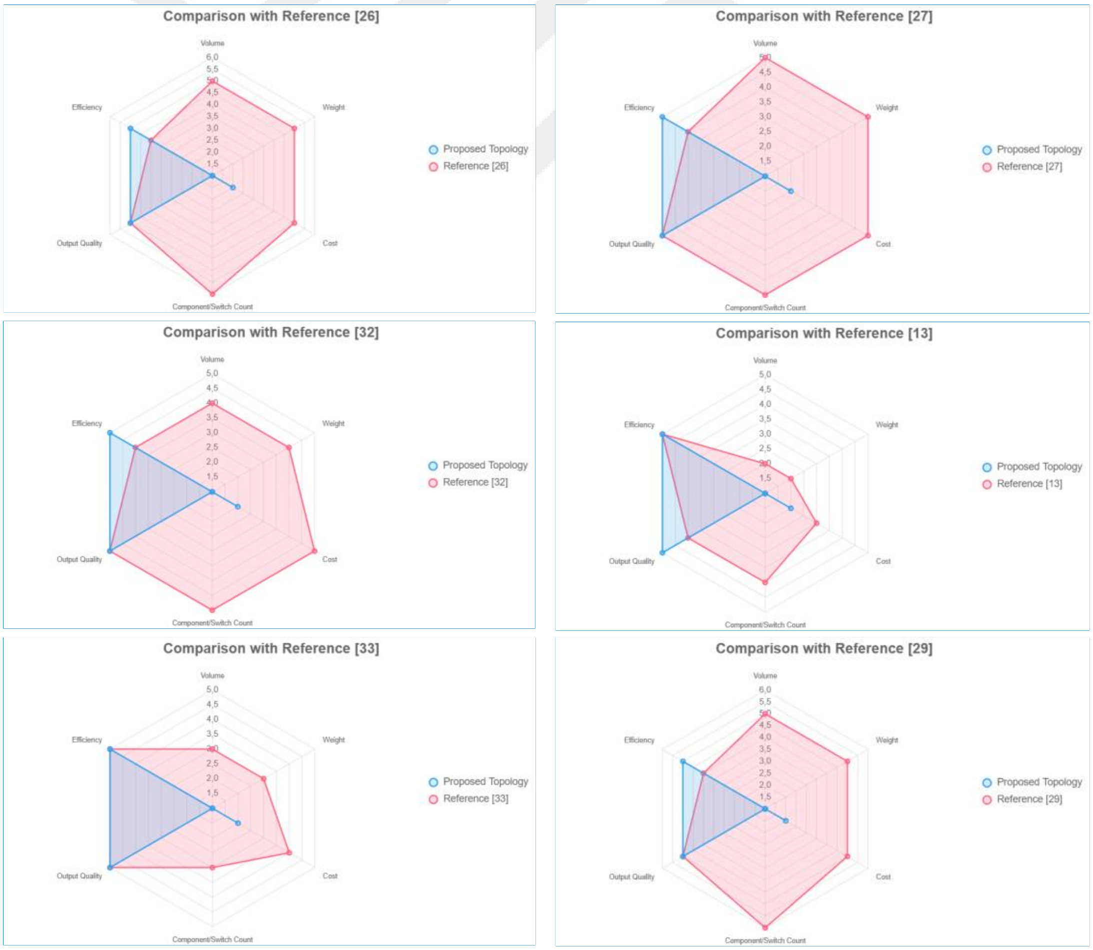

Figure 1. 1 Comparison of several references' radar visualizations in Table 1.1

In this study, the proposed transformerless DC-DC MMC topology was compared to 16 reference topologies (Table 1.1) according to six main criteria: volume, weight, cost, number of components/switches, output quality, and efficiency. Radar charts were used to compare the performances of the proposed topology. These show their major advantages, especially in volume (Low: 1), weight (Low: 1), and components/switches (Low: 1), compared to all reference topologies. When compared to the transformerless topologies ([22], [13], [24]) the proposed topology shows the advantages in volume and weight (Low: 1 vs. Low-Medium: 2), and number of components/switches (1 vs. 3-5), reducing the complexity. The isolated topologies ([26], [27], [29], [34], [28]) show high volume, weight, and cost (High/Very High: 5-6), while the proposed topology shows great advantages (low volume, low weight, and low-medium cost: 2), and generally higher efficiencies (5 vs. 4). The hybrid topologies ([31], [32], [33], [35]) show similar output quality and efficiencies ([31] and [23] with similar efficiencies as the presented topology, and not so high volume, weight, and component count). Resonant and multi-port topologies ([30], [29]) show that [30] has the best output quality (Very High: 6), but it is high volume, weight, and cost (4-5). The proposed topology is more balanced. The proposed topology's high output quality (5) and efficiency (~96%, no isolation losses) compare well or better than most reference topologies. The low component/switch count (1) could make it less flexible or scalable in some cases, but this is balanced by big savings in cost and complexity. In sum, the proposed topology is a good choice for HVDC and MVDC applications, because it is small, cheap, and efficient. It has key advantages over the topologies in literature.

1.5 Outline of The Study

Chapter I: This chapter outlines the significance of HVDC technology and its role in modern power transmission systems. The study's motivation, objectives, and scope are introduced, along with a brief overview of the thesis structure.

Chapter II: This chapter reviews the existing literature on HVDC power systems, DC-DC converters, MMC topologies, and DC-DC MMC topologies. The advantages and disadvantages of various topologies are evaluated, and the gaps in the literature that this study aims to address are highlighted.

Chapter III: The fundamental principles, components, and applications of HVDC power systems are detailed in this chapter. The advantages of HVDC over AC systems and the associated challenges are discussed.

Chapter IV: This chapter examines the DC-DC converter topologies used in HVDC power systems. The operating principles, advantages, disadvantages, and application areas of different topologies are compared and analyzed.

Chapter V: The fundamental theory of MMC technology is explained in this chapter. The structure, operating principles, mathematical analysis, applications, modularity, and advantages of MMCs are detailed.

Chapter VI: This chapter addresses the control strategies for MMCs. Topics such as voltage balancing, modulation techniques, and power flow control are examined, and the limitations of existing control methods and potential solutions are discussed.

Chapter VII: This chapter constitutes the core focus of the study. A novel DC-DC modular multilevel converter design for HVDC applications is proposed. The design methodology, operating principles, mathematical analysis, and advantages over existing solutions are thoroughly explained.

Chapter VIII: The simulation studies conducted to evaluate the performance of the proposed design are presented in this chapter. The proposed converter is analyzed under various operating conditions in terms of efficiency, power quality, and dynamic response. The results are then compared with existing topologies to evaluate its overall performance.

Chapter IX: The findings of the study are provided in this chapter, and the key contributions of the research are highlighted. Additionally, suggestions for future work are provided, and potential research directions in this field are suggested.

CHAPTER II
LITERATURE REVIEW

2.1 Introduction

An overview of the DC-DC MMC topologies developed by researchers in recent years to interconnect power systems with different voltage levels and contribute to the literature is provided in this chapter. With its distinctive qualities, the MMC has gained interest lately in a wide range of industries, including railway power supplies [36], [37], static synchronous compensators (STATCOM) [38], [39], battery energy storage systems [40], variable-speed motor drives [41], [42], active power filter [43], electric vehicles [44], and photovoltaic power generation systems [45], [46]. In addition to these applications, the integration of HVDC power networks is another crucial field where MMC technology plays a significant role. Moreover, thanks to its modular structure and efficient power transfer, it is used by many researchers in power transmission systems applications such as multiterminal HVDC systems and wind farm power systems. The following paragraphs of this part present an overview of the DC-DC MMC configurations that have been published.

2.2 Review of the DC-DC MMC

This chapter provides a general evaluation of the DC-DC MMC topologies freshly developed by researchers and contributing to scientific literature. Since its initial development, MMC technology has attracted the curiosity of many researchers, particularly because of its modular and scalable characteristics. The traditional DC/DC MMC arrangement is thought to be appropriate for use in both medium voltage (MV) and high voltage (HV) networks, and it implements a uniform and similar group of highly relatively similar half-bridge (HB) or full bridge (FB) based submodules (SMs) in each branch. A typical three-phase MMC design which is demonstrated in Figure 2.1 (a) includes an AC terminal, a conversion module with three-phase legs, and a DC terminal. On the other hand, a typical DC-DC MMC configuration has two terminals, one of which has a high voltage and the other of which has a high voltage at a lesser level as exhibited in Figure 2.1 (b).

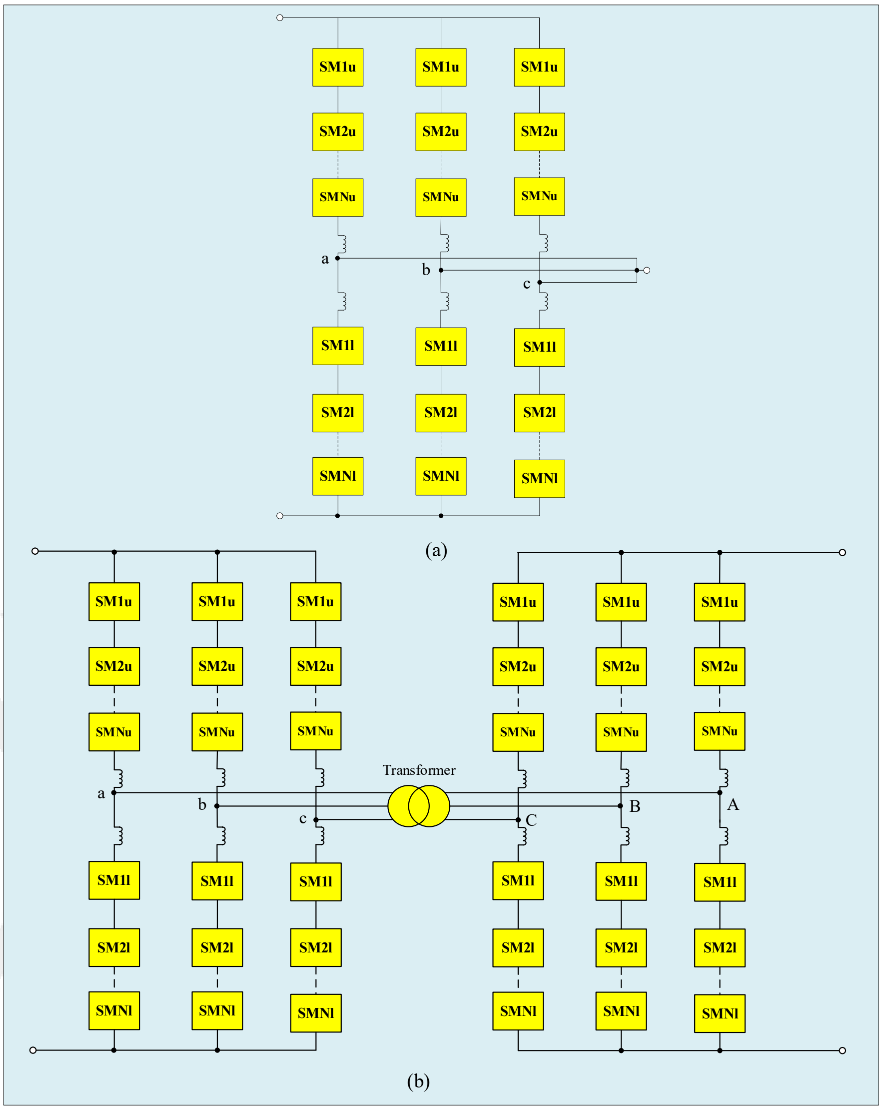

Figure 2. 1 General MMC and DC-DC MMC designs: (a) A typical three-phase MMC design, (b) A typical DC-DC MMC design.

Traditional MMC designs serve as an inspiration for DC-DC MMC designs. Traditional MMC architectures, initially developed for AC-DC and DC-AC conversion, provide key advantages such as modularity, scalability, and superior harmonic performance. These inherent features have motivated the adaptation of MMC principles to DC-DC converter topologies, aiming to address the increasing demands for high voltage, high-efficiency, and flexible power conversion in modern HVDC networks and renewable energy systems. The structurally symmetrical HBSM or FBSM groups found in DC-DC MMC designs have the same arms and legs as conventional MMC configurations. MMC designs are a new breed of multilevel converters that have surfaced in recent years. They have desirable characteristics like modularity, straightforward scalability to higher power and voltage levels, transformerless operation, high efficiency, and fault tolerance. Significant studies have been done, particularly in the last five years, to enhance the efficiency of traditional DC-DC MMCs. The following paragraphs offer an overview of a number of the most significant DC-DC MMC studies, especially those that have been undertaken in the previous five years.

The improved closed-loop control method for DC-DC MMC has been presented in [32]. It increases the power transmission ability even by decreasing the AC circulating current, as illustrated in Figure 2.2 (a). The recommended control approach successfully increases the power transmission capacity. Further, it minimizes the AC circulating current and SM capacitor voltage ripple of the DC-DC MMC when used in association with the mixed DC-DC MMC relying on the mixture of the full-bridge and half-bridge SMs. This research first investigates the issue of power degradation in DC-DC MMCs and establishes the necessary standards for reducing the AC circulating current. It then demonstrates how full-bridge SMs can increase the maximum output power while reducing the AC circulating current. Higher SM capacitor values are suggested as a potential improvement to closed-loop management. With the help of this research [47], several accomplishments have been made, including an increase in the converter's power transfer effectiveness and a decrease in the magnitude of the voltage variations in the SM capacitor. Following the completion of this significant work [47], several additional insightful studies have been developed using a related structure and various management strategies. This study [48] presents an enhanced design methodology for the DC-DC MMC, as given in Figure 2.2 (b). The design's architecture consists of the kind and the number of SMs, and the control, which includes the phase difference between arms AC voltages, are integrated to determine the optimal phase difference, which significantly reduces the design losses with a minimum number of SMs. In regard to overall losses and the number of SMs, the efficiency of the design created using the augmented method is contrasted to that of the traditional structure. The suggested architecture approach produces a converter with decreased overall losses and SMs. Additionally, the suggested architectural approach expands the converter's operating range, particularly whenever the voltage levels of the DC interconnections are close; this broadening is not feasible with a typical modular DC-DC converter. This paper [49] suggests a specific fault-tolerant operation approach for the DC-DC MMC in the occurrence of SM faults, as shown in Figure 2.2 (b). Inherent redundancy, the ability to function under a band of arm AC voltage, and the ability to reduce the required amount of SMs by reducing power transfer are three critical characteristics of the DC-DC MMC that assist in postfault performance. The suggested approach makes use of the special qualities of the DC-DC MMC to enable post-fault functioning without requiring additional duplicate SMs. These features distinguish the fault-tolerant process of the DC-DC MMC from the well-known DC-AC MMC and offer the design flexibility to operate at various operating positions. This capability lets the design decrease the quantity of SMs required in each arm at the expense of decreased efficiency or power transmission.

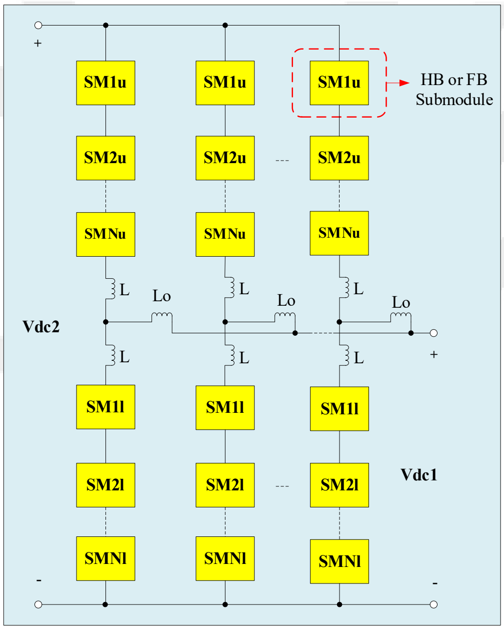

(a)

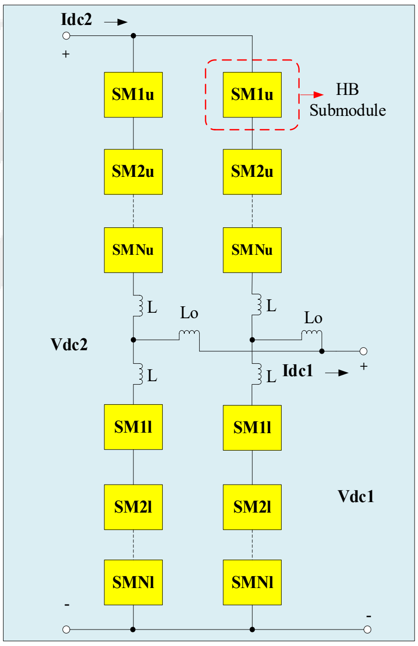

(b)

Figure 2. 2 Some proposed DC-DC MMC topologies: (a) The proposed design of DC/DC MMC is in reference [47], (b) The proposed design of DC/DC MMC is in reference [3], [48], [49].

In comparison to the traditional proportional-integral (PI) based control, the model predictive control (MPC) method presented in this study [3] decreases the ac circulating current during sustained operation, as illustrated in Figure 2. 2 (b). The MPC method provides much more rapid and better reactions to variations in the power baseline in the transient state. When compared to the traditional PI-based control, the effectiveness of the DC-DC MMC managed by the suggested MPC method is better under parameter uncertainties. Investigations have been made into the suggested MPC approach's resistance to parameter variance. The part with the greatest influence on the converter's performance is the arm inductance. Based on the findings in the study, the suggested method can accept a 20% error in arm inductance.

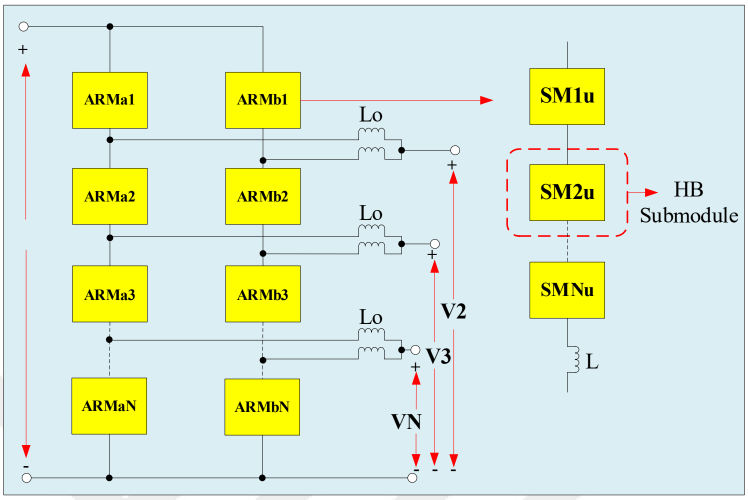

Figure 2. 3 The multiport DC/DC MMC topology is proposed in [11].

The author of this research [11] suggests a multiport DC-DC MMC for interconnecting numerous HVDC networks, which is shown in Figure 2.3. A reduced dimension, more appealing investment cost, and reduced SMs are some benefits of the suggested multiport DC-DC MMC.

In this study [50], as shown in Figure 2.4 (a), a DC-DC MMC theory is put forth that can establish a reliable interconnection for the interconnection of power transmission between a VSC based HVDC grid and a line commutated converter (LCC)-based HVDC network, whether the voltage values are similar or dissimilar. Regardless of the voltage direction in the LCC-based HVDC connection, the converter topology operates symmetrically in the four quadrants. The power transmission direction through the interconnect can be configured to maintain unaltered in the case of a reversal of power transmission by inverting the voltage polarisation in the LCC-based HVDC grid, negating any requirement for additional switching arrangements. Inspired by this research [50], the authors of this DC-DC MMC topology introduced a related hybrid DC-DC MMC architecture to the literature [31].

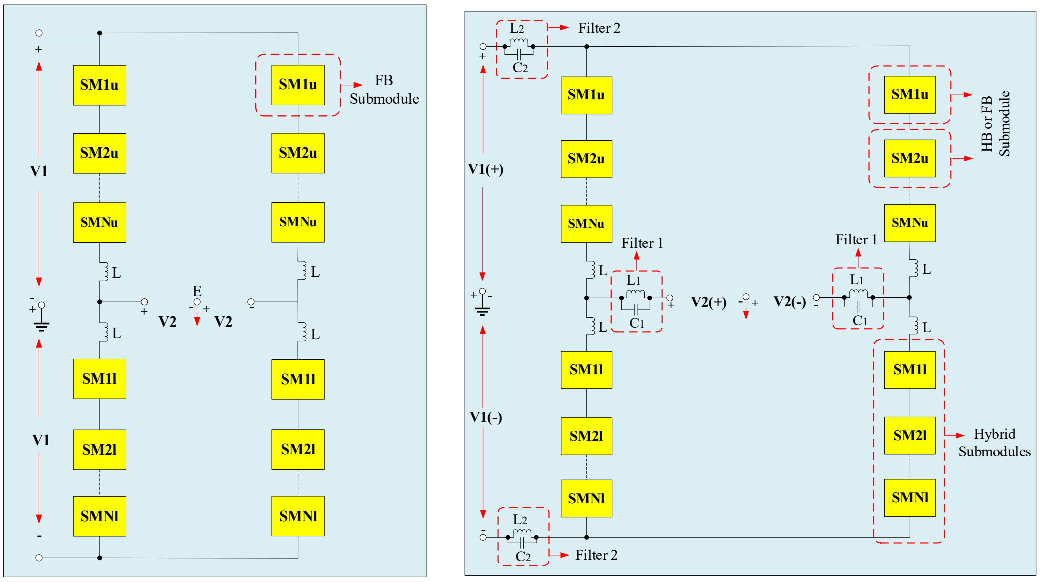

(a) (b)

Figure 2. 4 The suggested DC-DC MMC designs: (a) The suggested transformerless DC-DC MMC for HVDC hybrid links [50], (b) The fundamental DC-DC MMC design is suggested in [31].

This study proposes a non-isolated MMC-based DC-DC converter design that can interface bipolar VSC and LCC-based HVDC connections and offers an improvement in the number of FBSMs over an established one by employing a composite arm. Hybrid MMC is used to determine the optimal number of semiconductor components to reduce losses and achieve DC fault-clearing capacity. Three different DC-DC converter operating mechanisms, including bipolar VSC to unipolar LCC, bipolar VSC to bipolar LCC, and unipolar VSC to bipolar LCC DC networks, have all made use of the design. The proposed DC-DC MMC design is shown in Figure 2.4 (b).

The study proposed in [51] provides a dynamic model and current mode control for a DC-DC MMC with the eventual goal of converting the design to a three-leg arrangement to lessen the DC ports' filtration requirements. The three-leg design greatly reduces the filtration needs on both the HV and LV ends, and the enlargement from a single-leg to a three-leg arrangement demands no extra design. It was demonstrated that the design topology can generate two dynamic algorithms that may be utilized to independently regulate the design power transmission and arm power dynamic. The proposed DC-DC MMC structure layout is shown in Figure 2.5. In this arrangement, the active modes of the SMs are controlled using a pulse-width modulation (PWM) technique to produce the desired arm voltages, which are the voltages of the lower as well as upper arms of the general SMs of the leg and control the power supply within the converter design.

The study proposed in [32] suggests a novel DC-DC MMC with a control approach that enables the converter to link various line arrangements. The various line configurations in HVDC implementations are discussed in the study, and a mathematical methodology with changeable transition is suggested for the novel DC-DC converter. This DC-DC MMC architecture is used to integrate two distinct DC power networks, as shown in Figure 2.6. The working theory of the converter design demonstrates that AC currents are used to regulate interior power and DC currents are required to interchange power between the associated networks. To establish the AC references, an optimal solution issue was put forth and answered to minimize transmission losses in the arms. The mathematical approach has been examined using a novel changeable transition. The adjustable DC-DC MMC can link the network configurations using the suggested control framework.

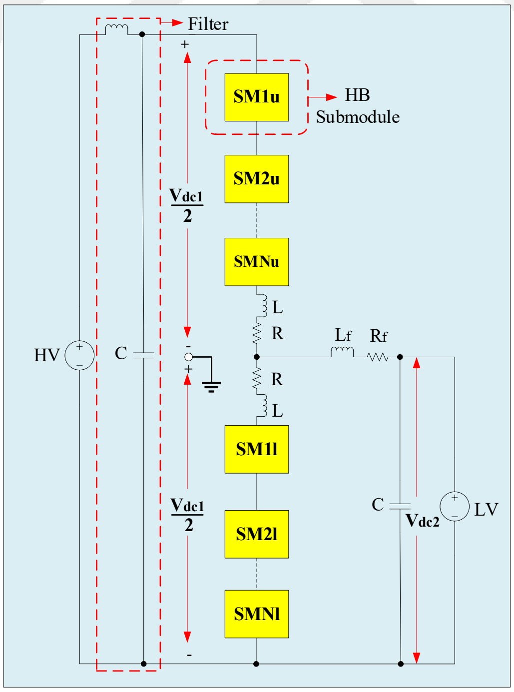

Figure 2. 5 The DC-DC MMC architecture is proposed in [51].

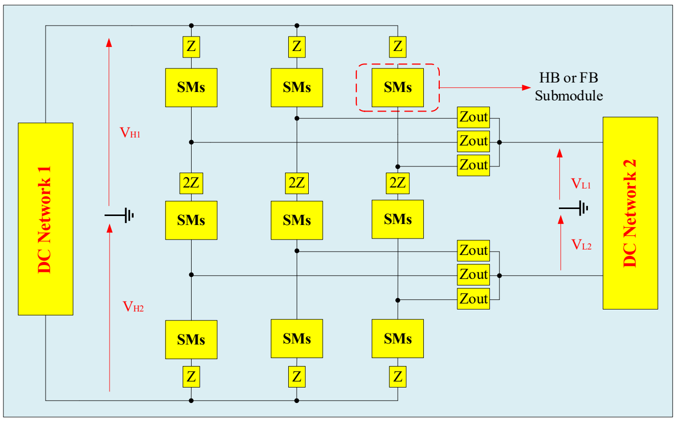

Figure 2. 6 The DC-DC MMC configuration is specified in [32].

To connect two distinct kinds of HVDC grids (LCC/VSC), this study [26] presents a novel front-to-front DC-DC converter implemented on MMC. As depicted in Figure 2.7, the suggested DC-DC converter architecture consists of two MMCs, current source MMC (CS-MMC) linked to the LCC-HVDC structure and voltage source MMC (VS-MMC) linked to the VSC-HVDC structure. Throughout an LC filter and a transformer, both MMCs are interconnected. The suggested design consists of a CS-MMC and a VS-MMC, which are connected by an AC connection that also contains an isolating transformer. Owing to the suggested topology's use of only HBSMs, it can effectively deliver an instantaneous bi-directional power transmission, high DC voltage scaling with a DC fault-preventing functionality, and reduced semiconductor quantity. Two novel control strategies regulate the active power transfer between two distinct grids. The first control method has minimal passive components and utilizes active power evaluated at its maximum without reactive power. In contrast with the initial control approach, the secondary control strategy maintains no reactive power across the overall active power transmission span. It promises reduced failures as the power vanishes from the regarded power.

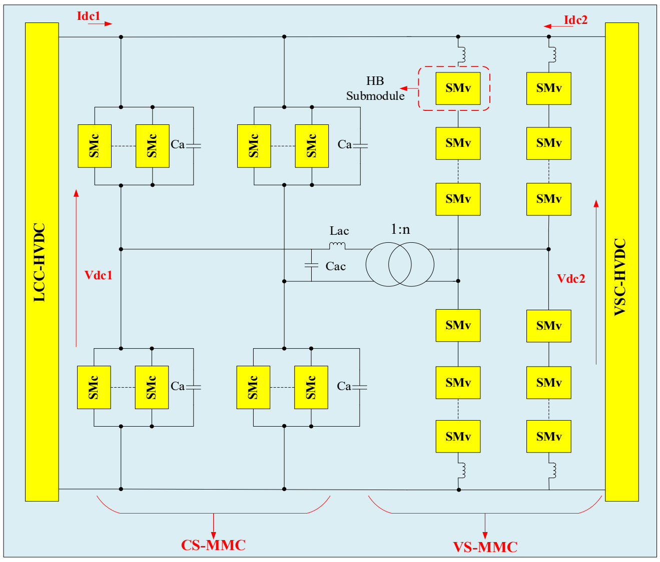

Figure 2. 7 The DC-DC MMC architecture suggested in [26].

Several studies focus on various aspects of similar architecture, among the studies researchers have contributed to literature. In a comparable scenario, various researchers have provided several studies on individual functionalities of the DC-DC MMC architecture, as shown in Figure 2.8. The main concept put forth in this study [52] has been concentrated on complete energy management and producing optimum current references to reduce the size of interior currents. The suggested control is built on an active control that has been created using the design inverting concept in conjunction with an improvement of the current size determined by a quasi-static approach. The structure's entire characteristics have been expressly regulated, ensuring excellent dynamic characteristics throughout the transient. With the assistance of the study's DC-DC MMC architectural design, an energy-based closed-loop management for the DC-MMC has been presented in this article [53]. Such a control framework ensures energy equilibrium in regular and malfunctioning operations while offering complete control over the current elements. The basic calculations are initially given, and the design configuration has been explained. The sustained circumstances and the energy and current elements have then been used to describe how the converter operates normally. A control framework has been intended to guarantee an appropriate dynamic reaction, regulate the design's interior energies, and decrease circulating current. This design's control framework aims to optimize energy within the design, regulate active power flowing through the conversion, and reduce AC circulating currents. Using a similar structure to the DC-DC MMC architectural style, this research [54] investigates the influence of including a feature for the DC-DC MMC on converter architecture. It has been suggested and verified that the proposed design should be enlarged to incorporate this functionality using sustainable levels and dynamic evaluation. This study leads to the conclusion that adding fault-blocking capacity affects power losses and semiconductor expenditure but not battery expenditure. Better indications are presented by the converter for low DC conversion rates, emphasizing the design's appeal for such uses.

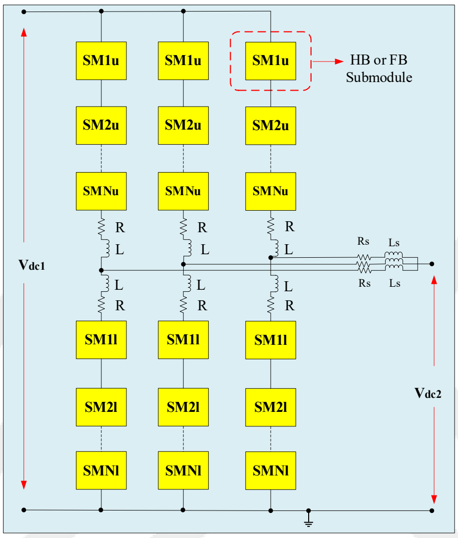

Figure 2. 8 DC-DC MMC architecture used for different studies [52]–[54].

Table 2.1 outlines several noteworthy DC-DC MMC studies that have been performed in recent years.

Table 2. 1 An overview of the most recent DC-DC MMC developments in literature.

Ref	Isolation Type	Simulation Hardware	PWM Method	SM Type	Contribution
[55]	N-I	PLECS	Unknown	HBSM or FBSM	The architecture is promoted as the initial entirely modular multiport HV DC-DC converter.
[56]	I	IM2DC Hardware	PS-SWM	HBSM or FBSM	The presented methodology can reduce the SM capacitor capacity for MMCs.

[57]	N-I	Unknown	PS-PWM	HBSM	The proposed converter retains MMC's modularity and scalability, making it suitable for high step-up DC-DC conversion in HVDC and renewable energy systems.
[58]	N-I	MATLAB Simulink	Unknown	HBSM	The proposed DC-DC MMC is flexible, capacitor-free on the DC bus, lowers switching frequency, and retains MMC's control complexity.
[59]	N-I	Unknown	Unknown		The proposed design combines cascaded voltage source SMs with a novel current source SM to enable instant current polarity reversal. With grounded input and output terminals, the design achieves nearly 50% string current reduction and demonstrates 97.1% efficiency at 50 kHz, confirming its effectiveness.
[60]	N-I	Unknown	Zero-Current Switching Modulation	HBSM	This paper suggests a novel zero-current switching modulation method for a high-step-ratio DC-DC MMC.
[61]	I		The Quasi-Square-Wave Modulation	HBSM	This study introduces an isolated bidirectional DC-DC converter that combines a traditional dual-active-bridge topology with an MMC, aimed at interconnecting medium- and low-voltage DC grids.
[62]	I	MATLAB Simulink	Two Level Modulation	HBSM or FBSM	To regulate output voltage towards the set point, a finite control set approach predictive control is suggested in this article.
[63]	N-I	Unknown	Unknown	HBSM and FBSM	This article proposes a non-isolated hybrid DC-DC MMC architecture with reduced AC circulating currents. The delta-connected arms eliminate bulky AC filters and improve fault tolerance.
[64]	N-I	MATLAB Simulink	Square Wave	HBSM	The modulation technique, which has a high DC usage ratio, enables this design to surpass the problems of

			Phase Shift PWM		magnetic saturation and the extra bulk of the transformer and to keep the capacitor voltage with minimal output fluctuation successfully.
[65]	N-I	MATLAB Simulink	PSC-PWM	HBSM and middle cell	This study presents a non-isolated DC-DC MMC with the suggested middle cells.
[66]	I	MATLAB Simulink	Nearest Level Modulation (NLM)	HBSM	This article shows a DC-DC MMC with a high step ratio for MV and HV uses, and a set of control circuits and an energy regulator have been introduced.
[67]	I	MATLAB/ Simulink	PS-PWM	HBSM	The suggested converter can exchange tens of megawatts of electric power with the established HVDC grids.
[57]	N-I	Unknown	PS-PWM	HBSM	The suggested converter maintains MMC's flexibility, effortlessness, and scalability, making it suited for high step-up DC-DC power conversion in renewable energy production and HVDC grids.

2.3 The Importance of the DC-DC MMC Architectures

Conventional DC-DC converter topologies such as buck, boost, flyback, and full-bridge structures are commonly employed in low and medium voltage DC power transmission systems, offering satisfactory performance for specific applications. However, these topologies become technically inadequate for HVDC transmission systems. The primary limitations stem from the inability of semiconductor switching devices to withstand extremely high voltage stress, the increased insulation requirements, and the considerable efficiency losses caused by switching and core losses in isolated converter designs. Furthermore, conventional converters lack the modularity, scalability, and operational flexibility that HVDC systems inherently demand. More critically, they are not equipped with appropriate fault management mechanisms to detect and isolate DC-side faults, such as pole-to-pole or pole-to-ground short circuits, which pose serious threats to system reliability. Therefore, the development of advanced DC-DC converter topologies with high efficiency, modular architecture, and robust fault-handling capabilities has become essential for modern

HVDC applications. Due to these drawbacks of the traditional DC-DC converters for high-level voltage grids, DC-DC MMC technology is crucial for HVDC power transmission networks. In this regard, since it was first presented in the literature, MMC technology has attracted the curiosity of an extensive number of researchers due to its modularity and scalability, two of its most significant characteristics. MMC technology is also favored in HVDC power transmission networks and has been used in several applications. Many researchers have performed extensive studies on DC-DC MMC technology and have contributed their findings to the literature. In these investigations, some researchers provide alternative control methods for DC-DC MMC topologies that have already been presented, while others exhibit a unique DC-DC MMC structure. The common objective of these studies is to achieve power transfer with minimum losses and maximum efficiency. In the decades to come, it will be important to look into the following aspects of DC-DC MMC technology. The DC-DC MMC is capable of transferring a specific volume of power during operation in various working locations. However, depending on the procedure at each working point, varying the number of SMs in each arm is necessary.

Additionally, each working location has a distinct AC circulating current. This will have an impact on the converter's original price and effectiveness. Therefore, identifying the ideal functioning recognize is vital. Earlier investigations demonstrated that the power transmission capacity of the DC-DC MMC could be indefinitely increased. However, analysis and modeling observations indicate that the unbalanced capacitor voltages restrict this converter's ability to operate. Hence, a comprehensive study of this occurrence is required. Different DC-DC MMC topologies and superior control and modulation methods must be utilized in HVDC power transmission networks to achieve the highest possible efficiency of power transfer.

CHAPTER III
HVDC TECHNOLOGYHVDC TECHNOLOGY

3.1 Introduction

In recent decades, the demand for efficient, reliable, and environmentally sustainable methods of electrical power transmission has intensified. HVDC transmission technology has emerged as a viable solution to meet these demands, offering advantages over traditional AC transmission systems. Nowadays, high voltage-based power transmission needs to be provided due to a higher requirement for significant amounts of electric power. Electrical energy was solely delivered via an AC 3-phase network till 1960. Utilizing AC and an appropriate transformer that has been changing the voltage from one level to another is fairly straightforward. Additionally, huge generators can produce power using solely AC [7]. Many issues, such as alterations to voltage patterns, diminished power transmission, and the production of reactive power [7], arise in the current AC systems when transmitting electrical energy from the small group of existing facilities that produce electrical energy using traditional energy sources and from the facilities that produce electrical energy using renewable energy sources, most of which are located very far away from the load centers. High voltage is utilized rather than low voltage to reduce power losses during power transmission. Long-distance electrical power transmission reduces electrical losses while the current is low. According to this point of view, HVDC technology is essential to power systems due to its many benefits, which include efficient power transmission, asynchronous grid interconnections, adaptability, limited reactive power, limited short-circuit currents, decreased losses, and the ability to transmit power from offshore wind farms to onshore power plants. It also connects asynchronous AC systems and allows for the transmission of power from many places that require subterranean and underwater lines to the mainland. In addition, DC power transmission is taken into consideration and has been developed recently for underwater power transmission, longer-distance transmission of power, connecting two asynchronous AC networks featuring distinct frequencies, and improving power system durability as a parallel interconnection alongside an existing AC power system [7]. HVDC transmission involves the transmission of electrical power using direct current (DC) at high voltage levels. Unlike AC transmission, which periodically reverses direction, DC transmission maintains a constant polarity. HVDC systems typically consist of converter stations located at both ends of the transmission line, which convert AC to DC at the sending end and DC back to AC at the receiving end. The commercialization of mercury arc converters in the 1930s marked the beginning of the advancement of HVDC power transmission networks. The initial industrial HVDC power transmission network agreement was awarded in 1941. Berlin was to receive 60 MW of power via a 115-kilometer underground power cable. This framework was prepared for use in 1945. Nevertheless, the structure was disassembled and never put into use because of the conclusion of World War II. The first HVDC power transmission network in Gotland came into service in 1954. HVDC power transmission networks have been an advanced technology throughout the 1960s and have been crucial for power network connectivity and power transmission over long distances [68]. Table 3.1 provides a detailed comparison between AC and DC transmission systems based on several technical and economic parameters [69], [70]. This chapter provides an overview of HVDC transmission, including its principles, components, applications, advantages, and challenges.

Table 3. 1 Comparison between AC and DC power transmission systems

Criteria	AC Transmission	DC Transmission
Transmission Medium	Three-phase AC	Bipolar or monopolar DC
Voltage Conversion	Easily transformed using transformers	Requires power electronics (converters/inverters) for voltage level adjustment
Reactive Power	Requires compensation due to inductance and capacitance	No reactive power; purely active power transmission
Line Losses	Higher due to skin effect and reactive components	Lower, especially over long distances
Line Charging Current	Present, limiting efficiency for long-distance cables	Absent; more efficient for long submarine or underground cables
Cost (Short Distance)	More economical for distances < 500 km	Less economical due to high converter station costs
Cost (Long Distance)	Becomes less economical	More economical for distances > 500–800 km
System Control	Less flexible for fast and precise power flow control	Highly controllable using modern power electronics
Stability	Susceptible to synchronization and transient issues	More stable; asynchronous interconnections are possible

Right-of-Way Requirement	Larger due to multiple conductors and insulation spacing	Smaller footprint due to fewer conductors
Fault Detection and Isolation	Relatively straightforward with existing protection schemes	Complex due to lack of natural zero crossings
Environmental Impact (EM Fields)	Higher electromagnetic interference (EMI)	Lower EMI due to constant polarity
Application Examples	Conventional power grids, urban distribution	HVDC links, offshore wind farms, intercontinental transmission lines

3.2 Basic Structure of HVDC

Figure 3.1 shows the basic structure of an HVDC system. The HVDC power transmission systems are made up of three fundamental components which are a transmission line, which is made possible by overhead power lines or power cables; a converter in rectifier, which converts power from AC to DC; and a converter in inverter, which converts power from DC to AC. Converter stations are the primary components of an HVDC system and are located at both ends of the transmission line. Each converter station typically consists of several converter units. One station converts AC power into DC, and the other converts DC back into AC. Each converter station has a number of converter units, which are often made up of semiconductors like insulated-gate bipolar transistors (IGBTs) or thyristors. These devices convert AC power to DC power and the other way around. Converter transformers are used to interface the converter units with the AC system. They step up or step down the voltage levels as necessary. The DC transmission line is the physical connection between the two converter stations. It carries DC power from one station to the other. In addition, HVDC transmission lines are designed to carry high voltage DC power over long distances with minimal losses. They may consist of overhead lines, underground cables, or submarine cables, depending on the specific application. Filters and smoothing are often employed to smooth the DC voltage and current, reducing harmonics and improving the quality of the transmitted power. HVDC systems require sophisticated control and protection systems to ensure stable operation and to protect the equipment from faults. Control and protection systems monitor parameters such as voltage, current, and temperature and take corrective actions in case of abnormalities or faults. A grounding electrode is usually provided at each station to ensure proper grounding of the HVDC system.

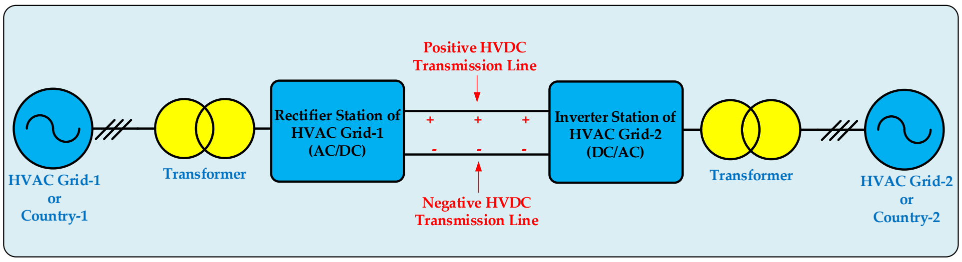

Figure 3. 1 Basic HVDC structure.

3.3 HVDC System Configurations

Numerous HVDC system architectures can be distinguished based on the purpose and placement of the conversion facilities [71]. Depending on the objective, these configurations can be taken into consideration for implementations based on CSC or VSC, either with or without transformer interconnection [72]. The several commonly encountered HVDC architectures and operation methods for HVDC power transmission have been shown in Figure 3.2 [73]. HVDC system frameworks can be based on MMC, VSC, or LCC in power systems. Power systems also utilize hybrid HVDC topologies, combining MMC and LCC structures. Figures 3.3 through 3.9 demonstrate frequently utilized MMC-based HVDC configurations [74], [75]. Hybrid HVDC structures using a combination of MMC and LCC HVDC topologies are shown in Figures 3.13 and 3.14. Two-terminal HDVC and multiterminal HVDC constructions are possible based on the number of converter stations. Only some multi-terminal HVDC facilities have been implemented to date, and the majority of HVDC systems presently in functioning have two separate terminals [76]. In essence, the four fundamental types of HVDC transmission systems-monopole, bipole, back-to-back, and multiterminal layouts-are employed depending on the distinctive characteristics.

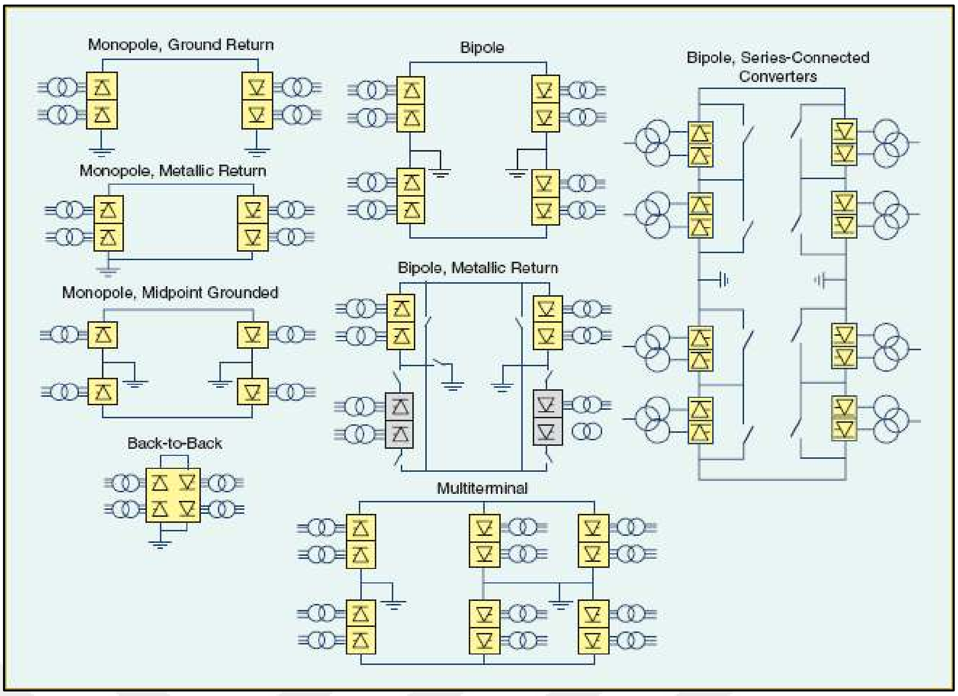

Figure 3. 2 Configurations of HVDC systems [73].

Monopolar systems are the most straightforward and affordable option considering moderately powerful transfers, given that they merely need one high voltage insulated power cable or power line conductor and two converter stations. In order to transport the current that is returned in underwater power cable intersections, these types of networks have been employed utilizing seawater electrodes and low-voltage electrode lines. Several regions do not support monopolar ground or seawater returning. The result might be observed in places featuring considerable ground resistance, power cable connections over water, or densely populated regions. Under these situations, the DC network employs a straightforward localized grounding mechanism for possible guidance alone and utilizes a metallic neutral or low-voltage power wire for the returning pathway [73].

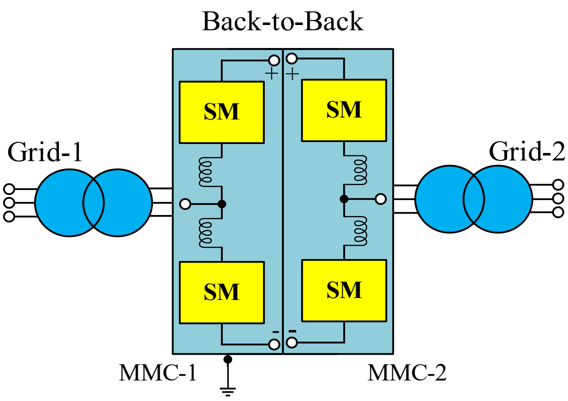

Figure 3. 3 MMC-based back-to-back HVDC structures [74], [75].

Since back-to-back arrangements use AC interconnections on both ends, they are the ideal architecture for linking asynchronous power grid networks. This HVDC design eliminates the requirement for power wires. As a result, there is no transmission loss, and the cost is decreased. Because of the extremely minimized losses, a higher effectiveness degree of voltage is therefore achieved [72], [73], [77], [78]. Electrical power is usually transmitted between unsynchronized AC grids using back-to-back HVDC converters. They are additionally employed within an interconnected power system to supply a designated power transfer. The two converter units of a back-to-back HVDC power station are situated at their respective location, and electrical power is not transmitted throughout great distances via a DC power link. Figure 3.3 demonstrates a simplified schematic of a back-to-back HVDC power system based on MMC. The frequencies of the two interconnected AC systems could be different or identical. An HVDC power transmission system that does not require a transmission line is called a back-to-back HVDC converter design. Nonetheless, certain further advantages may be obtained since the two ends of the design are situated in the same location. Commonly, the power electronic converters connected to either side of the link are situated inside a single building, described as a valve hall. Controlling settings can consequently be actively transmitted between the two converter structures with no risk of any information distortion or communication latency. Since there aren't any power losses during power transmission to take into account because the DC interconnection distance is zero, the typical demand for DC power transfer-maximizing transmission power in order to minimize power transfer losses is meaningless [78]. As seen in Figure 3.2 and Figure 3.3, the rectifier and inverter ends of the HVDC power transmission are directly connected by narrow bus bars in back-to-back HVDC converter architecture. A structure common to many application domains, including clean energy technological advances, is the VSC-based back-to-back HVDC converter, which regulates the transfer of electrical power. The importance of this structure stems from its capacity to independently adjust reactive and active powers [79]. Because of MMC technological innovation's reduced switching frequency, limited harmonics, a high degree of adaptability, and simplicity of redundancies construction [10], [80], [81], it is additionally employed in back-to-back HVDC converter designs.

There are two fundamental types of HVDC power grid configurations: bipolar and monopole. Asymmetrical and symmetrical arrangements of monopoles can also be differentiated more extensively. The asymmetrical setup is characterized by a single active conductor, where the return path for the current is established through the ground or a seawater medium. While this approach minimizes infrastructure expenses and simplifies implementation, it raises concerns related to long-term environmental effects, including electrochemical corrosion and unintended ground current dispersal. On the other hand, the symmetrical monopolar scheme incorporates two conductors carrying voltages of equal magnitude but reversed polarity, enabling a closed-loop current path that does not involve the earth. Although this structure requires higher insulation standards and material costs due to the dual-conductor design, it offers improved system balance and mitigates ecological impact. Furthermore, symmetric systems may continue to operate, albeit with reduced capacity, in the event of a conductor failure, thereby enhancing operational resilience. Ultimately, the choice between these two topologies hinges on technical, economic, and environmental priorities specific to the transmission application. Figure 3.2, Figure 3.5, and Figure 3.6 show the asymmetric monopolar mechanism. This HVDC arrangement consists of two ground electrodes, a single terminal line, and two conversion facilities. Based on a financial standpoint, this arrangement is the most favorable and least complicated. The ability to expand to a bipolar if needed is an additional superiority. The reality is that the current return passes across the ground; nevertheless, it frequently calls for authorization and may cause environmental issues. A different strategy that incorporates a smaller metallic return alongside the prior approach has been put out to address this problem. This second type is utilized to return the current, and as a result, no ground current can be generated since it is not needed for high voltage insulating. A setup technique like this is used in a lot of HVDC power transmission systems involving undersea interconnections [82]. This approach necessitates complex installation as well as advanced components for the grounded electrodes. Moreover, subterranean items, including interaction cables, oil pipelines, and magnetic instrument devices, face deterioration due to returning current. There isn't yet an achievable endeavor that shows how the earth's current is reversing. There have been efforts to use current reversing across saltwater to carry power over sea channels. A metallic conductor is inserted as the recirculating route to prevent the issues mentioned previously. Although the monopolar structure's use of two conductor cycles seems financially illogical, certain feasible HVDC facilities have used two wires in monopolar HVDC systems at an initial phase in the development of bipolar HVDC. This is because HVDC facilities may be funded and developed in sections [76].

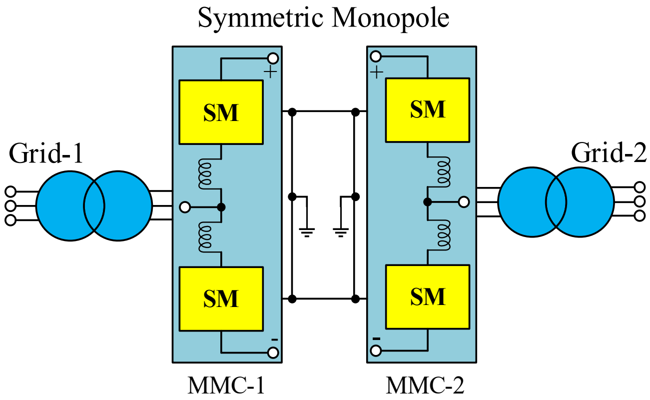

Figure 3. 4 MMC based symmetric monopole HVDC structures [74], [75].

Two power cables with opposing polarity interconnect the DC ends of the designs in a symmetrical arrangement. In VSC-HVDC infrastructure, the center position of capacitance needs to be grounded at the DC connection; otherwise, this arrangement often does not require ground at the DC end of the structure. The HVDC design's grounding method significantly influences the features of the DC short circuit trip. Because the AC end of the transformers in that construction is not subjected to DC voltage tension, it has the benefit of having a straightforward layout. Furthermore, the AC-side currents do not supply the DC side during DC-side pole-to-ground failures with this configuration. It is inexpensive and has little power degradation in transmission. On the other hand, this architecture forms the foundation of most VSC-based HVDC power transmission networks. Every terminal has a single converter design; however, the two units are interconnected together by two power DC cables, both for each terminal's positive and negative polarization. This allows the cables to be exposed solely to halfway of the DC voltages, which transmits half of the power. As demonstrated in Figure 3.4, the design's central region is typically grounded [75]. Two high voltage wires with uniformly dispersed voltages to the earth are used in this transmission architecture.

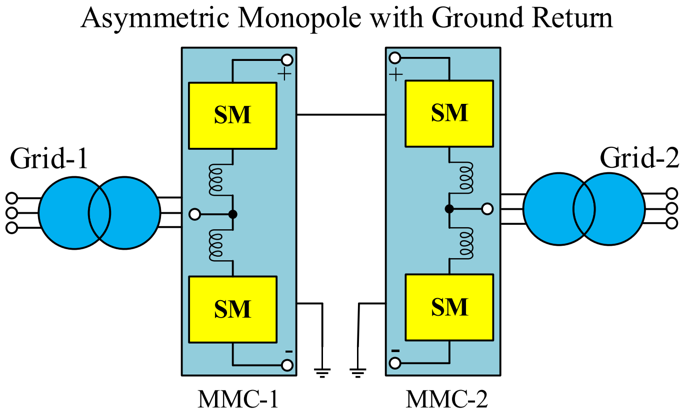

Figure 3. 5 MMC-based asymmetric monopole with ground return HVDC structures [74], [75].

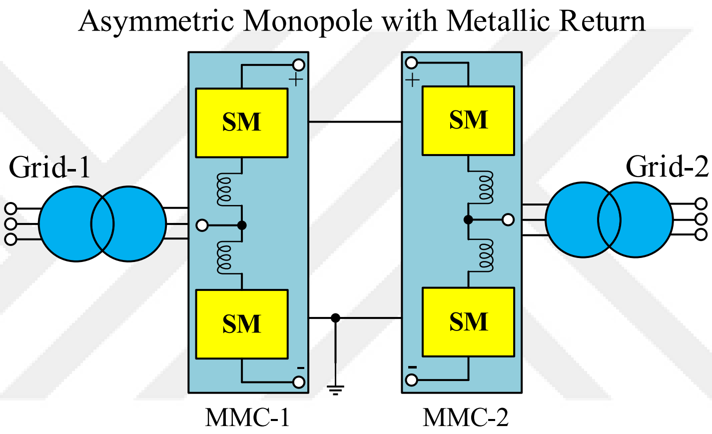

Figure 3. 6 MMC-based asymmetric monopole with metallic return HVDC structures [74], [75].

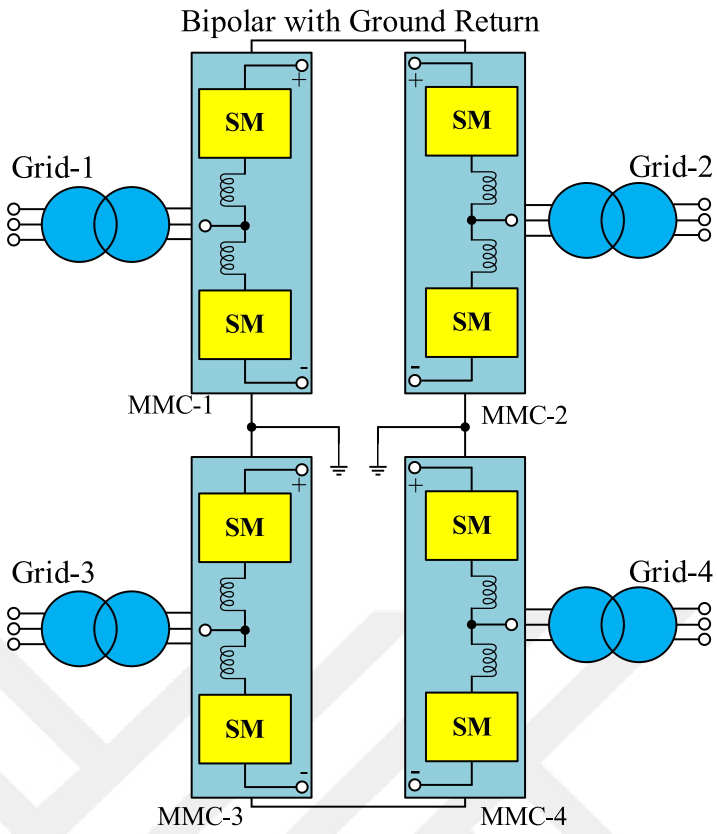

Figure 3. 7 MMC-based bipolar with ground return HVDC structure [74], [75].

The bipolar HVDC scheme comprises two independently operational asymmetric monopole structures. Bipolar HVDC structure offers more reliability and adaptability when compared to monopole topologies [83]. Bipolar layouts, similar to monopole architecture, are made up of conduction circuits that have either a metallic or ground return. In bipolar HVDC power systems, each station includes two converters to obtain maximum nominal power and lower aberrations for systems utilizing conventional current source conversions. In essence, bipolar HVDC structures are made up of two asymmetrical monopole HVDC structures that are coupled in serial and have polarities that are reversed yet have identical DC magnitudes. The benefit of this is that the second pole can continue to function as a monopole HVDC arrangement even in the event that one pole breaks [84]. The bipolar HVDC structure, similar to the monopolar HVDC structure, can be constructed with VSC, CSC, and MMC technologies. Figure 3.7 demonstrates where the inverter and rectifier's neutral terminals connect to the grounding electrode and the earth or seawater, respectively. A bipolar HVDC system with connected endpoints along with both neutral locations resembles dual monopolar HVDC systems with the backflow pathway being either underwater or on the ground.

Due to the opposing orientations of each of the return currents, the true current for the symmetrical operating is rather tiny. 50% of the power generated can continue to be delivered by a second pole utilizing the ground or saltwater as the backflow route, even if a single pole stops operating due to deficiencies. As a result, the above arrangement significantly improves DC transmission efficiency and stability. The bipolar HVDC structure in the neutral wire form is demonstrated in Figure 3.8. Two stations of HVDC converter neutral terminals that are simultaneously grounding can be represented by a second wire. 50% of the electrical current can travel via the ground or saltwater whenever a monopolar breakdown arises, allowing the neutral wire's intended capability to be decreased. In bipolar HVDC functioning, the neutral terminal of the current's electromagnetic influence can be minimized by a reduced unbalance in the electrical current that passes via the neutral connection [76].

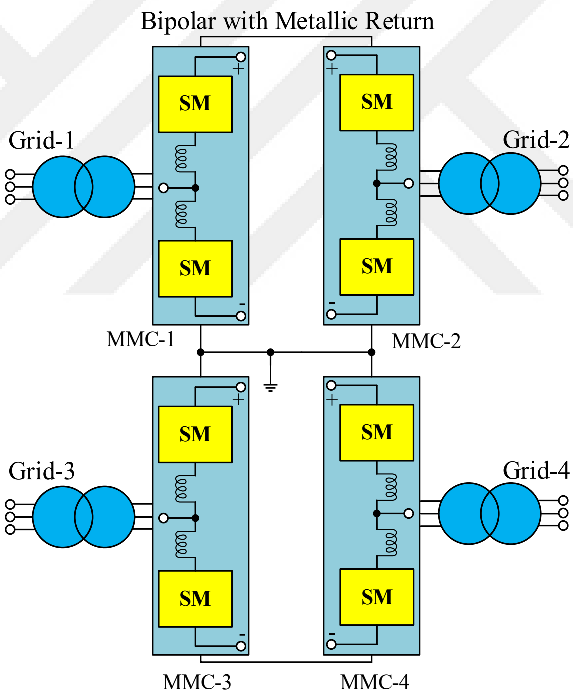

Figure 3. 8 MMC based bipolar with metallic return HVDC structure [74], [75].

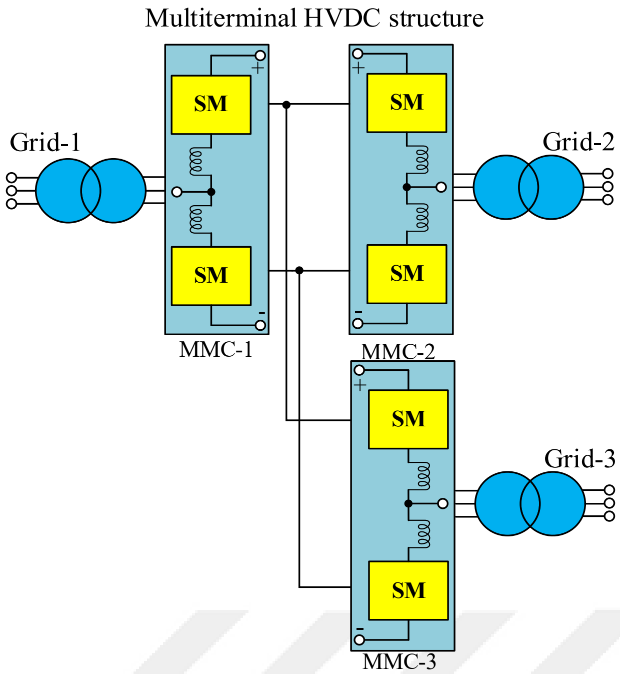

Figure 3. 9 MMC based multiterminal HVDC structure [74], [75].

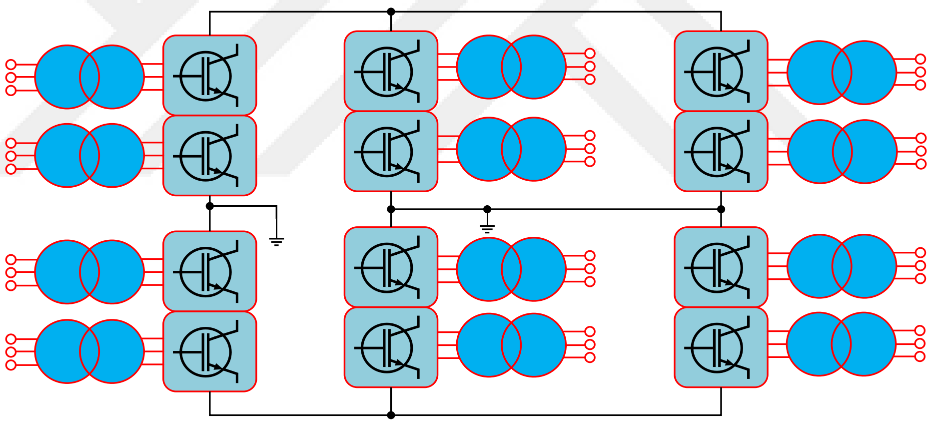

Figure 3. 10 VSC-based multiterminal HVDC structure.

In circumstances where there are over three converter stations, the HVDC facilities are commonly referred to by the expression multiterminal HVDCs. Depending on the power converters' connecting arrangement, the multiterminal HVDC infrastructure can be classified as parallel or serial [76]. For the transmission of energy generated from renewable sources from extensive and faraway locations, such as tide-generated power, massive wind farms off the coast, or sand photovoltaic power, multiterminal HVDC is a desirable choice [85], [86]. It is possible to create multiterminal HVDC structures using both VSC or LCC and MMC technologies. Figure 3.9 demonstrates an HVDC structure based on MMC technology, whereas Figure 3.10 illustrates an

HVDC structure based on VSC technology. Integrated interconnections between regional power grids and different forms of renewable energy are made easier by multiterminal HVDC power systems, which boost supply effectiveness and dependability. MMC technology offers numerous benefits over VSC technological devices, including reduced voltage limits, superior efficacy, improved power appropriateness for unrefined operations, inherent fault acceptance, and fault-avoiding capabilities to maximize the effectiveness of inability interruption in MMC-based HVDC power systems [87]. Because it can provide interconnection between three or more faraway power networks to improve consistency and dependability as well as reduce loss of electricity throughout planned maintenance, multilevel HVDC power systems have drawn a lot of research interest currently [72], [88]–[90].

LCC, VSC, and MMC technologies can be employed independently in HVDC power system topologies, as well as in hybrid HVDC systems, which combine various iterations of these systems. It is straightforward to apply various iterations of these three technologies in rectifier and inverter units for both two- and multi-station HVDC power networks.

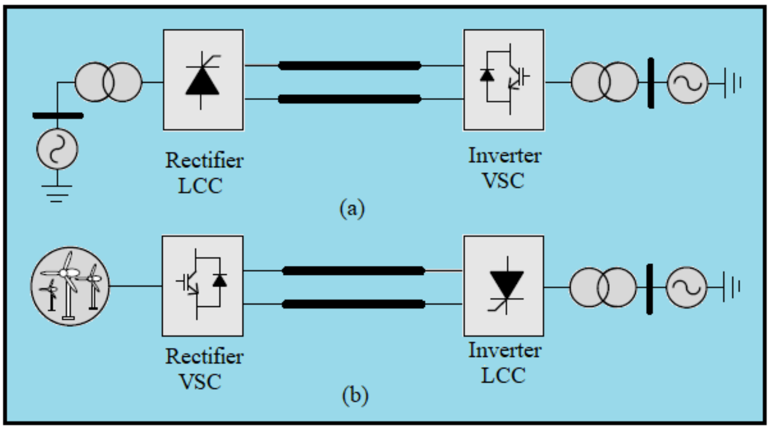

Figure 3. 11 Hybrid HVDC power system: (a) Version 1 and (b) Version 2 [91].

Since the late 20th century, there has been an attraction to the arrangement of LCC HVDC and VSC HVDC technologies [91]. Figures 3.11(a) and 3.11(b) demonstrate two distinct configurations of a two-station HVDC power system with a hybrid construction. Two variations of a multi-station HVDC power system with a hybrid construction are illustrated in Figures 3.12(a) and 3.12(b). IGBT has evolved into the primary component of voltage source power converters because of the fast improvement of power electronic technology. An LCC HVDC alongside a two-level, three-level, and multilevel VSC can comprise a hybrid HVDC power structure. Nevertheless, given the demands of contemporary operations, the hybrid LCC-two level-VSC as well as LCC-three level-VSC schemes are less practicable than the integrated system of LCC HVDC and modular VSC HVDC because of its reduced capacity to handle high power and voltage specifications [91], [92].

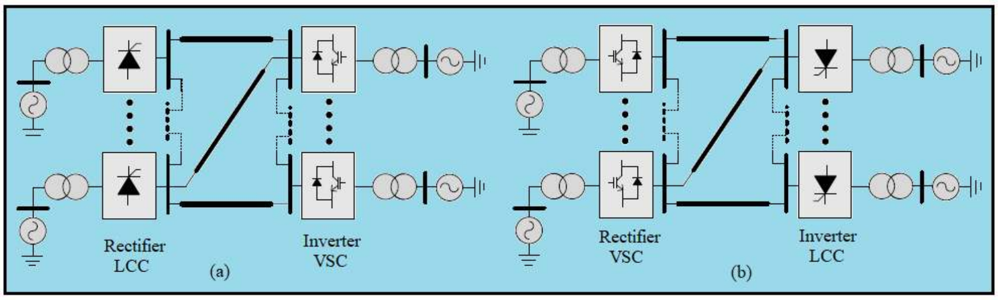

Figure 3. 12 Hybrid multiterminal HVDC power system: (a) Version 1 and (b) Version 2 [91].

Because traditional and customizable VSCs have comparable exterior properties, studying hybrid HVDC power systems founded on traditional VSCs often opens the door to combining LCC HVDC systems and modular VSCs HVDC systems [91]. The MMC technology is the most appropriate alternative to hybrid HVDC power designs since it is the most advanced VSC configuration; most existing hybrid HVDC developments implement the LCC-MMC combination [91], [93], [94]. The MMC portion of the hybrid LCC-MMC HVDC power configuration can employ various SM structures to fulfill varied demands because of the various SMs [91]. Figure 3.13 demonstrates the various hybrid HVDC power structure designs that are currently possible. Figure 3.13(a) illustrates hybrid monopole structure development, including a 12-pulse LCC-based HVDC power system and an MMC-based HVDC power system. Additionally, the bipole hybrid HVDC power network can be configured in four different ways. As indicated by Figure 3.13(b), a pair of 12-pulse LCC structures and an MMC configuration can be implemented; nevertheless, in the event two MMC structures have been employed, the multilevel HVDC system can operate in monopole mode (Figure 3.13(d)). Additionally, each converter station has the option to use hybrid architecture, which is demonstrated by Figures 3.13(c) and 3.13(e), where a 12-pulse LCC structure and an MMC configuration are positioned at both the negative and positive poles, correspondingly.

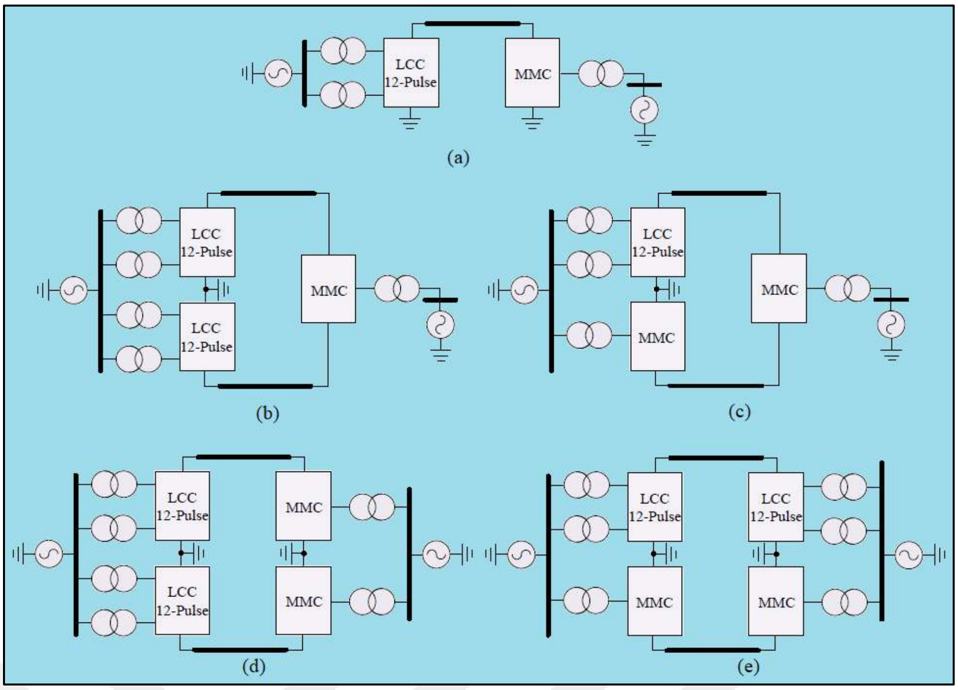

Figure 3. 13 Possible arrangements of hybrid HVDC systems: (a) Monopole arrangement, (b) Bipole arrangement 1, (c) Bipole arrangement 2, (d) Bipole arrangement 3, and (e) Bipole arrangement 4 [91].

Additional HVDC power converters can be positioned inside a single facility, as illustrated in Figure 3.14, in hybrid HVDC power transmission networks. The typical arrangement, which is illustrated in Figure 3.14(a), involves a pair of 12-pulse LCC-based HVDC power converter structures and MMC-based HVDC power arrangements, which are connected in serial mode and arranged at every pole's separate unit. Figures 3.14(b), 3.14(c), and 3.14(d) illustrate the manner in which, depending on the usual established one MMC-based HVDC or a 12-pulse LCC-based HVDC in every pole might be substituted with the additional one to form distinct architectures. Furthermore, the capability concern with MMC technology can be remedied by connecting HVDC power converters in parallel, also referred to as a collection of MMC architectures. Smoothing systems can be set up in these arrangements to restrict current flow during breakdown situations [95]. Akin to LCC and MMC-based hybrid HVDC power systems, the SM configurations of mixed multiterminal DC power plants depend on LCC and MMC technologies. The mixed HVDC power structure can be expanded to the widely utilized hybrid three-terminal HVDC power framework, illustrated in Figure 3.15(a), by adding more MMC systems to the inverter terminal. Furthermore, as demonstrated in Figures 3.15(b) and 3.15(c), several LCC-based and

MMC-based HVDC power networks at the rectifier or inverter ends of HVDC power networks can create complicated hybrid multiterminal DC power networks or straightforward DC power networks. As seen in Figure 3.15(d), LCC technology can additionally function as the sending end for substantial power transmission across extended distances to a DC power network made up of MMC-based power networks.

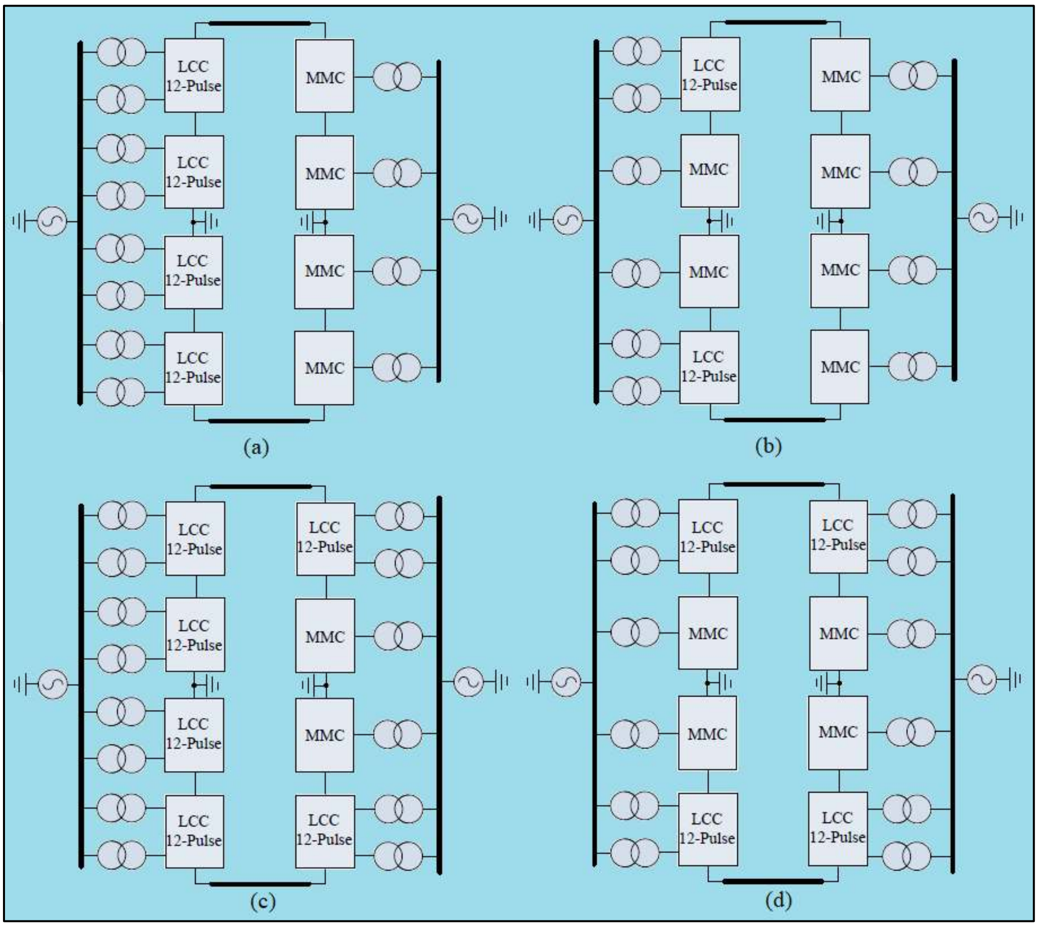

Figure 3. 14 Possible arrangements of hybrid Ultra HVDC systems: (a) Arrangement 1, (b) Arrangement 2, (c) Arrangement 3, and (d) Arrangement 4 [91].

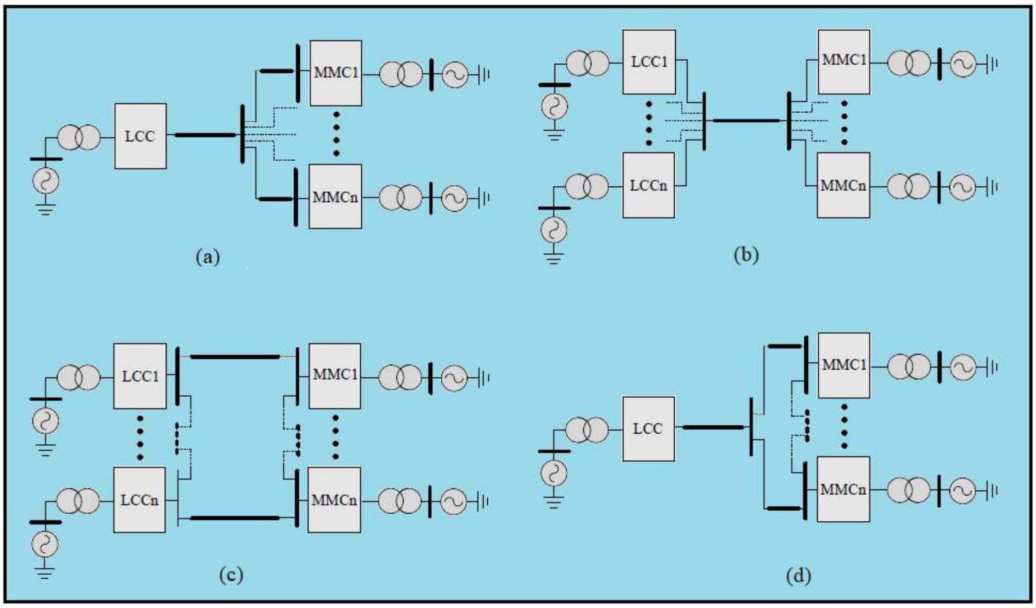

Figure 3. 15 Possible combinations of hybrid multiterminal HVDC Power structures: (a) Arrangement 1, (b) Arrangement 2, (c) Arrangement 3, and (d) Arrangement 4 [91].

Considering the three-terminal hybrid HVDC power structure as an illustration, six fundamental configurations of a typical hybrid multiterminal hyper HVDC power network are demonstrated in Figure 3.16. LCC and MMC-based bipole functioning configuration, LCC and MMC-based monopole functioning configuration (ground return), LCC and MMC based monopole functioning configuration (metallic return), LCC and MMC-based two-terminal functioning configuration, LCC and MMC-based bipole-monopole hybrid functioning configuration, and LCC and MMC based single valve group functioning configuration HVDC power concepts are depicted in Figures 3.16(a), 3.16(b), 3.16(c), 3.16(d), 3.16(e), and 3.16(f), respectively. The adaptability of bipole performance allows the three-terminal HVDC hybrid power network to transition towards a single execution. The power system can effortlessly transition towards a dual station operating option whenever a malfunction occurs at a single receiving station. Furthermore, in a hybrid multiterminal DC power structure, provided an individual valve collection or one terminal of the receiving endpoint has been isolated, the bipole-monopole hybrid configuration and the individual valve collection configuration can be used. Because they have many working forms of transportation, hybrid multiterminal DC power structures can often handle a variety of scenarios, including malfunctions and legitimate requirements [91], [96].

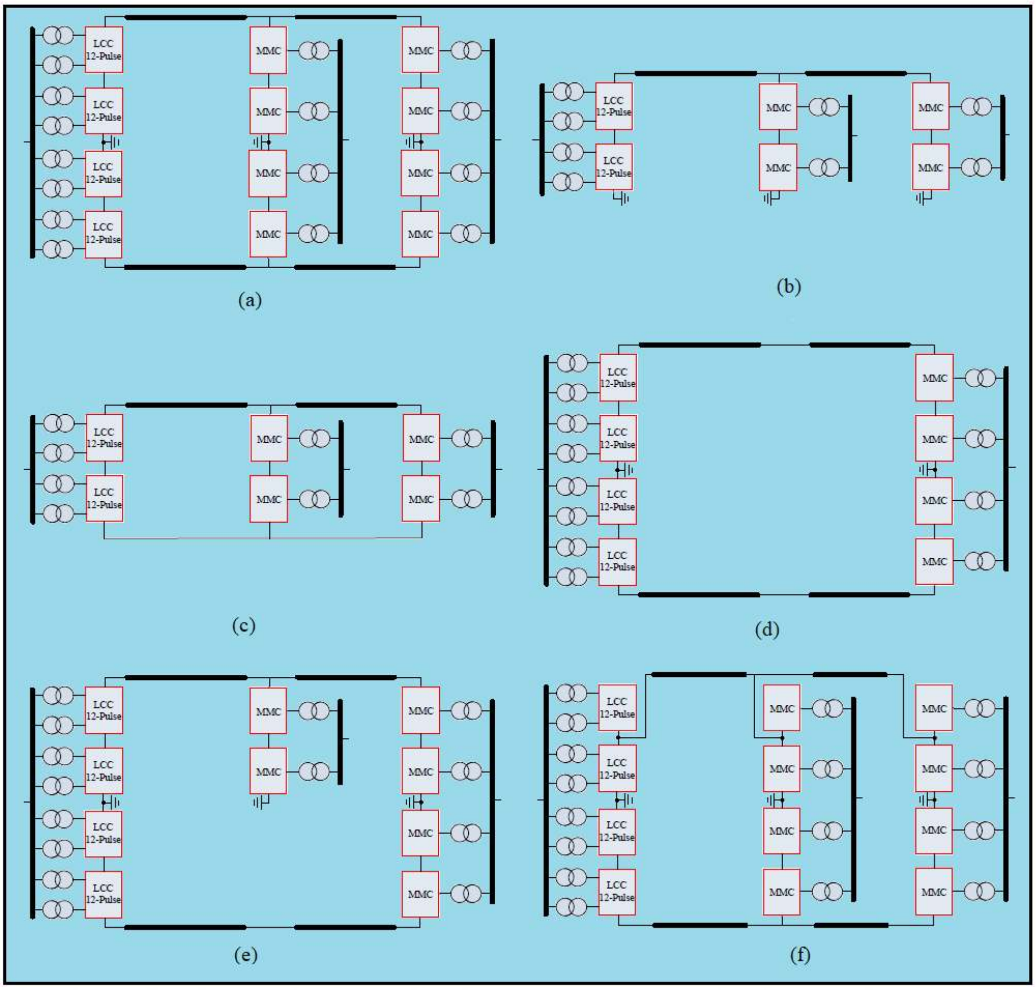

Figure 3. 16 Operational approaches of the three-terminal hybrid HVDC power network: (a) Bipole operational approach, (b) Monopole operational approach (ground returning), (c) Monopole operational approach (metallic returning), (d) Two-station operational approach, (e) Bipole-monopole hybrid operational approach, and (f) Singular valves groups operational approach [91].

3.4 HVDC Converter Technologies

HVDC power systems are divided into two classes: main circuit components and auxiliary circuit components. While the main circuit components provide power transfer between HVDC power networks, auxiliary circuit components are circuit control and protection systems that ensure this power transfer occurs safely and efficiently. Depending on which way the power is flowing, the converter systems at the basis of the HVDC power transmission system are called rectifiers or inverters. HVDC technology is an AC-DC-AC power electronics conversion circuit considering an architectural perspective. The majority of power converters utilized in HVDC installations are made up of a thyristor, a half-controlled mechanism known as a LCC or LCC-HVDC, which requires an AC power supply to facilitate modulation. VSC-HVDC has been around for several years and is becoming more and more popular since it can achieve synchronization by using the device's capacity to switch off. In order to achieve enhanced control qualities and faster reactions, the VSC-HVDC power transfer structure converter uses fully-controlled self-commutated power electronic devices like integrated gate commutated thyristor (IGCT), gate-turn-off thyristor (GTO), and insulated gate bipolar transistor (IGBT). Power electronic equipment is largely employed in power systems due to the swift growth and implementation of HDVC power systems [76]. Although HVDC power systems are frequently categorized into two distinct categories, VSC-HVDC and LCC-HVDC [97]–[99], MCC-based HVDC power systems have recently become more popular in power systems due to the impact of remarkable advancements in power electronics. The fundamentals of three technological advances, along with their benefits and limitations.

3.4.1 Line-Commutated Converter (LCC) or Current Source Converter (CSC)

The great features of HVDC technology have led to its substantial position in power networks in recent decades. Most modern power systems are designed to be DC-based in this perspective. Nevertheless, converting conventional AC power systems to DC power systems is crucial. Before the mercury arc rectifying device was invented in 1902, the sole way to convert electrical power from AC to DC power was to utilize motor and generator combinations. Beginning alongside the semiconductor diode and triode, the mercury arc rectifying device is a member of the vacuum tube category of electronics systems. The electrical power capacity was raised by replacing the absence of a vacuum with conduction gas, and the mercury arc switch and thyratron were created. By utilizing fluid mercury's repairing ability, the mercury arc valve's architecture was significantly less complicated, and its lifespan was extended than that of motor and generator combinations. However, the gate polarity of the valve can't be switched off until it is activated. The power supply ends after the electrical grid voltage is reversed during the second phase of the AC period. Line-Commutation is the term used to describe this specific method [100]. The HVDC system based on a Line Commutation converter (LCC-HVDC) is illustrated in Figure 3.17 with its one-line schematics [101].

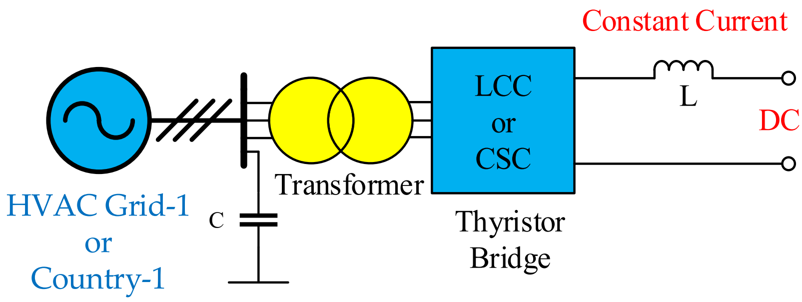

Figure 3. 17 LCC-HVDC one-line schematic [101].

Despite the fact that semiconductor-based power electronic systems for HVDC systems were initially developed in the 1930s, their initial commercialized implementation was not achieved till 1954 [102]. The LCC or CSC technology was used to construct The Gotland HVDC grid, the initial commercialized HVDC power transmission that utilized mercury-arc valve technologies [103]. The latter interconnects Sweden's Gotland Island to Sweden by an undersea cable that spans 98 km, has an operating voltage of 100 kV, and a peak power capacity of 20 MW [104], [105]. Since the thyristor semiconductor first appeared in 1950, novel HVDC technologies that solely use solid-state components have been suggested [82]. A significant number of mercury arc switches had been utilized in HVDC power architectures prior to the 1960s solid-state electronic technologies innovation. In addition to semiconductor diodes, triodes, and thyratrons, the electricity sector experts also produced silicon-based semiconductor rectifiers, power semiconductor diodes, and thyratrons. The silicon-based rectifier technology sometimes referred to as thyristor, superseded mercury arc switches because of its greater dependability, less expensive upkeep, and ecological hazards [104]. The invention of semiconductor thyristor-based HVDC power systems dates back to the 1970s. Thyristor gates are reminiscent of mercury arc gates in that they may be switched on at the gate mechanism yet not shut. The semiconductor thyristor-based HVDC power systems require a separate controlling component to switch on the gate since it operates through mainline commutation [100]. The Eel River project, implemented in Canada in 1972, was the initial full HVDC network that utilized thyristor actuators [100]. This technique is called LCC because the converter design's modulation procedure is driven by the AC network voltage to which the converter design is attached, and the substantial inductance on the DC end maintains a slight fluctuation in the DC. Thyristor-based LCC or CSC innovation prevailed in the HVDC market because of its benefits in terms of power ratings, dependability, and compactness. It is currently regarded as an established advancement in HVDC power systems and typical tools for DC power converter facilities [82], [103]. Since then, thyristor-based LCC or CSC technology has been widely used and developed for HVDC power systems. Figure 3.18 demonstrates the fundamental two-terminal LCC-HVDC power transmission system.

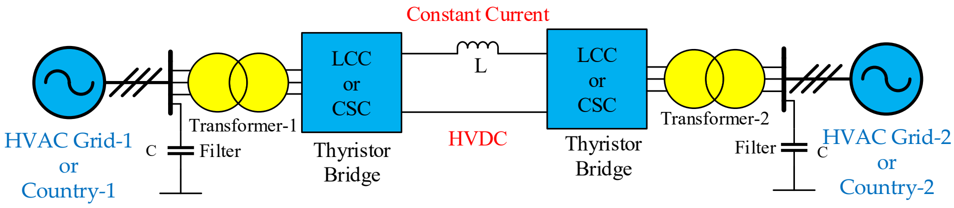

Figure 3. 18 LCC or CSC-based HVDC transmission system.

The fundamental functioning of this kind of converter technology is comparable to that of a three-phase bridge rectifying device. It starts with an equilibrium three-phase voltage at the input side and can change the positive or negative semi-cycle of every phase to produce uninterrupted negative or positive signals at the final stage, depending on whenever the thyristors are activated, respectively [106]. Because thyristors in LCC-based HVDC systems have HV and high current ratings, this earliest established innovation continues to represent the greatest effective option for large amounts of transmission of power. Nevertheless, there are certain drawbacks to LCC-based HVDC configurations, including restricted DC current flow and diminished power reverse processing capacity; potential conversion errors primarily resulting in high AC voltage decrease; reactive power compensation needed since there is reactive power consumption within the AC framework; and extra filtering instrument purchases due to typical and unusual harmonic distortion in the AC station and DC side produced by the naturally occurring transformation procedure [91]. A typical LCC-HVDC structure consists of components such as converters (inverter and rectifier), DC and AC filters, DC smoothing reactor, AC transformers, AC reactive support, electrodes, DC lines, and AC circuit breakers. Converter stations are primarily used to execute conversion operations from DC to AC on the component end of the inverter and from AC to DC on the rectifying end. The components within these converters are coupled in a six- or twelve-pulse pattern and comprise an actuator bridge that functions similarly to three-phase rectification bridges. The converter design produces harmonic voltages and currents across the AC and DC ends of the converter design. Such harmonics can conflict issues in the exchange of information systems and lead to capacitance overheating and disturbance around electric power plants. AC and DC filters are thereby utilized in both AC and DC stations. Having all of the converter end's poles connected in sequence, the DC smoothing reactor's large inductance, roughly 1 Henry, makes it up. The primary purposes of DC smoothing reactors include lowering harmonic currents and voltages in continuously flowing lines, preventing inverter conversion mistakes, preventing inconsistent current waveforms in illumination loads, and restricting the maximum current in the rectifying device phase when creating an alternative route in the DC line. Particularly designed for HVDC projects, AC transformers experience an equilibrium DC bias on the secondary windings. Reactive power usage may increase throughout brief periods of time. Since a connection and the AC structure have demands, compensating elements near conversion devices are necessary for strengthening AC networks. These compensating elements are capacitors attached to the creation; synchronized capacitors or static var compensating elements can be used as a portion of the reactive supply.

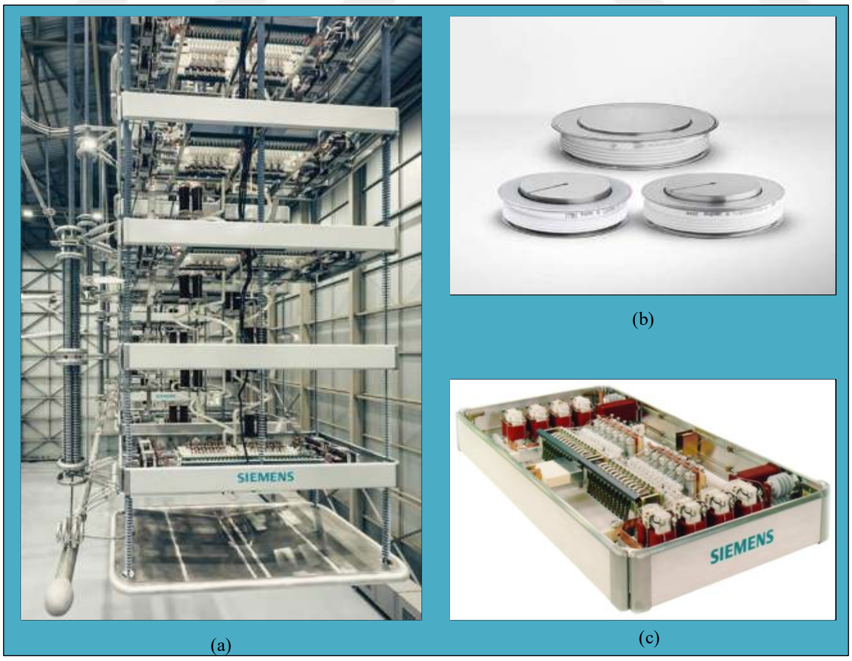

Figure 3. 19 LCC-based HVDC facility produced by Siemens company: (a) major facility, (b) high-power thyristor devices (4-inch, 5-inch, and 6-inch), and (c) thyristor structure [91], [107].

Additionally, the capacitors are connected to the current filtering devices, adding to the reactive power. Ground is intended to be used as a neutral conductor for a brief duration in the majority of DC circuits. Because of the aforementioned, in order to reduce stress variations and current densities, a ground interconnection needs a conducting material featuring a substantial surface area. This conductor, referred to by the term electrodes, is confined to the current flowing by way of the ground. DC and AC power lines are nearly identical, with the exception of the quantity of wires and construction area needed. DC power lines can be underground or utilized as atmospheric wires. An automated breaker is employed at the power supply station to fix problems with the transformers. These breakers are not utilized to eliminate DC failures because the converter design's switching operation and management strategy are capable of handling this type of malfunction management [82], [106]

3.4.2 Voltage Source Converter (VSC)

Many conventional HVDC power systems keep employing thyristor-based LCC technology, which first appeared in power systems. As a result of LCC's drawbacks, including harmonic distortions, switching breakdowns, an unwillingness to regulate reactive power, restricted DC current flow, and diminished power reverse processing capacity [74], [91], power systems researchers have come upon VSC technology, which offers several benefits over conventional LCC technologies, as a consequence of their researches for revolutionary power converter technologies. The core components of VSC-HVDC power transmission are distinct from what is found in typical LCC-HVDC power transmission due to the semiconductor-based power electronic components implemented. Conventional HVDC power switch thyristors can potentially be customized to activate; nonetheless, they cannot be switched off provided an additional system causes the current to decrease under the amount that holds electrical current. Consequently, to accomplish commutation, classical HVDC has to depend on a separate power source. The thyristor power switch is now the biggest power electronic component used to transfer electrical energy. Completely controllable semiconductor-based power electronic components that may be switched on or off via initiating pulse include Injection-Enhanced Gate Transistors (IEGT), IGBTs, GTOs, and MOSFETs. These power commutation components are a class of continually growing semiconductor-based power electronic components [76]. The IGBT, which was developed in the 1980s, was made possible by metal-oxide-semiconductor technological devices, which had previously been in usage since the

1970s [72]. The IGCT, which was initially described in 1999, represents a further advancement in thyristor technology [108]. HVDC power system development has benefited greatly from the creation of completely programmable semiconductor-based power switching devices, particularly IGBT. A novel converter architecture called the Self-Commuted Converter or VSC has been used for HVDC applications because of its turn-on/turn-off functionalities [109]. The converter design, commonly referred to as the VSC-HVDC power system, is regarded as the third version of HVDC power systems because of its completely controlled semiconductor-based power electronics [100]. Figure 3.20 illustrates the single-line diagram of the VSC-based HVDC system. In this configuration, the DC voltage on the DC side remains constant, while the AC current is governed by the interaction between the AC network voltage and the inverter's output voltage.

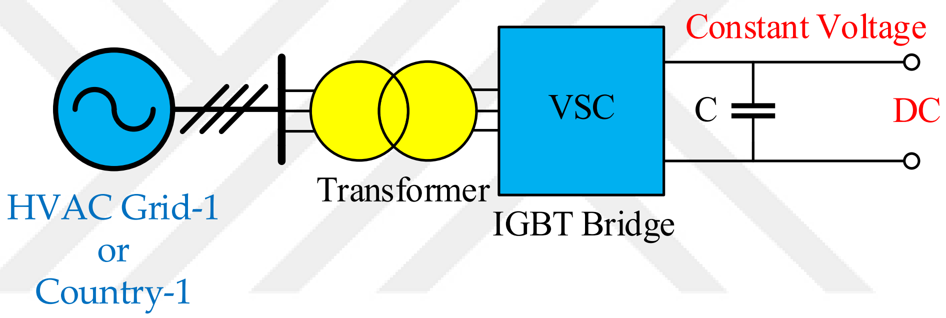

Figure 3. 20 VSC-HVDC one-line schematic [101].

The growth of VSC-based HVDC architectures and the voltages of the semiconductor component can withstand are directly correlated alongside the electrical power output provided for these converter configurations. Figure 3.21 demonstrates a simple setup of these VSC-based HVDC power interconnections with two terminals. The electrical power delivery is controlled in equilibrium by altering the direction of the mean current applied to the DC power line. The initial VSC-HVDC project, known as HVDC Light, was the HVDC Hellsjön-Grängesberg (Sweden) by ABB company, which established the achievement of these converter systems [110]–[112]. It was constructed at the start of 1997 and is a PWM-controlled technology [113], [114].

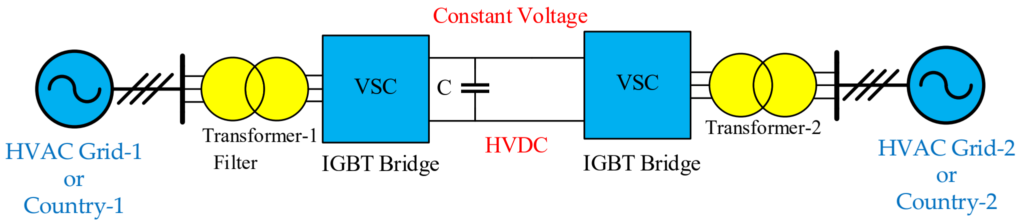

Figure 3. 21 VSC-based HVDC power system structure.

In contrast, VSC-based HVDC systems provide several advantages over LCC-based HVDC systems, which are listed below [71], [73], [84], [91], [97], [100], [115]–[118]:

- IGBT, GTO, and IGCT are completely regulated semiconductor-based power-switching devices that do not experience commuting failures in the event of an AC interruption in the grids.
- Operating the VSC-HVDC structure at the unity power ratio achieves reduced harmonics and reduced filter capacity.
- The switching method ceases to require transformers, which lowers costs and increases dependability.
- Multiterminal HVDC power systems are becoming increasingly common in the power infrastructure of the foreseeable future, and VSC technology facilitates their more straightforward implementation.
- It is achievable to independently and bidirectionally regulate reactive and active power parameters, which results in decoupling P-Q regulation.
- HVDC power systems with a VSC foundation prevent synchronization breakdowns brought on by interruptions.
- Possession of PWM techniques functionality. Even though the volume of the filtering system is reduced, this contributes to a rapid reaction to change and higher-quality wave shapes, resulting in lower prices.
- VSC-based HVDC technology also allows for the establishment of multiterminal interconnections and weak and inactive AC power network services.
- Black starting the offshore power network is possible using a VSC-HVDC power infrastructure.
- Ability to use techniques with a regulated current for protection regarding high AC short circuit defect electrical current.

- It can be possible to integrate inactive power systems with VSC-HVDC power systems.
- Capability to interconnect components on the side of the DC in pairs. Multiterminal VSC-HVDC power systems have become possible as a consequence.
- Less equipment is needed for VSC-based HVDC power systems, which significantly lowers the total cost. This phenomenon greatly increases the VSC-HVDC power system's controllability and scalability.
- Using ordinary transformers with VSC-HVDC power systems with a reduced unit dimension is possible.

VSC technology performs power conversion and transmission in HVDC power systems using fundamental components, including converters, DC capacitors, AC inductors, AC transformers, and AC filters. The functions of these components can be clarified as follows: Within the HVDC connection, the conversion device serves as one of the basics. Their key responsibilities include limiting shortcut electrical currents via switching components and controlling both reactive as well as active power. The electrical impedance of switching equipment' semiconductors is defined by the combination of transformers and reactive conversion impedance. The capacitors in the VSC architecture maintain a stable voltage on the DC system. As an alternative to placing the capacitance inside every pole, it is split and dispersed across every single switching cell. Every time the semiconductor device is engaged, its capacitance fluctuates between charge and discharge based on the amount of current flowing. The VSC architecture requires the AC inductor to regulate the supply currents properly, perform like a low-pass filtering system, and restrict the degree of rising in electrical current observed through the IGBT power switches. The secondary voltage level is able to be configured utilizing any one transformer arrangement. An AC filter is required when the generated voltage is a sinusoidal waveform with an intermediate harmonic component. The criteria for filtering effectiveness, such as allowable voltage fluctuation and the amount of harmonics grid impedance at the linking point, primarily determine the necessity of such filters [82], [106]. Figure 3.22 shows an HVDC power facility with VSC technology manufactured by ABB company.

Figure 3. 22 HVDC power facility with VSC technology manufactured by ABB company [91], [119].

3.4.3 MMC

VSC and LCC technologies typically constitute the focus of the converter systems found at the HVDC power technology's connecting locations [80]. However, due to the latest developments in semiconductor-based power electronics technological advances, multilevel converter technologies are scheduled to predominantly be employed in HVDC power technologies. Higher voltages and greater capacities are necessary for substantial power transferring in HVDC power networks. Generally, in conventional HVDC power systems, there are several barriers to widespread and efficient usage of the sequential interconnection method of powering instruments to increase productivity, including voltage distribution, the number of harmonics, and power converters' component tension. Numerous innovative multilevel architectures for HVDC power networks or modular combining methods have been developed by power system researchers. MMC technology, as a multilevel configuration, has garnered significant attention in the HVDC industry due to its favorable features, such as high power quality, improved efficiency, reduced switching frequency, modularity, ease of scalability, transformerless operation, fault tolerance, and the use of standardized, readily available components within a simplified control structure [10], [17], [74], [80], [120]–[124]. MMC technology has recently become the preferred converter technology in HVDC power systems due to its outstanding features mentioned above. Figure 3.23 shows the architecture of traditional MMC technology. It continues its presence in power systems together with traditional LCC and its upgraded version of VSC technology. MMC technology is a converter design that solves the disadvantages of VSC technology to a great extent and is a higher version of VSC technology. In other words, MMC technology is the fourth version of VSC technological advances and is a multilevel converter architecture [125]. While MMC technology has gained a significant presence in existing AC power systems, it has also gained a substantial footprint in modern HVDC power systems.

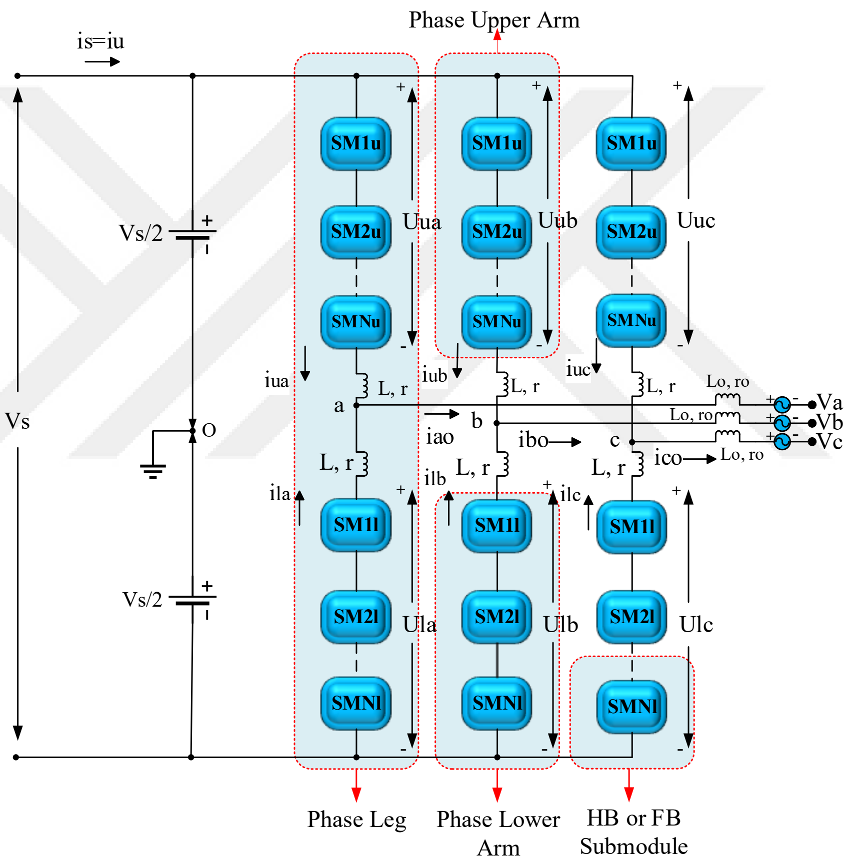

Figure 3. 23 The architecture of traditional MMC technology.

Figure 3.23 depicts the traditional MMC architecture that was first proposed in a German patent by Prof. Marquardt in 2001 [16]. The mentioned invention shows the DC to three-phase converter construction, which consists of a series of linked SMs, as well as the inductances inside each arm and the half-bridge (HB) and full-bridge (FB) SMs. The standard MMC structure offers the flexibility to operate as an inverter (DC-AC) or as a rectifier (AC-DC) for an extensive range of purposes. As shown in Figure

3.23, each phase in the conventional MMC structure consists of two arms: the upper arm and the lower arm. Every single upper arm and lower arm is composed of an arm inductor (L, r) and HB or FB SMs linked in serial sequence. A phase inductor (L_o, r_o) links the three-phase AC terminals $(V_a, V_b$ and $V_c)$ of the circuit to a branch leg that starts at each phase's midpoints (a, b, and c). Stated differently, the DC ends of the layout are connected between the top and lower arms of the phases, while the AC terminal is connected to the middle of each phase. Together with the proper DC and AC design voltages, each arm produces controlled voltages at specific endpoints that result in the necessary AC and DC currents.

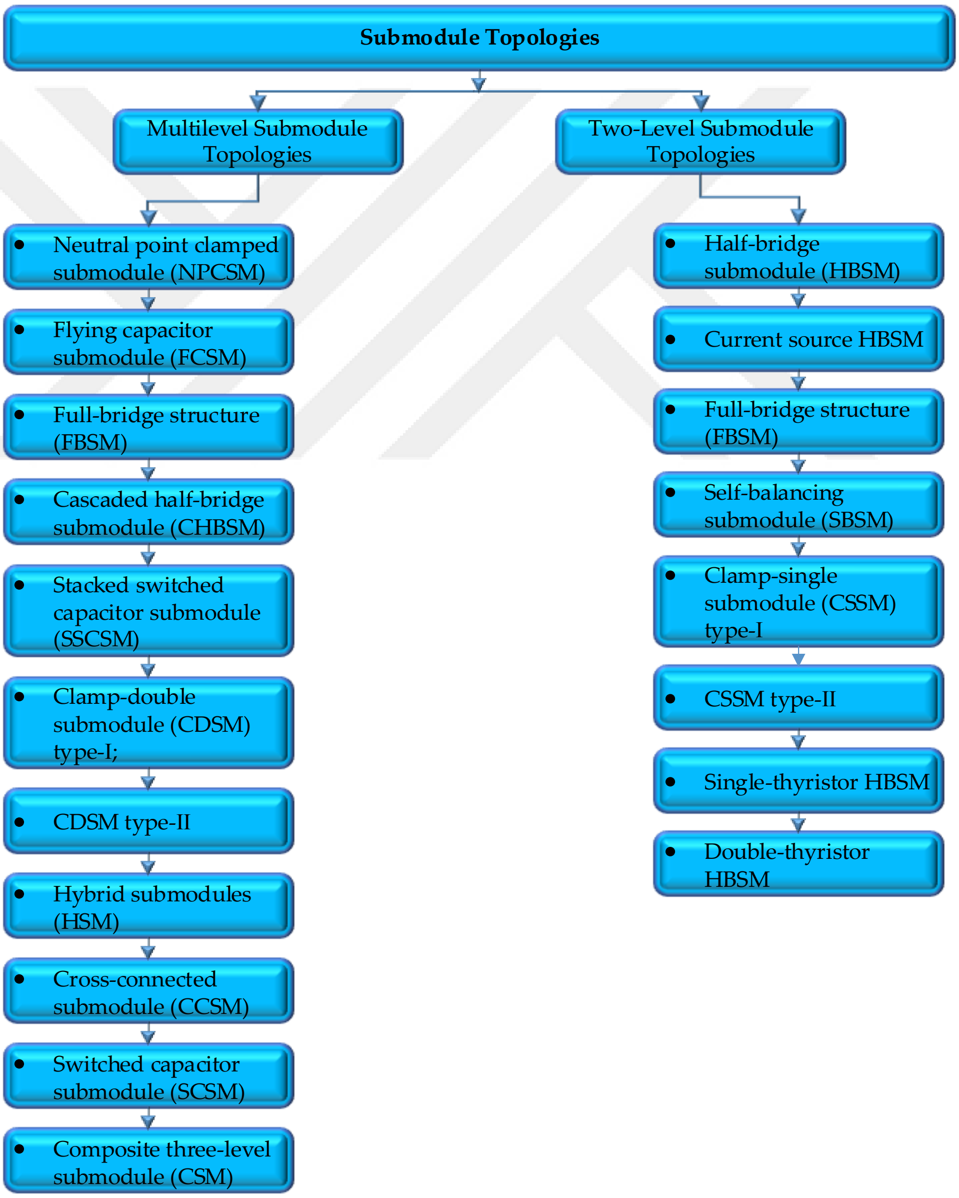

Figure 3. 24 SM topologies employed in MMC architectures.

The SM structure is fundamental to MMC concepts. Numerous researchers have created SM configurations since the MMC design was first published in the literature. SM architectures can be divided into two main groups based on the output voltage level, as shown in Figure 3.24: multiple-source multilevel SM topologies and single-source two-level SM configurations [124]. The notable developments in the field of semiconductors are unquestionably one of the main reasons for the current rise in interest in MMC technological advances. Since power switching devices in MMC technologies are semiconductor-based, SM structures provide their foundation. Due to its simple design, the unipolar semiconductor-based circuit architecture known as HB arrangement is most frequently utilized in SM designs. Since its construction is simple, HBSM has lower losses in power. The FBSM design construction relies on semiconductors and consists of two HBSMs and one floating capacitor. FBSM construction offers good protection against DC fault currents. Yet, compared to HBSM construction, there are more semi-conductor-based power-switching components, which results in greater power inefficiencies [22]. In MMC designs, Figure 3.25 shows the most often used SM topologies by scholars. Figures 3.25(a) and 3.25(b) exhibit IGBT-based HBSM and FBSM designs. Figure 3.25(c) presents the MOSFET-based HBSM form, whereas Figure 3.25(d) illustrates the MOSFET-based FBSM design.

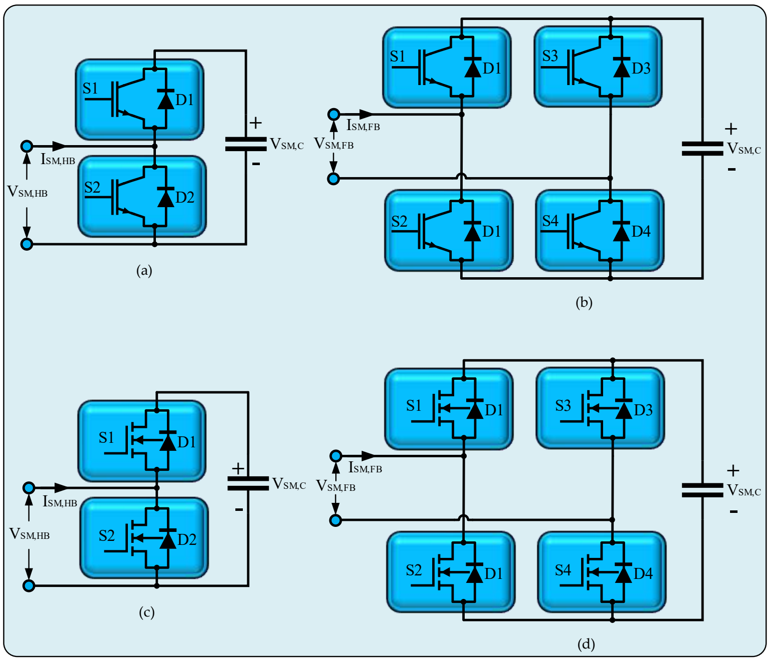

Figure 3. 25 The SM topologies that are frequently employed in MMC structures: (a) IGBT-founded HBSM; (b) IGBT-founded FBSM; (c) MOSFET-founded HBSM; (d) MOSFET-founded FBSM.

Siemens' Transbay Bay Cable Project, which spans the bay from San Francisco to Pittsburgh and was put into service in 2010, was the initial MMC-HVDC power network [126]. Beginning with the Pittsburg power converter unit within San Francisco's northeast towards the Potrero power converter facility within the city's center, the electric power route is identical. A 55-mile (88-kilometer) undersea XLPE DC power cable submerged in the Suisun, San Pablo, San Rafael, and San Francisco bays connects the power converter plants [126]. Figure 3.26 illustrates an MMC-based HVDC power system interconnecting two different power systems. An MMC structure created by Siemens is shown in Figure 3.27. Figure 3.27 illustrates the key components of the proposed MMC system, where Figure 3.27(a) shows the overall converter station layout, Figure 3.27(b) presents the detailed arm structure, and Figure 3.27(c) depicts the SM configuration.

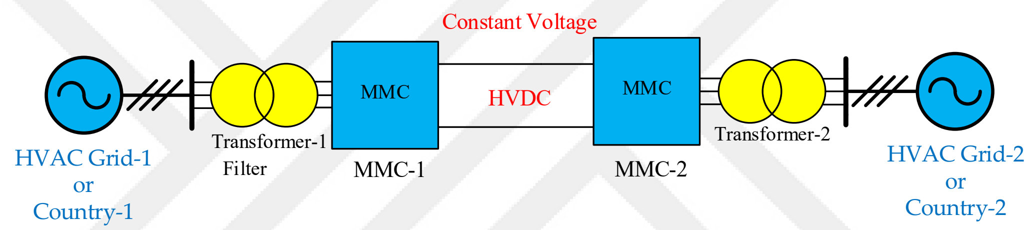

Figure 3. 26 MMC-based HVDC transmission system.

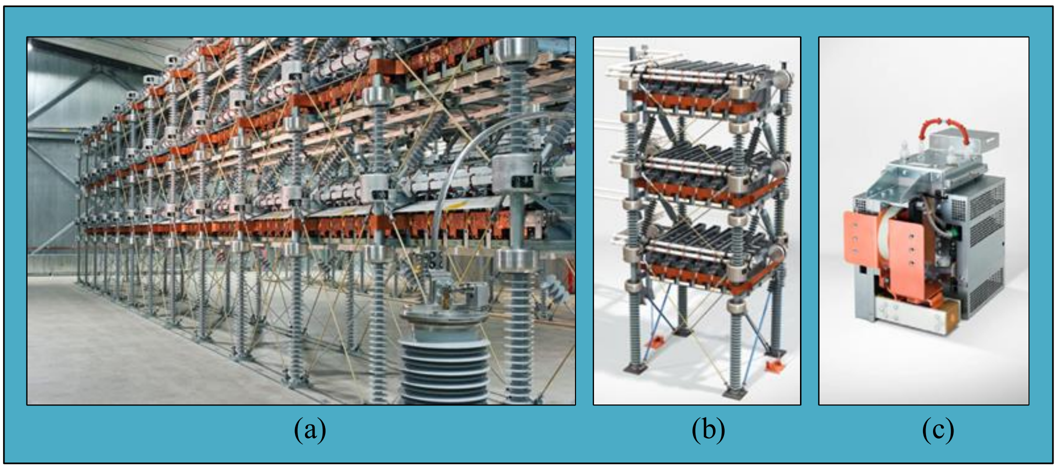

Figure 3. 27 Siemens-made MMC structure: (a) Main MMC architecture station; (b) MMC arm component; (c) MMC SM structure [91], [127], [128].

3.5 Applications of HVDC Technology

Massive amounts of electrical energy can be readily transmitted over tremendous distances via minimal losses thanks to HVDC power transmission technology [93],

[101], [129]. Specifically, HVDC is an extremely successful technological breakthrough in power transmission systems that enables the following: reduced power losses, controllable nature, ecological considerations, limited short circuit currents, massive power transfer capability, asynchronous power grid interconnections, high-efficiency generation of power, connecting enormous wind farms located offshore to the main network, decreased volume of overhead power lines, and successful power distribution throughout extended distances using underground and submerged wires [72], [117], [130]–[136]. In addition, providers are encountering additional difficulties due to the development of renewable energy sources-based power plants, which can simultaneously fulfill the community's electrical power requirements and become more ecologically friendly. Increasing amounts of electrical power originate with clean energy sources that are positioned distant from demand power grids. Sophisticated power transmission systems are needed to distribute the power sustainably and effectively. HVDC technology is the ideal solution for incorporating massive amounts of electrical power generated from renewable sources across immense distances. HVDC technology has gained an effective place in many application areas due to its extraordinary features, especially the ability to effectively integrate power systems based on renewable energy sources into load centers over long distances with minimum power losses. As previously described, the fundamental applications for HVDC technology are outlined in Figure 3.28. The following are explanations for the sections in Figure 3.28 that have numbers associated with them [68]:

1) Power transfer of substantial electrical power throughout the long-distance overhead wire.
2) 2 Mass electrical power transfer via subsea power line.
3) Rapid and accurate regulation of the electrical power transfer across an HVDC connection to modulate the transmission of electrical power utilizing a back-to-back architecture to positively diminish electromechanical disturbances and improve the power grid's reliability.
4) An HVDC connection is often employed to connect power networks with distinctive frequencies utilizing an asynchronous back-to-back power system, as it has no restrictions upon the frequency and angle of phase within the two AC power networks.

5) Utilizing a multiterminal DC power network to provide a link to possible counterparties in the regions crossed can be professionally and politically required once electrical power is needed to be transported from a faraway generating point throughout various nations or distinct regions inside a particular nation.
6) In cases where sustainable energy sources are positioned distantly beyond the end user, including wind power, an HVDC power transmission line might be employed to interconnect them.
7) There is an increasing amount of interest in VSC-based HVDC technologies. Significant progress in the invention of the IGBT power switch has rendered this novel innovation conceivable. Unlike the traditional HVDC power systems with thyristor-based VSC, PWM technique can additionally be utilized for the VSC technology in this sort of power system. Connecting renewable energy from the wind to the existing power network is an excellent fit to supply this type of technology.
8) Reactive power cannot be transferred via a DC power network; therefore, two AC power grids can be joined across an HVDC power network without generating more short-circuit power. This method is helpful when connecting power generators.

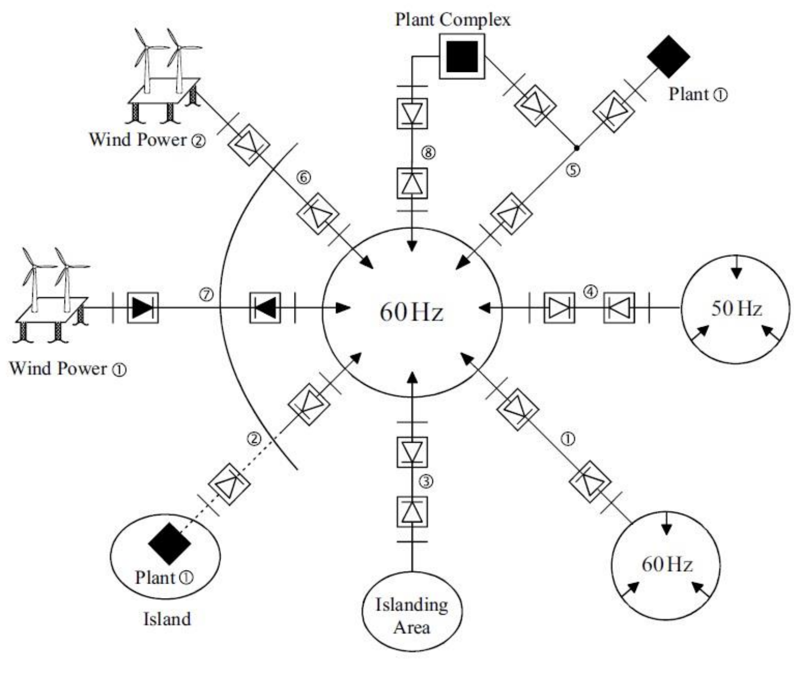

Figure 3. 28 Fundamental applications of HVDC technology [68].

In recent years, the interaction between neighboring power networks using HVDC networks is needed to increase the unpredictable nature of novel generating supplies. Asynchronous electrical networks can be effortlessly linked thanks to HVDC technology, which also provides the controller with precise management of the electrical power transmission across these two power networks. It additionally makes it possible for industries that would not alternatively become able to integrate, which has advantages including lesser intermittent operation, smaller circulating reserves, more perseverance, and the ability to profit from price differences. A back-to-back power arrangement should be employed when the power networks are located close to each other. In this particular situation, there is no need for an overhead power line or cable because the two converter stations can be placed side by side in identical structures and locations [137]. Several existing AC power systems can be connected asynchronously by implementing an HVDC back-to-back converter station. Back-to-back arrangements involve the placement of the rectifier part and inverter part in a single facility. They are typically utilized to provide an asynchronous link between two AC power systems that may or may not have an identical frequency. Utilizing a back-to-back arrangement to split up a power system that is too powerful in order to mitigate the currents that short out has additional advantages. A fundamental instance of a back-to-back converter station is presented in Figure 3.29.

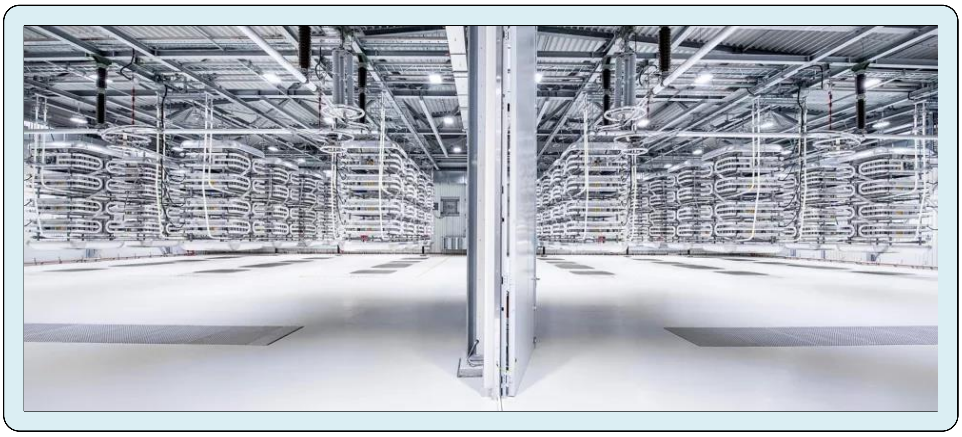

Figure 3. 29 Back-to-back power converter arrangement [138].

The phenomenon of making trades has been brought to the electrical power industry in various locations worldwide via permitted electrical power markets. Investment in the electrical power industry is made possible through combining marketplaces for electricity using grid interrelationships. Such interconnections can occur between different power networks inside an individual country's power grid or between national power networks. For the trades of electrical power to perform successfully in paired electrical markets or at all, stable and regulated power transfers are necessary, and HVDC technology provides this phenomenon. Distinct nations' power systems can have developed considerably in various ways, with radically differing regulations and technology. Marketplaces for electrical power that function with various frequencies and are unsuitable in distinct manners can solely be connected via HVDC power systems, which enables systems to collaborate on electrical power without necessitating the exact synchronization of a synchronized power system [138]. With the worldwide population becoming more urbanized, electricity demands in settlements rise. To keep up with this growth in electrical power demand, larger city's electrical power grids are constantly being upgraded. Due to the scarcity and high land cost, significant challenges occur anytime an entirely novel route needs to be acquired to transmit more electrical power via conventional power transmission networks. Another significant concern for the continued growth of existing electrical power grids is the possibility of surpassing the short-circuit capabilities of current substation systems along with additional system parts as existing power transmission capacities rise. Metropolitan electrical power grid development approaches need to consider concerns, including quality of electrical power and executives, noise contamination, auditory and electrical noises, licenses, and electrical power blockage [138]. HVDC technology can answer almost all the problems mentioned above thanks to its extraordinary features. Thanks to its compact structure and easy controllability, it plays a critical role in solving such problems. A representation of an electrical power infeed for a city center is shown in Figure 3. 30.

Figure 3. 30 An example of a city center electric power infeed [138].

HVDC technology is essential for transferring electrical energy across long distances to load centers and city centers and offering exceptional solutions in city centers. Fossil-based resources are the primary source of energy produced currently; however, their consumption has an adverse effect on the ecosystem as well as being a limited resource. Sustained emissions-free alternative power generation is going to become more significant in the electrical power industry as they grow and become more challenging to discover and harvest. In order to address the issues of limited energy resources and rising electrical power demand, which, at present, concerning development, is predicted to multiply within 30 to 40 years, wide-scale incorporation of green energy suppliers has become the most viable, overtime answer. Substantially incorporating energy from renewable sources within the electrical power system is not without hurdles. Installing electrical power facilities that can be completely and effectively used is necessary for them to succeed; often, these places are located far from the centers of load with the greatest electrical power requirements. Thus, it is necessary to significantly boost electrical power transmission performance and availability to integrate green energy production on an extensive level. Thanks to HVDC power transmission technologies, hundreds of thousands of users currently get electrical power from hydroelectricity, wind power, and solar power facilities daily. Since the ideal places for electrical power generation are typically in isolated locations, energy produced on top of mountains, far away deserts, and oceans frequently travels far away before reaching its intended destination. The most dependable and effective method for obtaining this is via HVDC technology. Thanks to low-loss DC power transmission technologies, almost all renewable electrical power is guaranteed for customer delivery [138].

In case of a major disruption, including an electrical blackout, HVDC technology offers prompt electrical power reconstruction with enhanced trustworthy and optimal management over a power grid's power delivery. Although these attributes are technically indispensable, key characteristics such as enhanced power quality, precise power flow control, ancillary support capabilities, system stability reinforcement, and congestion alleviation are frequently overlooked or inadequately weighted in the cost-benefit analyses of transmission infrastructure investments. A higher accurate and controlled electrical power transfer is expected to originate from an expanding percentage of DC power transfers integrated into conventional AC power grids. DC innovation provides faster electrical power recovery in case of a major disruption, such as an electrical power failure, alongside improved robust and optimal management over the distribution of the electrical loads in the power grid. An electrical power grid can be stabilized with DC power transports because they are able to adjust for variations in electrical power and voltage. Moreover, additional DC power lines can enhance electrical power transmission capacities, lower system interruptions, and enhance the reliability of the electrical power [138].

The greatest onshore areas for wind power plants are currently being established in several nations; therefore, appliances have shifted to offshore places. Operating offshore is mostly appealing due to the vast amount of windy electrical power that is accessible. The electrical power output produced can reach up to 70% more than upon the earth, with median wind velocities as much as 20% higher than usual. The absence of impediments like hillsides and the typically flat ocean surface contribute to the wind-based electrical power's increased dependability. As further and bigger offshore turbine facilities are planned, significant expenditures are required to figure out how to put electrical power into the electrical grid. Due to the substantial reactive power required by the power wires, which AC technologies utilized in the beginning, near-shore offshore wind power plants are progressively approaching their breaking point. HVDC technology is the most efficient way to deliver electrical power to the coastline from wind energy facilities that are away from the coast while maintaining high electrical power excellence. The HVDC power converter installations' lightweight and compact facility structure is particularly advantageous for offshore facilities. Figure 3.31 depicts the Dogger Bank Wind Farm, which is an offshore wind farm. Developed by Hitachi Energy, the Dogger Bank Wind Farm will be considered the world's biggest offshore wind power station by 2026 [138].

Figure 3. 31 Offshore Dogger Bank Wind Farm [138].

The offshore facilities can receive and transmit electrical power using HVDC technological advances. Offshore structures have historically produced their energy by consuming fossil-based fuels to operate diesel engines or gas-powered generation systems onboard. Implementing an electrical power transmission network to provide electrical power to remote offshore sites from the coast is an approach. Platform's carbon dioxide footprints can be completely eliminated with a power-from-coast option by removing onboard electrical power-producing equipment that consumes natural gas or petroleum-based fuels. It additionally renders more workspace accessible, lightens the load upon the platform, and enhances the employment environment.

Furthermore, HVDC power technologies require less maintenance compared to conventional generators. DC electrical power is capable of being delivered to many platforms within a multiterminal system, or the power converter unit can be placed on one platform, and electrical power can be transferred to the platforms through AC connections [138]. Figure 3.32 shows an example of an offshore platform (Troll A Platform). Troll A platform built by Hitachi Energy. Hitachi Energy operates the entirety of HVDC power-from-shore installations currently deployed worldwide. Troll A 1&2 from Statoil, completed in 2005; Valhall from BP, completed in 2011; Troll A 3&4, completed in 2015; and Johan Sverdrup from Equinor, completed in 2018. Every facility is situated in the North Sea.

Figure 3. 32 An illustration of an offshore platform (Troll A Platform) [138].

In most typical HVDC power structures, power transmission cables are overhead. Exceptionally high-power transfers over extremely long distances, which are roughly 600 km or more, often originating from distant power-producing units, are the main cause of the phenomenon. Given that HVDC technology is less expensive than comparable AC power transmission systems, it is an appealing solution for these kinds of systems. Whereas an AC power transmission line requires three main wires, a DC power transmission line only requires two wires, and DC losses of electrical power are much reduced. Although HVDC converter stations require significantly higher initial investment compared to AC systems, HVDC transmission becomes economically viable beyond certain distances due to lower line losses and the absence of reactive power requirements. The break-even distance varies by application: for submarine cables, HVDC is typically cost-effective beyond 50 km; for underground cables, the threshold ranges between 50-100 km; and for overhead lines, it generally exceeds 500–800 km. These values serve as useful guidelines for evaluating the cost-effectiveness of HVDC systems in long-distance power transmission. Installations for extended distances HVDC power systems that use overhead wires have been utilized in the USA, Canada, Brazil, China, and India, among other countries [138]. Figure 3.33 illustrates an example of overhead power transmission lines for HVDC technology.

Figure 3. 33 A particular instance study of HVDC technology's overhead electrical power transmission lines [138].

3.6 Advantages of HVDC Architectures

Particularly given that in comparison with traditional existing HVAC power frameworks, HVDC technology's characteristics such as its adaptability, productivity, affordability, technological benefits, environmentally friendly habits, narrowing power transmission line expenditures, suitability for high power enormous scale transfer over long distances, combination with asynchronous power networks, submarine power cable association, protection against deviations in phase angle, frequency, impedance, or voltage, along with its capacity to maintain independently frequency and generator management make it indispensable to today's power applications [15], [68], [101], [139]–[143]. Among the remarkable qualities previously mentioned, HVDC technology has become more significant in the power systems industry in recent years, particularly with regard to power transfer over great distances and undersea power lines. The following are some of the most significant advantages of HVDC technology over conventional HVAC technologies [7], [68], [101], [114], [139], [144]–[146].

- Regarding expenditures on investments and power transmission losses, HVDC power transmission technologies are more cost effective than traditional AC power transmission methods. The economic viability of HVDC depends on the application: beyond 50 km for submarine cables, 50-100 km for underground cables, and over 500-800 km for overhead lines.
- Comparing HVDC to HVAC, a large quantity of electrical power can be transmitted throughout extensive distances, having minimal power losses and a lower initial cost. The corresponding costs of AC and DC power transmission methods are illustrated in Figure 3.34.

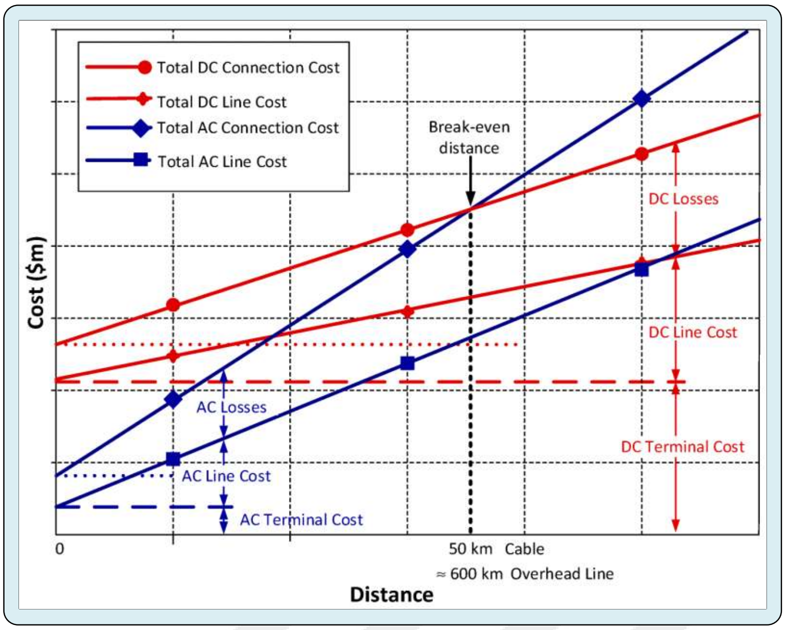

Figure 3. 34 AC and DC power transmission technologies' relative costs [144].

- Electrical power can be transported via underwater cables using HVDC technology, particularly for distances over 50 km. The key physical limitations of conventional AC power cables, whose overall active power transmission potential is reduced because of the reactive power fraction and capacitive currents, do not pertain to HVDC power lines.
- For the purpose of transferring electrical power to the power system's faraway power distribution networks, HVDC technology requires lower power wires and smaller poles.
- An HVDC power line's right-of-way size is significantly less than an AC power line. This makes it easier to choose appropriate pathways in places involving problematic landscapes and in areas inhabited by significant populations.
- HVDC technology can be used to establish links between asynchronous power systems.
- HVDC power transmission makes it possible to efficiently use power sources that are located far away from load center locations.
- In comparison to HVAC power technology supplying an equivalent level of electrical power throughout an identical distance, HVDC technology provides with the greatest effectiveness and an extremely short breakdown removal duration owing to the lack of reactance within DC.

- Among many crucial variables that can be controlled for HVDC power transportation is the transfer of electrical power.
- Following an interruption, stability or synchronized functioning throughout the power transmission must be preserved momentarily and dynamically.
- Because expense is a significant factor, HVDC technology is relatively more economical than HVAC technology in numerous respects.
- There are fewer DC line losses (no proximity impact, no skin impact).
- Whatever combination of voltage and frequency between the two AC power networks can be used with an HVDC power association. The load frequency management that is currently in place in all networks is able to function correctly since a standalone regulation is accessible for transferring electrical power.
- It allowed voltage fluctuation throughout predicted load rates and transmission routes.
- In cases where electrical power transmission from a faraway power generating facility requires traveling across national borders or various regions with a single nation, it could be politically as well as economically imperative to establish a link among attainable counterparts in the affected regions. It is possible to use multi-terminal DC power technology for this particular kind of application.
- The characteristics of the corona phenomena differ significantly between DC and AC power transmissions.
- Seasonal average corona losses are often greater advantages for the bipolar DC power line of transmission compared to the AC scenario for power transmission lines having nearly identical transmitting electrical power potential and rms wire voltages to ground. This is exceptionally accurate in adverse weather conditions.
- Corona discharges around the power lines cause high-frequency electrical currents within the power wires that produce electromagnetic fields, which leads to radio disturbances. Investigations of electromagnetic emissions have demonstrated that electromagnetic pollution on DC power lines is significantly less than that of AC power lines with comparable volume.
- The audible noises produced by equivalent DC and AC power lines are identical in ideal weather conditions. Nonetheless, the advantages of DC power

lines over AC power lines, such as their superior functionality and decreased interference levels, come into play during rainy seasons.

3.7 Summary

In this chapter, HVDC technology is covered in broad circumstances. A thorough examination has been conducted of the evolution of HVDC technology for power systems, its fundamental operating principles and structure, system topologies, converter technologies (LCC, VSC, and MMC), application areas, and remarkable advantages. Concerning its numerous benefits, such as efficient power transmission, asynchronous grid interconnections, adaptability, limited reactive power, limited short-circuit currents, reduced losses, and the capacity to transmit power from offshore wind farms to onshore power plants, HVDC technology is vital to power structures. It also facilitates the connection of asynchronous AC systems and the transfer of electricity from various locations that need underground and underwater cables to the mainland. Additionally, DC power transmission is taken into account and has recently been developed to connect two asynchronous AC networks with different frequencies, transmit power underwater, and enhance power system durability by connecting in parallel with an already-existing AC power system. LCC, or CSC, was the foundation upon which conventional HVDC systems were initially established. Later on, HVDC technologies based on VSC were developed. These two HVDC structures are still utilized in power systems today; however, with the advancement of VSC technology, MMC-based HVDC technologies have substituted these two HVDC structures in power systems. There are now multiple innovations available to strengthen the power transmission networks. Frequently and often used technologies include HVDC power network links, network upgrading, electrical power transfer regulating components, and AC power overhead lines and cables. HVDC technology is seen to be the greatest opportunity of these advancements as it enables architectural modifications through the use of cabling technological advances. More precisely, the development of a DC power network is thought to be the optimum solution that has the potential to change people's perspectives and pave the way for a power system of tomorrow that will rely heavily on renewable energy sources.

The fourth chapter will examine traditional DC-DC converter topologies, which are essential to HVDC technology.

CHAPTER IV

DC-DC CONVERTER TOPOLOGIES

4.1 Introduction

A DC-DC converter topology transforms the input DC voltage to a different DC voltage value by utilizing the DC source voltage. In other words, these architectures that transform a constant DC voltage level into a variable DC voltage level are known as DC-DC converter topologies. The schematic layout of a typical DC-DC converter is demonstrated in Figure 4.1. It is essential to transform a constant voltage DC supply to an adjustable voltage DC supply for several industrial applications, such as renewable energy applications, including those involving photovoltaic and wind energy structures, DC power networks, electric or hybrid vehicles, fuel cell vehicles, variable frequencies operation systems, energy storage systems with batteries, railroads, aircraft, low and high power applications, etc. Undoubtedly, the remarkable advancements in semiconductor technology are the primary cause of the widespread use of DC-DC converter systems in modern industrial applications. This state of affairs is mostly due to the fact that DC-DC converter topologies are developed utilizing semiconductor technology. Particularly, the outstanding expansion of DC power networks has been assisted by the recent spectacular advancement of semiconductor-based DC-DC converter systems. It is indisputable that HVDC power systems have become remarkably prevalent in DC power systems recently. DC-DC converter systems are critical, specifically for the integration of HVDC power networks.

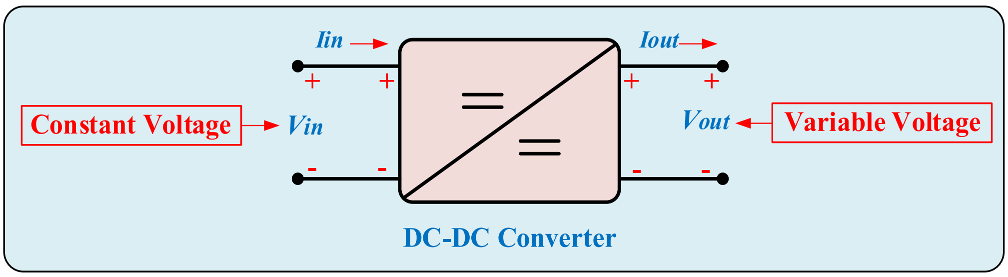

Figure 4. 1 The block layout of a DC-DC converter.

4.2 Conventional DC-DC Converters

Typical DC-DC converter architectures can differ greatly from their counterparts. These variations change depending on the industrial scenario in which they are employed. Some varieties increase (boost) or decrease (buck) the DC source voltage and can have two or more terminals (multi-level). Nonetheless, the primary categorization of DC-DC converters is based on the presence or absence of a transformer between the input and output terminals of DC-DC converter designs. There are two fundamental classifications of conventional DC-DC converters, which are isolated and nonisolated architectures [147]–[151]. A transformer is used to link the input and output circuits in isolated DC-DC converter topologies; nevertheless, no transformer is needed in non-isolated DC-DC converter topologies, and the input and output circuits are connected directly. Figure 4.2 summarizes the DC-DC converter configurations observed in the present-day literature.

4.2.1 Isolated DC-DC Converter Topologies

In the framework of DC-DC converter topologies, isolation is defined as galvanic isolation, which emphasizes the nonexistence of a physical connection between the converter primary and secondary terminals. In other words, an isolated DC-DC converter physically divides the system into two parts, isolating the input terminal from the output terminal and eliminating direct current flow through the input and output terminals of the DC-DC converter. This is usually accomplished by employing a transformer. Each of the isolated structures has a unique grounding in the isolated DC-DC converter designs. The isolated DC-DC converter topologies first transform the DC voltage waveform to AC voltage waveform, which is then rectified to the DC waveform after passing through a high-frequency transformer. Typically, isolated DC-DC converter topologies have a larger voltage gain compared to their non-isolated counterparts. In isolated DC-DC converter designs, nevertheless, reducing the influence of leakage inductance and the transformer construction process are crucial [152]. These types of converter topologies are examined through a topological perspective in the next parts.

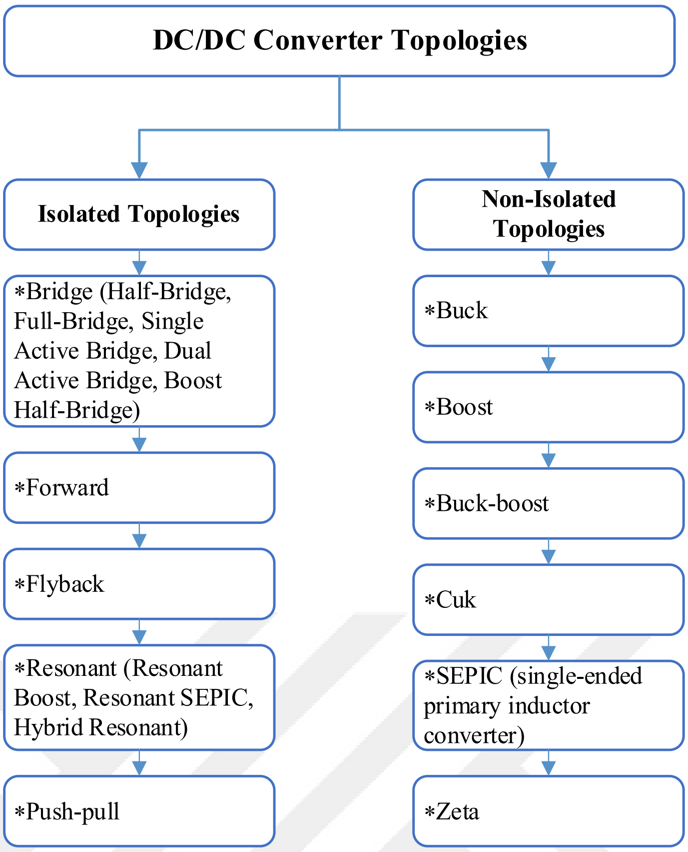

Figure 4. 2 Traditional DC-DC converter topologies.

4.2.1.1 Bridge Topologies

The isolated bridge converter framework represents a versatile category of DC-DC converters characterized by their integration of bridge configurations and multiple power switching elements combined with a high-frequency transformer. Commonly encountered topologies within this category include the half-bridge, full-bridge, single active bridge, dual active bridge, and boost half-bridge converters. Figure 4.3 showcases various bridge-based DC-DC converter configurations, including the full-bridge (Figure 4.3(a)), half-bridge (Figure 4.3(b)), and dual active bridge (Figure 4.3(c)) designs. The full-bridge DC-DC converter, illustrated in Figure 4.3(a), is engineered to deliver a double output voltage compared to the half-bridge configuration due to its higher number of switching elements [153]. Consequently, this topology provides a significantly greater power output. The primary terminal voltage of the transformer can be positive (+Vs), negative (-Vs), or zero, depending on the activation state of switches S1, S4, S2, S3. The secondary voltage is rectified from the AC voltage produced on the transformer's secondary side, fluctuating from zero up to the maximum achievable voltage (Vs), dictated by the transformer's turns ratio and the PWM control strategy.

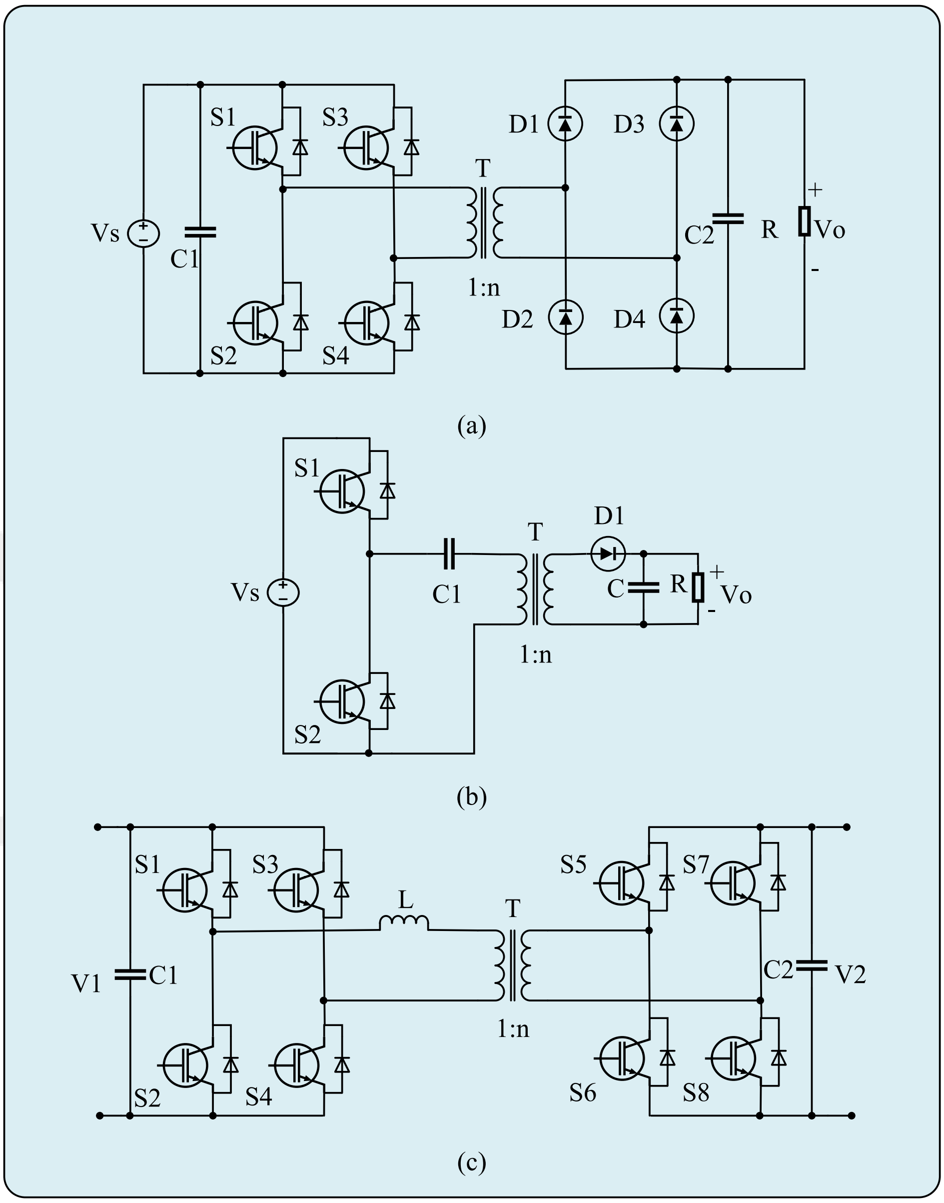

Figure 4. 3 Bridge DC-DC converter structures: (a) Full-bridge DC-DC converter topology, (b) Half-bridge DC-DC converter topology, (c) Dual active bridge DC-DC converter topology [154]–[157].

Conversely, the half-bridge DC-DC converter, depicted in Figure 4.3(b), employs a high-frequency transformer to provide electrical isolation, allowing for output voltages that may exceed, be lower than, or be opposite in polarity to the input voltage. This topology supports dual-ended DC-DC conversion and enables efficient power transmission. During operation, semiconductor switches (e.g., MOSFETs, IGCTs, FETs, and IGBTs) manage the transfer of power between the primary and secondary terminals, with switches S1 and S2 operating in tandem. As presented in Figure 4.3(c), the dual active bridge DC-DC converter is an advanced architecture designed for highly efficient bi-directional power transfer. It integrates two DC-AC conversion stages connected via an inductor and a high-power transformer, a concept initially introduced by de Doncker et al. [158]. This configuration excels in efficiency through optimal management, extensive voltage conversion capability, and the elimination of voltage stress during switching, making it highly desirable across various industries [159].

The dual active bridge design is particularly valued for its functional elegance, ease of process enhancement, excellent efficiency and power density, uniform power switching, galvanic isolation, and minimal inactive components [160]–[164]. This topology involves two H-bridge pairs connected to a high-frequency transformer, utilizing winding leakage inductance for both isolation and energy storage [165]. The single active bridge DC-DC converter is an ideal choice for unidirectional power transfer applications due to its cost-effectiveness and control flexibility. Its fundamental design includes an active and passive bridge linked by a high-frequency transformer [166]. Furthermore, the single active bridge DC-DC converter design is a single-directional version of the well-known dual active bridge DC-DC converter design that is bilateral and has a high rating for power. One of the simplest methods for increasing galvanically isolated DC-DC converters that can regulate multiple input voltage variations is to boost half-bridge DC-DC converter structure development [167], [168]. This paper [169] presents an established norm boost half-bridge DC-DC converter architecture. These present studies [169], [170] also discuss a modified boost half-bridge DC-DC converter topology that has evolved from the conventional boost half-bridge DC-DC converter design. Concerning its minimized voltage fluctuation related to diode reversed recovery, zero voltage power switching, smaller input filtering system, expansive input voltage level utilization, extensive duty cycle span, zero DC magnetization of the power transformer, and zero circulating current properties [169], [171], the conventional boost half-bridge DC-DC converter topology can be applied in various industries, including DC distribution structures [170], photovoltaic systems [172], fuel cell mechanisms [173], electrical and hybrid vehicle applications [174], HV and high-power network systems [175], and so on. The excessive DC magnetization current of the power transformer, a higher percentage of electromagnetic elements, a significant amount of uncontrolled power within the power transformer, and HV tension and significant shutdown voltage fluctuation of the secondary's rectifier diodes are nevertheless the primary drawbacks of the boost half-bridge DC-DC converter. Additionally, in response to quickly fluctuating audio alerts, it can be disrupted via an external inductor, which can produce a significant immediate output electrical current [169].

4.2.1.2 Forward DC-DC Converter

The forward DC-DC converter is an isolated DC-DC conversion topology designed to provide a stable and isolated DC output from an unregulated DC input source. This configuration can be theoretically applied to any transformer-based DC-DC converter with multiple outputs [153]. The transformer's winding ratio determines the output voltage, which can result in an output voltage that is either higher than, lower than, or equal to the input voltage. The forward DC-DC converter operates similarly to the flyback converter topology, making it prevalent in low-power applications due to its dynamic performance, cost-efficiency, and operational simplicity. However, it is less suited for high-line input scenarios due to the increased voltage stress on the primary switch, which can lead to higher power switching losses [176].

Figure 4.4 depicts the fundamental architecture of a forward DC-DC converter. Unlike the flyback converter, the forward converter allows simultaneous current flow through the transformer's primary and secondary sides when the power switch (MOSFET) is activated, thereby energizing the circuit. The transformer's induction facilitates concurrent current flow through the secondary side. The secondary voltage is influenced by the transformer's turns ratio, with diode D1 conducting while diode D2 remains open. When the power switch is deactivated, current ceases through both primary and secondary sides. The induced voltage on the secondary side inductor counters abrupt current changes, causing diode D2 to conduct while diode D1 remains open. This cyclic process continues indefinitely, with the power switch controlled by PWM technique.

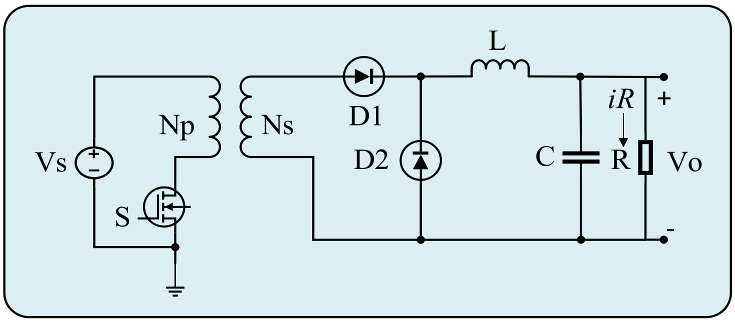

Figure 4. 4 Typical forward DC-DC converter structure [177].

4.2.1.3 Flyback DC-DC Converter

The basic structure of flyback DC-DC converters originates from the conventional buck-boost DC-DC converters. Stated differently, flyback DC-DC converters are an isolated kind of buck-boost DC-DC converter design. Thanks to their straightforward design and isolation, flyback DC-DC converter topologies are frequently employed in low and medium-power applications. The transformer's turn ratio allows them to attain a substantial boost voltage enhancement. It is preferred for multiple electrical power applications owing to its straightforward design, inexpensive cost, uncomplicated controlling method, and galvanic isolation properties [178]–[181]. Figure 4.5 illustrates a conventional flyback DC-DC converter construction. One benefit of flyback DC-DC converter topology is its extremely minimal component number. It is possible to achieve numerous results with the least various additional components. The only equipment that is needed for every single supplementary result is supplementary coil, diode, and capacitor components. Insufficient lateral control is a drawback of the flyback DC-DC converter design compared to buck-originated transformer-isolated converters similar to the forward and full bridge topologies [182]. Although conventional permanent frequency-controlled flyback DC-DC converter designs are easier to construct and manage, they exhibit considerable losses during voltage strain switching and challenging MOSFET power switching [183]. The flyback DC-DC converter topology's operation can be explained as follows. Increasing the primary side electrical current enables the power transformer's windings to accumulate electrical power whenever the primary side power switch is turned on, and the flyback DC-DC converter structure is activated. In such a circumstance, the contrary generating the secondary side voltage that is generated causes the diode D1 in the circuit structure to become energized in the opposite direction and transition to the threshold status. The process consequently results in zero electrical current running on the secondary end of the transformer. Since the secondary portion of the power transformer is not receiving any electric current, there is not any electrical transmission through the primary side towards the secondary side. The system component which supplies the required voltage to load within this operating state of the system is the C capacitor component. If the power switch is switched off, the transformer windings' polarities are altered by the magnetic field, causing the voltage to be rectified by the circuit that includes the rectifier structure. All the electrical power in the core gets delivered towards the load, and this process is repeated till the electrical power of the core is reduced or the power switching mechanism is activated.

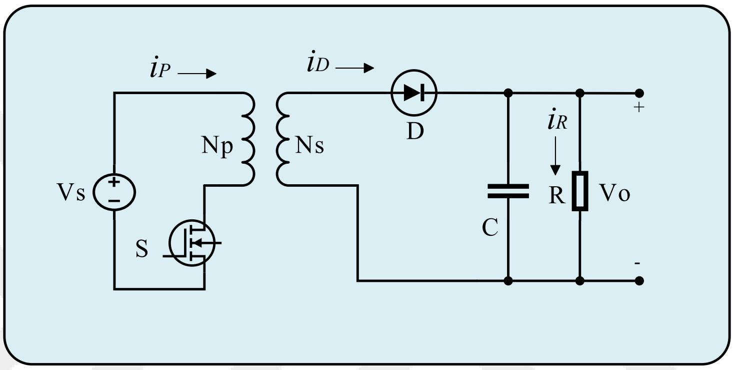

Figure 4. 5 Conventional flyback DC-DC converter design [184], [185].

4.2.1.4 Resonant DC-DC Converter

Resonant DC-DC converters epitomize a remarkable class of power electronics, distinguished by their capacity to achieve superior efficiency and precise control in energy conversion processes. In contrast to conventional power switching power supplies, resonant DC-DC converter designs mitigate switching losses, thereby facilitating enhanced operational efficiency. This discourse endeavors to elucidate the fundamental principles, architectural components, and diverse application domains of resonant DC-DC converters. Resonant DC-DC converter topologies are tried-and-true technological advances primarily utilized in industries requiring stable DC voltage improvement [186]. A substantial power bulk, smoother patterns of waveforms, exceptional performance, higher switching frequencies via selective switching configurations, outstanding quality of power conversion, and a significantly lower number of electromagnetic parts, including power transformers and filtering elements, are all features of resonant DC-DC converter topologies [186], [187]. Recently, boost rectifying devices have enhanced DC-DC resonant converter designs. In [188], an extensive examination of contemporary DC-DC resonant converter architectures is provided.

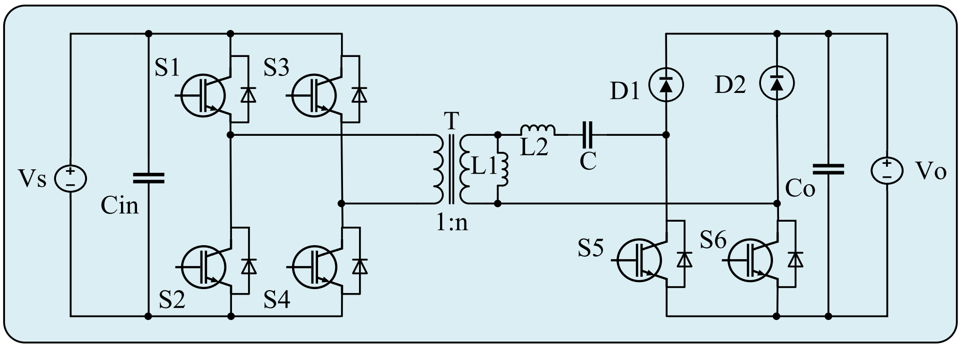

Figure 4. 6 Hybrid resonant DC-DC converter [189], [190].

Resonant DC-DC converters predominantly operate utilizing LC (inductor-capacitor) circuit configurations. These circuits strategically optimize the performance of switching devices at a designated resonance frequency, substantially minimizing energy dissipation during transitions. Two principal resonant modes are noteworthy: series resonant DC-DC converters and parallel resonant DC-DC converters. The series resonant DC-DC converter designs are predominantly employed to elevate the voltage across the load. By operating at elevated frequencies, series resonant DC-DC converters exhibit a notable reduction in switching losses, concurrently delivering high output efficiency. The parallel resonant DC-DC converter designs are commonly utilized in applications requiring a stable voltage source; this mode is adept at maintaining constant output voltage, thus enhancing the system's overall stability. DC-DC converter structures with resonant designs include mixed resonant, resonant boost, and resonant SEPIC models. Figure 4.6 presents a combination of a resonant serial DC-DC converter design utilizing a supplementary boosted converter architecture. This DC-DC converter design uses a regular electrical source in a serial resonant converter configuration to deliver the highest possible efficiency. The structure of the resonant converters behaves just like a buck DC-DC converter mechanism whenever the source voltage occurs below the highest level conditions, with phase changing on the primary terminal and integrated converting on the secondary terminal, and it also acts as a boost DC-DC converter mechanism whenever the source voltage is beneath lower-level conditions, with primary side full bridge and secondary side boost capability [189]. By significantly curtailing switching losses, resonant DC-DC converters can achieve remarkable levels of energy efficiency, often exceeding that of traditional counterparts. The inherent design of resonant DC-DC converters facilitates the production of reduced high-frequency noise, thereby alleviating electromagnetic interference concerns. These converters are capable of maintaining stable performance across a diverse spectrum of load conditions, rendering them versatile for various applications. Besides the advantages of the resonant DC-DC converter designs mentioned above, there are also some disadvantages. The intricacies associated with the design of resonant circuits often necessitate advanced engineering expertise, making the development process more challenging. The requirement for specialized components and meticulous design parameters can lead to increased manufacturing costs. Resonant DC-DC converters have carved a niche in numerous sectors, including HV applications, electrical vehicle systems, medical applications, etc. In summation, resonant DC-DC converters constitute a pivotal advancement in the realm of power electronics, characterized by their exceptional efficiency and minimized electromagnetic interference. As technology progresses, the potential for designing and implementing increasingly sophisticated and efficient systems continues to expand. Future research endeavors are poised to optimize these converters' performance while exploring novel application frontiers.

4.2.1.5 Push-Pull DC-DC Converter

The push-pull DC-DC converter constitutes a pioneer topology within the field of power electronics, celebrated for its remarkable efficiency and adaptability in facilitating the conversion of DC from one voltage level to another voltage level. A particular form of DC-DC converter known as a push-pull DC-DC converter utilizes a power transformer, PWM algorithms, and a controlling mechanism to alter the voltage of a DC source. There are numerous implementations for push-pull DC-DC converter architecture. However, this DC-DC converter configuration is particularly advantageous in applications demanding electrical isolation and substantial power transfer capabilities. This kind of DC-DC converter architecture is common within intricate buildings that incorporate numerous sources of clean energy, including pumps, photovoltaic power systems, and battery control technologies. The various power sources can be connected to both traditional and innovative intelligent networks thanks to push-pull DC-DC converter topologies. The above uses of the push-pull DC-DC converter designs demonstrate its value and practicality in managing the transfer of power in a variety of electric power frameworks, including those that are off the electrical network and in remote locations without facilities [191]. Figure 4.7 shows the fundamental structural schematic of a push-pull DC-DC converter design.

Push-pull DC-DC converter structures, characterized by their uncomplicated circuit designs, facilitate voltage regulation, galvanic isolation, high voltage transformation ratios, low-side switching, straightforward gateway driver circuits, and enhanced transformer utilization, making them advantageous for low-voltage industries [192]–[194], and it is frequently utilized in medium to high power systems [195].

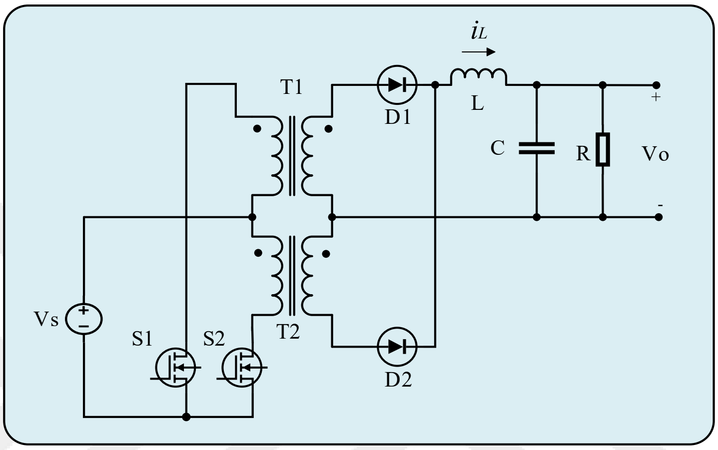

Figure 4. 7 Typical push-pull DC-DC converter structure [196].

Push-pull DC-DC converter designs are capable of achieving exceptional efficiency due to their effective utilization of transformer coupling and reduced switching losses. The inherent design of the transformer provides electrical isolation between input and output, enhancing the safety and reliability of the overall system. This topology accommodates flexible voltage step-up or step-down capabilities, rendering it suitable for a myriad of applications. At its core, the push-pull converter operates on the fundamental principle of alternately energizing two inductors through a transformer. This transformer performs the crucial function of voltage transformation and provides galvanic isolation between the input and output stages. A control circuit alternately activates two semiconductor-based power switches (commonly MOSFETs or IGBTs). When one switch is engaged, the current traverses one-half of the transformer, thereby inducing a corresponding voltage in the secondary winding. Upon the deactivation of the first switch, the second switch is actuated, allowing current to flow through the opposite half of the transformer. This alternation fosters continuous energy transfer to the output. The voltage induced in the secondary winding is subsequently rectified and filtered, yielding a stable DC output voltage suitable for load requirements. The primary terminal source voltage is transformed into the secondary side output voltage utilizing the power transformers, contingent upon the state of operation of the $S1$ and $S2$ electrical power valves. A typical push-pull DC-DC converter structure functions based on a particular principle: The magnetic field that exists at $T1$ rises in tandem throughout the interior core when electrical current passes across the primary side of the transformer whilst the $S1$ power valve is in a switched state. A voltage is provided at $T1$'s secondary by a rising magnetic field that exists. Since the pole orientation is conversely biased, the $D2$ diode is biased toward the front, and the $D1$ diode is shut down. The secondary terminal capacitance of the structure is charged by the inductive element in response to an input from $D2$. Whenever the $S2$ valve is switched on state, and the $S1$ valve is switched off, the high polarization of the $T1$ transformer is adversely uploaded. In this instance, the $D2$ diode is biased forward, and the $D1$ diode is shut down. The secondary terminal power transformer is where current flows across diode $D2$ and inductance L. In the initial case, the output side capacitor is energized and cannot allow any current to pass across it; in the second scenario, it can act like an electrical source and discharge, supplying current to the system. Consequently, the electrical current and the capacitor's discharging current flow throughout the load concurrently. Following a while, the $S1$ valve becomes active, the $S2$ valve becomes inactive, and the cycle is repeated [196].

4.2.2 Non-isolated DC-DC Converter Topologies

Considering the ability to convert electrical power through a DC voltage value to a different DC voltage level without establishing galvanic insulation between the primary terminal and secondary terminals of the DC-DC converter, non-isolated DC-DC converter structures are essential circuits in the field of power electronics. In case of non-isolated DC-DC converter architecture, no galvanic electrical isolation exists between the primary and secondary ends [147]. Better efficiency, small form factors, and affordability are their design characteristics, making them indispensable in a wide range of applications. More efficient and compact solutions are made possible by the circuit architecture's simplification in the absence of electrical galvanic isolation. Several topologies can accommodate a broad range of voltage and current needs, such as buck, boost, buck-boost, cuk, SEPIC, and Zeta DC-DC converters. This means that these converters are essential to current electrical engineering since they are used in everything from sophisticated power supply systems to portable technological devices.

Therefore, several research that offer issue identification and tracking techniques associated with these kinds of DC-DC converters have been reported in the literature [197]. Those of non-isolated DC-DC converter designs surpass the advantages of isolated DC-DC converter designs. These converter structures are nonetheless a greater sensible option over isolated arrangements, notwithstanding a few specialized limitations including a large duty cycling proportion, poor voltage gain, as well as additional components [147].

4.2.2.1 Buck DC-DC Converter

An important architecture in power electronics is the buck DC-DC converter, which effectively steps down a larger input electrical voltage into a lower output voltage in addition to retaining a high-power transformation effectiveness. In other words, the non-isolated DC-DC converter, a particular kind known as a buck DC-DC converter, has an output secondary side voltage that is smaller than the input source primary side voltage [198], [199]. Concerning its exceptional functionality and straightforward utilization, particularly originating in its own distinctive uniform and minimum phase framework, the buck DC-DC converter design has traditionally been considerably more extensively utilized in industry. Many different types of electronic mechanisms employ buck DC-DC converters, often known as step-down converters [200]. A diminished general layout is an appealing characteristic in tiny electronic structures, and it is achieved in part by the design's minimalism and low necessity for passive components. A key player in the development of modern electrical power engineering, the buck DC-DC converter architecture is an essential part of the electrical power transformation landscape. Its performance, small design, and adaptability make it an indispensable instrument. In addition to their affordability and ease of utilization, buck DC-DC converter designs are presently found in many industries; nevertheless, because of their rough power switching and inadequate functionality at higher power switching frequencies, buck DC-DC converters are a major source of electromagnetic radiation degradation [201].

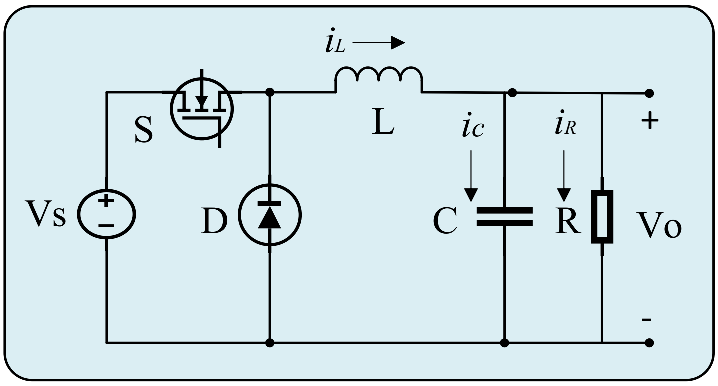

Figure 4. 8 Traditional DC-DC buck converter schematic [202]–[204].

Figure 4.8 exhibits the construction of a conventional buck DC-DC converter architecture. The power switching valve in this arrangement is activated, and the electrical current is transferred to the converter’s secondary end. The transfer of electrical current to the secondary side of the system is initially stopped due to power absorption in the inductive component, but, with a period, both the electrical charge upon the capacitance component and the electrical current entering the load gradually increase. Considering there is guaranteed to be a sizable voltage on the diode cathode terminal, the diode is going to be biased in the opposite direction. Ultimately, whilst the power valve is turned off, the electrical power accumulated in the electromagnetic field around the inductive device is brought back into the system's circuit. The voltage that exists over the inductive element has changed to be precisely the inverse of the voltage on the inductive component in one phase, and the electrical current can continue to circulate for a brief period while the electrical switch remains switched on thanks to the received electrical power from the diminishing electromagnetic field. The current travels between the biasing forward diode element and the load, which is placed at the secondary side of the system throughout the system because of the voltage around the inductive element. The current can flow across the load until the subsequent period begins after the inductive device gives back a significant portion of its own produced electrical power to the circuit, and the voltage across the load keeps dropping. At that stage, the electrical power in the capacitance device takes over as the main source of electrical current.

4.2.2.2 Boost DC-DC Converter

A non-isolated step-up DC-DC converter with an output voltage higher than the input voltage is identified as a boost converter topology. The regulation of the duty cycle using passive and semiconductor devices is feasible, provided that the boost converter's output voltage remains higher than its input voltage [205], [206]. A typical boost DC-DC converter architecture is demonstrated in Figure 4.9. Boost DC-DC converters include precise switching strategies and inductive components, and their operation is based on several fundamental concepts. These converter designs' power transformation procedure can be clustered into several interrelated steps, including inductive element charging, transmission of power, and output filtering and control. DC-DC converter architecture, a DC voltage is produced on the inductive element whenever the power valve is activated. The electrical current that passes via the inductive element rises while the power switch is in the on position. The features of the inductive device cause the current flowing across it to change gradually. Because of this, the inductive element acts as an electrical power source by continuing to supply electrical current to the system even after the power valve is switched off. The load that is associated with the system experiences a voltage that is greater than the DC primary voltage of the system whenever the switching mechanism is switched on and off periodically. The output voltage of the system is altered and controlled by the PWM signal that is transmitted to the power valve. In this arrangement, the secondary side voltage rises in tandem with a boost in the duty cycle of the PWM signal supplied to the power valve. On the other hand, the secondary side voltage similarly decreases, considering that the PWM signal's duty cycle has decreased.

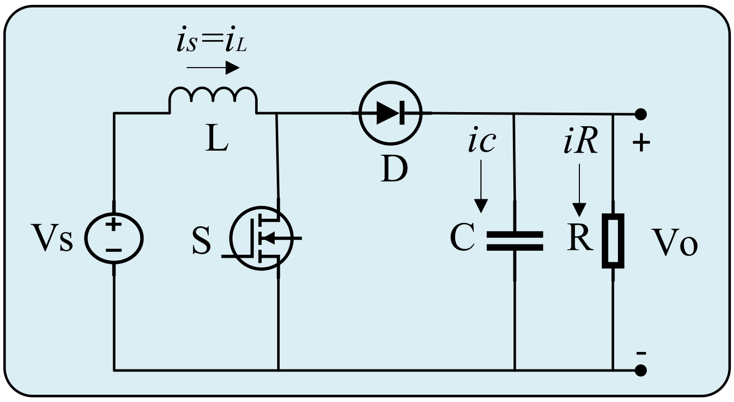

Figure 4. 9 Traditional DC-DC boost converter schematic [148], [207].

Boost DC-DC converters are essential components of present-day electrical power management techniques because of their outstanding effectiveness and small size, which meet the various energy requirements of today's technologies. The ongoing development of electrical power systems and technological electronic elements is probably going to improve these converter topologies' effectiveness characteristics and increase their range of purposes, guaranteeing their continued significance in the rapidly evolving field of electrical and electronics engineering.

4.2.2.3 Buck-Boost DC-DC Converter

A vital approach in power electronics, buck-boost DC-DC converter topologies provide a flexible way to control the output voltage. This converter can either step up (boost) or step down (buck) the primary side voltage. Furthermore, a non-isolated buck-boost converter architecture has a boost converter configuration featuring a secondary side voltage larger than the primary side voltage and a buck converter configuration with a secondary side voltage smaller than the primary side voltage. The duty cycle percentage dictates whether the converter design performs in boost or buck mode [208], [209]. In Figure 4.10, a traditional buck-boost DC-DC converter is demonstrated.

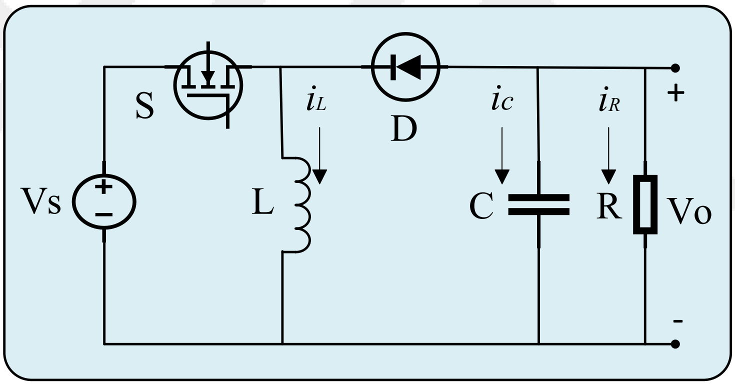

Figure 4. 10 Traditional DC-DC buck-boost converter schematic [210]–[212].

In a manner comparable to other DC-DC converter designs, buck-boost converter topologies are examined in two stages according to the cut-off or power transfer state of the power switching component. The manner in which the power storage and transformation procedures collaborate is essential to the performance of buck-boost converter designs. A power-switching device, an inductive element, the semiconductor diode, and a capacitor are the essential components found in such converter topologies. The buck and boost approaches are the two essential phases in which they operate. Whenever the power valve is activated, the system's inductive device is energized by the electrical current circulating through the inductive element from the primary side DC voltage source. Considering the diode element remains in the shutdown state, the current through the circuit is not transmitted to the other side of the diode in this circumstance. Since the inductive device's average voltage and the capacitor's current are zero in DC circuit frameworks, the inductor's voltage is reversely produced, and the capacitor's current travels in the other direction whenever the design's power switch is switched off. Whenever the power valve is off, the semiconductor diode is biased toward the front condition, which causes the circuit current to pass through to the other end. The capacitor, which formerly transmitted the electrical energy to the load side, is reenergized with the power passing from the inductive device in the second circumstance, while the coil supplied by the input source in the first scenario releases its energy on the capacitor and the load in this functioning step of the converter structure. This procedure continues by repeatedly turning the power switch on or off state. Similar to other DC-DC converter mechanisms, the buck-boost DC-DC converter structures use PWM technique to manage power switching.

Buck-Boost converter topologies have several benefits, such as the ability to function throughout a wide range of voltages and customization options. Implementing them in various applications, such as power systems, battery storage systems, renewable energy solutions, electrical vehicle systems, etc., is made easier by their interoperability with different input and output voltages. Additionally, they are recommended in many situations because of their outstanding effectiveness and tiny dimensions. Future developments in these converter topologies and their incorporation with advanced technology should significantly improve the efficiency of power facilities.

4.2.2.4 Cuk and SEPIC DC-DC Converters

The Cuk and SEPIC converter architectures stand out among the many varieties of DC-DC converter designs because of their flexibility and versatility. The output voltage of the non-isolated Cuk converter topology is polarized in the opposite direction as the source voltage, and it can be possibly greater or lesser [213]. The Cuk converter design is unique in that it can be used for both step-up and step-down applications. The key features of the Cuk converter architecture contain an excellent conversion proportion, capacitive isolation between the power source and the load device, buck-boost skill, persistent input and output currents, a low-side switch, continual source current, and capacitive power transfer [214], [215]. One of its key characteristics is the Cuk converter's capability to control the output voltage separately from the source voltage. Moreover, it is especially useful for specific applications because it generates a negative output voltage.

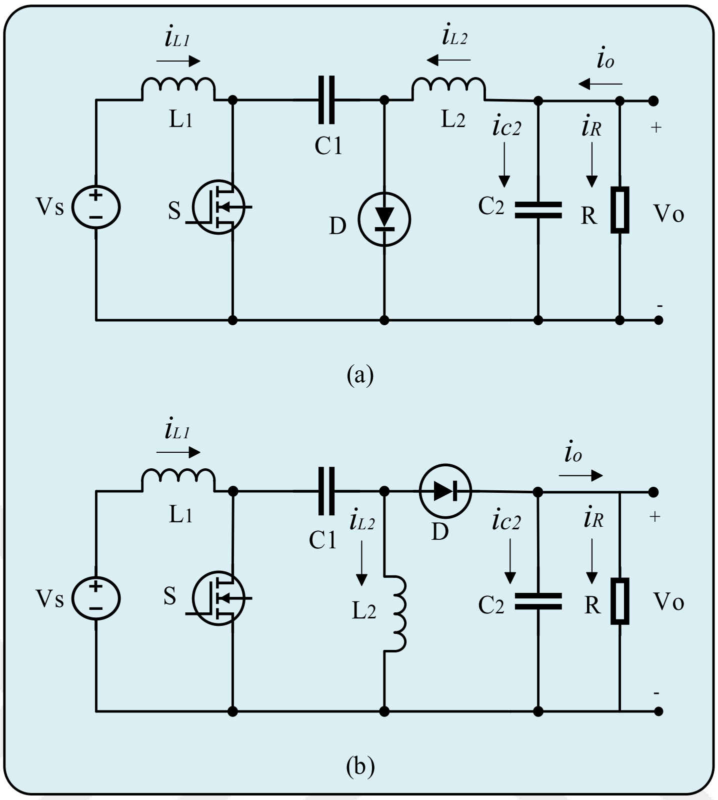

Figure 4. 11 The fundamental Cuk and SEPIC DC-DC converter schemes: (a) Cuk DC-DC converter, (b) SEPIC DC-DC converter [216]–[219].

A relatively straightforward cuk DC-DC converter design is demonstrated in Figure 4.11(a). A non-isolated SEPIC converter design functions by periodically turning a semiconductor-based power switch on and off. Its output voltage is either higher or lower than the original source voltage and does not invert polarization [213]. The SEPIC converter architecture is based on a boost-buck construction. It has minimal fluctuation in input current and provides an output voltage that is not inverted, contrary to the Cuk converter architecture. The bulk of traditional DC-DC converter topologies are less efficient than SEPIC [220]. An uncommon version of the SEPIC and Cuk converter has the capability to acquire two outputs with the same voltage yet distinct polarity [217], [221]. A relatively straightforward SEPIC DC-DC converter design is demonstrated in Figure 4.11(b).

PWM technique and a control approach are used to regulate the power switch's position in order to facilitate the effective operation of these converter topologies. The circuit can be split into two distinct parts based on whether the power switch in Cuk converter designs is switched on or off. As indicated by Figure 4.11(a), the $L1$ inductor becomes operational when the power valve is in the on position, permitting current to flow throughout it. In the aforementioned scenario, the reversely polarized diode corresponds to where the current passes whenever the power valve in the Cuk DC-DC converter arrangement is switched off. A voltage having identical polarization with the input source voltage charges the $C1$ capacitor owing to the closed loop to the diode's left side of the circuit. In the present instance, the power acquired in the circuit's previous mode is transferred by the $L1$ inductive element. Through the D diode, the load is supplied by the electrical power stored in the inductive element $L2$ and capacitor $C2$. The SEPIC DC-DC converter architecture's behavior is comparable to that of the Cuk DC-DC converter architecture and can be outlined as follows: With the left part of the circuit exhibiting positive polarization and the right part of the circuit having negative polarization, as illustrated in Figure 4.11(b), inductive component $L1$ is induced by the source voltage owing to current coming from the voltage source whenever the power valve is switched on. The capacitor $C1$ provides a current to the left of the system since it is charged in the initial situation. A voltage that is polarized in the contrary orientation from the primary side voltage source is generated over the inductive element $C2$ by the current in question. In the second circumstance, the electrical energy stored in inductive element $L1$ is oriented in the reverse direction from its original state whenever the power valve is switched off. In the present situation, current launches flowing into the system from the primary side voltage source and the inductive element $L1$. The capacitor $C2$ is initially energized by this streaming current and then discharged upon activation of the power valve. In a comparable manner to inductive component $L1$, inductive component $L2$'s polarization similarly varies. The circuit structure receives current from the $L2$ inductor in addition to the overall system current. The capacitor $C2$ is charged by the total of these currents passing on toward the circuit's output terminal, which has a voltage that is identical in polarization to the primary side voltage source. The load receives current flowing from the capacitor $C2$ in addition to the overall system current once it has been charged. The polarization of the input and output voltages is identical when they are acquired on the load. Likewise, in other converter structures, a control technique and a PWM technique are used to switch the power valve on and off, repeating this procedure continuously.

The Cuk and SEPIC DC-DC converter topologies, which provide adaptable and effective solutions for a variety of applications such as power systems, photovoltaic systems, DC microgrid applications, wind induction generators, electrical vehicle systems, are essential to the development of power control systems. Their importance in both personal technologies and manufacturing processes is highlighted by their capacity to adjust to changing input and output circumstances. Since semiconductor-based power electronics developments have tremendous potential to improve energy consumption and system effectiveness in a globe that is becoming more and more energy-aware, future studies ought to concentrate on enhancing the effectiveness, small dimensions, and serviceability of these types of converter designs. These converter topologies will keep coming to be crucial in determining how power networks develop in the years ahead, thanks to continuous advancement.

4.2.2.5 Zeta DC-DC Converter

The fundamental purpose of DC-DC converter designs is to alter a particular DC voltage value into a different one. The Zeta DC-DC converter topology is distinguished from other types of DC-DC converters by its special architectural characteristics and functionalities. Zeta converter topologies are non-isolated, fourth-order, non-linear DC-DC converters that have the capability to increase or decrease the applied source voltage [222], [223]. As is the case of Cuk and SEPIC converter architectures, zeta DC-DC converter structures have positive polarization for both the primary and secondary of the converter and can be adopted in both boost and buck operations. The zeta DC-DC converter structure, in other words, has input and output voltages with an identical polarity [224], [225]. Featuring a continuous feedback mechanism that permits higher voltage availability, greater workload transients, less output-voltage fluctuations, and more straightforward rectification, Zeta DC-DC converter designs operate superior to SEPIC DC-DC converter designs [226]. Because of its straightforward design and ability to function effectively as a buck-boost converter that produces non-inverted results [227], it regards utilized for numerous kinds of purposes, including high voltage conversion applications [228], photovoltaic platforms [229], [230], LED driver systems [231], energy controlling frameworks [232], and brushless DC motor drive structures [233]. Figure 4.12 exhibits a conventional DC-DC zeta converter layout.

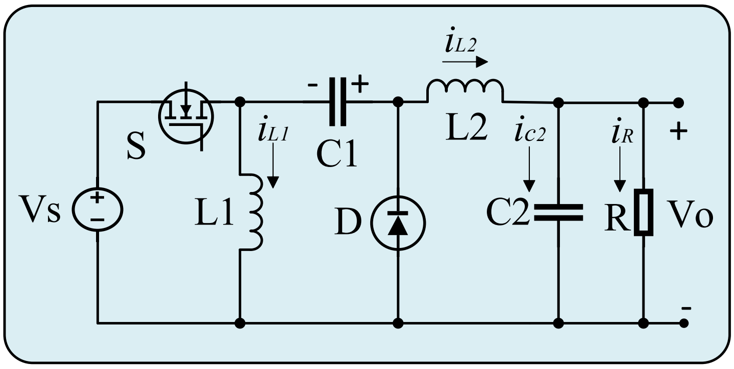

Figure 4. 12 Traditional Zeta DC-DC converter structure [225], [229], [234]–[236].

Generally, a switching component, semiconductor diode, two inductive components, and capacitor comprise a zeta DC-DC converter architecture. Power preservation and voltage control can be managed together with this arrangement. The Zeta DC-DC converter layout, which uses two inductive components, is appropriate for several purposes since it can support both voltage boost and buck capabilities. The switching mechanism is precisely controlled to regulate boost and buck forms, allowing for accurate output voltage modifications. In such a configuration, the diode D turns reverse-biased whenever the power valve is turned on, and the inductive devices $L1$ and $L2$ start charging via the power supply's same polarity. Stated otherwise, the power source voltage, or Vs, is the voltage across the two inductive devices. The voltage transmitted via the inductive elements $L1$ and $L2$ continues to be negative polarity while the power valve is off, and the semiconductor diode D is in the on condition [229]. The semiconductor diode device guides the current flow while the switching portion is off to ensure effective power transfer. To support both boost and buck processes, the Zeta DC-DC converter topology utilizes two inductive components, which are an essential part of its power storage system. The capacitor component ensures a steadier voltage profile by stabilizing the generated voltage and reducing oscillations.

4.3 Multilevel DC-DC Converters

Multilevel DC-DC converter topologies, an outstanding instance of sophisticated power transformation mechanisms, have become a game-changing technology in the field of semiconductor-based power electronic systems. These converter structures are specifically developed to reduce distortion caused by harmonics, increase power effectiveness, and make it easier to achieve higher voltage outputs. Multilevel converter designs operate on the fundamental tenet of strategically deploying many voltage ranges to provide the appropriate output voltage, which reduces switching mechanism tensions and improves the system's overall efficiency. It is possible to construct multilevel DC-DC converters as either isolated or non-isolated. Diode-clamped, flying-capacitor, and cascade H-bridge architectures are used in non-isolated multilevel DC-DC converter architectures. Designing the diode-clamped circuit is straightforward, and the cost of the converter is relatively little.

Nevertheless, increasing clamped diodes limits its application at high voltage levels. The flying capacitor converter architecture's limited efficacy has been found to be satisfactory. On the other hand, employing medium voltage is difficult due to the massive number of flying capacitors [237]. Flying capacitor converter structures have long been used in high voltage, high-power DC-AC applications. Flying capacitor multilevel converter topologies provide notable advantages in terms of efficiency and power production compared to several conventional configurations [238], [239].

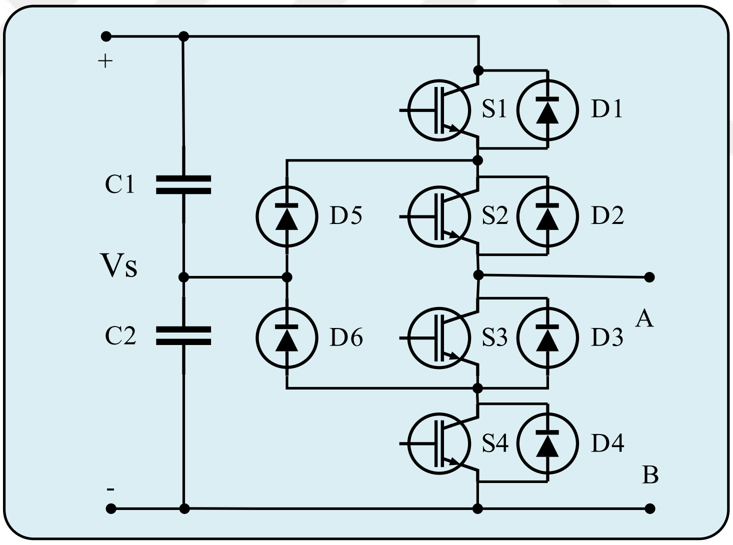

Figure 4. 13 Diode clamped multilevel DC-DC converter layout [240].

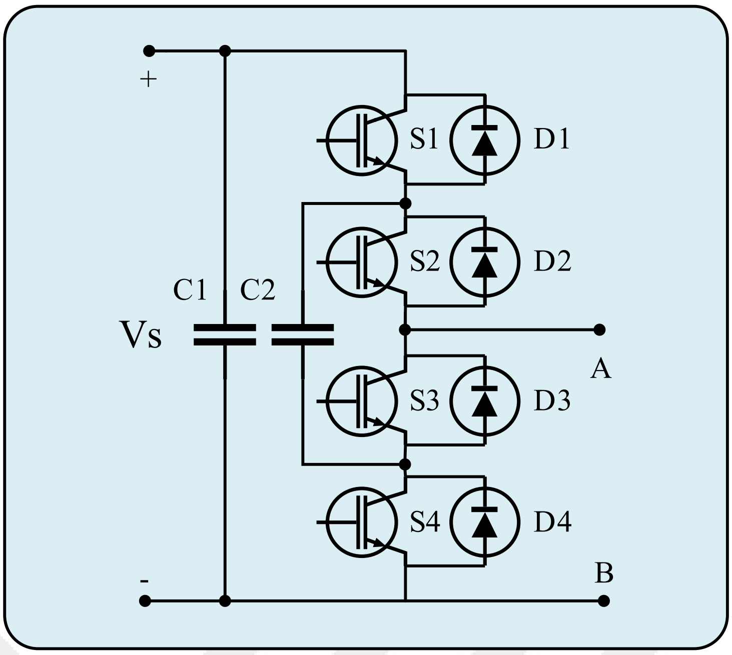

Figure 4. 14 Flying capacitor multilevel DC-DC converter layout [240].

The cascading H-bridge converter structure is one of the most often used multilevel converter technologies. An H-bridge that is cascaded is constructed by serially linking identical H-bridge topologies. The cascaded H-bridge DC-DC converter designs have the advantage of having the capability to accomplish high output voltage levels with superior quality. A cascaded H-bridge design composed of many individual cells is used to attain these outcomes. Moreover, cascaded H-bridge designs present a fundamental breakdown capability due to their exceptional adaptability, resulting in their appropriate implementation in appropriate mechanisms [241]. The cascaded H-bridge architecture is an outstanding candidate for medium and high-power applications because it can provide a very high output voltage whilst preserving exceptional signal consistency [242]–[244]. Multilevel DC-DC topologies diode clamped, flying capacitor, and cascade are illustrated in Figure 4.13, Figure 4.14, and Figure 4.15, respectively.

Numerous associated capacitors in the design's secondary side divide the system's primary side voltage into distinctive output voltage ranges in multilevel DC-DC converter architectures. Stated differently, the consecutive connections of capacitors produce distinct voltage ratings. In a diode-clamped multilevel DC-DC converter architecture, demonstrated in Figure 4.13, interconnected capacitors can split the primary side source voltage into three separate levels. The output voltage levels of diode-clamped multilevel DC-DC converter architectures are controlled by diodes, which essentially clamp the voltage to predetermined values. Power switches (MOSFETs, IGBTs, etc.), diodes, and capacitors constitute a diode-clamped multilevel DC-DC converter structure. Switching devices regulate the current switching to reach the required voltage level. For effective functioning, fast-switching products must be chosen. Diode components are essential in this structure because they clamp the output voltage at particular values. Thanks to them, every degree of voltage is successfully improved or restricted. The output is stabilized, and the voltage is smoothed using capacitors. Usually, a capacitor is connected to every voltage degree in the converter to reduce voltage fluctuations and enhance efficiency. Minimal harmonic distortion, excellent effectiveness, high voltage and power transportation, and less stress due to temperature are some of the unique benefits of diode-clamped multilevel DC-DC converter topologies. Thanks to these advantages, they are especially well-suited for utilization in electric vehicles, power systems, energy storage systems, renewable energy systems, and other industrial applications. Nevertheless, there are still obstacles that need to be resolved, such as their intricate architecture, increased production expenses, and possible voltage balance problems. The functionality and suitability of diode-clamped multilevel DC-DC converters are expected to continue to increase with improvements in semiconductor technologies and control strategies, increasing their employment in outstanding performance power systems of tomorrow.

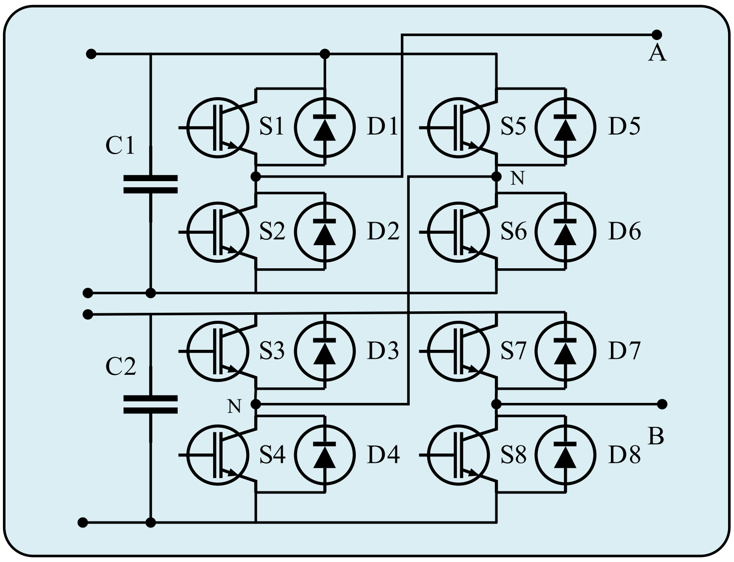

Figure 4. 15 Cascade multilevel DC-DC converter layout [240].

In a flying capacitor multilevel DC-DC converter architecture, as demonstrated in Figure 4.14, desired secondary side voltage levels are achieved by distributing voltage across the linked capacitors. The capability of the flying capacitor multilevel DC-DC converter architecture to provide many different voltages without the need for extra restraining components such as diodes makes it very appealing. This converter architecture uses flying capacitors that are dynamically swapped into the circuit to provide the required voltage objectives. Despite flying capacitor multilevel DC-DC converters having drawbacks with capacitor voltage regulation and operational intricacy, they are particularly helpful in situations requiring high voltage and effective performance. High voltage, high-power systems needing effective operation and less harmonic distortions might find a convincing answer in the flying capacitor multilevel DC-DC converter topologies. It is very helpful in industrial power systems, electric vehicles, energy storage mechanisms, and renewable energy systems since it can supply varied voltage levels. However, some issues, such as capacitor voltage balance, control intricacy, and system costs, need to be properly considered. With continuous improvements in management techniques and the technology behind semiconductors, the flying capacitor multilevel DC-DC converter architecture might be a significant part of power electronics in the near future.

A cascade multilevel DC-DC converter topology is another configuration of a multilevel DC-DC converter where several H bridge converters with various power sources are sequentially linked one after the other, illustrated in Figure 4.15. A sophisticated approach is represented by cascade multilevel DC-DC converter topologies, which employ multiple phases of converters in series to provide larger output voltage levels with less harmonic distortion and more effectiveness. A tiny percentage of the primary side voltage is stepped up or down by each of the many linked components that make up cascade multilevel DC-DC converter systems. Each phase is usually linked in serial to combine the distinct contributions of every step and produce a high output voltage. A complex solution for applications that require significant power needing high voltage converting with enhanced effectiveness, less harmonic distortion, and adaptability is a cascade multilevel DC-DC converter structure. They are a desirable option for contemporary power electronics infrastructure due to their capacity to manage high voltages via a sequence of stages functioning at lower voltages. For the system to function at its best, issues with design, including isolation, temperature control, synchronization, and electromagnetic interference reduction, must be appropriately handled. Cascade multilevel DC-DC converter designs have the potential to be a significant component of power transformation industries in the future, especially in electric vehicles, renewable energy frameworks, uninterruptible power supply mechanisms, and commercial power supplies, provided the controlling procedures and semiconductor manufacturing techniques keep continuing to move forward. Table 4.1 provides a comparative analysis of the conventional DC-DC converter topologies discussed in this chapter, evaluating them based on the number of components and elements utilized, their respective application domains, as well as their power and voltage characteristics.

Table 4. 1 Comparison of traditional DC-DC converter topologies.

Converter Topology	Isolation	Component Count and Complexity	Typical Applications	Power and Voltage Range
Bridge (HB, FB, Single Active Bridge, Dual Active Bridge, Boost Half-Bridge)	Isolated	High number of switches, transformers, and passive elements; complex control	High power applications such as grid interfaces, HVDC, renewable energy systems	Medium to high power; MV to HV
Forward	Isolated	Moderate complexity with transformer, switch, and diode count	Medium power supplies for industrial and telecom	Medium power; MV
Flyback	Isolated	Low component count; single switch and transformer	Low power applications, battery chargers, small power supplies	Low to medium power; LV to MV
Resonant (Resonant Boost, Resonant SEPIC, Hybrid Resonant)	Isolated	Complex due to resonant tank circuits and switches	High efficiency applications requiring soft switching	Medium power; variable voltage
Push-Pull	Isolated	Moderate complexity; two switches and a center-tapped transformer	Medium power converters, low-cost isolated supplies	Medium power; MV

Buck	Non-Isolated	Simple topology with one switch and diode/inductor	Step-down DC-DC applications in battery-powered devices	Low to medium power; LV to MV
Boost	Non-Isolated	Simple; single switch, diode, inductor	Step-up applications such as LED drivers, power factor correction	Low to medium power; LV to MV
Buck-Boost	Non-Isolated	Moderate complexity; combines buck and boost elements	Inversion or regulation applications	Low to medium power; LV to MV
Cuk	Non-Isolated	Higher complexity; requires additional inductors and capacitors	Applications needing inverted output voltage and low ripple	Low to medium power; LV to MV
SEPIC (Single-Ended Primary Inductor Converter)	Non-Isolated	Moderate complexity; multiple inductors and capacitors	Applications requiring output voltage above, below, or equal to input	Low to medium power; LV to MV
Zeta	Non-Isolated	Moderate complexity; similar to SEPIC with different topology	Power regulation where voltage conversion flexibility is needed	Low to medium power; LV to MV

4.4 Summary

The DC-DC converter topologies are thoroughly evaluated in this section. To perform this assessment, DC-DC converter designs are separated into non-isolated DC-DC converter topologies and isolated DC-DC converter topologies. DC-DC converters have become essential parts of contemporary power and electrical systems. These converters have evolved significantly, becoming more portable, efficient, and versatile due to the constant quest for greater energy efficiency and the growth of high-performance, renewable, and portable applications. Fundamentally, DC-DC converters reduce energy losses while regulating voltage precisely and steadily, allowing a wide range of systems and devices to function seamlessly, from sophisticated industrial power infrastructures to low-power consumer appliances. High efficiency, which minimizes energy loss and lessens heat dissipation, is the main benefit of DC-DC converters. This results in longer device lifecycles and increased operational dependability. This feature is particularly important in applications like power systems, electric vehicles, renewable energy mechanisms, and portable electronic applications where energy saving and temperature control are crucial. Furthermore, in renewable energy systems, DC-DC converters play a crucial role in converting variable input voltages from solar arrays, wind turbines, and various other energy sources into steady, suitable power, which improves the integration of sustainable energy technological advances. Future developments in digital control methods and integrated circuit structure will likely influence the ongoing development of DC-DC converter technologies. These converters will be able to satisfy the increasingly complicated needs of contemporary power systems thanks to the integration of advanced digital controllers and the shrinking of componentry, which will allow for better levels of effectiveness and flexibility. Future DC-DC converters are also expected to offer improved programming capabilities, which will allow them to be tailored to a wider range of specialized purposes and accomplish even greater levels of performance due to continuous advancements in semiconductor innovations and materials science. The development of DC-DC converters is related to the growing need for low-energy, sustainable approaches in various industries. These converters will keep pushing the limits of energy conversion efficiency by emphasizing more sophisticated switching strategies, lower-loss parts, and improved control systems. Therefore, in a world where energy control, sustainability, and minimizing environmental effects are becoming increasingly important, DC-DC converters will continue to be essential to the optimization of energy circulation. In summary, it is impossible to overestimate the influence of DC-DC converters on the development of power electronics and energy networks as they are a technical and environmental pillar in the continuous quest for sustainability and energy effectiveness.

CHAPTER V
MMC THEORY

5.1 Introduction

In contemporary power systems, the need for advanced technologies that enhance energy efficiency, transmission reliability, and operational sustainability has never been more critical. Among the most promising innovations in power conversion technologies is the MMC, which has garnered significant attention due to its exceptional performance in high-power and high voltage applications. Prof. Marquardt initially recommended MMC technology in a German patent in 2001 [16]. The MMC's inherent modularity, scalability, and adaptability make it a key component in systems requiring efficient conversion of electrical power, such as HVDC power transmission networks, renewable energy integration, and electric vehicle technologies. Multiple MMC topological modifications were put forward in earlier articles, such as a one-phase to a one-phase MMC structure [245] and a one-phase into three separate phases MMC structure [246]. These converter topologies were suggested to obtain traction purposes. Additionally, those studies demonstrated a simple single-phase framework incorporating a fundamental AC and DC management system readily adaptable to the three phases of MMC architecture [247]. The MMC stands in contrast to traditional converter topologies, offering distinct advantages in terms of output quality, system fault tolerance, and flexibility. However, realizing the full potential of the MMC necessitates the development of sophisticated control strategies and robust management frameworks to mitigate the complexities inherent in its operation. This chapter aims to examine the MMC's structural composition, underlying principles of operation, key advantages, and contemporary applications.

5.2 Traditional MMC Theory

The MMC technology stands as a transformative technology in power electronics, renowned for its efficiency, scalability, and high-quality performance in handling high-power systems. Incorporating renewable energy power systems and large-scale industrial motor control technologies is particularly valuable in HVDC power systems.

The MMC technology is a modern solution to the challenges posed by conventional power conversion technologies. Its underlying principles are anchored in a modular design that enhances its adaptability and reliability across various demanding applications, making it an essential component in contemporary power systems. The MMC technology was conceptualized as an innovative alternative to traditional VSC technologies, which were constrained by power handling capacity and efficiency when operating at high voltages. MMC technology differentiates itself from its predecessors' modular architecture, which uses multiple identical SMs connected in series to generate output voltages. This modular framework allows for scalable and efficient power conversion and introduces a level of fault tolerance that enhances operational reliability. Over time, MMC technology has expanded its reach, finding applications in HVDC systems, renewable energy systems, and industrial motor drive technologies, all of which require the ability to manage substantial power without compromising quality.

5.2.1 MMC Structure

MMC technology is defined by its unique modular architecture, as indicated in Figure 5.1, wherein multiple SMs (or cells) are connected in series to achieve high voltage and power output levels. This modular design enables a highly flexible and scalable solution to power conversion challenges. The distinctive feature of the MMC is its modular design, wherein each phase leg is composed of multiple SMs connected in series. These SMs contain capacitors and semiconductor-based power switches, and their series arrangement determines the overall output voltage. This modular approach makes the MMC technology highly scalable, enabling it to handle significant power levels while avoiding using heavy and space-inefficient components such as large transformers. Moreover, the fault-tolerant nature of this design ensures that the failure of one or more SMs does not incapacitate the converter but instead results in a controlled reduction in performance, preserving the system’s functionality. MMC concept outlines a DC-to-three-phase converter structure composed of interconnected SMs, inductances within each arm, and HB and FB SMs. The standard MMC architecture is highly flexible and capable of operating as an inverter (DC to AC) and a rectifier (AC to DC), making it suitable for a broad spectrum of applications.

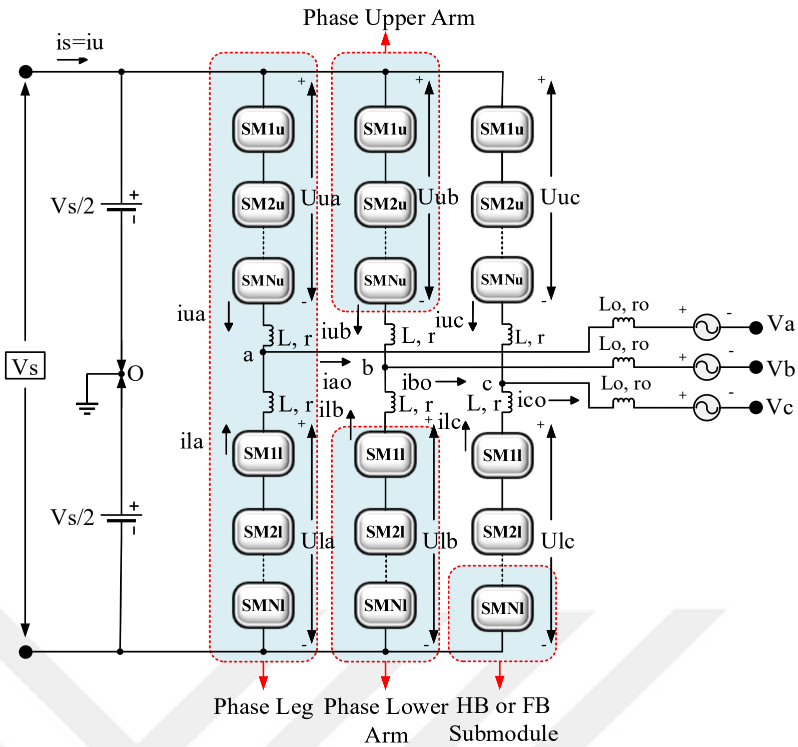

Figure 5. 1 Conventional MMC Structure.

As shown in Figure 5.1, each phase in the traditional MMC structure comprises two main components: the upper and lower arms. Each arm contains an arm inductor (L, r) and a series of HB or FB SMs. The connection between the AC network and the converter is facilitated by a phase inductor (Lo, ro), which links the three-phase AC terminals (Va, Vb, Vc) to the midpoints of each phase leg (a, b, and c). Arm inductors (L) restrict the circulation of fault currents triggered via DC terminal failures and arm current harmonics that inherently pass within phase legs of MMC [1], [82]. In essence, the DC connections are made between each phase's upper and lower arms, while the AC connection is established at the midpoint of each phase. This configuration, combined with appropriate DC and AC voltage levels, allows the arms to produce controlled voltages at specific points, thereby ensuring the proper flow of AC and DC currents for the conversion process. Each SM is composed of a DC energy source, typically in the form of a capacitor, and switching elements such as IGBTs and MOSFETs. These SMs operate independently, each contributing a portion of the total output voltage. The modular nature allows for easy scaling of the system by adding more SMs, thus enabling high voltage operation while maintaining low individual voltage ratings for each SM. Power electronics in MMC systems rely heavily on high-performance switching devices such as IGBTs, which facilitate the conversion of DC power into AC. These devices control the voltage output of each SM, ensuring that the overall converter output is a smooth, multi-level sinusoidal waveform. Each SM integrates capacitors to store energy and maintain voltage stability. The capacitors help smooth out voltage fluctuations and support the dynamic power balancing across the system. Effectively managing these capacitors is critical for ensuring the converter’s efficiency and long-term stability.

The operating principle of the MMC revolves around the interaction of the individual SMs to form a composite AC voltage output. In essence, each SM generates a small voltage level, and the aggregate output is achieved by combining these voltage contributions. The MMC can produce a high-quality AC waveform with minimal harmonic distortion through precise control of the switching elements. A key characteristic of the MMC is its ability to independently control the voltage of each submodule, which allows for the creation of a staircase-like voltage waveform at the converter output. This multilevel voltage structure significantly reduces the harmonic content compared to traditional two-level converters. Furthermore, the ability to balance individual submodules' voltages ensures the entire system's stability and reliability, especially under varying load conditions.

Various modifications of the MMC architecture have been explored in the literature, each tailored to enhance specific functionalities or address particular challenges within power systems [18], [248]. These alternative topologies are illustrated in Figure 5.2. From a broader MMC perspective, one key goal is optimizing operational efficiency through distinct configurations of converter legs and arms. Hybrid arrangements of arms and legs are pivotal in balancing factors such as cost, energy loss, and fault-tolerant behavior in DC systems [124]. The Alternate Arm Converter (AAC), depicted in Figure 5.2(a), has gained attention as a viable alternative to traditional MMCs for HVDC applications due to its reduced submodule count, lower energy storage demands, and robust DC fault tolerance [249]. Particularly, in terms of both design and control, the AAC provides superior DC fault tolerance, placing it in the same category as advanced MMC designs [250].

Each arm of the AAC architecture depicted in Figure 5.2(a) is made up of a number of linked FBSMs, an inductor, and a direction switch [125], [250]–[253]. The direction switch chooses the electrically powered arm, and the FBSMs produce multilevel voltages. This ensures that the lower arm provides a minus half period of AC voltage, whereas the upper arm of the design provides the positively charged AC voltage halfway period. Consequently, compared to conventional MMC setups, converter losses are significantly decreased [125]. The AAC-MMC introduces a paradigm shift in multilevel power conversion by dynamically reconfiguring its conduction paths to minimize operational losses. In this architecture, each phase leg alternates between upper and lower arm conduction via high-speed director switches, effectively decoupling the dc and ac current paths during switching intervals. This unique operational modality not only curtails redundant submodule switching but also alleviates voltage stress across semiconductor devices, a persistent limitation in conventional MMCs. Empirical studies suggest that the AAC-MMC's discontinuous arm operation enhances transient response during asymmetric grid faults, though its efficacy hinges on precise synchronization of director switch commutation. A salient challenge lies in mitigating circulating currents induced by arm alternation, which necessitates advanced harmonic suppression techniques.

The DC-DC Push-Pull MMC, presented in Figure 5.2(b), requires fewer submodules to achieve the same DC voltage level as conventional MMCs. A center-tapped single-phase transformer is used to connect the converter's phase components to the AC system, providing galvanic isolation. This configuration is well-suited for applications that require high voltage and low-current operation, as it reduces the number of power semiconductor switches and passive components while maintaining the flexibility of the MMC [254]. Emerging as a transformative solution for high-power DC-DC conversion, the push-pull MMC topology synergizes the voltage-multiplying capability of modular multilevel architectures with the inherent fault tolerance of push-pull switching. This configuration employs complementary operation of interleaved SM clusters, where alternating conduction phases achieve continuous power transfer while maintaining balanced capacitor voltages. The topology's distinctive feature lies in its magnetic coupling - a high-frequency transformer provides galvanic isolation while enabling voltage ratio adjustment through winding turns. Unlike conventional MMC-based DC-DC converters, the push-pull variant eliminates the need for bulky DC-link capacitors by leveraging phase-shifted arm current modulation.

The Flying Capacitor MMC, as shown in Figure 5.2(c), incorporates capacitors placed between the upper and lower arms in each phase. These cross-connected capacitors help balance the power between the arms and reduce voltage ripples in the capacitors, without increasing the common-mode voltage in the converter [237], [255]. The FC-MMC represents a transformative advancement in multilevel power conversion, uniquely integrating the voltage-splitting capabilities of flying capacitors with the modularity of MMC architectures. This topology employs distributed flying capacitors within each SM, enabling dynamic voltage balancing through interleaved charge redistribution, a feature absent in conventional MMCs. The FC-MMC's distinctive operation hinges on decoupled capacitor charging cycles, where sequential switching states autonomously regulate voltage sharing without relying on centralized control algorithms. Recent experimental validations demonstrate their superior performance in HVDC applications, particularly in mitigating voltage imbalance during asymmetrical grid faults. However, the topology introduces nonlinear dynamics in capacitor charge-discharge cycles, necessitating advanced MPC strategies to stabilize transient responses.

Figure 5.2(d) illustrates the schematic of the active cross-connected MMC topology, featuring three phase units, each comprising a pair of upper and lower arms interconnected by a bridging branch. Each arm is partitioned into two parallel sub arms, with their junction node linked to the central bridge branch. The external terminals of the sub arms interface with the DC or AC distribution bus via current-limiting inductors. The number of series-connected half-bridge submodules per arm and bridging branch is dictated by the operational voltage requirements and the withstanding capability of individual semiconductor devices. Typically, the bridging branch mirrors the submodule count of the main arms, with identical voltage and current specifications across all submodules to ensure uniform power distribution [256]. The active cross-connected MMC introduces a paradigm-shifting architecture in high-power energy conversion by integrating dynamically controlled cross-branches between conventional upper and lower arms. Unlike passive cross-connection methods, this topology employs actively switched SMs within the bridging paths, enabling real-time power flow redirection and enhanced fault current management. Each phase leg comprises two primary arms (upper/lower) and an active cross-branch, with all three paths containing identical half-bridge or full-bridge SMs rated for matched voltage/current levels.

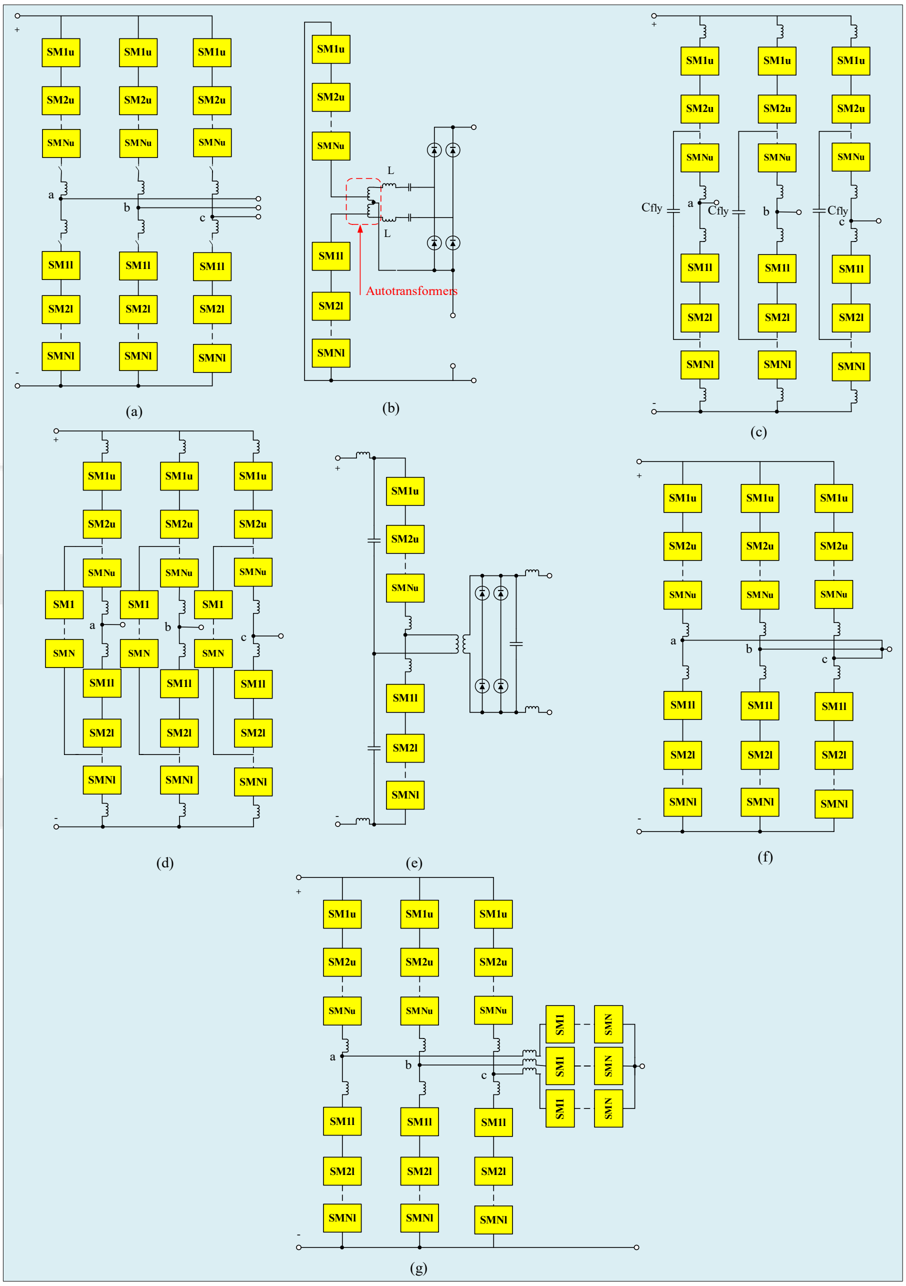

Figure 5. 2 Various MMC designs: (a) AAC MMC, (b) DC-DC push-pull MMC, (c) Flying-capacitor MMC, (d) Active cross-connected MMC, (e) DC-DC MMC with high-frequency transformer, (f) Conventional MMC, (g) MMC with output SMs.

Figure 5.2(e) illustrates the implementation of a DC-DC converter design with a one-phase MMC design in an HB arrangement, utilizing a one-phase semiconductor rectifier and a transformer. It is easier to link medium voltage and high voltage systems using this design [66], [257]. The high voltage section incorporates two series-connected stacks of HB SMs arranged in a single-phase MMC structure, complemented by arm inductances. The transformer's primary side is placed between a central phase point and a virtual neutral, derived using two capacitors connected across the DC bus. On the low-voltage side, a conventional diode-based full-bridge rectifier links the transformer secondary to an energy buffer capacitor. To suppress AC ripple and restrict oscillatory currents to within the converter, passive damping circuits composed of inductors and resistors are employed on both sides. The conventional three-phase MMC architecture, as shown in Figure 5.2(f), can also function as a DC-DC converter design when a single terminal is interconnected with every other terminal. In this setup, a control mechanism is needed to regulate the DC output voltage while circulating currents help balance the capacitor voltages [258]. Lastly, an improved version of the MMC design is shown in Figure 5.2(g), where three more branches are inserted across the secondary terminal and the middle point for every phase of operation. By separating the inner circulatory current with the primary and secondary terminal DC currents, these additional arms reduce the complexity of the control. This improved topology offers significant benefits over alternative designs, including a smaller AC filter, fault ride-through capabilities for both DC and AC-side failures, and lower switching power ratings [259]. Regarding energy dissipation, fault tolerance, system adaptability, and control complexity, all of the preceding MMC architectures have unique benefits. By utilizing these topologies, engineers can enhance HVDC systems' efficiency, fault management, and scalability. The illustrated topology presents a distinctive variation of the MMC, where each phase leg comprises a cascaded arrangement of upper and lower arm SMs, and the converter output is augmented with additional output-stage SMs. These output SMs are positioned beyond the transformer interface and are directly involved in shaping the final AC output waveform. Such a configuration enhances voltage scalability and waveform quality while facilitating local voltage regulation and improved fault-handling capabilities. The arms of the converter include energy storage capacitors and switching elements to generate stepped voltages, whereas the output submodules contribute to finer waveform resolution and dynamic compensation under varying load or grid conditions. This design is particularly suitable for applications requiring modularity, redundancy, and high-power quality such as MV drives, HVDC converters, and advanced solid-state transformers where space and efficiency constraints preclude bulky filtering. The inclusion of output SMs, while increasing the complexity of control and coordination, offers significant benefits in terms of operational flexibility and performance reliability.

5.2.2 Mathematical Model of MMC

The mathematical modeling of the MMC is a crucial aspect in understanding its operation, ensuring efficient power conversion, and optimizing performance in high voltage applications and additional industries where MMC technology can be implemented with great effectiveness. This section presents a comprehensive mathematical formulation of the conventional MMC topology, which also serves as a foundational basis for deriving the mathematical representation of the proposed DC-DC MMC configuration.

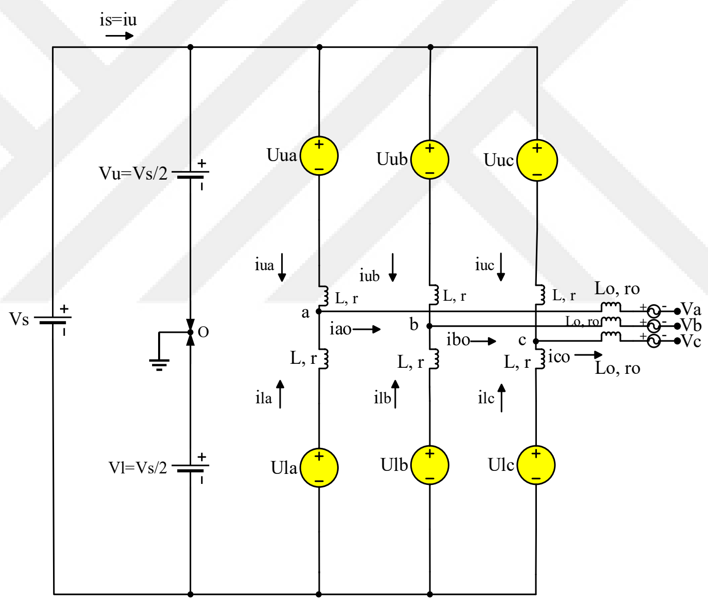

Figure 5. 3 MMC arrangement incorporating the arms' ideal voltage sources.

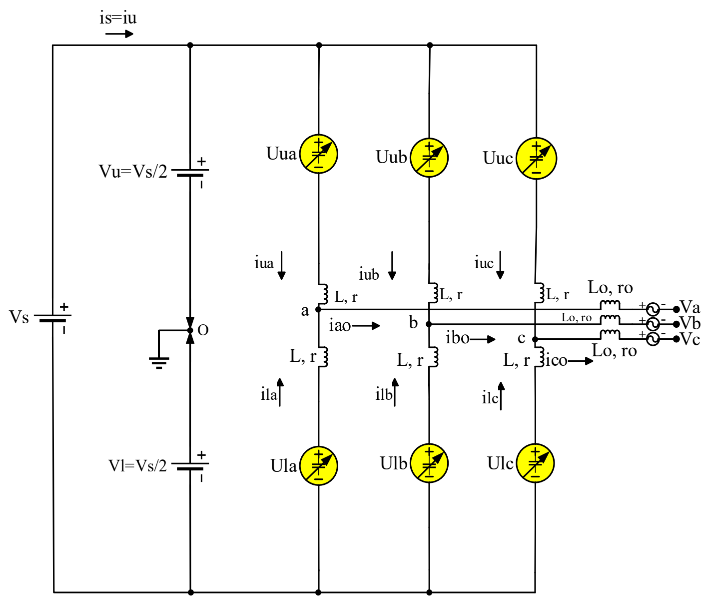

Figure 5. 4 MMC arrangement with the arms' non-ideal voltage sources.

To successfully achieve the mathematical analysis of the typical MMC architecture shown in Figure 5.1, clarified equivalent circuits should be established. Figures 5.3 and 5.4 demonstrate the MMC arrangement incorporating the arms' ideal voltage sources and MMC arrangement with the arms' non-ideal voltage sources equivalent circuit models of the conventional MMC architecture, respectively. The MMC topology's phases all have the same structure; hence, it is acceptable to do mathematical analysis for one of them because the other phases will require identical mathematical analysis.

The analogous one-phase circuit, shown in Figure 5.5, is used as the foundation for modeling the conventional MMC architecture, as illustrated in Figure 5.1. The a-phase of the MMC serves as the primary reference for circuit analysis, with similar methods applicable to the remaining phases (phase-b and phase-c). Given the large number of cells in the MMC, the mathematical modeling process can become highly complex and simulating such a system can be computationally expensive. Numerous methods have been put out in scientific literature to solve this problem by simplifying the model and reducing the amount of time needed for simulations. The operation of the MMC is determined by the number of switching submodules, which can be approximated as ideal, continuous DC voltage sources. In Figure 5.3, a simplified equivalent model of a three-phase MMC is presented, where the voltages at the terminals of the SMs in each arm are aggregated into a single equivalent voltage source [121], [123], [260]–

[263]. This approach reduces the complexity of the model while preserving the essential features of the converter's operation.

Additionally, Figure 5.4 illustrates a representation in which each MMC arm is modeled as a capacitor with a time-varying sinusoidal capacitance. The voltage across this capacitor is treated as a controllable voltage source, which can dynamically adjust to fluctuations in the system's voltage requirements. The power produced in each arm is used to regulate the capacitor voltage, compensating for variations in the voltage levels over time. The top and bottom arm power are adjusted to match the load's active power requirements. Furthermore, to keep the balance across the top as well as the bottom arms, the power differential between them is regulated. This voltage equilibrium ensures the converter operates symmetrically and efficiently, optimizing the system's overall performance. The MMC can maintain stable operation through these control mechanisms while accommodating varying load conditions.

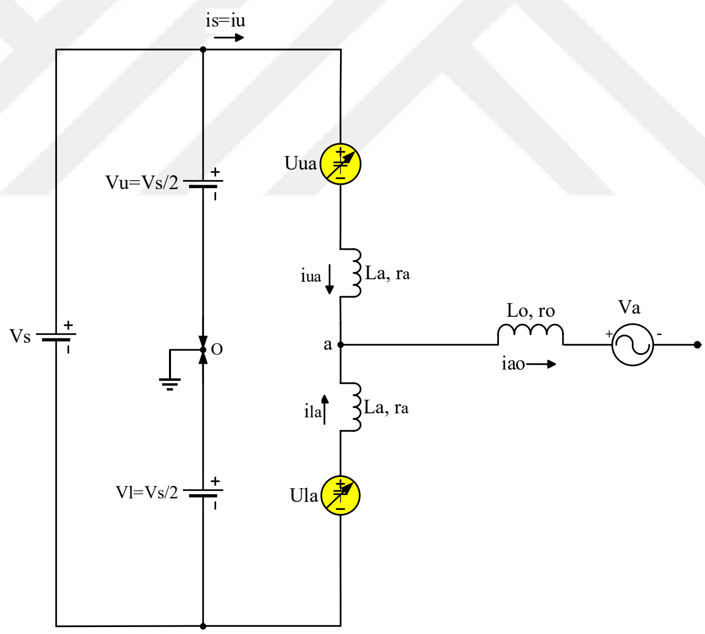

Figure 5. 5 The traditional MMC's one-phase equivalent.

A one-phase corresponding circuit of the traditional MMC design is produced, as shown in Figure 5.5, for a less complicated mathematical analysis of the traditional three-phase MMC topology, which is shown in Figure 5.1.

Considering Kirchhoff Voltage Law (KVL) [18], [121], [125], [261], [264]–[267] alongside Figure 5.5, the following expressions have been provided:

$$\frac{V_S}{2} - U_{ua} - r_a i_{ua} - L_a \frac{di_{ua}}{dt} - v_a - r_o i_{ao} - L_o \frac{di_{ao}}{dt} = 0 \quad (5.1)$$

$$\frac{V_S}{2} - U_{ua} - r_a i_{ua} - L_a \frac{di_{ua}}{dt} = v_a + r_o i_{ao} + L_o \frac{di_{ao}}{dt} \quad (5.2)$$

$$-\frac{V_S}{2} + U_{la} + r_a i_{la} + L_a \frac{di_{la}}{dt} - v_a - r_o i_{ao} - L_o \frac{di_{ao}}{dt} = 0 \quad (5.3)$$

$$-\frac{V_S}{2} + U_{la} + r_a i_{la} + L_a \frac{di_{la}}{dt} = v_a + r_o i_{ao} + L_o \frac{di_{ao}}{dt} \quad (5.4)$$

The phase-a upper and lower arm voltages are obtained from Figure 5.5 by

$$V_u = \frac{V_S}{2} = U_{ua} + L_a \frac{di_{ua}}{dt} + r_a i_{ua} + L_o \frac{di_{ao}}{dt} + r_o i_{ao} + v_a \quad (5.5)$$

$$V_l = \frac{V_S}{2} = U_{la} - L_a \frac{di_{la}}{dt} - r_a i_{ua} - L_o \frac{di_{ao}}{dt} - r_o i_{ao} - v_a \quad (5.6)$$

The upper and lower arm currents of phase-a are determined based on the one-phase corresponding circuit demonstrated in Figure 5.5 by

$$i_{ua} = \frac{i_{ao}}{2} + i_{CC} \quad (5.7)$$

$$i_{la} = \frac{i_{ao}}{2} - i_{CC} \quad (5.8)$$

Here is where i_{CC} signifies the MMC topology's circulation current. The phase-a AC circuit current is provided as

$$i_{ao} = 2i_a + 2i_{cmc} \quad (5.9)$$

Here is where i_a signifies the phase-a AC secondary side current and i_{cmc} signifies the common-mode-current of the MMC system.

In a comparable manner, the current that passes through the top and lower DC terminals of MMC topology is provided by

$$i_u = i_{ua} + i_{ub} + i_{uc} = 3i_{cmc} \quad (5.10)$$

$$i_l = i_{la} + i_{lb} + i_{lc} = 3i_{cmc} \quad (5.11)$$

The result of subtracting the arm's upper voltage in (5.5) from the lower arm's voltage in (5.6) is

$$V_S = u_{ua} + u_{la} + L_a \frac{d(i_{ua} - i_{la})}{dt} + r_a(i_{ua} - i_{la}) \quad (5.12)$$

In a similar vein, the addition of the upper and lower arm voltages in (5.5) and (5.6) yields the following expression:

$$0 = U_{ua} - U_{la} + L_a \frac{d(i_{ua} + i_{la})}{dt} + r_a(i_{ua} + i_{la}) + 2L_o \frac{di_{ao}}{dt} + 2r_o i_{ao} + 2v_a \quad (5.13)$$

Equation (5.13) can be rearranged to get the distinction between phase-a's upper and lower voltages in the following manner:

$$U_{ua} - U_{la} = L_a \frac{d(i_{ua} - i_{la})}{dt} + r_a(i_{ua} - i_{la}) - 2L_o \frac{di_{ao}}{dt} - 2r_o i_{ao} - 2v_a \quad (5.14)$$

Given that it causes losses in the structure, circulating current is especially critical in MMC architecture. Therefore, the circulating current needs to be mathematically described in MMC implementations. The converter legs are the only area where the circulating AC flows. A circulating current's amplitude in phase-a is established by

$$i_{CC} = \frac{i_{ua} - i_{la}}{2} \quad (5.15)$$

According to (5.10) and (5.11), the common-mode current intensity (i_{cmc}) is determined in the following manner:

$$i_{cmc} = \frac{i_u + i_l}{6} \quad (5.16)$$

Whenever (5.9) and (5.16) are substituted into (5.13), a particular expression is produced:

$$0 = U_{ua} - U_{la} + 2L_a \frac{di_{cmc}}{dt} + 2r_a i_{cmc} + 2L_a \frac{di_a}{dt} + 2r_a i_a$$
$$+4L_o \frac{di_{cmc}}{dt} + 4r_o i_{cmc} + 4L_o \frac{di_a}{dt} + 4r_o i_a + 2v_a \quad (5.17)$$

The AC output current is equal transmission between the upper and lower arms. The AC secondary side current of phase-a has been established by (5.7) and (5.8).

$$i_a = \frac{i_{ua} + i_{la}}{2} - i_{cmc} \tag{5.18}$$

5.2.3 Submodule Topologies of MMC

MMCs have emerged as pivotal technology in high-power applications due to their modular structure, scalability, superior efficiency, and harmonic reduction performance. The fundamental building blocks of MMCs are the SMs, which are connected in series to form a multilevel converter. Each SM typically includes a capacitor and two power switches (e.g., IGBTs or MOSFETs), and the arrangement of these SMs defines the voltage levels that the converter can generate. The design of these SMs significantly influences the converter's performance, reliability, and operational efficiency. Since the inception of the MMC concept in literature, researchers have proposed and refined a multitude of SM topologies. As illustrated in Figure 5.6, SM structures can be assigned to two main groups according to the output voltage level: single-source two-level SM topologies and multiple-source multi-level SM topologies [124]. A significant factor driving the surge of interest in MMC technology can be attributed to the significant advancements in semiconductor technology. SM structures, which constitute the foundational element of MMC systems, are composed of semiconductor-based power-switching devices. These components are particularly valued for their exceptional characteristics, such as operating at elevated temperatures and reducing switching losses. MOSFETs and IGBTs, especially those incorporating cutting-edge elements, including silicon carbide and gallium nitride, are employed in MMC architecture due to their high switching capabilities and superior performance in high-power applications.

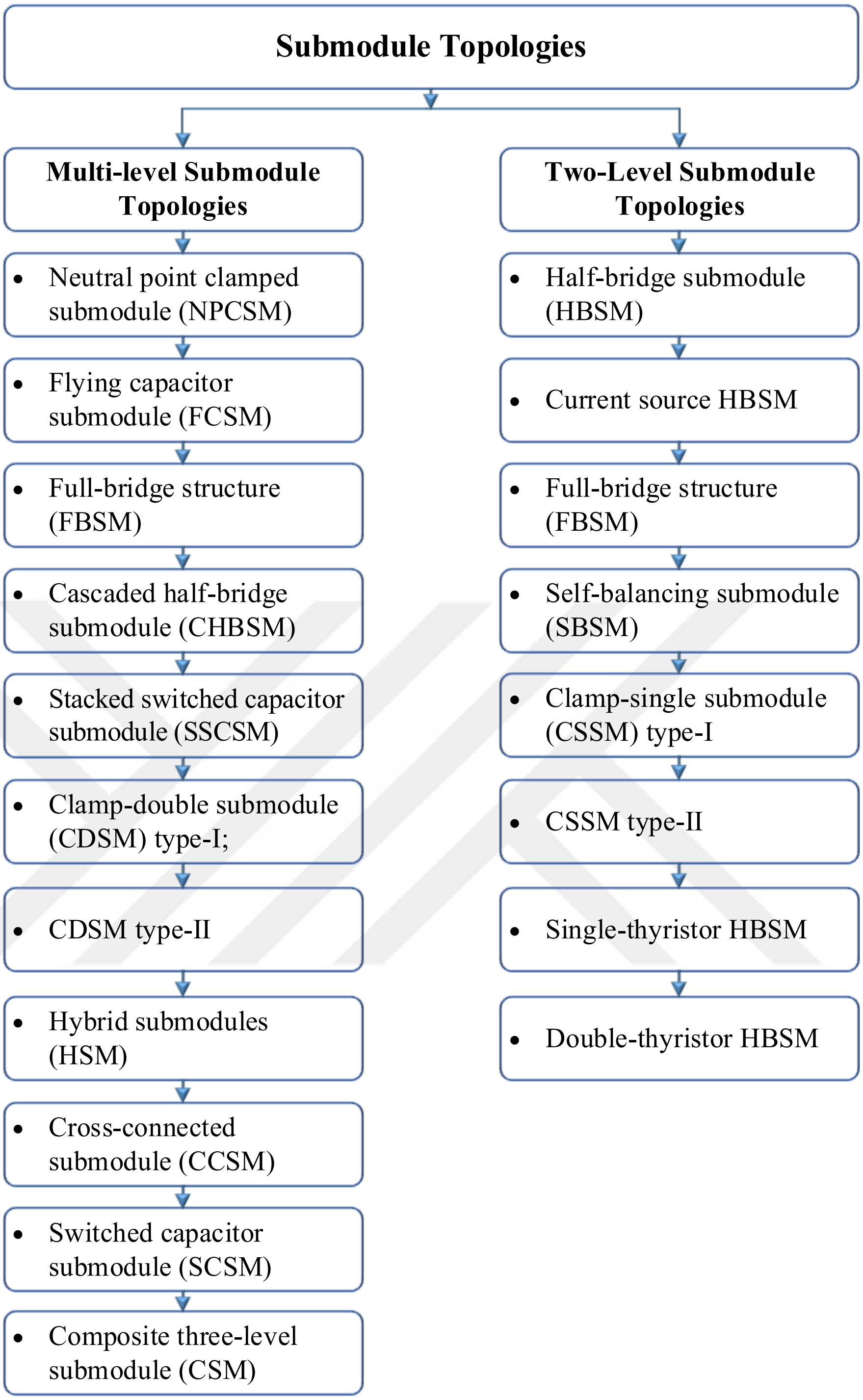

Figure 5. 6 SM topologies used in MMC architectures [74].

Among the various SM topologies, the HB configuration is the most commonly utilized unipolar semiconductor-based circuit due to its simplicity in design. The HBSM is particularly noted for its reduced power losses, which can be attributed to its straightforward structure. In contrast, the FBSM is a more sophisticated configuration, consisting of a floating capacitor in conjunction with two HBSMs. While the FBSM topology offers enhanced protection against DC fault currents, it incurs higher power losses owing to the greater number of semiconductor switches required compared to the HBSM configuration [124].

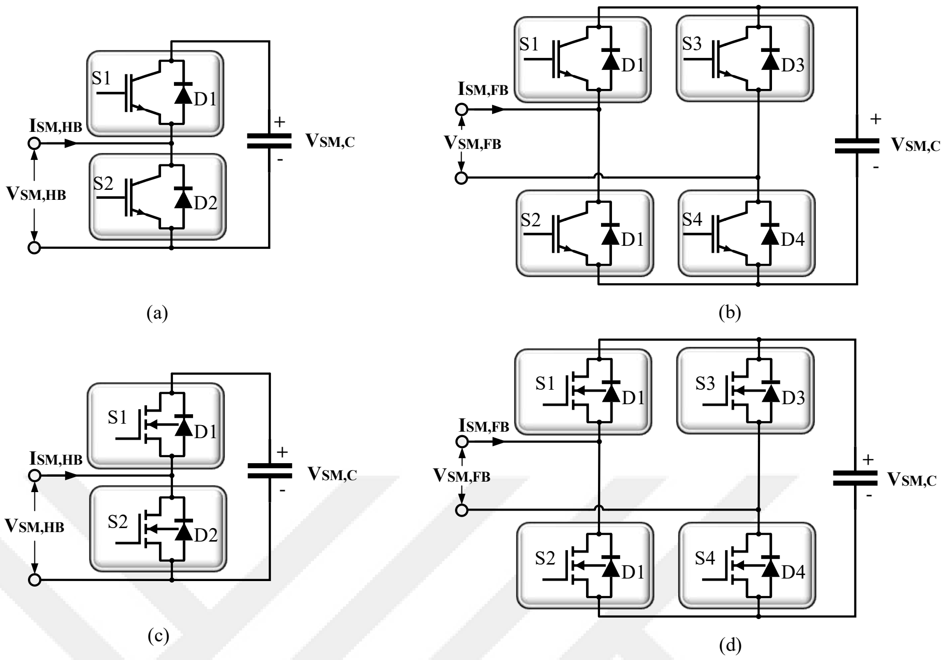

Figure 5. 7 The predominant SM topologies used in MMC systems: (a) IGBT-based HBSM; (b) IGBT-based FBSM; (c) MOSFET-based HBSM; (d) MOSFET-based FBSM.

The selection of an appropriate SM topology in MMC systems plays a crucial role in determining the converter's performance, efficiency, and cost. Each topology offers distinct advantages and is suited to different application scenarios. The HBSM remains the simplest and most cost-effective option, while the FBSM provides greater voltage flexibility and control. Hybrid and floating topologies offer a balance between performance and complexity, while asymmetric designs cater to highly specialized needs. [124] study provides an extensive examination of the SM topologies utilized in MMC technology. Ultimately, the choice of SM topology must align with the specific operational requirements of the application, balancing factors such as voltage control, complexity, cost, and energy efficiency. Figure 5.7 presents the most prevalent SM structures utilized in MMC architecture. Specifically, Figures 5.7(a) and 5.7(b) depict IGBT-based HBSM and FBSM topologies, while Figures 5.7(c) and 5.7(d) showcase the MOSFET-based HBSM and FBSM structures, respectively.

5.2.4 Applications of MMC Technology

The MMC has recently gained significant attention due to its exceptional properties, making it an attractive option for a variety of advanced applications. It has shown considerable promise in areas such as HVDC power transmission systems [80], [268], [269], electrical railway traction technologies [270], [271], and the supply of power to railway networks [272], [273]. Additionally, MMC technology has been explored for its potential in STATCOMs [38], [274], energy-storing solutions [275], and the growing field of electric maritime vessels [276], [277]. Other noteworthy applications include its use in variable-speed motor drive mechanisms [278], [279], electric vehicle charging structures [280], and active power filtering [43]. Moreover, MMCs are being integrated into battery electric vehicle systems [281], [282], and solar power generation networks [46]. As a form of multilevel converter, the MMC represents the latest advancement in VSC technology [125], offering significant advantages in terms of efficiency, adaptability, and scalability across various domains.

HVDC power transmission is recognized as one of the most efficient methods for transmitting electricity over long distances. Unlike traditional AC power transmission, HVDC systems reduce energy losses and minimize the required infrastructure. MMCs act as the system's backbone in HVDC applications, efficiently converting AC to DC power. This is especially crucial for incorporating offshore wind farms and other renewable energy sources into the overall grid. The inherent features of MMCs, such as low harmonic content and excellent voltage regulation, make them ideal for ensuring that high voltage power is transmitted reliably and with minimal distortion across long distances. MMCs are highly effective in these applications due to their ability to convert low-voltage AC power generated from renewable sources into high voltage DC, which can then be transmitted to the grid. For instance, MMCs ensure smooth energy transfer in wind power plants by converting the electricity produced by turbines into a form compatible with the grid.

Similarly, in photovoltaic systems, MMCs enable DC power conversion into AC power for grid injection. The modular nature of MMCs makes them well-suited to the scalable and distributed nature of renewable energy systems, ensuring their reliability even in the face of variable energy outputs. The advent of electrical-based transportation systems and electrically powered cars underscored the need for efficient power conversion technologies that can control the circulation of electricity in these structures. MMCs are increasingly utilized in the charging infrastructure for electric vehicles, as well as in the management of electric buses, trains, and other forms of electric transport. The modular design of MMCs allows for efficient DC-AC conversion, providing flexibility to scale the power capacity as required for different types of electric vehicles and transport systems. By reducing energy loss and minimizing size and weight, MMCs help improve the performance and sustainability of electric transportation solutions. In various industrial sectors, high power levels are often required to drive large motors, machinery, and generators. MMCs are integral to the efficient conversion of power in these high-demand applications. By employing MMCs, industrial systems can benefit from improved power quality, reduced energy losses, and enhanced system reliability. MMCs also ensure that industrial equipment operates with minimal harmonic distortion, contributing to cleaner energy usage and prolonging the machinery's lifespan.

Furthermore, their ability to manage dynamic power loads makes them especially suitable for applications requiring precise control, such as heavy manufacturing, mining operations, and large-scale production systems. The evolution of smart grid technologies has created the need for advanced solutions that can efficiently manage the dynamic flow of electricity in modern power distribution networks. MMCs are crucial in the operation of smart grids, particularly in applications involving energy storage and load balancing. MMCs and energy storage systems cooperate to regulate power flow, ensuring grid stability regardless of production and consumption of power oscillate. This is especially crucial as the system incorporates additional sources of sustainable energy, some of that are sporadic. The modular design of MMCs makes them adaptable, enabling smart grids to scale effectively and respond to the changing demands of both producers and consumers of electricity. Motor drives, which are essential components in many industrial and commercial applications, benefit greatly from the use of MMCs. These drives require precise motor speed and torque control, typically in real time. MMCs excel in motor control systems by providing high-efficiency AC-DC-AC conversion, ensuring that motors operate smoothly and efficiently.

Additionally, MMCs help to minimize harmonic distortion in the power supplied to motors, which reduces wear and tear on equipment and improves overall system reliability. The scalability and modularity of MMCs also make them ideal for motor drive systems, allowing them to be tailored to the specific power requirements of different industries. In the broader discipline of power electronics, MMCs are essential for improving the effectiveness of energy conversion and distribution facilities. With their potential for achieving AC-DC-AC conversion with minimal losses, MMCs are crucial in applications such as power factor correction and energy storage management. Their modular structure allows for easy adaptation to varying power demands, making them well-suited for use in modern power distribution networks.

MMCs represent a groundbreaking technology in the realm of power conversion, offering unparalleled efficiency, flexibility, and scalability. Their applications span a wide range of sectors, from renewable energy systems and electric vehicles to industrial power systems and smart grids. MMCs will greatly influence the future developments of power electronics and electrical distribution as the demand for sustainable energy solutions rises. Their ability to adapt to evolving energy needs and provide efficient, reliable power conversion ensures that MMCs will remain at the forefront of technological innovation in the power industry for years to come.

5.3 DC-DC MMC Theory

MMC technology has drawn a lot of interest because of their remarkable high-power conversion capabilities, especially in systems that need high voltage DC-AC conversion. Known for their low harmonic distortion, scalability, and efficiency, MMCs have become integral to various modern energy systems. A specialized variation of traditional MMC topology, the DC-DC MMC architecture, focuses on converting DC voltage from one level to another with high efficiency. This type of MMC system is particularly advantageous for HVDC power structures, power transmission, and the incorporation of renewable energy sources-based power systems. The DC-DC MMC is designed for efficient conversion of DC voltage, either stepping it up or stepping it down, while maintaining high energy efficiency. This technology finds significant applications in scenarios like renewable energy systems, energy storage, and electric vehicle power management. The operational principles of the DC-DC MMC are based on several core mechanisms: modular SM configuration, series and parallel configurations, switching and modulation techniques, and energy conversion, etc. Each SM in the DC-DC MMC comprises a switching device and a capacitor, both of which work in tandem to regulate voltage and convert energy. The modules collectively manage the input DC voltage and convert it to the desired output level. To obtain the desired voltage level, the SMs are linked in serial, and the converter's ability to handle current is increased by parallel connections. This flexible topology allows the DC-DC MMC to efficiently convert a wide range of voltage and current levels. The operation of the DC-DC MMC relies on precise control of the switching elements through advanced modulation strategies, such as PWM technologies. These approaches modify the duty cycles of the switching components to control the voltage produced. The primary function of the DC-DC MMC is to convert the DC voltage to a different level while maintaining minimal energy losses. The SMs store and transfer energy via capacitors, ensuring high efficiency in the conversion process. Figure 5.8 shows a typical isolated DC-DC MMC layout for enhanced comprehension of the DC-DC MMC structure [263], [283], [284].

DC-DC MMCs offer several notable advantages that make them an ideal solution for high-power, high-efficiency conversion, such as superior conversion efficiency, low harmonic distortion, scalability, effective voltage and current conversion, and enhanced reliability. The modular architecture and advanced switching techniques enable the DC-DC MMC to operate with minimal energy losses, ensuring high overall efficiency in power conversion. This is crucial in applications that require large-scale power handling. The multilevel structure of the MMC ensures that the output voltage waveform is smooth, with significantly reduced harmonic distortion compared to conventional converters. The modular design of the DC-DC MMC offers the ability to scale the converter by adding more submodules, thus increasing its power capacity as needed. This flexibility allows for efficient operation across a broad range of power levels. The DC-DC MMC can efficiently handle high voltage and current, making it suitable for applications requiring large power conversion, such as long-distance energy transmission and industrial power systems. By operating each SM at lower voltages, the DC-DC MMC reduces the stress on individual components, thus enhancing the system's overall reliability. Furthermore, the modular design allows for easier maintenance and faulty isolation.

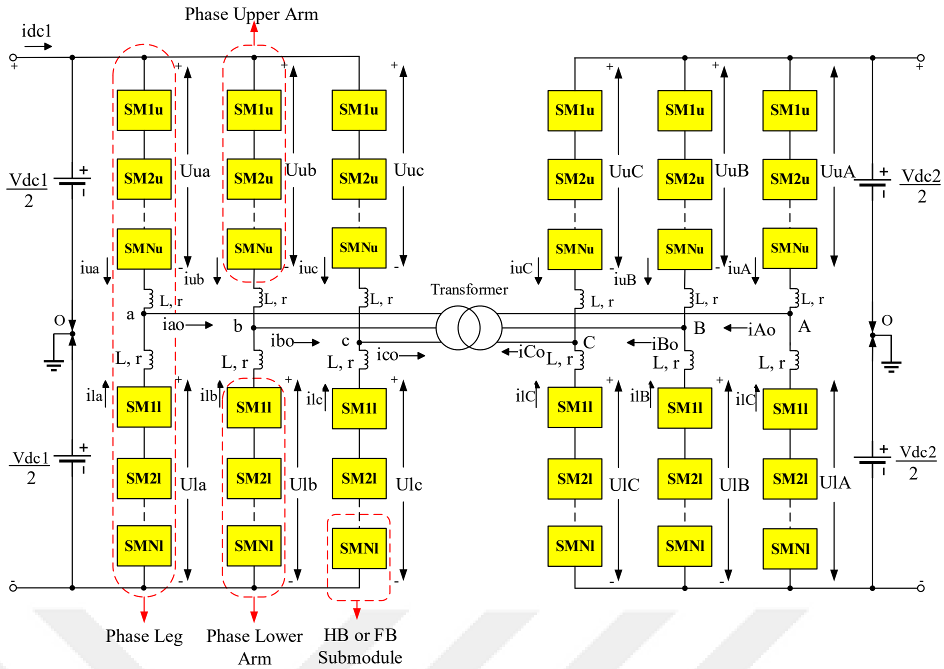

Figure 5. 8 A typical DC-DC MMC configuration [263], [283], [284].

The versatility and efficiency of the DC-DC MMC make it suitable for a wide range of applications in various industries, such as HVDC power systems, electric vehicle technologies, renewable energy sources-based power systems, power electronics applications, and power grid interconnections. DC-DC MMCs are essential components of HVDC power systems used for long-distance power transmission. These systems benefit from the modularity and efficiency of the DC-DC MMC, which enhances reliability and reduces transmission losses. DC-DC MMCs are employed in battery charging and overall power management in the electric vehicle sector. The ability to efficiently adjust the voltage ensures optimal performance of the battery and reduces energy losses during the charging process. The DC-DC MMC architectures are critically crucial for renewable energy power applications, including solar and wind power, because they transform the DC voltage produced by these power facilities into appropriate energy storage or grid integration levels. In industrial power electronics, such as motor drives and power supplies, the DC-DC MMC is used to provide clean and efficient power conversion. Its low harmonic distortion and high efficiency make it ideal for demanding industrial applications. DC-DC MMCs are increasingly used in power grids to facilitate the integration of renewable energy sources, enabling smooth voltage conversion between different levels and improving the grid's entire performance and reliability.

5.3.1 Mathematical Model of Typical DC-DC MMC

Mathematical analysis is essential in DC-DC MMC topologies, similar to conventional MMC systems. This is because of the fact that control strategies are developed employing mathematical models, which are essential for guaranteeing effective power transmission across converter systems. In isolated DC-DC MMC configurations, it is necessary to thoroughly investigate the architecture of the converter topology employed for such analyses. Figure 5.8 illustrates a widely recognized isolated DC-DC MMC arrangement [263], [283], [284]. Within this framework, a power transformer featuring a medium frequency connects the primary side and secondary side of MMCs, offering galvanic isolation between the two DC networks and facilitating power transmission. Similarly to other MMC mechanisms, the isolated DC-DC MMC's primary and secondary portions have a three-phase configuration. A number of the same SMs and an arm inductive device constitute every single phase's upper and lower arms. Each phase contains two arms, with each arm containing N SMs, meaning each leg has a total of 2N SMs [263], [283], [284].

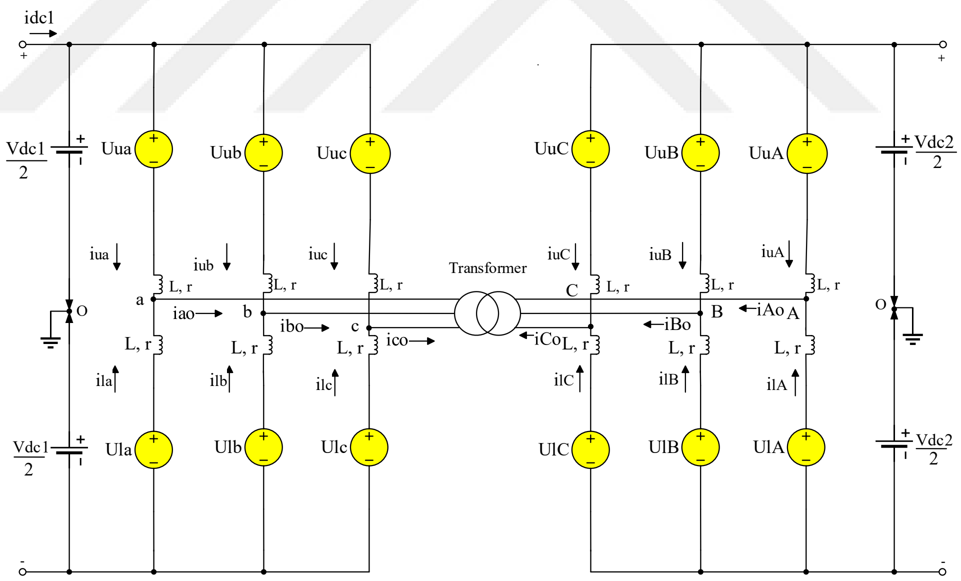

Figure 5. 9 The isolated DC-DC MMC design's equivalent arrangement.

A crucial role of the arm inductors is to control transient currents and balance the voltage differentials across the upper and lower arms of the MMC design that arise from the switching of the SMs [263], [283], [284]. Phase-a of the MMC, which is situated on the main side of the isolated DC-DC MMC arrangement, is the subject of the mathematical study presented here. The same analysis can be applied to the remaining phases. As stated in the mathematical analysis section of conventional MMC systems, every arm of the MMC can be considered a non-linear capacitor with a time-varying sinus-shaped capacitance. The voltage across this capacitor is modeled such a voltage source that can be controlled, as shown in Figure 5.9. The corresponding circuit for the typical isolated DC-DC MMC design indicated in Figure 5.8 is illustrated in Figure 5.9.

By using Kirchhoff's Current Law (KCL) and KVL, the appropriate approximations for both the upper and the lower arms of the MMC design can be obtained from Figure 5.9:

$$i_{ao} = i_{ua} + i_{la} \tag{5.19}$$

A varying current, known as i_{dif}, flows throughout this converter's legs because of the differences in voltage across the DC terminal and phase legs of the system. In addition, the AC seems to be distributed equally across the lower and upper arms. The following is the result of obtaining mathematical equations (5.20) and (5.21).

$$i_{ua} = i_{dif} + \frac{i_{ao}}{2} \tag{5.20}$$

$$i_{la} = i_{dif} + \frac{i_{ao}}{2} \tag{5.21}$$

In phase a, i_{ua} and i_{la} advocate for the upper and lower arm currents, correspondingly. The abbreviation i_{ao} represents the current phase of phase a. The following is the current i_{dif} that can be derived from mathematical equations (5.20) and (5.21).

$$i_{dif} = i_{ua} - \frac{i_{ao}}{2} \tag{5.22}$$

$$i_{dif} = i_{la} + \frac{i_{ao}}{2} \tag{5.23}$$

The following is the result of integrating these two equations (5.22) and (5.23):

$$i_{dif} = \frac{i_{ua} + i_{la}}{2} \tag{5.24}$$

The formulations that follow can be determined by employing KVL.

$$-\frac{V_{dc1}}{2}+n_u U_{ua}+r_a i_{ua}+L_a\frac{di_{ua}}{dt}+Uao=0 \quad (5.25)$$

$$\frac{V_{dc1}}{2}-n_l U_{la}-r_a i_{la}-L_a\frac{di_{la}}{dt}+Uao=0 \quad (5.26)$$

Wherein the DC terminal and AC phase voltages can be identified by V_{dc1} and U_{ao}, correspondingly.

$$U_{ua}=U_{la}=\frac{V_{dc1}}{2} \quad (5.27)$$

In this case, $U_{ua}$and U_{la} specify the respective voltages throughout each upper and lower arm of the design. The output voltage is determined to some extent by the n_u and n_l, which indicates the total quantity of SMs contained in each arm of the design. Mathematical equations (5.25) and (5.26) are subtracted to produce expression (5.28) in the following manner:

$$\frac{di_{dif}}{dt}=\frac{V_{dc1}}{2L_a}-\frac{n_u U_{ua}+n_l U_{la}}{2L_a}-\frac{r_a i_{dif}}{L_a} \quad (5.28)$$

Thus, we acquire the following formula (5.29) in the following fashion:

$$\frac{di_{dif}}{dt}=\frac{V_{dc1}-(n_u U_{ua}+n_l U_{la})-2r_a i_{dif}}{2L_a} \quad (5.29)$$

In the state of stable operation situation, the MMC operating features allow the arm current to be expressed as a combination of the common and differentiated pattern components.

$$i_{ua}=\frac{i_{ao}}{2}+i_{CC} \quad (5.30)$$

$$i_{la}=\frac{i_{ao}}{2}-i_{CC} \quad (5.31)$$

In this case, i_{CC} indicates for the MMC structure's circulating current. The AC structure's phase-a current is provided as

$$i_{ao}=2i_a+2i_{cmc} \quad (5.32)$$

Here is where i_a stands for the phase-a AC output current, and i_{cmc} for the MMC design's common-mode current.

In a comparable manner, the current that passes through both the upper and lower dc-terminals of MMC is supplied by

$$i_u = i_{ua} + i_{ub} + i_{uc} = 3i_{cmc} \tag{5.33}$$

$$i_l = i_{la} + i_{lb} + i_{lc} = 3i_{cmc} \tag{5.34}$$

Therefore, equations (5.30) and (5.31) are used to calculate the magnitude of a circulating current for phase-a.

$$i_{CC} = \frac{i_{ua} - i_{la}}{2} \tag{5.35}$$

The following is an equation for the calculation of the common-mode current intensity (i_{cmc}) using equations (5.33) and (5.34):

$$i_{cmc} = \frac{i_u + i_l}{6} \tag{5.36}$$

5.4 Summary

As very effective and advanced power conversion architecture, the MMC technology is especially well-suited for high voltage and high-power purposes. In contrast to traditional multilevel converter topologies, the MMC technology is exceptional at providing significantly lower harmonic distortion and enhanced effectiveness. The creation of almost perfect sinusoidal wave shapes whilst reducing inefficiencies is made possible by these characteristics, which are crucial in improving the entire structure's effectiveness. High voltage operating equilibrium, minimal power switching losses, inherent flexibility, and the simplicity of maintenance and adaptability provided by its modular architecture are some of the crucial benefits of MMC technologies. Fundamentally, the MMC architecture is made up of several SMs, each of which integrates individual energy preservation elements, usually capacitors and semiconductor-based power electronic switching devices. These SMs operate in sequence to gradually raise the DC voltage levels, making producing large output voltages easier. Because every SM can be independently controlled by the modular architecture, efficient voltage stabilization and the ability to isolate errors in the case of SM breakdowns are guaranteed. The capacity of the MMC to function at very low switching frequencies is one of its distinguishing features. This greatly reduces electromagnetic interference, leading to smoother output patterns of waves as well as improved reliable system functionality. The perfect voltage regulation between the modules constitutes a crucial architectural concern because of each SM's restricted power storage capability. Complicated procedures continuously regulate the amounts of voltage throughout the modules to accomplish this balance, reducing disparities and guaranteeing outstanding performance. Such voltage control prolongs the operating life of the SMs in addition to increasing the converter's performance and dependability. A substantial level of failure tolerance is also provided by the MMC's modular architecture, which allows any faulty SM to be easily detached without affecting the system's overall efficiency, guaranteeing dependable and uninterrupted performance. MMC technology is used in various fields; nevertheless, it is most well-known in commercial power transformation, electric vehicle powertrains, renewable energy-based power facilities cooperation, and HVDC power transmission networks. MMC technological advances are essential for providing effective extended-distance transmission of power alongside minimized losses in the HVDC infrastructure framework whilst promoting network stabilization.

Furthermore, the MMC technology is becoming more widely acknowledged for its capacity to improve power systems' resistance to abrupt changes in demand and grid disruptions, providing a very adaptable and reliable approach for contemporary power networks. In conclusion, MMC technology is a game-changing innovation in power electronics that provides unmatched dependability, effectiveness, and adaptability. It is positioned as a key innovation for future power transformation and transportation infrastructure because of its smooth incorporation into dynamic power networks, high voltage projects, and facilities utilizing renewable energy. The MMC technology will play an increasingly significant role in forming the forthcoming generations of electric power networks as worldwide energy requirements continue to evolve.

CHAPTER VI
MMC CONTROL THEORY

6.1 Introduction

Contemporary power infrastructures are based on the effective generation, distribution, and transportation of electrical power. Increasingly complicated and effective power transformation strategies have been made possible in recent decades by developments in power technological devices, which are essential for satisfying the changing needs of outstanding performance electrical power systems. Power converter architecture has become increasingly sophisticated because of the rising incorporation of renewable energy sources-based power facilities, rising demand for improved power effectiveness, and the capacity to control large-scale power networks. Regarding them, MMC technology has attracted a lot of interest because of its exceptional behavioral traits in industries requiring accurate management, high voltage, and high-power architectures. The flexible structure of the MMC architecture sets it apart, allowing for the self-regulating management of each SM. This property makes it possible to optimize the characteristics of dynamic systems, guaranteeing robust effectiveness, minimal harmonic interference, and outstanding effectiveness. Because of the aforementioned upsides, the MMC structure is especially well-suited for uses like commercial drive mechanisms, electrical car charging infrastructures, the transmission of HVDC power, and the incorporation of renewable energy-based power networks. The fact that MMC topologies are widely used in a variety of sectors shows how revolutionary an innovation they can be for contemporary electrical power structures. Notwithstanding the benefits that MMCs provide, their efficient functioning depends on the application of strong and advanced management techniques. Because the converter's architecture is adaptable, controlling voltage and current transmission among various SMs is crucial to maintaining the system's stability and highest possible efficiency. Nevertheless, since MMCs have numerous associated SMs and require exact synchronization between them, their control is intrinsically more difficult than that of classical converter topologies. Because of this complexity, it becomes extremely difficult to preserve structure correctness, equilibrium, and dependability throughout a variety of operational circumstances. The background knowledge required to comprehend the management problems associated will first be provided by an examination of the basic principles of operation and architectural benefits of MMC topologies. Following that, a thorough analysis of the control strategies presently used to accomplish these goals will be provided, along with a detailed discussion of the main goals of MMC system control, including voltage regulation, power flow governance, and harmonic elimination. As load circumstances and operating needs change, one of the main goals of MMC controlling is to maintain system efficiency and dependability. Fuzzy logic control mechanisms, high-performance PID control structures, MPC systems, and artificial intelligence-based control approaches are some of the advanced controlling strategies that can be investigated to address these issues. Through greater accuracy in controlling the levels of voltage, current, and power transfer, these cutting-edge techniques allow MMCs to operate greater adaptably and efficiently. The wider difficulties with power control and management in MMC-based structures, such as power efficiency and design reliability, are also examined. These difficulties are especially important in high-power and large-scale purposes; wherein dependable and effective network performance depends on superior control systems. In the continuously expanding fields of control philosophy and MMC implementation of technologies, new developments and possible future innovations can impact the establishment of MMC control methods. Providing a thorough examination of the control approaches currently employed for MMC structures, assessing their effectiveness critically, and suggesting possible directions for further investigation and improvement in the area are the primary goals of this chapter. This chapter aims to further the comprehension of MMC control methodology and its real-world implementations to improve the productivity, effectiveness, and dependability of MMC-based power mechanisms.

6.2 Traditional MMC Control Theory

The execution of a suitable and accurate control technique is crucial to the functioning of MMCs. A wide range of methodologies and approaches are integrated into the conventional control framework that governs MMCs in order to handle the intrinsic complexity of these converter topologies, maximize performance, and guarantee mechanism reliability. In particular, MMC technological advances are critical for HVDC power systems owing to their advantages, which include high-quality output waveforms, fault tolerance, transformerless functioning, flexibility, and scalability of voltage and power. Thanks to contemporary control systems, MMCs can be operated securely, dependably, and effectively. Such control techniques are very efficient, flexible, and somewhat consistent.

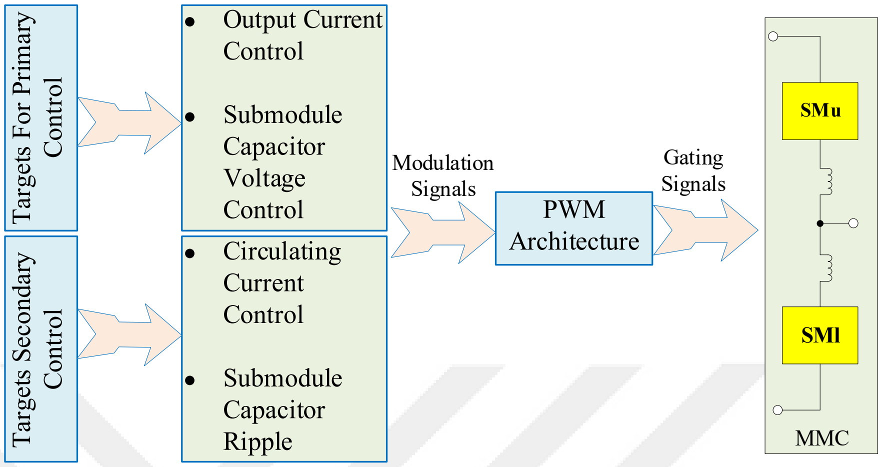

Figure 6. 1 The typical MMC control mechanism.

MMC control is inherently challenging, as illustrated in Figure 6.1, due to the involvement of various performance criteria that must be simultaneously addressed [18], [120]. Primary control in a traditional MMC control arrangement typically comprises SM capacitor voltage control and output current control. On the other hand secondary control comprises SM capacitor fluctuations and circulating current control. An effective modulation mechanism and regulator need to be employed to benefit from the exceptional power fulfillment of the MMC.

The primary goal of traditional MMC control theory is voltage control, in which the voltage of each SM is individually controlled. The SMs' charging and discharging stages are controlled to keep the output voltage at the target level. Usually, PWM methods are used to accomplish this kind of control. For every SM, PWM produces a switching signal that modifies the SM's voltage levels. To retain the intended system output while controlling the SM voltages, the process of switching ratio modulation makes sure that the output voltage is accurately managed. In conventional MMC control strategies, both closed-loop and open-loop control techniques are frequently adopted. Depending on the particular requirements of the structure and its surroundings during operation, each of these strategies has unique benefits. The resultant variables of open-loop control structures are established using predetermined input variables; the output of the system does not provide feedback. Although this approach is often faster and more straightforward, it is intrinsically less robust against outside disruptions and system errors. Due to its failure to take into consideration dynamic changes in the system, open-loop control techniques can be less accurate when responding to modifications in the load or the surrounding circumstances. On the other hand, closed-loop control techniques constantly minimize errors between the intended and realized results while examining the system's output in real-time. The output voltage or current in MMC technologies is monitored, and a system controller (usually a PID controller) processes undesirable signals to modify the system's behavior appropriately. Because it allows the entire system to adapt dynamically to changing conditions, closed-loop control offers higher accuracy and stability, which makes it more appropriate for high-performance applications where accuracy is crucial.

6.2.1 SM Capacitor Voltage Control Mechanism

An essential aspect of MMC control lies in precisely controlling the terminal voltages and currents to facilitate seamless energy exchange between the converter's input and output. Serving as a dynamic interface for power conversion, the MMC utilizes its submodule capacitors as transient energy reservoirs. For the converter to operate with high fidelity and stability, it is imperative to maintain a well-regulated average capacitor voltage throughout its operation [285]. As the number of SMs in an MMC increases, the corresponding operating voltage scales accordingly. Each SM contains capacitors whose voltages are inherently dynamic and must be regulated around a predefined reference level. Effective control of these capacitor voltages is crucial not only for ensuring the reliable operation of the MMC but also for maintaining waveform quality and operational integrity. This control strategy includes balancing the voltages across submodules, regulating the voltage across converter legs, and managing the energy distribution within the converter arms [125].

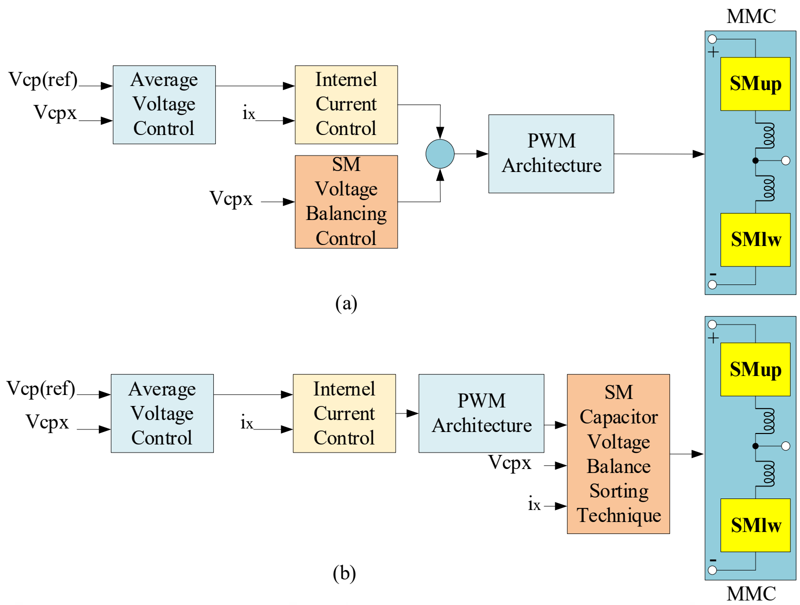

Figure 6. 2 Control methods utilized in MMC: (a) Voltage balancing performed prior to the PWM process, and (b) SM balancing executed subsequent to PWM.

To maintain MMC's satisfactory performance, capacitor voltage balancing is crucial. The categorization approach is commonly utilized in MMC technology to balance capacitor voltages in SMs. In this methodology, the initial step involves determining the individual capacitor voltages within the SMs and categorizing the voltages in the upper and lower converter arms. As the direction of branch currents reverses, the SM capacitors undergo alternating charging and discharging cycles. Specifically, a positive branch current leads to capacitor charging, while a negative current results in discharging. This bi-directional current flow inevitably introduces voltage imbalance across the arms. To address this issue, the capacitor voltages of all SMs are continuously monitored and methodically sorted [261]. Figure 6.2 illustrates the core principles of MMC control strategies and the implemented capacitor voltage balancing technique [261], [285]. In Figure 6.2(a), the outer control loop regulates the average submodule capacitor voltage and provides the reference signal for the inner current controller. The current controller determines the modulation index accordingly. Additionally, a voltage balancing mechanism supplements the modulation index by incorporating a correction term based on the voltage deviation and the direction of current. Although this approach is limited in its operational scope, subsequent enhancements have been introduced, notably through the implementation of an arm voltage balancing technique. Figure 6.2(b) presents a control scheme that maintains the same outer-loop average capacitor voltage regulation and inner-loop current control as its predecessor, yet differs by relocating the voltage balancing mechanism to the post-modulation stage. In this configuration, the modulation unit computes the required arm output voltage by determining the exact number of submodules to be activated. Subsequently, the balancing algorithm dynamically adjusts submodule selection to equalize capacitor voltages by selectively charging capacitors below the reference threshold and discharging those above it [286].

Effectively balancing the voltage across each SM is necessary for MMCs to operate at their peak performance. Individual SM voltage levels can shift over time, which might impair system performance and cause instability. The dynamics of the DC capacitors' charging and discharging frequently result in these voltage imbalances, which can lead to power losses and decreases in efficiency. To address this issue, traditional MMC control strategies incorporate voltage balancing algorithms. These algorithms monitor and correct voltage discrepancies between SMs to maintain equilibrium. Voltage balancing is essential not only for maintaining stable output but also for preserving energy distribution among the SMs. There are two primary methods for voltage balancing which are open-loop balancing and closed-loop balancing. In open-loop voltage balancing, SM voltages are maintained within a prescribed range, and adjustments are made independently for each SM. While this approach is simpler and computationally less intensive, it is less adaptable to dynamic system changes and external disturbances. Closed-loop voltage balancing, on the other hand, involves continuous feedback of the voltage levels of each SM, comparing them against the overall system output. The control system then dynamically corrects imbalances by adjusting the voltage of individual SMs in real time. This method offers greater stability and adaptability, making it particularly suitable for systems that experience frequent load or operational fluctuations.

Numerous researches on SM capacitor voltage balancing control in MMC technology have been conducted in the last few years. The following are some of the most popular studies discussed in this paper. The basic goal of the developers of presented this study imbalanced AC grid instances in MMCs is to enhance power stabilization [287]. Voltage balancing is achieved by adopting a novel control mechanism. By implementing the suggested control technique to a power network linked to traditional

MMC architecture, the feedback/feedforward control technique is examined in depth. This study presents a current-less submodule individual voltage balancing control (SMIVBC) to achieve capacitor voltage balancing in the MMC [274]. A new strategy is proposed in [274], introducing a current-less SMIVBC scheme. This method enables independent regulation of each SM capacitor voltage to its reference value without relying on capacitor current measurements. Instead, the technique manipulates the modulation of the DC-side equipment within each SM, eliminating the need for sorting algorithms and current sensing. As a result, this approach reduces the number of required sensors and sampled signals, lowers implementation costs, and enhances overall system reliability. In [288], a distinct technique is employed, wherein submodule gating signals are independently generated using a phase disposition PWM method. The modulation signals are periodically rotated among SMs to maintain voltage equilibrium. To ensure both high-quality output voltage and balanced SM capacitor voltages, the modulation index is dynamically adjusted. Addressing capacitor voltage imbalance is critical, as prolonged deviation can lead to overcharging of capacitors and degrading operational reliability. Therefore, maintaining proper voltage balance across all submodules remains a key design objective in MMC control strategies.

To enhance the limited customizable range of DC due to voltage and power inequalities, innovative feedback and feed-forward power balancing mechanisms that make use of enhanced choosing techniques are proposed in [289]. In power balancing management, the feed-forward management process provides fast, flexible behavior, while the feedback mechanism ensures very little and consistent errors. In a wider range of DC supplies, the mixed MMC can maintain the balance of power between HBSMs and FBSMs by employing the recommended controlling techniques.

An improved energy grading strategy for stabilizing every SMs capacitor energy in MMCs is described in [290]. Whenever the SM voltage technique is multiplied by a lot of degrees, nevertheless, the voltage disturbances and circulation current are becoming progressively complicated, resulting in higher voltage disturbances and circulation current. An increased voltage grading technique is presented to resolve the issue, which indicates an expanded control logical functionality for capacitor voltage equilibrium in the converter. The modulation index approach is used to identify the switching arrangement of every SM floating capacitor, which is subsequently by comparison to the mixed state situation in the MMC utilizing the arms' current direction.

The voltage balancing algorithm, which is based on reassigning switching periods, was developed in [291] to enhance the rebalancing effectiveness of capacitor energies with a lower operative frequency. A detailed description of the lower switching frequency voltage balancing method is provided. The correlation between switching timings, switching frequency, and capacitor voltage variation may then be determined using this information. The voltage variations in the positive and negative periods of the leg current are thoroughly investigated. Independent surveillance and controlling every SM are necessary in a traditional system for balancing a capacitor voltage, which adds to the converter's expense and load.

With no need for extra instruments or processors, [292] presents a simple logical method for regulating the capacitance energy within every SM. The capacitance energy of SMs is regulated using a simple rational procedure, which balances the capacitance voltage and decreases the voltage distortion of every capacitance.

The capacitor in every SM connecting to the converter is balanced using a voltage balancing approach proposed in [293]. The suggested approach additionally reduces capacitor fluctuation voltage. The phase placement carrier approach is first used to generate switching pulses for switching components, which are thereafter modulated by using a voltage balancing scheme and implemented in the converter.

6.2.2 Output Current Control

In recognition of MMCs to operate as efficiently as possible, the output current is required to be precisely controlled. Efficient power delivery is guaranteed by effective current control, which also reduces system losses and guards against any kind of component damage. Additionally, a regulated output current lowers the possibility of harmonics, which might have a negative impact on system dependability and power quality. Additionally, keeping the output current steady increases the converter's longevity and enhances its overall functionality. Therefore, a key component of MMC functioning is precise output current control [294], [295].

Various advanced control strategies have been developed for MMCs to ensure accurate output current regulation and enhance system performance. Among these, PID control remains a widely used method due to its simplicity and effectiveness. It improves system stabilization through proportional response to error, integral correction of steady-state deviations, and derivative anticipation of future errors. However, its performance heavily depends on meticulous tuning, especially under dynamic operating conditions [296]. Model-based control techniques, including state-space and linear-quadratic regulator approaches, require precise mathematical models of the MMC system. These methods forecast the converter's future behavior and adjust control actions accordingly, offering high performance even in nonlinear or time-varying environments [294]. Another critical challenge in MMCs is the mitigation of harmonics in the output current, which affects power quality. Harmonic mitigation techniques aim to reduce Total Harmonic Distortion (THD) using either advanced modulation schemes, such as selective harmonic elimination, or filtering approaches, to maintain near-sinusoidal output waveforms [297]. Model Predictive Control (MPC) is gaining popularity in MMC applications due to its ability to handle complex dynamics and constraints by optimizing control actions over a prediction horizon. MPC enhances converter behavior by preemptively modifying inputs based on future current trajectories, albeit at the cost of higher computational requirements [298]. Current tracking control, which includes techniques like sliding-mode and feedback-based methods, ensures the output current accurately follows a reference signal. It continuously adjusts the modulation to minimize tracking error and is particularly effective in systems requiring rapid dynamic response to disturbances or load variations [299].

6.2.3 Circulating Current Control

MMCs have a substantial disadvantage in terms of internal (do not flow outside) circulation current flowing among the phases. Internal circulating current can drastically raise system losses and diminish system lifetime, especially in high-power systems [300]. In general, circulating currents have a limited impact on the AC system's voltages and currents. However, if not properly managed, they can cause an increase in the root mean square (RMS) or peak values of the currents in the converter arms. This increase may exceed the design specifications of the equipment, leading to higher energy dissipation and variations in capacitor voltages [18], [125], [301], [302]. A practical method to mitigate circulating currents involves the addition of inductors to each phase or branch of the MMC. Through the implementation of a closed-loop control mechanism, the magnitude of circulating currents in each branch can be effectively restricted [125].

In an MMC, the voltage generated by the converter is essentially the sum of the voltages from each SM capacitor. If there are voltage imbalances between the SMs, circulating currents can arise. These currents can flow through the converter's internal circuitry and result in significant issues, including energy loss, thermal stress, and instability in the overall system. Circulating currents typically form due to several factors, such as voltage imbalances, transient responses, load asymmetry, and the system's dynamic behavior. Each SM has a capacitor, and the voltages across these capacitors need to remain balanced for optimum performance. Mismatches in the charging or discharging procedures of distinct SMs, as well as malfunctions or flaws in the switching devices, might result in voltage imbalances. Transients in the system's voltage can occur during switching processes or dynamic variations in load. These transients have the potential to provide pathways for circulating currents by momentarily altering the voltage between SMs. Circulating currents can occur because various arms of the converter cannot share the same load equally if the load across the converter is not symmetrical or fluctuates dynamically. Additional imbalances can occur from currents flowing between the SMs in the same arm because of such asymmetries. Circulating currents can be made severe by the fast-switching nature of MMCs and the intricate interplay between modulated signals, particularly in situations where the load or operating circumstances alter often. Voltage differentials brought on by a converter's reaction to transient states can result in circulating currents while the system tries to stabilize.

Effective control of circulating currents is essential for maintaining high efficiency and stable operation of MMCs. Several advanced techniques have been developed to minimize these currents, each with varying degrees of complexity and computational demands. One of the most straightforward methods to control circulating currents involves direct feedback regulation. In this approach, the circulating currents are actively measured, and the control system adjusts the SM voltages and modulation signals to counteract the currents. This method typically employs a feedback loop, such as PI control, which adjusts the switching strategy to minimize the circulating current. The challenge with direct regulation is the need for fast, real-time current sensing and rapid adjustments to maintain system stability. Maintaining a balanced voltage across all the converter's SMs is a basic technique to lower circulating currents. Circulating currents will probably occur when the system adjusts for any discrepancies in the capacitor voltages inside each SM. Capacitor voltages are actively controlled using voltage-balancing algorithms. To maintain voltage balance over time, these algorithms modify each SM's modulation schemes. Predictive or adaptive algorithms are used in advanced voltage balancing techniques to reduce voltage mistakes and eliminate the requirement for high-frequency switching. MPC is an innovative and advanced control method that effectively regulates circulation currents. MPC proactively modifies the control signals by forecasting future behavior using an MMC dynamic model. By reducing circulating currents and maintaining voltage balance, this predictive method enables the converter's functioning to be optimized. MPC's capacity to manage limitations like voltage and current restrictions is one of its benefits, which makes it perfect for MMC systems that must function in a variety of scenarios, including load variations and transient occurrences. A reliable control method for dealing with circulating currents, particularly in nonlinear and unpredictable systems, is sliding mode control (SMC). By forcing the system's trajectory to "slide" over a predetermined surface, this technique successfully reduces circulating currents even in the face of disruptions. Because SMC can manage nonlinearities and system uncertainties without necessitating exact models of every system component, it is very beneficial in MMCs. Even in the event of system disruptions, it can adjust to shifting operating circumstances while maintaining low circulating currents. PWM methods, particularly carrier-based PWM, are frequently employed in MMCs to regulate SM switching. PWM techniques that regulate the time and phase relationships between the switching signals, such as PS-PWM or LS-PWM, aid in lowering circulating currents. It is feasible to lessen voltage imbalances and, consequently, circulating currents by altering the modulation techniques (e.g., by changing the carrier signals' phase). In particular, PS-PWM can be useful for minimizing circulating current problems and balancing SM switching. Distributed control techniques can be used to regulate circulating currents across numerous SMs in large-scale MMC systems. To lower circulating currents, local feedback mechanisms allow each SM to be individually regulated. These controllers can then cooperate. Conversely, adaptive control methods adjust control settings according to the system's observed behavior in real-time. These techniques provide a great deal of versatility and can maximize the converter's performance in a range of operating environments.

Recent advancements have led to the development of various modulation techniques and control strategies aimed at reducing the losses associated with circulating currents in MMC systems. A novel approach known as Circulating Current Optimization Control (CCOC) has been proposed in [303] to minimize the peak currents in the converter arms. This method enables the use of switching devices with lower current ratings or enhances power handling capacity while maintaining similar-rated devices. Reference [304] introduces a coordinated control scheme to reduce power losses and stabilize capacitor voltages in AC-voltage-boosted full-bridge submodule MMCs by modulating the second harmonic components of the circulating current, ultimately decreasing MMC power losses. To prevent excessive circulating currents within an MMC, [305] presents an enhanced closed-loop control approach, which helps to mitigate capacitor voltage fluctuations while limiting circulating current. This method also reduces DC link voltage fluctuations under both steady-state and dynamic AC network conditions without the need for additional controllers. As a result, this circulating current control method lowers conduction losses, minimizes equipment ratings, and improves converter performance and efficiency. The impact of asymmetrical leg impedance on circulating current suppression (CCS) in MMC-HVDC networks is explored in [306], where a supplementary circuit-based approach is proposed to optimize CCS and boost the performance of the MMC-HVDC system based on mathematical models.

Additionally, [307] presents an innovative CCOC technique to reduce the maximum arm current in MMCs while maintaining consistent peak capacitor voltage fluctuations in the submodules. A simplified method for determining circulating current magnitude is also provided, along with a comparative analysis that highlights the advantages of the proposed approach over existing methods. Based on the derived formulas, two circulating current controllers are described that regulate the amplitude and phase angle of the second harmonic circulating current.

A key component of improving the functionality, dependability, and efficiency of MMCs is circulating current regulation. With the growing demand for large-scale and high-efficiency power conversion systems particularly in HVDC transmission and renewable energy applications the importance of effective circulating current control is expected to increase significantly. Promising approaches to controlling circulating currents and guaranteeing steady and effective operation include adaptive voltage balancing, SMC, and MPC.

6.2.4 SM Capacitor Voltage Ripple Control

The voltage across each capacitor in MMC is critical for the effective operation. However, power switching operations within MMC topologies lead to voltage ripple across the capacitors, which can degrade MMC system performance, reduce efficiency, and shorten component lifespan. Consequently, managing the capacitor voltage ripple is a key research area in the optimization of MMC technology performance. In MMC technology, the phenomenon of SM capacitor voltage fluctuation is a significant obstacle. In the MMC configuration, the capacitors within each SM serve as intermediary elements, facilitating power transfer between the input and output. However, the SM capacitors often experience undesired voltage ripple as a result of the power interchange process that occurs between the DC and AC sides of the system [308]. Particularly, the power flowing through the converter's top and bottom arms causes fluctuations in voltage across the SM capacitors to mostly fluctuate at the fundamental frequencies observed in MMC topologies [309], [310]. Furthermore, the capacitance of the SM and the associated angular frequency are inversely proportional to the amplitude of each harmonic element in the SM capacitor voltage ripple [310]. Research has demonstrated that minimizing the SM capacitors' ripple in the voltage helps in decreasing their mass and size, which are usually the main factors influencing the MMC system's overall weight and dimensions [308].

The capacitor voltage in each SM fluctuates due to the periodic charging and discharging process during switching operations. These fluctuations, referred to as capacitor voltage ripple, arise primarily from such as power switching dynamics, imbalanced load conditions, and capacitor size and system parameters. During the switching events, capacitors undergo charge and discharge cycles, resulting in voltage ripple. Under uneven load conditions, voltage sharing among the SMs can become unbalanced, exacerbating voltage ripple. The value of the capacitors and other system design parameters such as switching frequency and modulation strategies significantly influence the amplitude of the voltage ripple. Excessive ripple can cause various problems, including increased switching losses, thermal stress, and reduced operational life of the capacitors. Therefore, effective techniques for controlling and reducing this ripple are essential. Various control techniques have been proposed and implemented to mitigate the capacitor voltage ripple in MMCs. These strategies can be broadly classified as carrier-based PWM techniques, voltage balancing control, hybrid control approaches, energy storage, flyback control, active and passive filtering, etc. Carrier-based PWM methods are widely employed to mitigate voltage ripple by balancing the switching patterns across SMs [311]. These techniques distribute the ripple more evenly, which reduces the peak-to-peak variations in capacitor voltages. Although carrier-based PWM approaches aid in controlling the voltage ripple, they mainly target converter arm balance rather than the voltage regulation of individual SM capacitors. Voltage balancing techniques have been developed to directly control capacitor voltage ripple. These methods regulate the voltage of each SM by adjusting switching sequences based on real-time feedback. Hybrid control strategies enhance system performance by combining the benefits of several control techniques. When MPC and PI control are combined, for example, fast response time is possible while utilizing MPC's predictive power. Likewise, combining carrier-based PWM with voltage balancing approaches reduces ripple and guarantees effective operation.

In some MMC applications, supplementary energy storage devices such as supercapacitors or batteries can be employed to smooth out the power flow and absorb voltage ripple, especially in those with dynamic or variable load circumstances. These gadgets mitigate ripple effects and lessen the strain on the SM capacitors by acting as energy buffers. Flyback circuits offer an additional approach by storing energy during high voltage times and releasing it during low-voltage phases. By filtering high-frequency voltage ripples, flyback circuits smooth out the voltage waveform and lessen the strain on capacitors. To further reduce the high-frequency voltage ripple, active and passive filters can be used within the MMC system. Passive filters consist of components such as inductors and capacitors, while active filters utilize power electronic devices to inject compensating currents. These filters are designed to attenuate unwanted harmonic frequencies and smooth the capacitor voltage waveform.

With regard to operating as efficiently, reliably, and optimally as possible, the capacitor voltage ripple must be controlled. To lessen ripple, a number of control solutions have been developed, such as energy storage devices, voltage balancing methods, carrier-based modulation, and hybrid control systems. However, issues including fault tolerance, scalability, thermal management, and real-time processing continue to be major barriers to their widespread use. To enhance the performance and dependability of MMC mechanisms, further studies should concentrate on discovering fault-tolerant techniques, optimizing hybrid control methods, and investigating novel materials and components. These developments will make MMCs even more reliable and efficient as technology develops, opening the door for their wider use in high-power and dynamic applications.

6.3 DC-DC MMC Control Theory

The MMC is a sophisticated converter topology that, owing to its scalability and efficiency, has become crucial for high voltage and high-current power transformation structures. Particularly, DC-DC MMCs combine the modular structure of MMC with DC-DC conversion, offering advantages including high conversion efficiency, improved fault tolerance, and less harmonic distortion. The challenge of controlling DC-DC MMCs is crucial and intricate as it calls for precise management of both voltage and current, steady functioning, and loss minimization under various operating circumstances. The control strategies and techniques used in DC-DC MMCs include voltage regulation, current control, SM voltage balancing, modulation schemes, predictive control approaches, and efficiency optimization. The key objective control strategies and techniques are to ensure the converter's reliable performance, high efficiency, and effective handling of transient conditions and faults. To generate the desired output voltage in a DC-DC MMC system, the SMs supply voltage steps. The system can easily handle high voltage applications and scale due to its modular design. The output voltage can be regulated to the desired level by selectively engaging or bypassing each SM. Because of its adaptability, the MMC is particularly well-suited for installation in substantial power storage mechanisms, electric vehicle charging infrastructure, and HVDC networks.

It is crucial to design suitable DC-DC MMC architecture and a control strategy for effective high-power transmission in DC-DC MMC topology. Control innovations have been established in recent decades for the effectiveness and adjustable transmission of power in DC-DC MMC configurations and typical MMC configurations. These approaches depend on the implementation of the variables, including regulating the SM capacitor voltages [312], the arm voltage controlling [263], lowering the circulating current [312], specifically controlling the DC voltage proportion [313], active power management [314], and output voltage balance management [60]. The control concept of a traditional MMC and DC-DC MMC is generally separated into exterior control loops and interior control loops. The outer control loops handle the high-level voltage and current regulation, while the inner control loops manage the power-switching behavior of individual SMs, ensuring their operation remains stable and efficient. The preservation of the intended output voltage is the outer control loop's principal responsibility. This is accomplished by controlling the overall voltage that the SMs provide. In this loop, PI and MPC controllers are typically utilized. The duty cycle of the SMs is adjusted to account for any errors in the output voltage, which is continually monitored and compared to the reference voltage. An outside current control loop is also used in some DC-DC MMC systems, especially buck or boost converters [125].

In MMCs, balancing the voltage between the SMs' capacitors is a critical issue [315]. Maintaining the same voltage across each capacitor is essential since the SMs are connected in serial. To achieve equal voltages across all SMs, voltage balancing methods are employed within the inner control loops. This is typically done by controlling the charging and discharging cycles of each SM. Additionally, the inner loop also manages the switching of the SMs. Each SM can be either connected or bypassed to contribute to the overall voltage. The control system adjusts the switching times and duty cycles to regulate the voltage and minimize losses. PWM techniques are commonly used to generate power switching signals, which are crucial for ensuring high-quality voltage output and efficient operation. Various filtering techniques are applied to reduce harmonic content. Additionally, PS-PWM and SV-PWM are employed to minimize harmonics and produce smoother waveforms [316].

MPC is a sophisticated control technique that has grown in popularity. MPC forecasts future system states using the converter's dynamic model and then determines the best course of action for control. By predicting system behavior and modifying the control signals beforehand, this method reduces voltage and current variances. Because it can better manage the converter's non-linear dynamics, MPC has a number of benefits over more conventional control techniques like PID or PI controllers. MPC minimizes current ripple and voltage overshoot while improving transient response by optimizing the control signals. Applications requiring quick and accurate management, including electric car charging and renewable energy integration, benefit greatly from this technique [317].

Several new architectures, modulation methods, and control technologies have been presented to control the concept of DC-DC MMC topologies, and many more investigation studies are needed to increase its effectiveness [318]. This research [319] describes the implementing and governance of an innovative DC-DC MMC that allows offshore wind farms to be integrated into the HVDC power network. The suggested converter's flexibility allows for scaling across an extensive variety of voltage ranges. The suggested converter displays higher characteristics with respect to effectiveness, losses, and device usage. This study uses a proportional resonant (PR) controller to regulate the suggested converter that operates straightforwardly on the MMC's AC output in a stable standard reference. The PR regulator provides identical stable and dynamic characteristics like a synchronous chassis PI regulator, as well as various sub-control cycles such as SM voltage balancing management and circulating current reduction. The utilized controller performs straightforwardly on the primary side of the MMC AC, eliminating complicated transformations and ensuring structure solidity across network fluctuations. A schematic representation of the control technique used for this study [319] is given in Figure 6.3. In the proposed control approach, the transfer functions corresponding to the conventional PI (PI_1 and PI_2) controllers are directly combined with sinusoidal and sinusoidal reference waveforms. This strategy remains valid during both steady-state conditions and transient responses, owing to the fact that the PI controllers function within the synchronous d-q rotating reference frame. Importantly, the methodology does not require the use of Park or similar frame transformation techniques to transition between the stationary and rotating coordinate systems. This study modulates the MMC using the carrier phase shift PWM approach.

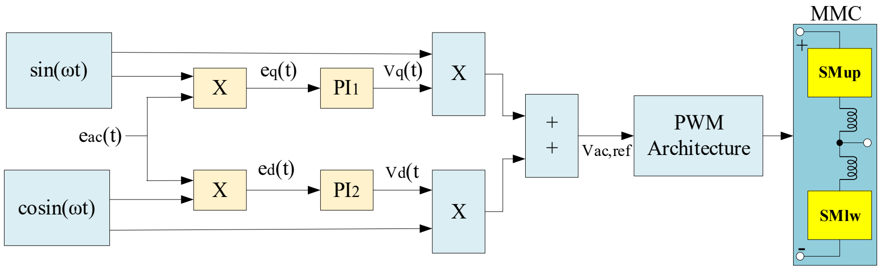

Figure 6. 3 Control structure are utilized in the proposed DC-DC MMC [319].

The output of the control system, $V_{ac,ref}$, is utilized to operate the power switches as modulating signals. This study's control strategy is examined in detail. Reference [320] presents a unique hybrid architecture for attaining effective high voltage DC-DC transformation. It has fewer semiconductor devices, lower initial expenses, a compact structure, and reduced power losses, making it desirable in interconnecting DC power grids with a voltage proportion of lower than two. NLC modulating and SM capacitor voltage stabilization, DC power management, circulating current control, thyristor activation control, and power storing regulation are all part of the control architecture shown in Figure 6.4 of the proposed DC-DC MMC. The referential current of the secondary side of the converter architecture is generated by the DC power management. Power balancing between primary and secondary is required to maintain the steady functioning of the DC-DC converter design. Because the power stored in the SM capacitors is affected by the power differential between primary and secondary sides, a storage technology controller is utilized to maintain the observed average voltage of all SM capacitors in every phase identical to the baseline SM capacitors voltage level. Optimizing the received current from the primary side of the converter accomplishes the above situation. The suggested research explains the comprehensive modulation and control technique in technical detail [320].

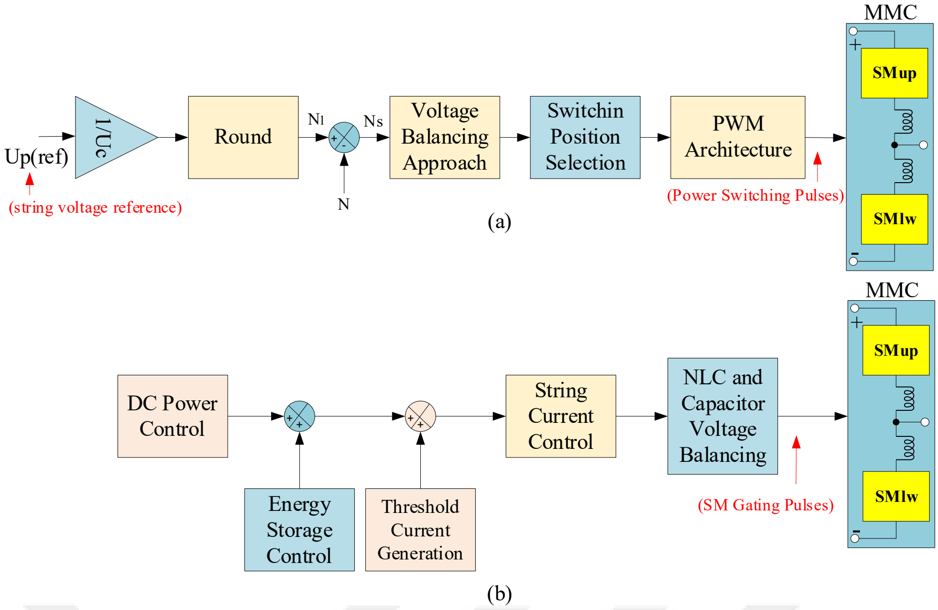

Figure 6. 4 Control technique for proposed converter design: (a) The NLC's control representation. (b) Control block diagrams for the converter design [320].

For output voltage management according to the setpoint voltage value and determining the ideal number of functional SMs rather than utilizing constant numbers like in two-grade modulating whenever the elevation parameter is adjusted, this research [62] offers a finite control set model predictive control topology. The above control approach establishes a cost function depending on the output voltage value and tries to optimize a limited number of SMs to be implanted in each design arm. It considers the current state of SM voltages together with a single-step forecast of the voltage's level. The output voltage achieved whenever that controlling approach is used is consistently closer to the desired voltage. Because the output voltage pursues the desired voltage level, the output current is likewise inside the limitations. The SMs' voltages must similarly be adjusted, with whole SMs having nearly the identical voltage, that is identical to the average of whole SM voltage values in a certain arm. The block diagram of the control technique used in DC-DC MMC design is given in Figure 6.5.

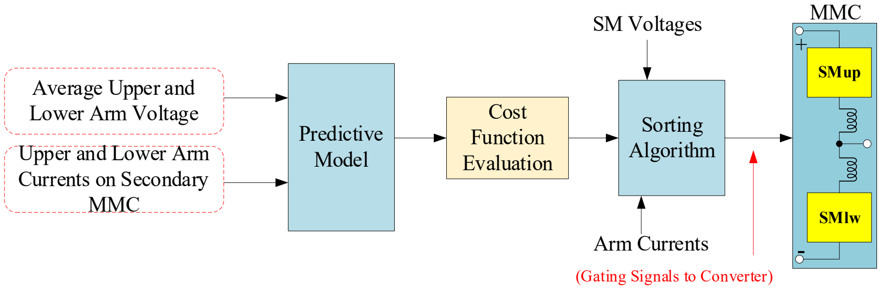

Figure 6. 5 Block diagram of control structure for proposed converter design [62].

A novel MPC for DC-DC MMC without arm inductance based on solid-state transformers is presented in this research [321]. In addition, this study suggested a PS-SWM MPC-centered power transfer and stabilizing controller combined with model-based directional controllers, as well as an enhanced dynamic methodology for the arm inductor-less design architecture. Novel improvements such as interest in using the model-based linear editors to build current references, utilizing an inductor-less arm structure for MMC design, high power productivity, and as well as obtaining inductor-less current management for MMC-based solid-state transformers can be specified in the proposed DC-DC MMC control technique. The controller created specifically for the suggested converter architecture is a closed cycle system element, a directional regulator and a model predictive controller, and a cell exchanging technique that works in an open cycle system, as shown in Figure 6.6. Notwithstanding the lower converter inactiveness, the improvement issue is formulated as an immediate, closed-form calculation within that unique control approach. Furthermore, it does not need a high sample speed to accomplish its controlling goals.

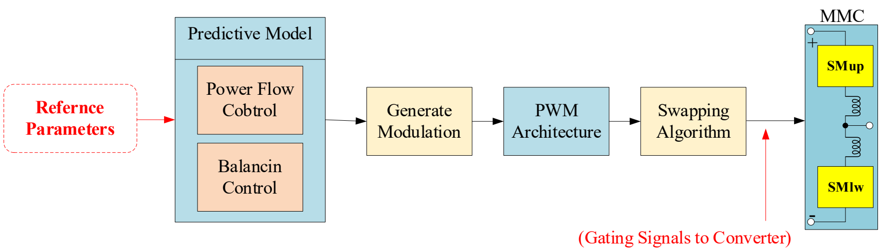

Figure 6. 6 The schematic diagram control structure for the proposed converter design [321].

The interior and exterior variations of the DC-DC MMC are included in the MPC methodology in this study [322], which results in a specialized MPC method. Three control targets are implemented to provide exact control throughout the converter design dynamics. Every one of these control targets is governed by the minimization of a distinct cost function. A fundamental product regulates one of the control targets, and a one-second product increases converter effectiveness according to the defined cost functions. Figure 6.7 depicts the complete control architecture of the DC-DC MMC.

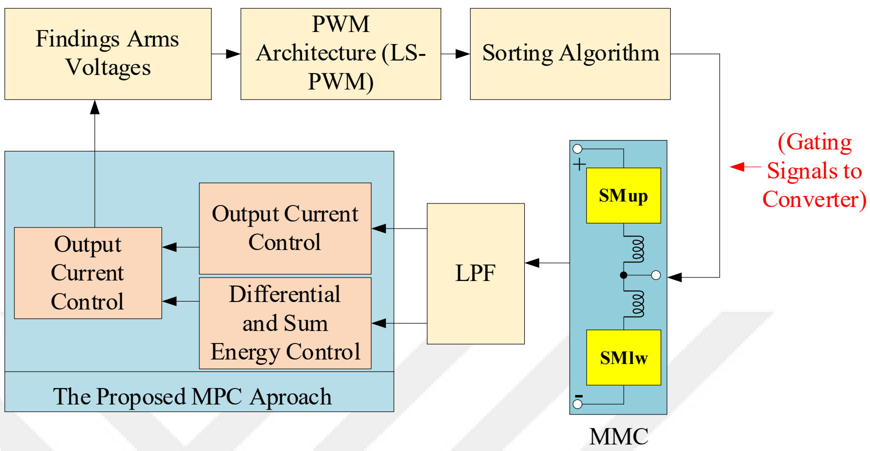

Figure 6. 7 The overall control structure for the provided converter design [322].

The suggested MPC approach improves interior dynamics, such as capacitor voltage beside arm currents, as well as exterior dynamics, such as implanted current flow to DC systems. In addition, in stable conditions, the suggested MPC technique is greater capable of lowering the circulating current. Therefore, the entire configuration's effectiveness improves. Owing to the gathered results, the suggested technique can withstand a 20% toleration in arm inductance of the design. Several good control techniques are provided in this research, which are commonly utilized in both conventional MMC and DC-DC MMC systems. These techniques are investigated thoroughly. Many other control approaches have been presented in the literature in addition to these control approaches.

The DC-DC MMC is an extremely complex power conversion system with exceptional scalability, efficiency, and dependability for high voltage applications because of its modular construction. In the control theory of DC-DC MMCs, a mixture of inner and outer control loops are employed to manage both voltage and current. Advanced modulation methods that improve voltage quality and reduce harmonics, such as PS-PWM and SV-PWM, improve performance. Through its ability to forecast future system states and modify the control signals appropriately, the MPC provides further optimization. Under a variety of circumstances, the DC-DC MMC can operate successfully by guaranteeing fault tolerance, harmonic reduction, voltage control, and current stability. It is an excellent choice for high-power applications such as energy storage structures, HVDC networks, and electric vehicle charging facilities owing to these features. As control algorithms continue to evolve, DC-DC MMC systems' performance, dependability, and efficiency improve, meeting the changing needs of contemporary energy systems and electrical grids.

6.4 PWM Technology

Control of DC-DC MMC topologies is equally essential as the discovery of novel architecture. The control of DC-DC MMC designs is made up of several sections. One of the most crucial elements of these elements is PWM technology. PWM technology is a method for producing a signal at its destination by altering the width of the impulses that will be created. In other words, PWM technology is a method of converting a signal that comes from the original source into impulses at assured times utilizing particular systems. PWM technology is essentially a form of power switching. The power switch is turned on or off in accordance with this signal width by adjusting the width of the pulse supplied from the reference source to the power switch in this technique. Three distinct PWM signals with duty cycle values of 30%, 50%, and 70% are displayed in Figure 6.8. The power switch will be open or active during these conditions. According to the PWM approach, a signal's period is determined by integrating the duty cycle's active and inactive durations. This statement can be modeled mathematically as the following equation:

$$\text{Period of the pulse} = \text{duty cycle}_{\text{active}} + \text{duty cycle}_{\text{inactive}} \tag{6.1}$$

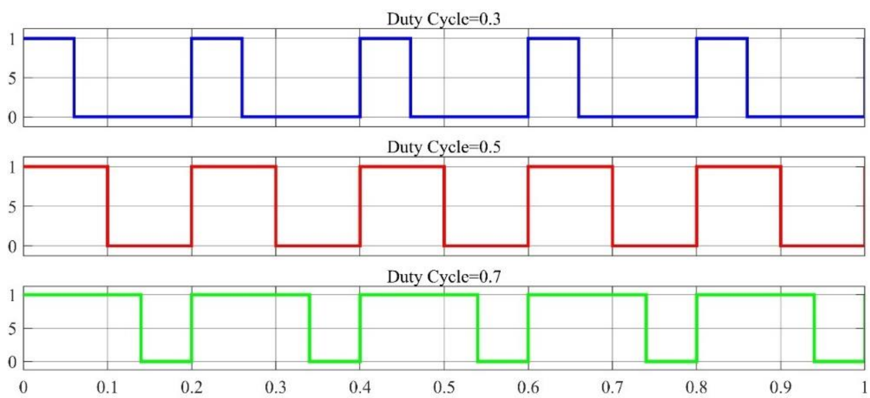

Figure 6. 8 Three PWM signals with duty cycle values of 30%, 50%, and 70%.

The modulation scheme's mission is to produce the intended signal with the smallest possible amount of deformation in low-order harmonics while shifting the inevitable distortions to greater levels to eliminate the need for filtration [125]. PWM signal control is often appropriate for systems and devices that can react rapidly to input. PWM technology frequently uses IGBT or MOSFET semiconductor power components, which have a high operating frequency. With respect to switching frequency, PWM techniques for applications have been separated into high switching frequency PWM modulation, low switching frequency PWM modulation, and fundamental switching frequency PWM modulation structures, as illustrated in Figure 6.9.

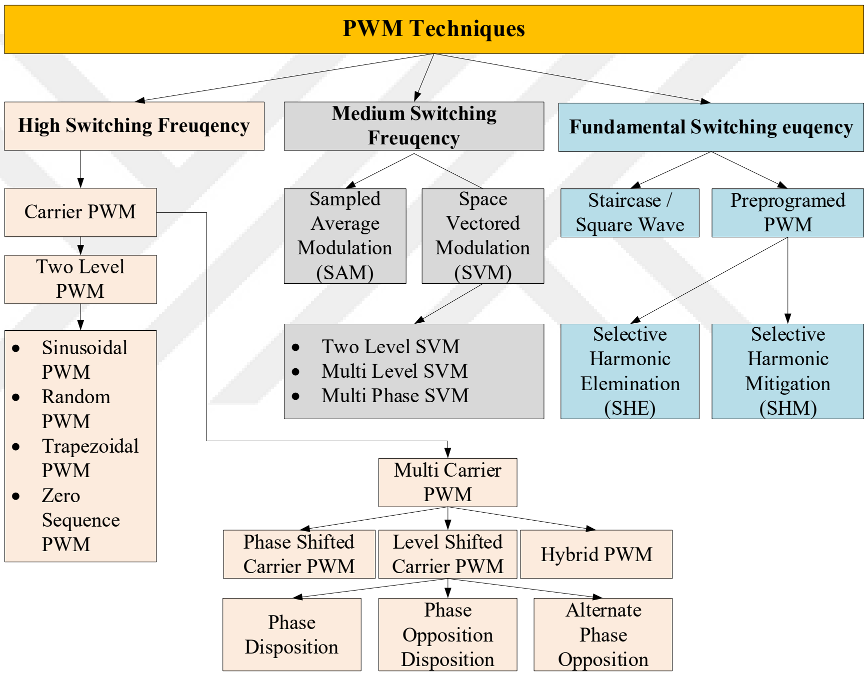

Figure 6. 9 PWM modulation structures [125].

In traditional and DC-DC MMC frameworks, several PWM approaches are more favored than the others for power switching, as shown in Figure 6.10. The methods used for modulation are intended to accomplish several controlling goals, including voltage adjusting, an improvement in common-mode voltage, a reduction in equipment switching frequency, a minimization of power distortions, and a reduction in current ripples. As illustrated in Figure 6.10, the PWM techniques for MMCs are divided into three categories depending on the switching frequency: fundamental switching frequency modulation, high switching frequency, and low switching frequency [323]. In other words, researchers prefer the PWM techniques given in

Figure 6.10 for a more efficient power transfer in conventional and DC-DC MMC designs.

Since multilevel converter architectures are becoming more prevalent, PWM method development and execution are pertinent and significant. The use of PWM techniques produces an output voltage with outstanding characteristics while enabling more precise control of its level and frequency. Carrier-based modulation and space vector modulation (SVM) are the two main categories used to categorize the multilevel PWM techniques demonstrated in Figure 6.11. The PWM architecture includes both of these modulations. Although it appears that the two approaches are considerably distinct from one another, no one strategy has been shown to succeed better [324]. Furthermore, the PWM techniques can be classified into two major categories in accordance with the operational domains in which they have used the state-space vector domain, where the approach depends on generating a set of voltage vectors throughout a period of time, and the period of time domain, where it is relying on the creation of voltage levels over an extended period of time. The various PWM multilevel approaches are identified according to the switching frequency they create. More often than not, lower switching frequency techniques are preferable for applications that require high power because of the reduced switching distortions, but high switching frequency techniques are more appropriate for exceptionally wide varying range operations owing to their superior output power efficiency and increased capacity [325].

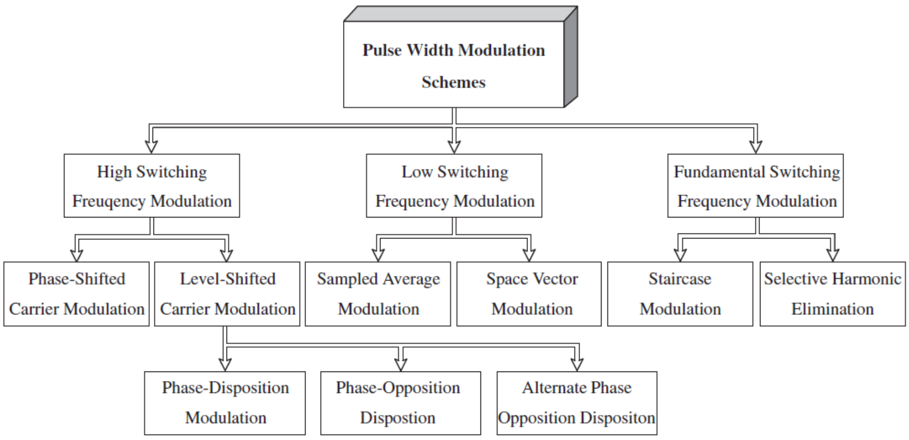

Figure 6. 10 PWM techniques for conventional and DC-DC MMC models [18], [323]**.**

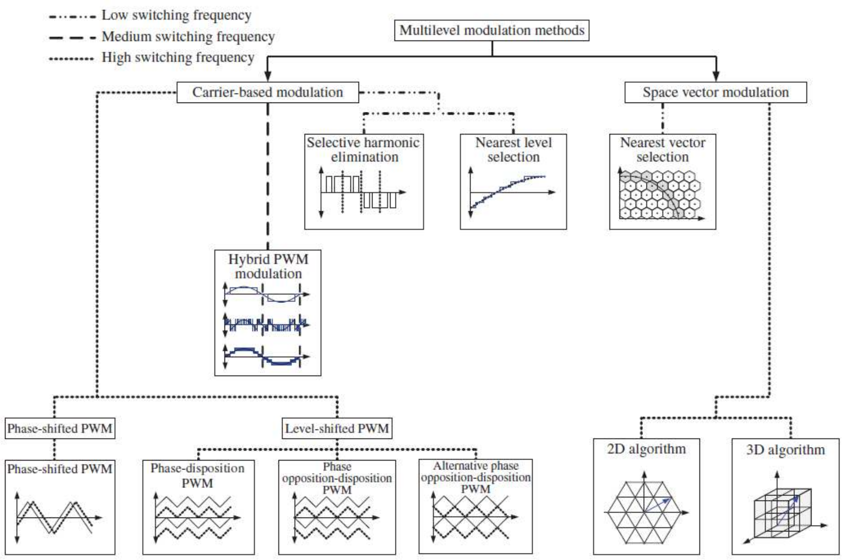

Figure 6. 11 Classifying modulation techniques for multilevel converters [324], [325].

6.4.1 Phase-Shifted Carrier Modulation

Phase-Shifted Carrier Modulation (PSC-PWM) is a high-frequency carrier signal-based modulation technique. The PSC-PWM PWM approach produces an output signal by comparing a reference signal with a sine waveform to N SMs in the phase arms of MMC designs, and N signals with a unique triangular carrier waveform of the same frequency and amplitude. The triangular carrier signals in PSC-PWM are arranged horizontally and have the same amplitude, as shown in Figure 6.12. For this technique, N identical triangular carriers that are positioned apart by an angle of $360^{\circ}/N$ from one another are required, with one carrier for each SM. The lag between the carrier signals is dependent on:

$$\mathrm{T_{lag}} = \frac{1}{\mathrm{N.f_s}} \tag{6.2}$$

Where f_s is the switching frequency in the carrier signal [106]. In the PSC-PWM technique, the same carrier set is used for both the upper and lower arms if the number of submodules for each arm is identical. The output phase voltage in the present scenario is $N + 1$ level.

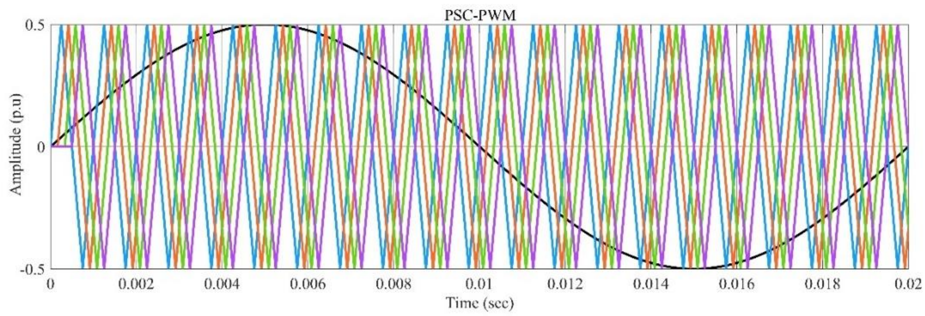

Figure 6. 12 PSC-PWM architecture (for four carrier signals).

6.4.2 Level-Shifted Carrier Modulation

LSC-PWM is a high-frequency carrier signal-based modulation technology similar to the PSC-PWM technique. High-frequency carrier signals are compared with a reference sinusoidal signal in the LSC-PWM approach. The resulting comparison provides an output signal for the power switches of the SM, which are used in MMC implementations. The carriers in the LSC-PWM technique have an amplitude equal to the sinusoidal reference signal's amplitude. The triangular carriers for LSC-PWM are arranged vertically and have identical amplitudes.

For the LS PWM approach, each carrier signal's magnitude is determined by dividing the reference signal's amplitude by the quantity of SMs. To divide the carrier signals into various ranges, the location of the carrier signals is modified by increasing their intensities [326]. The LSC-PWM techniques necessitate N consecutive displacements of N equivalent triangular carrier signals throughout the entire DC voltage value. Peak-to-peak magnitudes of the carrier signals, which have the frequency of f_s are made equivalent concerning each other to allow the utilization of circuit components that produce various levels of voltage [327]. The LSC-PWM technique is subsequently separated into three different categories, which are phase-disposition (PD-PWM), phase-opposition-disposition (POD-PWM), and alternate phase opposition-disposition (APOD-PWM).

6.4.2.1 Phase-Disposition PWM

In the PD-PWM method, the whole carrier signals employed in a carrier established have identical frequency and phase sequences. The amplitude of the reference signal is taken into account in this modulation approach to determine the magnitudes of the carrier signals. As observed in Figure 6.13, the carrier signals of the PD-PWM technique have been relocated in the DC voltage region to create an MMC with four SMs per phase arm.

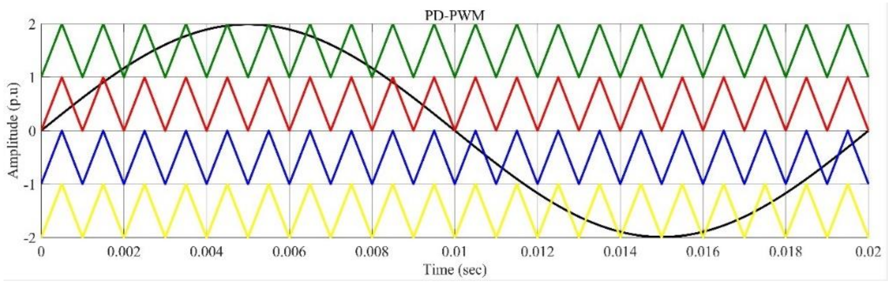

Figure 6. 13 PD-PWM structure (for four carrier carriers).

6.4.2.2 Phase-Opposition-Disposition PWM

POD-PWM is another level-shifted approach that is alike to the PD-PWM structure. The MMC's upper arm carrier signals, those considered positive ones, have a phase shift of 180 degrees in comparison to the MMC's lower arm carrier signals in the POD-PWM technique. In other words, the carrier signals in the POD-PWM technique are 180° beyond phase with respect to one another. The carrier's magnitudes can be changed similarly to PD-PWM techniques. Figure 6.14 illustrates the structure of the four carrier signals of the POD-PWM technique.

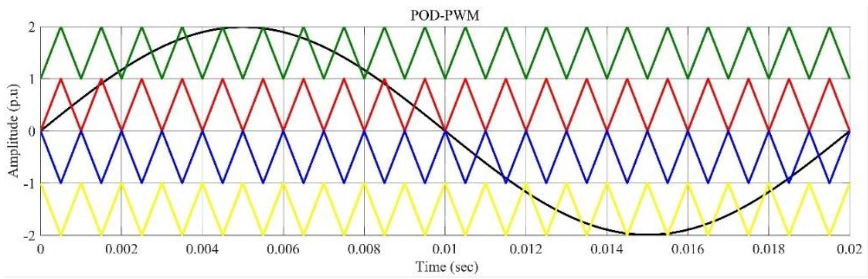

Figure 6. 14 POD-PWM carriers' structure (for four carrier carriers).

6.4.2.3 Alternate Phase Opposition-Disposition

The carrier signals in the APOD-PWM technique are 180 degrees out of phase for carrier signals under the zero axis as well as in phase for carriers over the zero axis. To put it another way, for each pair of carrier signals, the carrier signals are alternately shifted by 180°. In other words, every carrier signal in an arrangement of carrier signals representing a single arm has a 180° phase shift in comparison to its peer. Figure 6.15 illustrates carrier signals of the APOD-PWM approach.

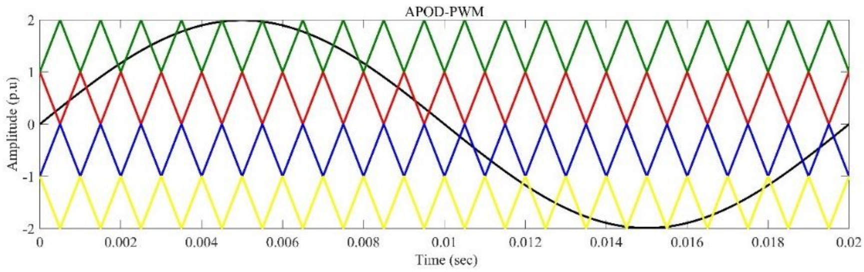

Figure 6. 15 APOD-PWM technique carriers' structure (for four carrier carriers).

6.5 Summary

PWM is crucial in identifying each SM's switching states, which influences the output voltage waveform, harmonic content, and MMC efficiency. Depending on the application, several PWM approaches control these switching patterns, each with unique benefits and trade-offs. Effective voltage and current management, in addition to PWM, is essential to MMC functioning. While current management algorithms precisely maintain the intended current profile, voltage balancing approaches guarantee constant voltage across each SM. Reference tracking control, linear and nonlinear control approaches control, and, more recently, MPC are popular control techniques that provide the best possible regulation of system performance even in the face of intricate and variable operating circumstances. Thanks to its modular architecture and a highly advanced power conversion system, the DC-DC MMC offers great scalability, efficiency, and reliability for high voltage applications. In the control theory of DC-DC MMCs, voltage and current are managed by combining inner and outside control loops (voltage and current regulation). MPC provides further optimization through the prediction of future system states and the subsequent adjustment of the control signals. In conclusion, optimizing these converters' performance, dependability, and efficiency requires carefully selecting PWM approaches in conjunction with the control theory underlying MMC systems. The strategies discussed in this section not only improve operating efficiency but also expand the spectrum of uses for MMCs in industries such as power transmission, renewable energy-based power structures, and electrically powered vehicles. MMC control theory research developments will probably concentrate on more sophisticated modulation strategies and control algorithms to further boost performance, reduce losses, and increase fault tolerance in intricate real-world systems.

In this study, PD-PWM, POD-PWM, and APOD-PWM techniques are employed due to their distinct advantages in multilevel converter applications. These carrier-based modulation strategies are chosen for their ability to enhance voltage waveform quality, reduce switching losses, and maintain voltage balance across converter levels. PD-PWM offers a straightforward implementation and effectively minimizes THD in line-to-line voltages, making it suitable for systems prioritizing high power quality. POD-PWM, as well as providing improved control of the neutral-point voltage, which is especially beneficial in neutral-point-clamped (NPC) converters. APOD-PWM contributes to a more uniform harmonic distribution by alternating the phase of carrier signals, thus improving electromagnetic compatibility and thermal performance. The use of these methods supports the overall objective of achieving efficient and reliable operation in advanced power electronic systems.

CHAPTER VII
A NOVEL DC-DC MODULAR MULTILEVEL CONVERTER DESIGN FOR HVDC INTERCONNECTION

7.1 Introduction

Power electronics-based DC-DC converter designs have undoubtedly played a significant role in the recent fast development of HVDC technologies. Due to recent improvements in semiconductor-based power electronics technology, multi-level converter systems are also utilized in HVDC technology. Day by day, the share of MMC-based HVDC technologies in power systems grows dramatically. In power systems, conventional MMC technology established in the literature can be implemented as an inverter station (DC-AC) and a rectifier station (AC-DC). Due to its increasing popularity, DC-DC MMC technology, accomplished through utilizing conventional MMC technology as a reference, has drawn the curiosity of many researchers. DC-DC MMC technology provides excellent results, particularly in integrating modern asynchronous HVDC power systems and new-generation HVDC power systems with existing asynchronous HVAC power systems. A unique DC-DC MMC design is introduced in this study to integrate two asynchronous HVDC power grids successfully. The operation of the fundamental nature, simulation-based parameter records, and mathematical analysis of the relevant topology have all been thoroughly analyzed. This study offers a novel DC-DC MMC design essential to fulfilling the demands of HVDC technology, which is gaining popularity among power system researchers and entrepreneurs daily. It provides an excellent approach to integrating modern HVDC power networks with varying voltage levels, which are increasingly used in power systems. A satisfactory power transfer was observed, considering the suggested arrangement was implemented in a simulated environment based on the simulation outcomes. Therefore, the suggested DC-DC MMC topology offers several improvements, novelties, and noteworthy achievements compared to the existing DC-DC MMC topologies in the literature.

7.2 Proposed Non-isolated DC-DC MMC Model

HVDC technology has recently played a more significant role in global power networks. Nonetheless, it is unavoidable that some integration issues exist between new-generation HVDC power systems with various voltage levels and conventional HVDC power systems. Simultaneously, combining HVDC power networks with HVAC power networks, which are more common worldwide, presents some integration challenges. Using multi-level converter systems is of the utmost importance at that stage. The novel non-isolated DC-DC MMC design proposed in this study provides a remarkable answer to the incorporation issues in power systems outlined above.

The innovative non-isolated DC-DC MMC technology has been developed with inspiration from the investigations in [12], [322]. Figure 7.1 shows the proposed innovative non-isolated DC-DC MMC design. The two-arm and one-arm architectural structures of the suggested non-isolated DC-DC MMC architecture are illustrated in Figure 7.2 and Figure 7.3, respectively. The proposed non-isolated DC-DC MMC design's architectural framework and mathematical analysis have recently been described. The novel DC-DC MMC architecture suggested is non-isolated (transformerless) in structure. The proposed converter topology benefits significantly from this method, which includes reduced volume, more appealing financing costs, fewer SM counts, lower weight, less power loss, etc. The construction of the suggested non-isolated converter is less complicated. This results in lower power loss and higher efficiency, which are crucial advantages, especially for energy conservation applications. Due to its more straightforward and less complicated construction, this converter is a cost-effective structure. Lower manufacturing expenses lead to lower overall system costs when isolating parts are absent. It also helps to save operating and maintenance expenses. This financial benefit becomes significant, particularly for large-scale power applications. Table 7.1 presents comparative data and numerical estimates for the recommended transformerless design based on criteria such as reductions in volume, weight, cost, and power losses. Conventional isolated DC-DC MMCs typically require bulky step-up/down transformers, resulting in converter volumes system weights for comparable power ratings. By removing the transformer stage and employing a compact three-arm symmetrical structure, the proposed design reduces the volume and the total weight of the design, corresponding to nearly 40%

reduction in both categories. Similarly, the hardware simplification significantly decreases the number of required semiconductors. Isolated topologies require a large number of switches depending on the design (for instance 146 HBSM=292 power switches [66]), the proposed configuration operates effectively with only 96 IGBT switches (3 arms × 4 SM sets × 4 HBSMs × 2 switches per HBSM). This reduction not only lowers costs but also minimizes switching losses. As a result, overall system costs are estimated to be approximately 30% lower than conventional designs, mainly due to the elimination of transformers and reduced SM counts.

Table 7. 1 Comparative evaluation of proposed topology vs. conventional isolated DC-DC MMCs

Criterion	Conventional Isolated DC–DC MMC (Literature)	Proposed Non-isolated DC–DC MMC	Improvement
Converter Volume	Bulky transformers & filters) 146 HBSM, 2 transformers [66], 16 HBSM, 4 FBSM, 4 transformers c, in primary side 20 FBSM, in secondary side 20 or 30 FBSM (dependind to selected company), 1 transformer [340]	Compact, 1 type 48 SM, eliminated transformer	Reduced volume
System Weight	High Level Heavy (Including HV transformer), 146 HBSM, 2 transformers [66]	Trasformerless design, 48 HBSM	Reduced SM, eliminated transformer
Semiconductor Count	16 HBSM, 4 FBSM, 4 transformers [328]	48 HBSMs power switches	Reduced quantities of SM
Estimated Cost	Based on SM and number of transformers	Lower cost compared to studies at the table and literature	Reduced cost
Power Losses	≈3-3.5% of rated power (96% efficiency) [26], 5-6% of rated power (>94% efficiency) [328]	<3% of rated power (>96% efficiency)	Reduced power losses

Efficiency	93–95% common for isolated MMC DC-DC prototypes [328]	≥96%	Improvement of efficiency
SM Capacitor Ripple	≈10% typical imbalance in isolated MMCs	±5% (simulation: Figs. 8.11, 8.20, 8.27)	Reduction ripple

In terms of efficiency, the proposed converter achieves >96% efficiency, outperforming typical isolated MMC-based DC-DC converters that reach 93–95%. Power loss analysis shows that total losses account for less than 3% of rated power, compared to 3-5% in traditional designs. Moreover, the capacitor voltage ripple is tightly controlled within ±5%, compared to reported in conventional systems, confirming superior dynamic stability and voltage balancing. These results collectively validate that the proposed non-isolated DC-DC MMC achieves a substantial reduction in volume, weight, cost, and power losses, while simultaneously improving efficiency and reliability, thereby demonstrating clear advantages over existing topologies in the literature.

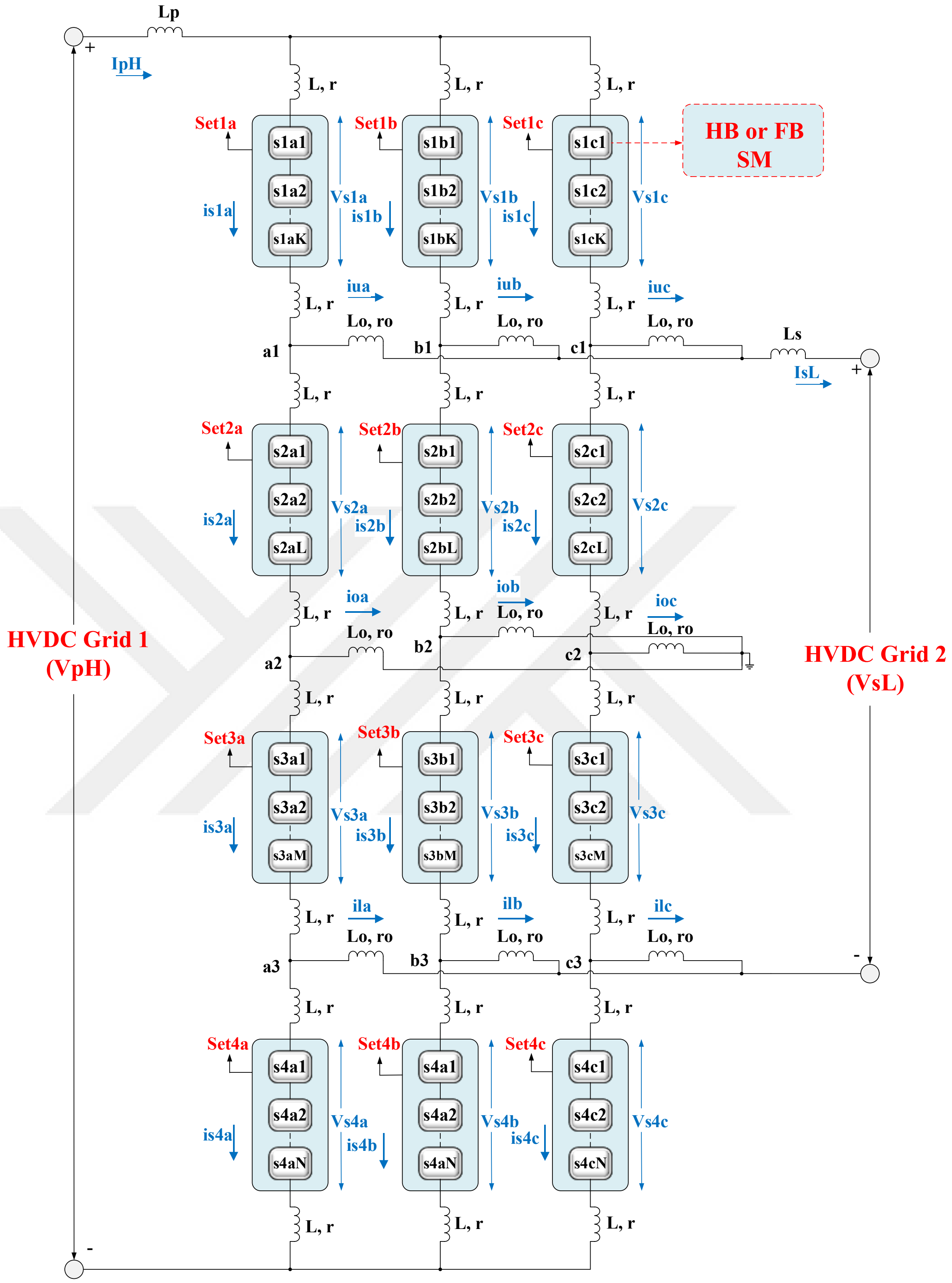

Figure 7. 1 Proposed innovative non-isolated DC-DC MMC topology.

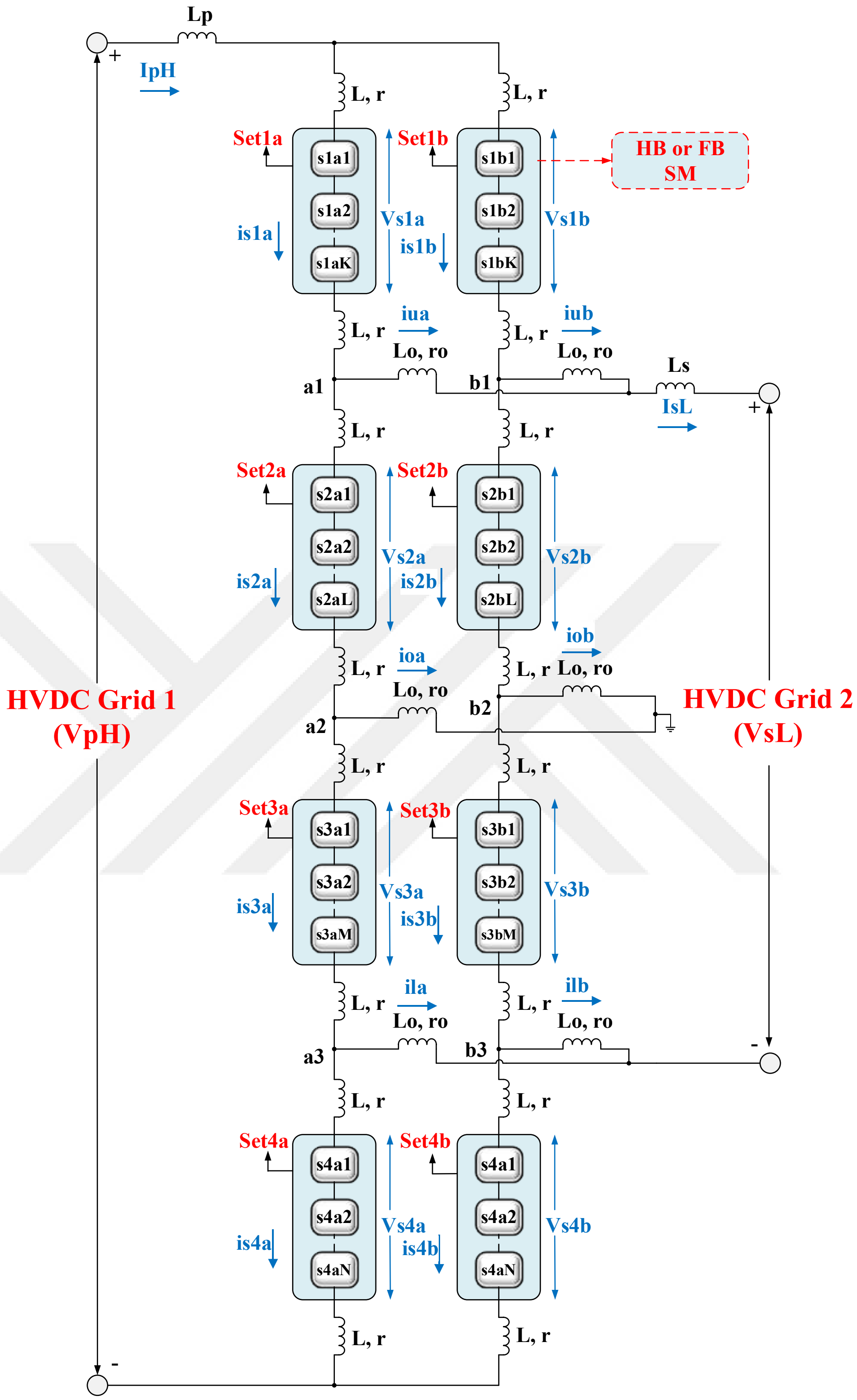

Figure 7. 2 Proposed unique DC-DC MMC topology with 2-arm structure.

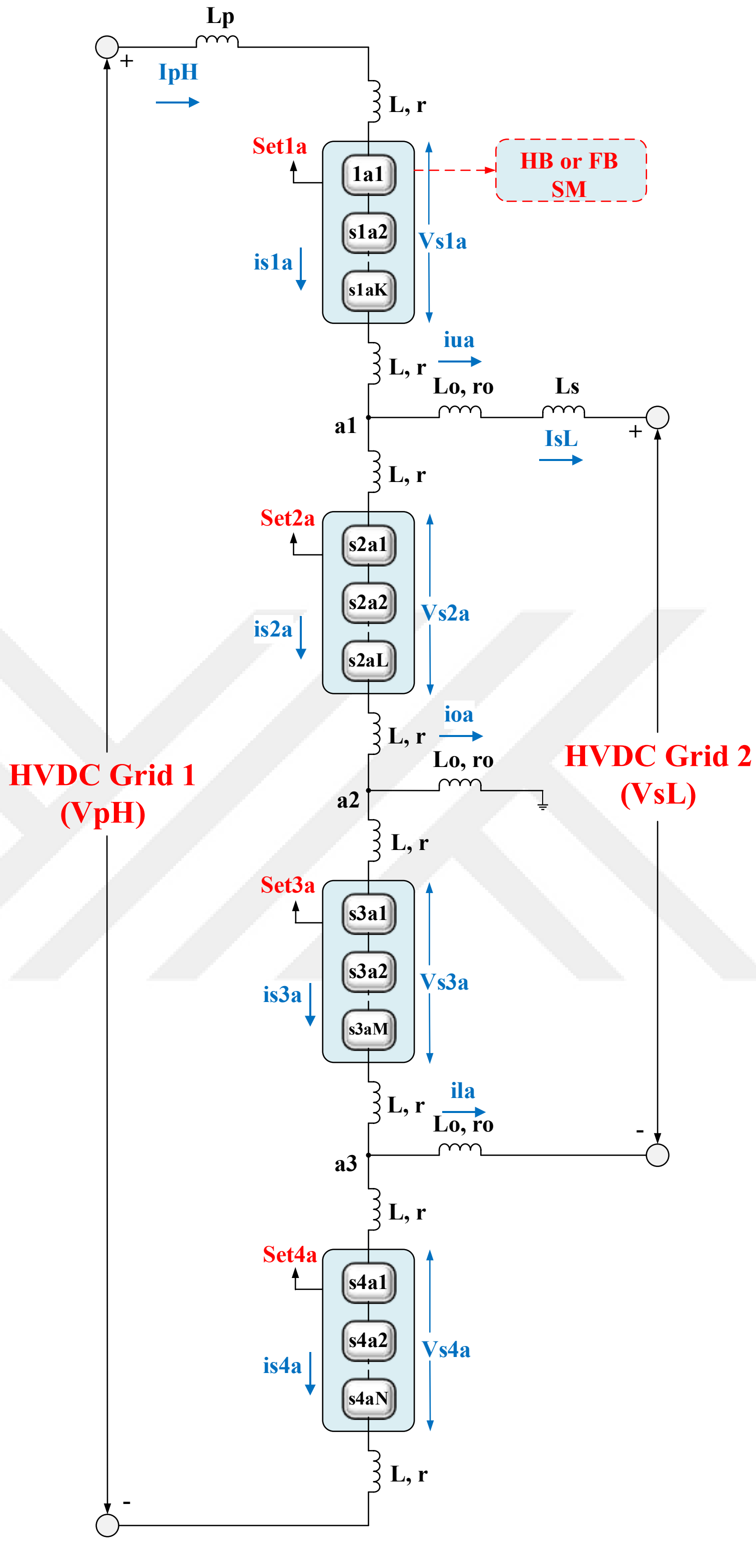

Figure 7. 3 Proposed unique DC-DC MMC topology with 1-arm structure.

Proposed DC-DC MMC topology results in a lightweight, non-isolated converter due to its more straightforward construction and fewer components. This functionality is quite beneficial, particularly for manufacturing and transportation procedures. The

DC-DC MMC topology can provide excellent power density because it is designed in a non-isolated configuration. This approach enhances power transfer by enabling the converter structure to generate greater electrical power. The following sections of this research will examine how the proposed non-isolated DC-DC MMC architecture integrates with existing HVAC power systems. Table 7.2 presents a selection of DC–DC MMC topologies reported in the literature that contribute significantly to the relevant research domains. It also provides a comparative evaluation between these existing topologies and the proposed DC–DC MMC configuration.

Table 7. 2 Some DC-DC MMC topologies' contributions to application areas.

DC-DC MMC	Application Area	Contribution to Literature
[80]	Hybrid HVDC grid interconnections	The suggested concept can connect HVDC networks utilizing VSC and LCC and operate in four quadrants.
[34]	MVDC grids	The study presents a bipolar MMDC operational approach to achieve stable performance in bipolar MVDC power distribution networks.
[26]	HVDC grids	The suggested arrangement using the fewest possible semiconductors can effectively deliver high DC voltage multiplication through a DC failure- avoiding ability and sustained bi-directional power transmission.
[11]	HVDC grid interconnections	The suggested design has several benefits, including a reduced volume, more appealing investment costs, and reduced SMs.
[330]	Rapid charging of electric vehicles	The suggested design reduces the control complexities and switching numbers using a single half bridge-MMC arm. It can naturally prevent DC faults, and a high voltage conversion rate can be obtained through galvanic isolation.
[331]	LVDC and MVDC grid interconnections	Decreased computational stress for power enforcement, circulating current mitigation, DC fault ride-through functioning, and transformer current optimization for improved effectiveness throughout the whole load range have been made possible by the suggested design.
[6]	MVDC and HVDC grid interconnections	This paper suggests using magnetizing inductance as a basis for an analytic analysis of the DC-DC MMC's performance. The difference method circulating current, converter powers, currents, capacitor voltage ripples, and soft-switching behavior are all shown to be significantly impacted by the magnetizing inductance.
[33]	LVDC and HVDC grid interconnections	The primary benefit of the suggested converter is that it utilizes a single bidirectional high-voltage valve and traditional MMC arms with HBSMs to achieve DC-DC transformation alongside appropriate capacitor voltages and restricted voltage ripples.

[332]	MV DC-DC interconnections	Compared to the MMC, the suggested design requires just one-third of the SMs, voltage, and current sensors to produce three-phase trapezoid outputs with a regulated sloping. The DC fault-blocking capacity, flexible grounding, and desirable voltage matching are all provided by the front-to-front arrangement of the suggested design.
[23]	DC distribution grids	In contrast to the conventional MMC, the suggested design allows the buck cell to produce smoother voltage control and a larger voltage band. The excellent efficiency of the MMC-based DAB unit is ensured by the assured voltage corresponding between the LV and MV ends over the whole voltage band.
[Proposed Study]	HVDC grid interconnections	This study presents a unique DC-DC MMC architecture that provides an excellent solution for integrating modern asynchronous HVDC networks and these modern HVDC power systems with existing HVAC power systems. The transformerless approach significantly reduces the converter's volume, weight, price, and power loss. The suggested converter exhibits several characteristics, including a straightforward circuit design, innovative structure, acceptable swift dynamic reaction, controllability, and bidirectional power flow. A power transfer control system is presented in this unique study to accurately regulate the power transfer across power systems with different or similar voltage levels.

7.3 The Proposed Non-isolated DC-DC MMC Design's Architectural Structure

Based on the fundamental concepts of the classical MMC approach, the suggested non-isolated DC-DC MMC architecture is intended to accomplish DC-DC MMC conversion rather than DC-AC conversion. Similar to the traditional MMC architecture, the unique DC-DC MMC model that has been suggested has many arms, each including numerous SM clusters. The recommended innovative DC-DC MMC design consists of three essential arms (arms a, b, and c), as demonstrated in Figure 7.1. Four independent SM sets, each involving four HBSM structures (Set1a, Set2a, Set3a, and Set4a for arm-a), combined to form each arm. In this case, the primary rationale for utilizing HBSM construction is its straightforward design, which strives to employ as few as conceivable power switches to minimize switching losses. Figure 7.4 illustrates the SM structures researchers most frequently utilize in traditional MMC and DC-DC MMC architectures. IGBT-based HBSM and FBSM architectures are depicted in Figures 7.4(a) and 7.4(b) correspondingly. The MOSFET-based HBSM form is illustrated in Figure 7.4(c), while the MOSFET-based FBSM architecture is presented in Figure 7.4(d). The IGBT power switch based on semiconductors was chosen for the HBSM construction. These SM sets have been identified individually for each arm as top SM set (Set1a for arm-a), bottom SM set (Set4a for arm-a), middle top SM set (Set2a for arm-a), and middle bottom SM set (Set3a for arm-a).

There is one arm inductance (L, r) for each arm that occurs before and after the corresponding SM sets. The recommended DC-DC MMC design's secondary side positive terminal is formed by the branch arms that arise for each arm between the top and middle top SM sets (points $a1, b1, and\ c1$). These branch arms are connected sequentially through the arm filtering inductor (L_o, r_o). The secondary side negative terminal of the recommended DC-DC MMC design has been formed like that of the system's output side positive terminal by a branch arm emerging between the bottom SM set and the middle bottom SM set (points $a3, b3, and\ c3$) for each arm and connected successively through the arm filtering inductor (L_o, r_o). The center ground branch arm of the proposed DC-DC MMC design is formed by a branch arm that emerges between the middle top SM set and the middle bottom SM set of each arm (points $a2, b2, and\ c2$). This branch arm is connected sequentially through the arm filtering inductor (L_o, r_o), reminiscent of the formation of positive and negative secondary side terminals. In the proposed design, arm filtering inductors (L_o) make confident that the AC portion of the cycle is sufficiently diminished while arm inductors (L) among the SM sets soak up the short-term voltage variations arising from the switching process of the SMs in the cycle comprising the primary side of the architecture and the DC-DC MMC arms. According to the current levels flowing through the SM sets, the established voltage balancing and control system and the implementation of arm inductors (L) in the suggested novel DC-DC MMC architecture minimize any circulation currents in the arms at acceptable levels. The ohmic power losses related to L and L_o are represented by resistances r and r_o, correspondingly. In the proposed DC-DC MMC design, L_p and L_s represent the filtering inductances of the design's primary and secondary side of the design, respectively.

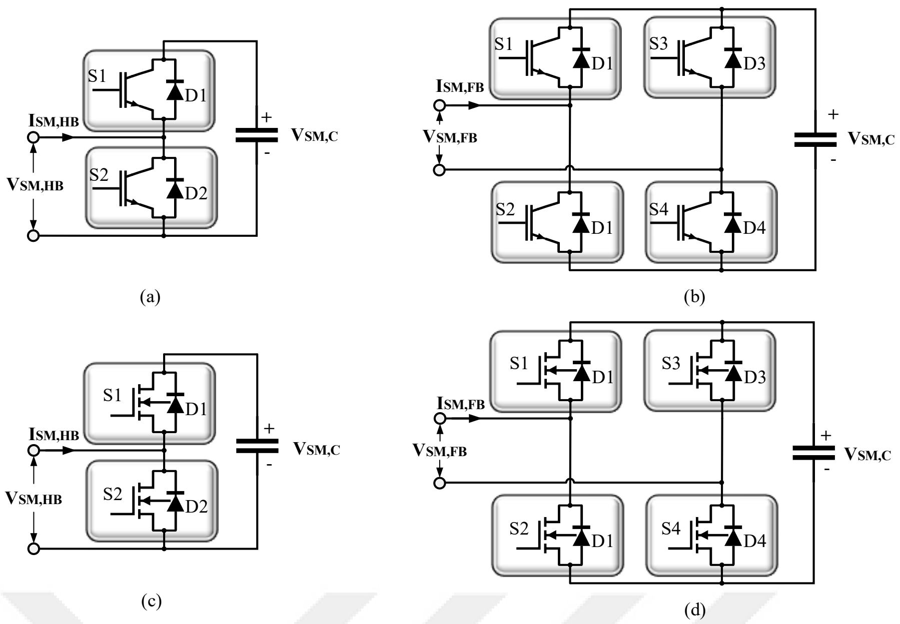

Figure 7. 4 The SM structures are most frequently utilized in MMC designs: (a) IGBT-founded HBSM; (b) IGBT-founded FBSM; (c) MOSFET-founded HBSM; (d) MOSFET-founded FBSM.

In contrast to previously reported DC-DC MMC configurations, the proposed topology introduces structural innovations that fundamentally differentiate it from existing approaches. First, while many conventional designs rely on complex transformer-based isolation stages, the presented architecture is entirely transformerless, which not only minimizes bulk hardware but also eliminates limitations in high-voltage scalability. Second, the SM configuration (HBSM) in the proposed structure is arranged in a symmetrical and modular manner, ensuring balanced operation across the arms with fewer switching components. This arrangement significantly reduces circulating currents and enhances voltage balancing without requiring sophisticated auxiliary circuits, which are often necessary in traditional MMC-based converters. Furthermore, the interconnection strategy between SM groups is deliberately simplified to achieve efficient bidirectional power flow with reduced control burden. Unlike earlier topologies that depend on multi-stage energy transfer or hybrid SM arrangements, the proposed design employs a compact three-arm structure where SM clusters are flexibly interconnected, leading to a more robust and cost-effective configuration. These structural distinctions highlight the novelty of the proposed DC-DC MMC and establish it as a practical alternative for large-scale HVDC interconnection applications. Additionally, this research provides an analysis of the integration of both contemporary DC power grids and current AC power grids, as well as strategies within the boundaries of DC-DC MMC topologies. In contrast, the majority of DC-DC MMC topologies in literature only suggest strategies within these boundaries. It is evident from the results that the suggested topology is vital for both conventional (HVAC) and contemporary (HVDC) power grids.

7.4 The Mathematical Model of Proposed Non-isolated DC-DC MMC

Power conversion system design, analysis, and optimization all heavily rely on mathematical modeling. Mathematical models contribute to the stability and functionality of the converter by offering a more thorough comprehension of the system's underlying dynamics, including both linear and nonlinear characteristics. Mathematical modeling is critical in adequately evaluating the recommended architectures in MMC technology. The mathematical analysis of the proposed DC-DC MMC topology is developed with reference to the equivalent circuit representations illustrated in Figures 7.5 and 7.6. The analysis systematically incorporates the three-arm configuration as well as the reduced two-arm and single-arm equivalent models to comprehensively capture the system's operational behavior.

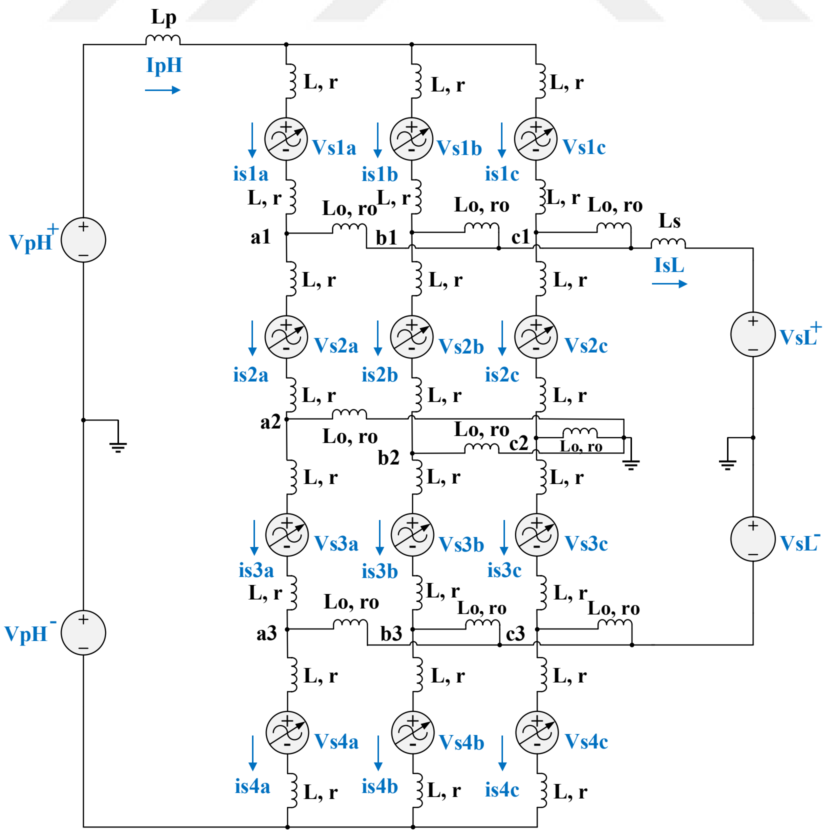

Figure 7. 5 The proposed DC-DC MMC design's equivalent circuit.

Figure 7.5 demonstrates the circuit equivalent to the novel DC-DC MMC design that has been suggested. The 2-arm and 1-arm equivalent circuit designs of the suggested DC-DC MMC design are illustrated in Figures 7.6(a) and Figure 7.6(b). A voltage source with a variable characteristic in this equivalent circuit structure represents each branch's SM groups. Voltage sources that alter over time consist of both DC and AC components. The mathematical counterparts of these DC and AC components are presented below.

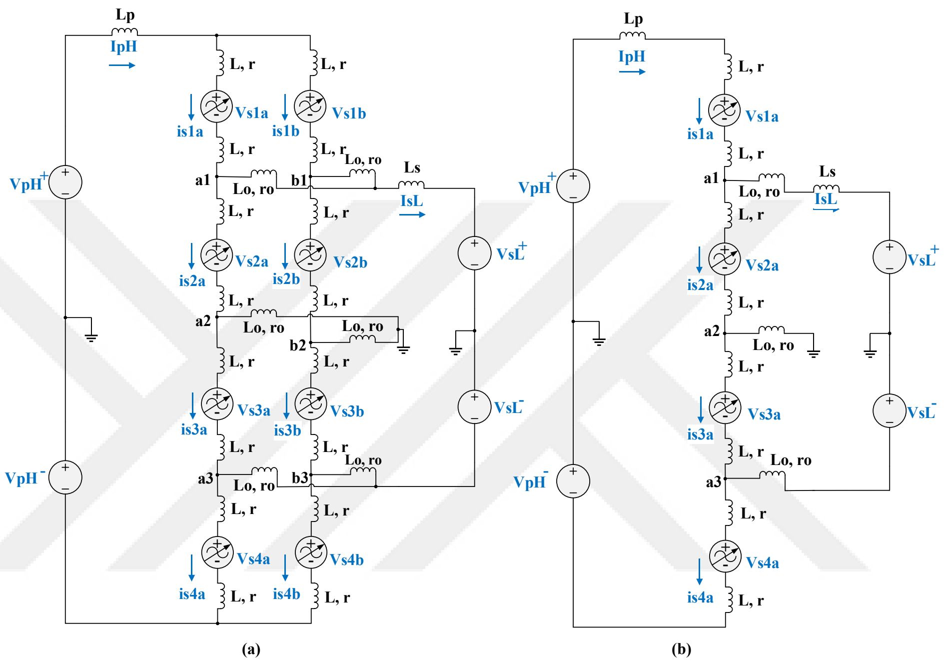

Figure 7. 6 The proposed novel DC-DC MMC design's equivalent circuits with 2-arm and 1-arm structures: (a) 2-arm equivalent circuit structure; (b) 1-arm equivalent circuit structure.

According to the 1-arm equivalent circuit model (arm-a) of the suggested DC-DC MMC architecture, the mathematical computations provided in the following section have been carried out. Since similar mathematical analyses are valid for the other arms of the design (arms b and c), this study does not include mathematical evaluations for the two arms under consideration. The following mathematical parameters can be determined by applying the fundamental KVL and KCL to the architecture of the 1-arm circuit illustrated in Figure 7.6(b). First and foremost, the following are the voltage equations for SM clusters.

$$v_{s1a} = v_{s1a,dc} + v_{s1a,ac} = \frac{V_{pH}}{2} - \frac{V_{sL}}{2} + 2L\frac{d}{dt}i_{s1a} + 2ri_{s1a} + V_{s1a,max}\sin\omega t \quad (7.1)$$

$$v_{s2a} = v_{s2a,dc} + v_{s2a,ac} = \frac{V_{sL}}{2} + 2L\frac{d}{dt}i_{s2a} + 2ri_{s2a} + V_{s2a,max}\sin(\omega t + \theta_1) \quad (7.2)$$

$$v_{s3a} = v_{s3a,dc} + v_{s3a,ac} = \frac{V_{sL}}{2} + 2L\frac{d}{dt}i_{s3a} + 2ri_{s3a} - V_{s3a,max}\sin(\omega t + \theta_2) \quad (7.3)$$

$$v_{s4a} = v_{s4a,dc} + v_{s4a,ac} = \frac{V_{pH}}{2} - \frac{V_{sL}}{2} + 2L\frac{d}{dt}i_{s4a} + 2ri_{s4a} - V_{s4a,max}\sin(\omega t + \theta_3) \quad (7.4)$$

$$i_{s1a} = I_{PH} = i_{s2a} + i_{s1a,uo} \quad (7.5)$$

$$i_{s2a} = i_{s3a} + i_{s1a,co} \quad (7.6)$$

$$i_{s4a} = i_{s3a} + i_{s1a,lo} \quad (7.7)$$

where $v_{s1a}, v_{s2a}, v_{s3a},$ and v_{s4a} denote the voltage expressions for the SM sets which are set1a, set2a, set3a and set4a in arm a, respectively. In keeping with the same logic $i_{s1a}, i_{s2a}, i_{s3a},$ and i_{s4a} represent the currents flowing through the SM sets which are set1a, set2a, set3a and set4a in arm a, correspondingly. The AC magnitude of the AC voltage of sets which are set1a, set2a, set3a, and set4a is represented by $V_{s1a,max}, V_{s2a,max}, V_{s3a,max},$ and $V_{s4a,max}$ respectively. $\theta_1, \theta_2,$ and θ_3 are corresponding initial phase angles of SM sets voltage expression for arm-a. The angular frequency is represented by ω. The primary and secondary DC voltage levels of the suggested DC-DC MMC design are denoted by the V_{pH} and V_{SL}, correspondingly. Secondly, the current expressions of SM clusters are as follows.

$$i_{s1a} = i_{s1a,dc} + i_{s1a,ac} = I_{pH} + I_{s1a,max}\sin(\omega t + \beta_1) \quad (7.8)$$

$$i_{s2a} = i_{s2a,dc} + i_{s2a,ac} = I_{pH} - \frac{V_{pH}}{Vs_L}I_{pH} + I_{s2a,max}\sin(\omega t + \beta_2) \quad (7.9)$$

$$i_{s3a} = i_{s3a,dc} + i_{s3a,ac} = I_{pH} - \frac{V_{pH}}{Vs_L}I_{pH} - I_{s3a,max}\sin(\omega t + \beta_3) \quad (7.10)$$

$$i_{s4a} = i_{s4a,dc} + i_{s4a,ac} = I_{pH} - I_{s4a,max}\sin(\omega t + \beta_4) \quad (7.11)$$

Examining the voltage and current expressions of the SM sets above reveals that each voltage and current parameter comprises two parts: DC and AC. The DC voltage components of the SM sets are represented by $v_{s1a,dc}$, $v_{s2a,dc}$, $v_{s3a,dc}$, and $v_{s4a,dc}$. $v_{s1a,ac}$, $v_{s2a,ac}$, $v_{s3a,ac}$, and $v_{s4a,ac}$, are the AC voltage components of sets of SM. Considering a comparable methodology, the AC components of the currents flowing through the SM sets are expressed by $i_{s1a,ac}$, $i_{s2a,ac}$, $i_{s3a,ac}$, and $i_{s4a,ac}$, while the DC components are expressed by $i_{s1a,dc}$, $i_{s2a,dc}$, $i_{s3a,dc}$, and $i_{s4a,dc}$. The AC magnitude of the AC voltage of sets which are set1a, set2a, set3a, and set4a is represented by $I_{s1a,max}$, $I_{s2a,max}$, $I_{s3a,max}$, and $I_{s4a,max}$ respectively. The phase angle of the currents flowing through the SM sets is represented by the letters β_1, β_2, β_3, and β_4. The following equation is the current flowing from point a2 through the grounding branch line. It is evident from equation (7.12) that the DC component is zero.

$$i_{s1a,co} = i_{s1a,co,dc} + i_{s1a,co,ac} = 2I_{s1a,co,max}\sin(\omega t + \gamma) \tag{7.12}$$

The power expressions have been presented as follows, following the voltage and current expressions of the SM sets. In this case, branch inductances and resistors are disregarded to prevent an excessively involved mathematical examination and provide a more efficient power assessment.

$$\begin{aligned} p_{s1a} = v_{s1a}i_{s1a} = &\left[\frac{V_{pH}}{2} - \frac{V_{sL}}{2} + 2L\frac{d}{dt}i_{s1a} + 2ri_{s1a} + \right. \\ &\left. + V_{s1a,max}(\sin\omega t)\right]\left[I_{pH} + I_{s1a,max}\sin(\omega t + \beta_1)\right] \end{aligned} \tag{7.13}$$

$$\begin{aligned} p_{s1a} = &\frac{V_{pH}}{2}I_{pH} + \frac{V_{pH}}{2}I_{s1a,max}\sin(\omega t + \beta_1) - \frac{V_{sL}}{2}I_{pH} \\ &- \frac{V_{sL}}{2}I_{s1a,max}\sin(\omega t + \beta_1 + V_{s1a,max}(\sin\omega t)I_{pH} \\ &+ V_{s1a,max}\sin(\omega t)I_{s1a,max}\sin(\omega t + \beta_1) \end{aligned} \tag{7.14}$$

$$\begin{aligned} p_{s1a} = &\frac{V_{pH}}{2}I_{pH} - \frac{V_{sL}}{2}I_{pH} + \frac{V_{pH}}{2}I_{s1a,max}\sin(\omega t + \beta_1) \\ &- \frac{V_{sL}}{2}I_{s1a,max}\sin(\omega t\frac{V_{sL}}{2}I_{s1a,max}\sin(\omega t + \beta_1) \\ &+ \frac{V_{s1a,max}I_{s1a,max}}{2}\cos(\beta_1) + V_{s1a,max}I_{pH}\sin(\omega t) \\ &- \frac{V_{s1a,max}I_{s1a,max}}{2}[\cos(2\omega t)\cos(\beta_1) - \sin(2\omega t)\sin(\beta_1)] \end{aligned} \tag{7.15}$$

Where, p_{s1a} represents the power of the SM set st1a of arm-a. As seen in equation (7.13), the power expression consists of both DC and AC components, as in the case of voltage and current parameters, since it is inherently the product of the voltage falling on the relevant SM set and the current flowing through it. The power expressions of the set 2a set 3a, and set 4a SM sets of arm-a have been gathered with a similar approach and provided as p_{s2a}, p_{s3a}, and p_{s4a}, correspondingly.

$$
\begin{aligned}
p_{s2a} = \ & v_{s2a} i_{s2a} \\
& = \left[\frac{V_{sL}}{2} - V_{s3a,max}\sin(\omega t \right. \\
& \left. + \theta_2)\right]\left[I_{pH} - \frac{V_{pH}}{Vs_L} I_{pH} + I_{s2a,max}\sin(\omega t + \beta_2)\right]
\end{aligned} \tag{7.16}
$$

$$
\begin{aligned}
p_{s2a} = \ & \frac{V_{sL}}{2} I_{pH} - \frac{V_{sL}}{2}\frac{V_{pH}}{Vs_L} I_{pH} + \frac{V_{sL}}{2} I_{s2a,max}\sin(\omega t + \beta_2) \\
& + V_{s2a,max}\sin(\omega t + \theta_1) I_{pH} - V_{s2a,max}\sin(\omega t + \theta_1)\frac{V_{pH}}{Vs_L} I_{pH} \\
& + V_{s2a,max}\sin(\omega t + \theta_1) I_{s2a,max}\sin(\omega t + \beta_2)
\end{aligned} \tag{7.17}
$$

$$
\begin{aligned}
p_{s2a} = \ & \frac{V_{sL}}{2} I_{pH} - \frac{V_{pH}}{2} I_{pH} + \frac{V_{sL}}{2} I_{s2a,max}\sin(\omega t + \beta_2) \\
& + \left[[V_{s2a,max} I_{pH} - V_{s2a,max} I_{pH}\frac{V_{pH}}{V_{sL}}\right]\sin(\omega t + \theta_1) \\
& + \frac{V_{s2a,max} I_{s2a,max}}{2}\cos(\theta_1 - \beta_2) \\
& - \frac{V_{s2a,max} I_{s2a,max}}{2}[\cos(2\omega t + 2\theta_1)\cos(\theta_1 - \beta_2) \\
& + \sin(2\omega t + 2\theta_1)\sin(\theta_1 - \beta_2)]
\end{aligned} \tag{7.18}
$$

$$
\begin{aligned}
p_{s3a}\, v_{s3a} i_{s3a} = \ & \left[\frac{V_{sL}}{2} + V_{s3a,max}\sin(\omega t \right. \\
& \left. + \theta_2)\ \right]\left[I_{pH} - \frac{V_{pH}}{Vs_L} I_{pH} - I_{s3a,max}\sin(\omega t + \beta_3)\right]
\end{aligned} \tag{7.19}
$$

$$p_{s3a} = \frac{V_{sL}}{2} I_{pH} - \frac{V_{sL}}{2}\frac{V_{pH}}{Vs_L} I_{pH} - \frac{V_{sL}}{2} I_{s3a,max} \sin(\omega t + \beta_3) + V_{s3a,max} \sin(\omega t + \theta_2) I_{pH} - V_{s3a,max} \sin(\omega t + \theta_2) \frac{V_{pH}}{Vs_L} I_{pH} - V_{s3a,max} \sin(\omega t + \theta_2) I_{s3a,max} \sin(\omega t + \beta_3) \tag{7.20}$$

$$p_{s3a} = \frac{V_{sL}}{2} I_{pH} - \frac{V_{pH}}{2} I_{pH} - \frac{V_{sL}}{2} I_{s3a,max} \sin(\omega t + \beta_3) - V_{s3a,max} I_{pH} + V_{s3a,max} I_{pH} \frac{V_{pH}}{Vs_L} \sin(\omega t + \theta_2) + \frac{V_{s3a,max} I_{s3a,max}}{2} \cos(\theta_2 - \beta_3) - \frac{V_{s3a,max} I_{s3a,max}}{2} [\cos(2\omega t + 2\theta_2) \cos(\theta_2 - \beta_3) + \sin(2\omega t + 2\theta_2) \sin(\theta_2 - \beta_3)] \tag{7.21}$$

$$p_{s4a}\ v_{s4a} i_{s4a} = \left[\frac{V_{pH}}{2} - \frac{V_{sL}}{2} - V_{s4a,max} \sin(\omega t + \theta_3)\right] [I_{pH} - I_{s4a,max} \sin(\omega t + \beta_4) \tag{7.22}$$

$$p_{s4a} = \frac{V_{pH}}{2} I_{pH} - \frac{V_{pH}}{2} I_{s4a,max} \sin(\omega t + \beta_4) - \frac{V_{sL}}{2} I_{pH} + \frac{V_{sL}}{2} I_{s4a,max} \sin(\omega t + \beta_4) - V_{s4a,max} \sin(\omega t + \theta_3) I_{pH} + V_{s4a,max} \sin(\omega t + \theta_3) I_{s4a,max} \sin(\omega t + \beta_4) \tag{7.23}$$

$$p_{s4a} = \frac{V_{pH}}{2} I_{pH} - \frac{V_{pH}}{2} I_{s4a,max} \sin(\omega t + \beta_4) - \frac{V_{sL}}{2} I_{pH} + \frac{V_{sL}}{2} I_{s4a,max} \sin(\omega t + \beta_4) - V_{s4a,max} I_{pH} \sin(\omega t + \theta_3) + \frac{V_{s4a,max} I_{s4a,max}}{2} \cos(\beta_4 - \theta_3) - \frac{V_{s4a,max} I_{s4a,max}}{2} [\cos(2\omega t + 2\theta_3) \cos(\theta_3 - \beta_4) + \sin(2\omega t + 2\theta_3) \sin(\theta_3 - \beta_4)] \tag{7.24}$$

7.5 Summary

This section provides general information on the proposed unique non-isolated DC-DC MMC topology, which is crucial for the interconnection of HVDC power systems, as well as a thorough analysis of DC-DC MMC topologies developed from existing MMC technologies. The suggested novel DC-DC MMC topology's architectural structure is described in depth. A detailed analysis of the architectural structure's distinguishing characteristics is conducted. Furthermore, a mathematical model study of the suggested DC-DC MMC architecture is carried out. Therefore, the significance of DC-DC MMC topologies, which are crucial for power systems, is highlighted in this part, along with the detailed presentation of the mathematical analysis and distinctive aspects of the suggested novel DC-DC MMC topology. The mathematical analysis presented in this section plays a pivotal role in the overall control strategy of the proposed DC-DC MMC topology. Based on the analytical results, the dynamic behavior of the topology was accurately modeled, and the control parameters were systematically optimized. Consequently, the developed control system enables highly accurate and stable bidirectional power transfer, ensuring the effective performance of the proposed converter architecture. The next portion of this paper provides the simulation analysis and functioning concept of the suggested DC-DC MMC architecture.

CHAPTER VIII
SIMULATION STUDIES

8.1 Introduction

Advanced power conversion technologies have been in high demand because of their vital role in improving energy efficiency in a variety of applications, including HVDC power systems, electric vehicles, manufacturing processes, and renewable energy-based facilities. In these systems, DC-DC converters are crucial parts that enable accurate voltage control while preserving high efficiency and reducing power losses. Nevertheless, conventional DC-DC converters have considerable difficulties in high-power applications, where their performance could not be satisfactory enough. DC-DC MMC topologies have become a competitive alternative to traditional power system topologies in this regard. MMC's modular architecture has several benefits, including increased scalability, efficiency, and reliability, which makes it ideal for high voltage and high-power applications. A viable strategy for getting beyond the drawbacks of conventional converters and accomplishing more effective energy transformation is the incorporation of MMC into DC-DC conversion systems. The operational concepts of the suggested innovative non-isolated DC-DC MMC topology are analyzed in this chapter, along with a simulation-based performance evaluation. An overview of the suggested DC-DC MMC architecture is presented in the seventh chapter, along with an assessment of its distinctive characteristics and applicability to DC-DC power conversion.

The following sections examine architectural aspects, performance measurements, and fundamental operating concepts related to the suggested DC-DC MMC architecture. A comprehensive simulation analysis is conducted in this section the research to evaluate the topology's viability, effectiveness, and productivity under various scenarios of operation.

8.2 Operational Principle of the Proposed DC-DC MMC Topology

The suggested DC-DC MMC design's key objective is integrating HVAC and HVDC asynchronous networks with various voltage levels. That is the design's fundamental concept of operation. Following the abovementioned desire, two approximately real-life asynchronous networks have been incorporated into the present investigation utilizing a simulation environment, as shown in Figure 8.1. The system presented in this research has a primary end featuring a DC voltage level of 266 kV and a power of 210 MW and a secondary end featuring a DC voltage level of 188 kV and a power of 204 MW. The rectifier station that converts HVAC voltages into HVDC voltages is positioned on both the primary and secondary sides of the system. The fundamental objective of these rectifier stations is to ensure that the suggested system integrates with existing HVAC networks. The primary and secondary sides of the proposed DC-DC MMC system receive network voltages from rectifier stations, which convert HVAC voltage to HVDC voltage.

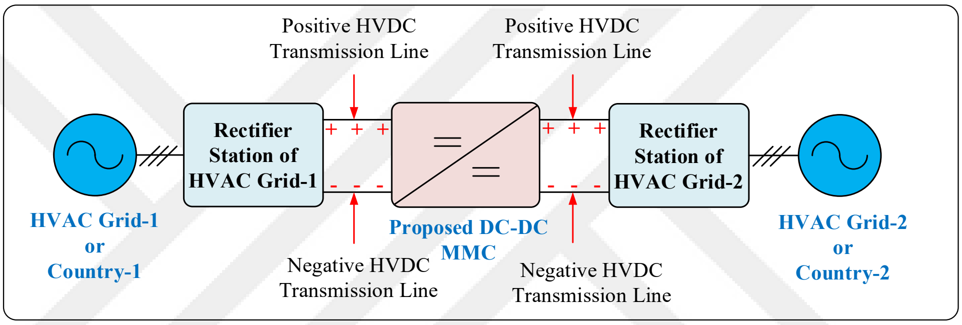

Figure 8. 1 Interconnect the two asynchronous HVAC power grids utilizing the proposed DC-DC MMC design.

The transformation and transfer processes under the control system's guidance are illustrated in Figure 8.2, which shows the overall control system of the proposed innovative DC-DC MMC design. This architecture consists of multiple hierarchical control blocks designed to ensure stable operation, high efficiency, and bidirectional power flow within the system. The control process begins with the block titled "Determining the Parameters of the Recommended System," which defines the fundamental operating conditions and system parameters. These values serve as the foundation for reference generation and are processed through the "Filtering System" to eliminate undesired harmonics from the input voltage and current signals.

The converter control algorithms rely on transforming the measured three-phase signals into an appropriate reference frame. This is achieved via Clarke and dq0 transformations, which first map the signals onto the α-β plane and then onto the synchronous d-q referential define. These transformations enhance the performance of the PI controllers by enabling faster and more accurate dynamic response.

At the core of the control architecture are the “Calculation of System Parameters,” “Power Control Unit,” and “Reference Currents Determination Unit.” These modules process real-time power demands to generate the corresponding d–q axis reference current components. These references are then sent to the “Currents Control Unit,” which compares them with the measured currents and generates the appropriate switching signals.

To maintain system stability, the architecture includes both a “DC Voltage Controller” and a “DC Voltage Equilibrium Management” block. These ensure voltage balance on the DC side. In particular, equalizing the voltages of each submodule capacitor is critical in MMC structures. These blocks provide active balancing strategies to prevent voltage deviation. The proposed control architecture presents an integrated approach that combines transformation operations, reference current generation, phase synchronization, voltage and current regulation, and efficiency analysis. This robust control structure enables the DC-DC MMC system to operate with high reliability and efficiency across a wide range of applications, including hybrid HVDC interconnections.

To achieve greater effectiveness in output power, the filtering system that filters the voltage and current values supplied from the networks to the DC-DC MMC architecture is depicted in Figure 8.3. At the initial stage of the control scheme, grid-related parameters (such as voltages, currents, and frequencies) along with the design-specific DC voltage values are introduced as input variables. These Input Parameters are subjected to a Filtering Model, which plays a critical role in removing harmonic distortions and measurement errors from the raw input signals. As a result, the system is provided with more stable and accurate data, enhancing the reliability of subsequent control operations. The filtered data are denoted as Output Parameters, which are then forwarded to the Clarke Transformation block. This transformation is essential for converting three-phase time-domain signals into a two-axis orthogonal reference frame, enabling effective control in the stationary α-β frame.

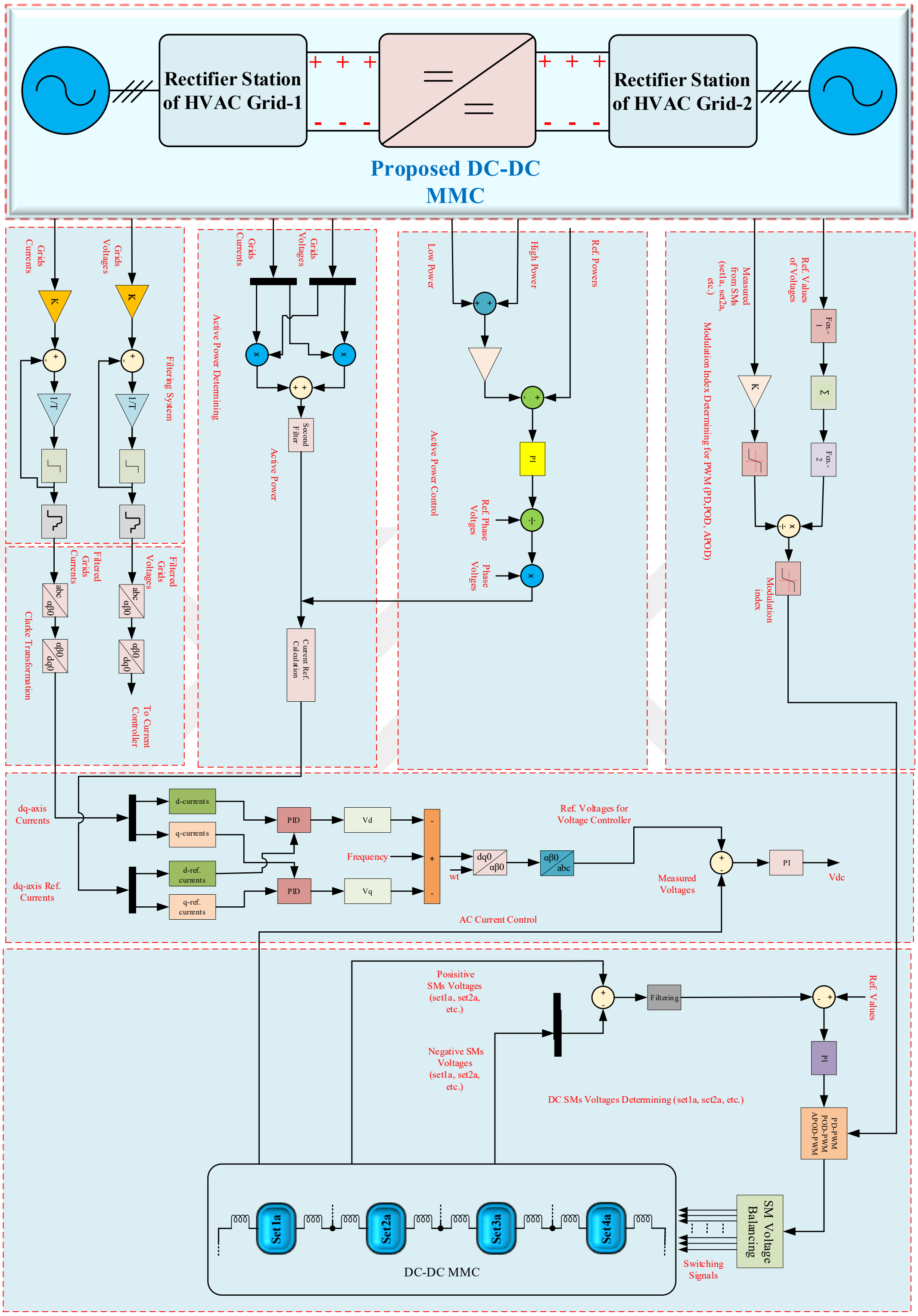

Figure 8. 2 Overall block diagrams of the proposed control system of unique DC-DC MMC topology

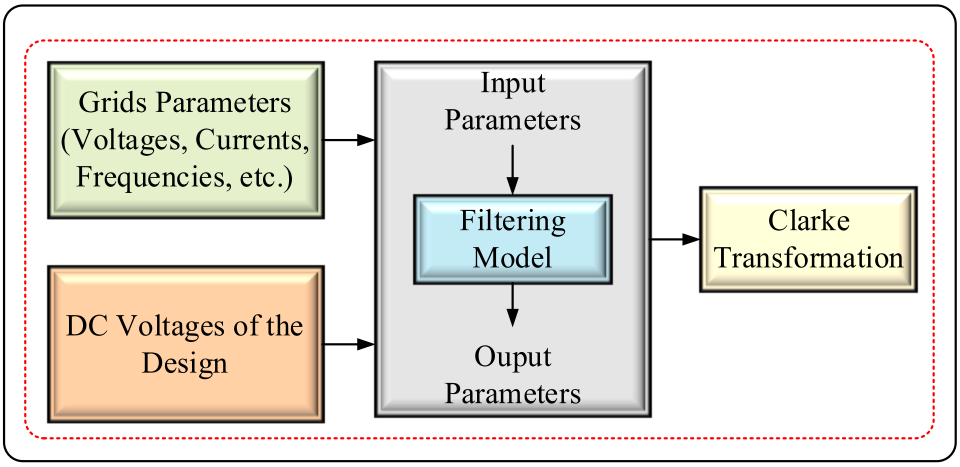

Figure 8. 3 Filtering system of control mechanism.

Figure 8.4 shows the Clarke transformation developed to determine the system characteristics needed for the suggested system and the circuit parameters required for an efficient DC voltage balancing system and effective power control. The sub-block diagram of the control system, which calculates the system parameters needed for the suggested topology, is displayed in Figure 8.5. The block diagram presented in this figure details a critical subsection of the overall control system for proposed converter design, specifically focusing on the measurement and signal processing subsystem. As shown, various parameters such as filtered DC voltages, AC voltages and currents, power, and frequency are initially filtered to remove noise, and then passed through a "Second Filtering System" to achieve optimized, high-accuracy signal quality for the control algorithms. This comprehensive filtering process minimizes potential distortions from external factors, thereby enhancing the reliability of the measured data. The "Measured Grids' Parameters" (voltages and currents) obtained after the second filtering stage are directly fed back to the converter's main current and voltage controllers, while the "Measured Grids' Powers" are transmitted to higher-level power control units and also to units responsible for analyzing system losses and efficiency. Furthermore, the PD-PWM block, which converts reference signals from the controllers into appropriate PWM signals for the converter's semiconductor switches based on the measured parameters, plays a crucial role in the system's dynamic response and precise control. This structured approach provides a robust foundation for effectively managing the DC-DC MMC's power flow, voltage and current regulation, and continuously monitoring its operational efficiency.

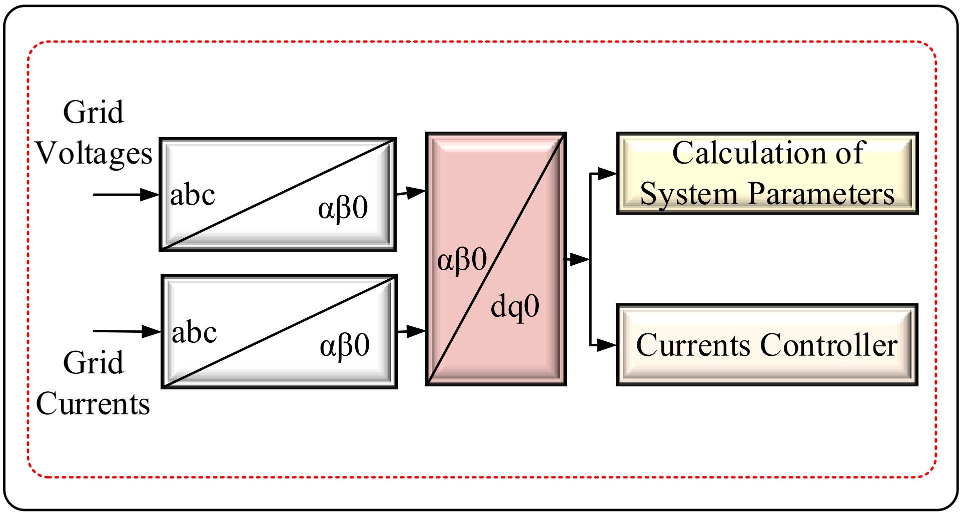

Figure 8. 4 Clarke transformation of control mechanism.

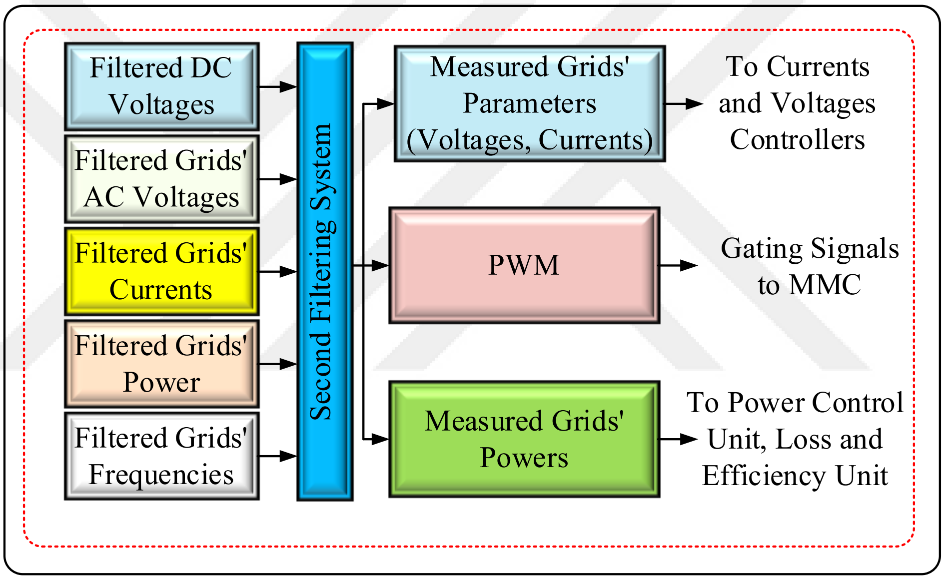

Figure 8. 5 Calculation of the system parameters diagram.

Lastly, the power, current, and DC voltage control units in the proposed control system are illustrated in Figure 8.6. Essentially, this control structure aims to manage active (P) and reactive (Q) power flow while simultaneously ensuring system safety and stability. "V, I Parameters" from the system and externally defined "PQ Parameters" are processed by a "PQ Controller" to determine the reference currents that the converter must realize. These reference currents are supervised and limited by a "Current Limiter Unit" to ensure they do not exceed the converter's physical boundaries. The safe reference currents output by the current limiter are then utilized by an "Inner Controller Unit", which generates the commands to be applied to the converter's semiconductor switches. In parallel, "Measured DC Voltages" are fed back to a "DC Voltages Control System" to maintain the converter's DC link bus voltage at the desired level, with this control also indirectly influencing the overall power flow. This integrated control architecture ensures that the converter meets desired power demands, regulates the DC bus voltage, and simultaneously preserves operational safety and system integrity.

The design variables associated with the suggested system have been determined, which can be witnessed in the control system; the corresponding values have been supplied into the framework with the help of a filtering mechanism. Current, voltage, and power control mechanisms based on PID Controller, and Clarke Transformation mechanism have been utilized for this data transmission. In the stable $\alpha\beta$ framework, the equilibrium two-phase orthogonal parts are obtained by applying the Clarke transformation to the equilibrium three-phase elements of HVAC Grid-1 and HVAC Grid-2 in the ABC referencing structure of the proposed topology.

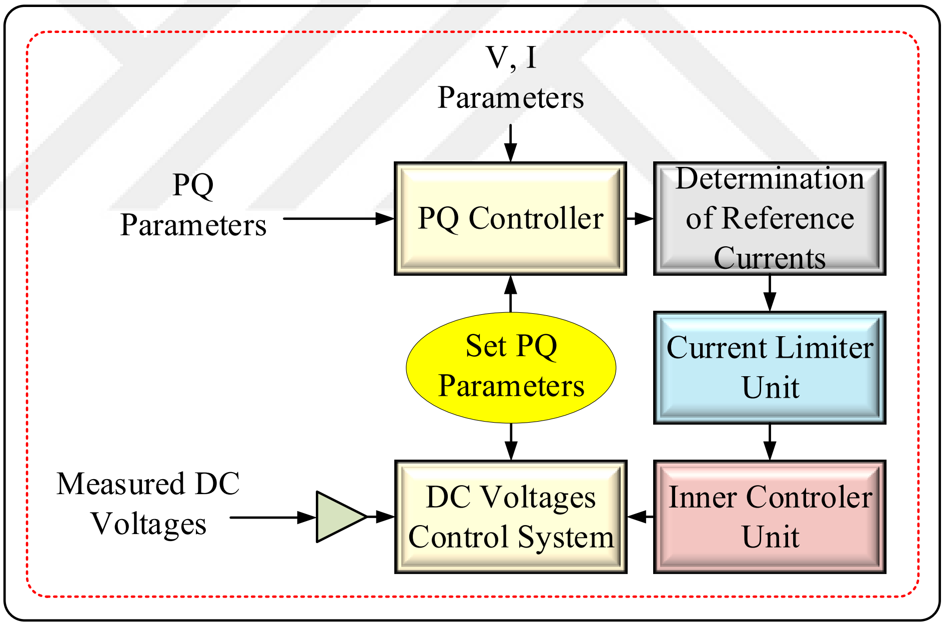

Figure 8. 6 Powers, currents, and DC voltages of the proposed controlling system for recommended topology.

Furthermore, the Clarke Transformation structure can generate the variables α, β, and zero by computing the Clarke transformation of the three-phase variables a, b, and c. The controller modifies the inner generator frequency to maintain a zero-phase shift. The controller system's $d - q$ transformation module utilizes the α and β variables obtained from Clarke Transformation to determine the quadratic axis (q) and direct axis (d) parameters. The signal computation section determines parameters under the values of the filter mechanism that the system controller implements. PID-based current, voltage, and power control units customize the required parameters to ensure the suggested DC-DC MMC system behaves reliably and steadily. A comprehensive efficiency analysis and loss model have been developed and applied to verify the proposed DC-DC topology's efficient bi-directional power transmission capability. General control diagram illustrates how the parameters from the power controller, current, and DC voltage control units are assessed in this efficiency model, along with information from the unit that calculates the system parameters needed for the designed converter topology's efficient power transfer. Even though DC-DC converter systems have losses from capacitors, inductors, switching, power transmission, etc., the proposed design offers bi-directional power transfer with high efficiency and low losses in comparison to conventional MMC designs because it settles on minimal SM structures (HBSM), uses an efficient PWM technique, has a symmetrical and compact structure, and has an innovative control system developed.

The filtering system is the first phase in the control process. It filters the measured and raw data, identified as the grid voltages and grid currents. This filtering operation processes raw data through a series of gain (K), integral ($1/T$) and limiting operations to reduce noise and unwanted harmonic content so that clean filtered grids voltages and currents can be produced. These filtering outputs are next fed into the Clarke transformation block, which converts the three-phase (abc) quantities into the stationary two-phase ($\alpha\beta$) and then into the rotating synchronous $dq0$ reference frame. The outputs in the $dq0$ frame represent essential inputs to the higher-level current controller and voltage controller. The modulation index determining block utilizes a sum of the ref. values voltages and measures SM voltages (scaled by the gain K) into a series of non-linear functions (Func-1, Func-2) to produce the modulation index. The modulation index is an important measurement to produce the gate signals which include the PD, POD and APOD PWM schemes. In the critical DC SMs voltage determining, the inherent capacitor voltage balance problem in MMC is eliminated by comparing positive and negative SMs voltages and producing a reference via a PI controller and a filtering step. Balancing values after being added to the PWM vector to form the switching signals. The main AC control is running in the dq-frame, which traces back the measured dq-axis currents to their reference currents. The V_d and V_q

voltage vectors are created by feeding the error signals into the PID controllers. The reference voltages for the voltage controller are obtained by concurrently transforming these and the frequency data to abc preceding back transformation ($dq0 \rightarrow \alpha\beta0 \rightarrow abc$). Lastly, the active power control block regulates the system's power flow by utilizing a PI controller, setting up high and low power reference signals, and modifying phase voltages to drive towards the ultimate active power output.

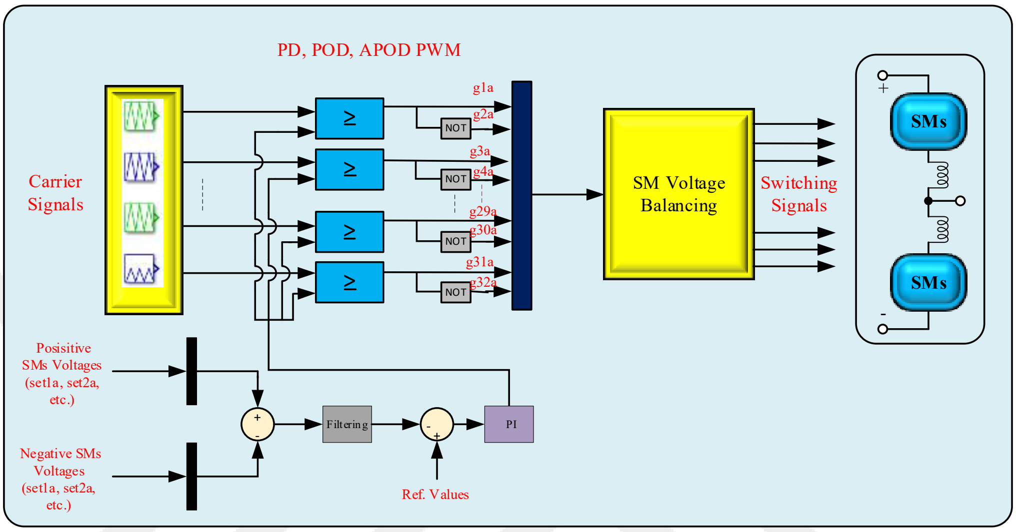

Figure 8. 7 Modulation strategy implementation process.

A structured block diagram, Figure 8.7, presents the detailed steps for the implementation of the PD-PWM, POD-PWM, and APOD-PWM strategies. First, carrier signals are generated concurrently with the measured SM voltages that are fed back and normalized to obtain the reference signals. These reference signals are compared with the carriers, and depending on the selected modulation strategy, different switching patterns are achieved: in PD-PWM all carriers are aligned in phase, in POD-PWM the carriers corresponding to the positive and negative arms are phase-shifted by 180°, and in APOD-PWM successive carriers are alternately shifted by 180°. The comparator outputs obtained are sent to the SM voltage balancing stage, where monitored and equalized submodule voltages are those that ensure the correct operation. Finally, the balanced switching signals, which are the result of both efficient modulation and stable submodule performance, are given to the DC-DC MMC. This depiction not only helps to understand the theoretical basis of the modulation strategies but also indicates their practical implementation systematically, thus responding to the reviewer's request for a clearer and more convincing description of the modulation process.

One of the most significant contributions of the proposed DC-DC MMC is its symmetrical arm design, which directly enables efficient bidirectional power transfer. In the developed three-arm architecture, each arm is constructed with four uniformly configured HBSM clusters. This symmetry ensures that both voltage and current stresses are evenly distributed among all arms, thereby minimizing imbalance during forward and reverse power flow.

Simulation results confirm the benefits of this design. Under nominal operating conditions, the system successfully transferred 210 MW at 266 kV on the primary side to 204 MW at 188 kV on the secondary side, while maintaining stable bidirectional operation. The observed capacitor voltage deviation across all submodules remained within ±5% (Figure 8.14, 8.24, 8.32), demonstrating precise balancing without additional auxiliary circuits. Furthermore, the system achieved a bidirectional transfer efficiency above 96%, supported by switching frequencies of 1 kHz, which is notably higher than the 93–95% efficiency commonly reported in conventional hybrid MMC converters.

The symmetrical configuration also reduces the computational burden of control. Since each arm exhibits identical electrical characteristics, the control system can employ streamlined PI/PID-based regulators rather than advanced adaptive controllers typically required in asymmetric designs. This simplification translates into approximately 30% fewer reference signals and modulation variables, lowering control complexity while preserving stability.

On the hardware side, symmetry minimizes the need for redundant current sensors and specialized protection units. Power waveforms from the simulations (Figures 8.11, 8.21, and 8.29) further validate that the converter tracks reference signals with excellent transient response, even under abrupt changes at 2.0 s and 3.14 s, ensuring reliable bidirectional operation.

In summary, the symmetrical design of the proposed converter not only enables high-efficiency bidirectional power transfer but also lowers control complexity and hardware requirements, thereby offering a scalable and economically viable solution for large-scale HVDC interconnections.

8.3 Simulation Analysis of the DC-DC MMC Topology

The proposed novel non-isolated DC-DC MMC architecture is evaluated through simulation in this phase of the study, with a focus on enhancing power conversion proficiency between two HVDC power grids and reducing power losses. The capability of MMCs to provide low harmonic distortion, excellent operational efficiency, and consistent performance across a broad range of voltage and current ranges has made them well-known in sophisticated power electronics. Because of their modular construction, MMCs provide notable benefits over traditional DC-DC converter designs in regard to efficiency, dependability, and flexibility. Because of its flexibility, MMCs can effectively manage high power demands, which makes them ideal for large-scale applications involving power storage, electric vehicles, and renewable energy facilities. DC-DC MMC topologies, developed based on the foundational principles of conventional MMC technology, must be carefully designed to retain the benefits associated with traditional MMC configurations. In addition to this, to ensure the effective operation of the MMC topology, it is crucial to develop advanced and robust control techniques that complement the original design. The proposed innovative DC-DC MMC design was developed in alignment with these principles, and a highly functional control system was also devised to support its operation. Power transfer between the two power systems was successfully facilitated through both the novel design and the accompanying control system, demonstrating the effectiveness and practicality of the proposed solution. Through an assortment of simulation investigations, the performance of the suggested DC-DC MMC topology is examined in this section of the study. Important metrics, including voltage control, current circulation, overall system efficiency, and dynamic responsiveness, are examined. This part of the study investigates potential enhancements in voltage equilibrium, power loss elimination, and other operational issues frequently faced by conventional converter systems. It is anticipated that the results of these simulations are offer insightful information for improving the architecture and functionality of the proposed DC-DC MMC topology, advancing more dependable, sustainable, and efficient power conversion approaches.

Table 8. 1 Parameters of the simulated novel DC-DC MMC design.

Parameters	Symbols	Values
HVDC Grid 1	VpH	266kV
HVDC Grid 2	VsL	188kV
Arm Filtering Inductor	Lo, ro^1	20mH
Arm Inductor	L, r^1	3mH
Number of HBSM per Sets	N	4
Number of Sets per Arm	M	4
HBSM Capacitor	VsC	10mF
Switching Frequency	$fswc$	1000Hz
Number of Arms, K	Arm-a, Arm-b Arm-c	3

[1]The internal resistances of the inductors r and ro were neglected in the simulation analysis.

Table 8. 2 Main control parameters of the simulated novel DC-DC MMC design

Parameters	Symbols	Values
Proportional gain of power control	Kpc	4
Integral gain of power control	Kic	4
Proportional gain of power regulator	Kpr	25
Integral gain of power regulator	Kir	25
Proportional gain of current regulator	$Kpcr$	1
Integral gain of current regulator	$Kicr$	1
Proportional gain of DC voltage regulator	K_{pv}	3
Integral gain of DC voltage regulator	K_{iv}	50

The suggested DC-DC MMC topology is simulated in the simulation environment to demonstrate the system's effectiveness and functionality. Table 8,1 summarizes the parameters of the proposed DC-DC MMC topology, which is given in Figure 7.1. Table 8.2 illustrates the main control parameters of the control strategy incorporated into the proposed converter architecture. The following sections present the simulation outcomes obtained using the suggested design regarding the data in Table 8.1. The present study has applied individual PD-PWM, POD-PWM, and APOD-PWM technologies to control power switching in SM architecture sets. An individual simulation study of the system was conducted for each of these three PWM approaches. IGBT power switches have been employed in the HBSM architecture of the suggested design, given that they have lower switching losses and a higher switching frequency and provide superior outcomes at higher voltage levels.

In carrying out the simulation studies of the proposed non-isolated DC-DC MMC topology, several practical assumptions and simplifications were adopted within the simulation environment to ensure computational efficiency and to emphasize the fundamental operational behavior of the converter. Semiconductor switches were represented according to their functional characteristics, and passive circuit elements such as inductors and capacitors were modeled based on their nominal values to focus on the system's steady-state and transient performance. The control system was implemented in a numerical simulation framework that enabled precise observation of voltage, current, and power flow responses without introducing external disturbances or communication delays. While the simulation environment inherently excludes secondary parasitic and thermal effects, the efficiency and loss analyses presented in the previous chapter were obtained from the converter's defined physical parameters such as arm and filter inductor resistances (r, r_0) and the reduced number of switching devices. This methodology ensures that the presented results accurately represent the system's expected performance while maintaining clarity and consistency throughout the analysis.

In practical applications, certain non-idealities such as thermal limitations and tolerances in passive components can cause slight variations in performance. However, the simulation results demonstrate that the proposed converter consistently maintains high efficiency (above 96%), low current total harmonic distortion (THD < 2.08%), stable capacitor voltage regulation within ±2–5%, and fast transient recovery times below 0.2 s under the tested steady-state and dynamic conditions. These quantitative results are derived from the electromagnetic transient simulations and correspond to measurable performance indicators presented in Figures 8.10, 8.21, and 8.29. Compared to conventional MMC-based converters reported in the literature, the observed improvements are substantial and are expected to remain valid under realistic operating conditions, with only minor deviations in absolute efficiency values due to physical non-idealities.

The numerical values reported in this section - such as the overall converter efficiency exceeding 96%, total power losses below 3% of the rated power, and capacitor voltage ripples within ±5% - are derived directly from the simulation analysis data of the proposed DC-DC MMC. The simulation results (Figure 8.17 and Figure 8.18) indicate that the current THD remained between 1.5% - 2.08% under steady-state conditions, confirming that the designed control and modulation strategies effectively suppress harmonic distortion. The THD of the proposed converter was evaluated to assess the waveform quality of the transferred power. This result validates the converter's capability to maintain high-quality current transfer while sustaining efficient bidirectional power flow. Simulation results were calculated by evaluating the instantaneous voltage and current waveforms at the input and output terminals of the converter in the steady-state period, after the transient response stabilized. The average power at both terminals was computed, and efficiency was determined as the ratio of output to input active power. The voltage ripple values were obtained from the submodule capacitor voltage profiles presented in Figures 8.14, 8.24, and 8.32. Accordingly, the stated performance indicators represent quantified simulation outcomes rather than qualitative estimations. This clarification ensures that the numerical values correspond directly to measurable quantities extracted from the simulation environment.

As a result, the assumptions utilized herein do not compromise the accuracy of the results; rather, they offer a precise, targeted illustration of the converter's intrinsic capabilities. The converter's structure is anticipated to retain its superior qualities in comparison to alternative designs when realistic device models and hardware non-idealities are later incorporated, thereby enhancing the dependability and usefulness of the suggested topology in HVDC interconnection applications.

8.3.1 Case Study 1

This study supports the effectiveness of the suggested DC-DC MMC architecture in interconnecting HVDC power networks and its significance in guaranteeing efficient electrical power transfer between these power networks, as supported by the outcomes of the simulation process. To enable the DC-DC MMC topology to carry out its assigned responsibility with great accuracy, an exhaustive control system has been developed in the framework of this simulation-based analysis. Three case studies have been carried out to assess the system fully; each corresponds to one of the three modulation strategies investigated in this study. In the first case study, simulation results were obtained utilizing the PD-PWM approach. In the second and third scenarios, distinguished simulation outcomes were derived utilizing the POD-PWM and APOD-PWM methodologies, respectively. The following section presents the simulation results from the first case study, the first of these three case studies, that were acquired using the PD-PWM approach. Figure 8.8 illustrates the primary side voltage (higher voltage level), primary side current, secondary side voltage (lower voltage level than the primary side), and secondary side current waveforms of the proposed DC-DC MMC design, respectively.

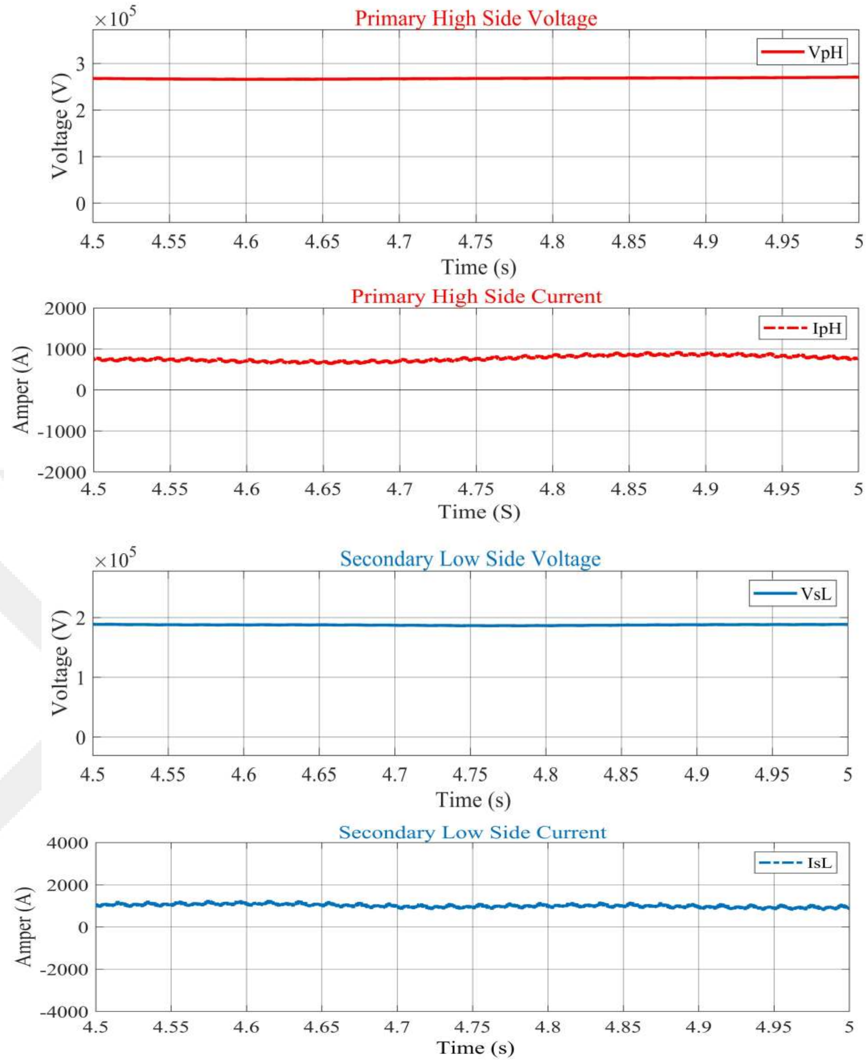

Figure 8. 8 Voltage and current waveforms of the primary and secondary sides of the proposed DC-DC MMC topology.

The input and output voltage measurements of the suggested system have been presented in Figure 8.8's first and third waveforms, respectively. In contrast, Figure 8.8's second and fourth waveforms display the input and output current measurements. The waveforms demonstrate a near-perfect DC characteristic for the voltage values, although harmonics cause some tolerable limited oscillates in the current values. These statistics, however, unambiguously demonstrate that the suggested system can transfer power and convert voltage from DC to DC. The voltage level of the primary side is 266 kV, while the secondary side is 188 kV, as demonstrated in Figure 8.8. The corresponding primary and secondary side currents for the abovementioned voltage levels are 780 A and 1040 A, respectively. As provided in the mathematical examination in Section 7.4, voltage and current expressions consist of AC and DC characteristics. This situation causes some fluctuations, albeit at low levels, especially in the system's primary and secondary current waveforms. The findings above indicate that the DC-DC MMC design provides an equilibrium power transfer between two power networks. In other words, the functionality of the suggested novel DC-DC MMC and related control mechanisms can be demonstrated by the simulation results.

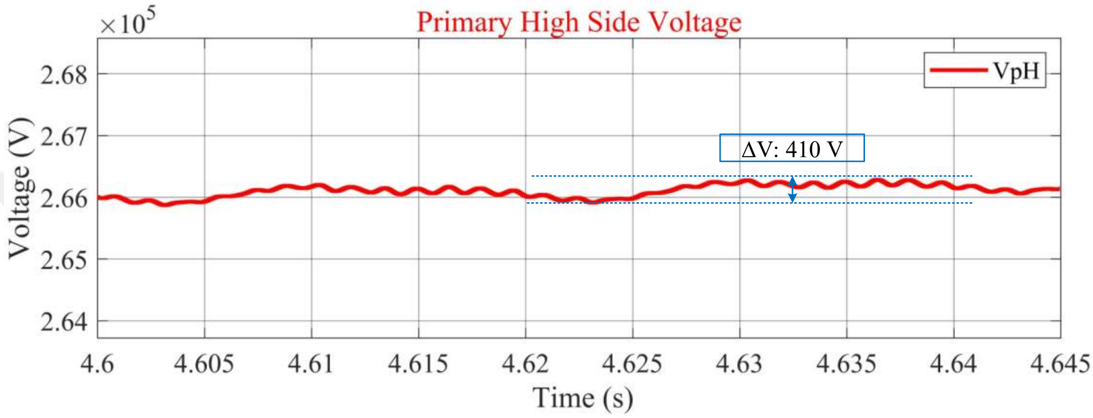

Figure 8. 9 Voltage waveform of the primary side of the proposed DC-DC MMC topology (Zoomed).

Figure 8.9 illustrates the steady-state voltage ripple characteristics of the proposed DC-DC MMC. The waveform labeled VpH in Figure 8.9 represents the voltage on the high-voltage terminal. The voltage remains nearly constant, with a small fluctuation of approximately $\Delta V \approx 410$ V, indicating that the control mechanisms effectively stabilize the converter operation. Figure 8.10 shows the corresponding secondary low side voltage waveform, where the observed voltage ripple is about $\Delta V \approx 448$ V. Although the absolute fluctuation appears comparable to that of the primary side, its relative magnitude is small when normalized to the nominal voltage, confirming that both converter sides maintain steady and well-regulated voltage levels. These results demonstrate that the proposed control structure efficiently suppresses voltage oscillations across the converter arms. The low and symmetric ripple amplitudes verify ensuring stable operation and consistent power transfer between the converter terminals.

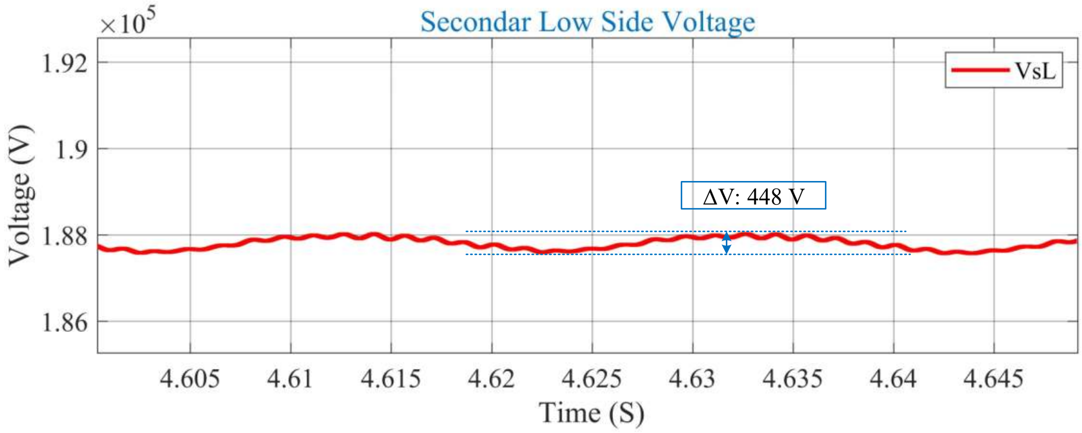

Figure 8. 10 Voltage waveform of the secondary side of the proposed DC-DC MMC topology (Zoomed).

These results verify that the proposed control approach ensures uniform current distribution, suppresses arm-level oscillations, and enables reliable power exchange under steady-state conditions. The suggested DC-DC MMC topology's bi-directional power transfers are demonstrated in Figure 8.11. The power transfer waveform from the primary side to the secondary side is depicted in Figure 8.11(a), and the power transfer waveform from the secondary side to the primary side is illustrated in Figure 8.11(b). Figures 8.11(a) and 8.11(b) show that the power transfer occurs 0.5 seconds after the system operates, with the control system executing a step activation. The primary and secondary power waveforms perfectly follow the reference signal. The power flow progressively exhibits behavior consistent with the 0.9 p.u. reference signal. The power signals exhibit an exceptional reaction to abrupt changes in the system, such as voltage and power, occurring at 2 and 3.14 seconds. After the post, the power transfer stabilizes and proceeds after 3.14 seconds, following the reference signal. It is clear from examining the primary and secondary power transfer waveforms that the suggested converter design performs successfully during abrupt changes in the system's voltage and power in the suggested DC-DC MMC architecture. Outstanding rapid transient characteristics have been observed in the power transfers from the primary to the secondary side and from the secondary to the primary side in response to unexpected alterations in the system's parameters. For electrical networks to operate safely and sustainably, transient performance assessments of the systems are essential. These studies support the process of comprehending how the system functions, forecasting any issues, and establishing approaches for intervention whenever required. Consequently, it is visible from analyzing the primary and secondary waveforms that the suggested DC-DC MMC architecture successfully facilitates power transfer between two asynchronous HVDC power grids.

Examining a system start-up procedure is vital for ensuring a system operates effectively and safely. It is essential to recognize potential start-up problems in a power transfer system and develop strategies to address them. Therefore, the system is more trustworthy and can provide solutions immediately if an issue arises. Future improvements depend on observing performance statistics, such as the time it takes for the system to start-up and the phases at which problems occur. This method can enhance performance, and system start-up time can be reduced. The system start-up technique must be tested regularly to assess the process's effectiveness. Whenever any problems arise, these circumstances ought to be resolved, and the procedure revised. The novel DC-DC MMC architectural structure and control mechanism have been developed based on this phenomenon's characteristics. The system's starting process is successful due to its established control mechanism. Figure 8.10 illustrates how the system launches power transfer in accordance with the start-up procedure. After 0.5 seconds, power is progressively transferred from the primary to the secondary and from the secondary to the primary side. After around 0.5 seconds of ramping control, the power transfer is complete. The planned system's start-up process was chosen to provide a secure and effective power transmission. Due to both networks' high power transfer rates, the start-up process is balanced with the established control mechanism to maintain the system's resilience to possible hazards.

The proposed converter enables stable, efficient, and well-controlled bidirectional power transfer between asynchronous HVDC networks, ensuring reliable operation with reduced complexity and minimal power losses. The HBSM with IGBT used in the converter study at a switching frequency of 1 kHz (see Table 8.1). This frequency was chosen to give a good compromise between low switching losses and fast dynamic control. The converter has switching losses of less than 1.5% of rated power at this frequency with a high control bandwidth. This way the converter achieves high energy efficiency and high control sensitivity. Simulation studies (see Figures 8.11, 8.21, and 8.29) clearly show that the system has a quick transient response. After step-change of reference power, the converter reaches steady-state power transfer within 0.5 s, and overshoot is less than 5% of rated power. Furthermore, at sudden disturbances (2.0 s and 3.14 s), the power waveforms on both primary and secondary sides follow the reference waveforms with settling time of less than 200 ms. The data reveal that the converter is even more robust to unexpected changes in the system. When comparing the proposed transformerless architecture with conventional isolated MMC-based DC-DC converters, one can see that the former has lower conduction and core-related losses. The measurements carried out by the Loss and Efficiency Analysis Unit embedded in the control system (Figure 8.2) demonstrate that the efficiency of the converter is higher than 96% under nominal loading conditions. This high efficiency rate is a big advantage over the standard isolated MMC-based DC-DC converters that are much slower in transient operation and less efficient. The results of this study prove that the advantages in theory for this non-isolated DC-DC MMC topology can be achieved also in practice; namely, the presented converter can deliver a fast dynamic response at high converter efficiency for bidirectional power transfer between the asynchronous HVDC grids.

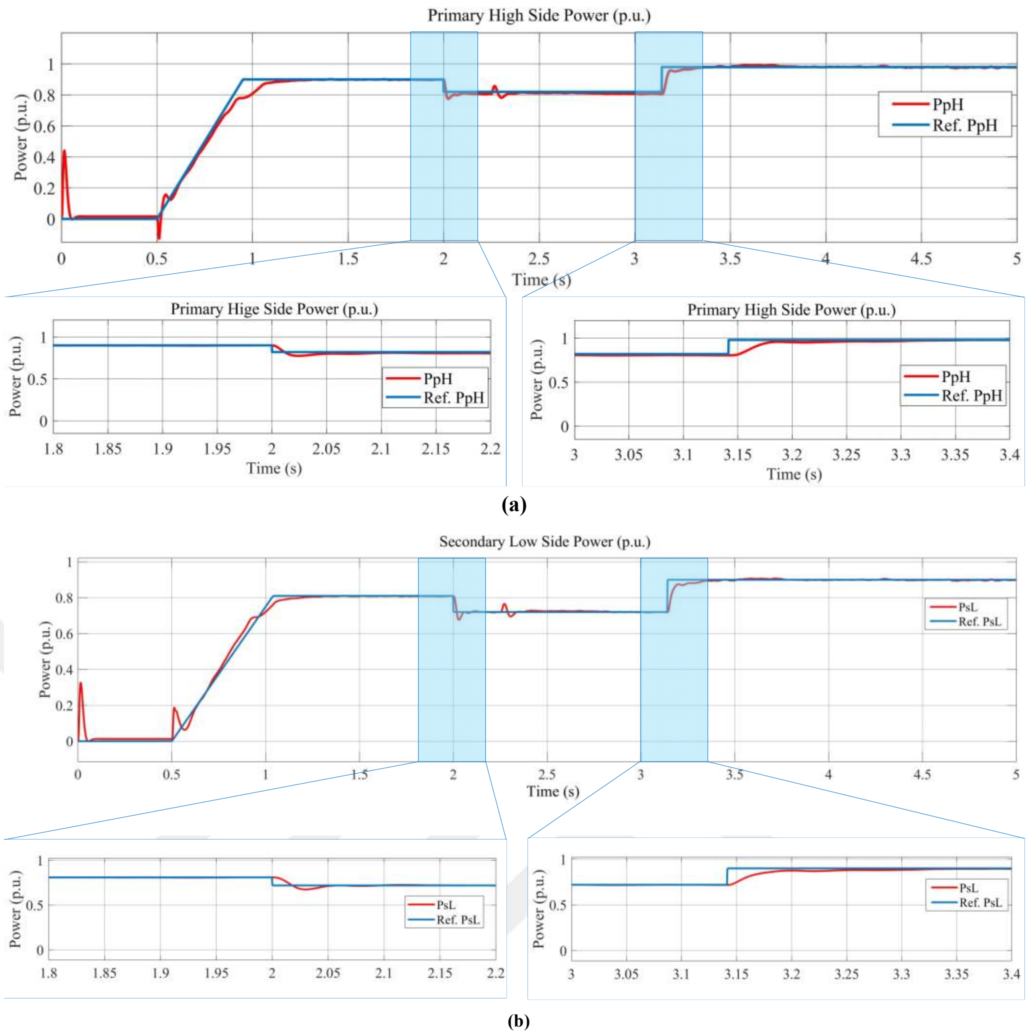

Figure 8. 11 Power waveforms of the primary and secondary sides of the proposed DC-DC MMC topology: (a) The power waveform transferred from the primary side to the secondary side; (b) The power waveform transferred from the secondary side to the primary side.

The voltage across the four SM sets in system arm-a and the currents flowing through the appropriate SM sets are shown in Figure 8.12 and Figure 8.13. The novel configuration that has been suggested has three arms, each of which has four SM sets, as shown in Figure 7.1. The PD-PWM approach, which operates based on reference signals with a 120-degree phase difference between each arm, has been employed for switching the power switches. The voltage and current waveforms of the SM set on arm-a are given to keep the research from getting excessively extensive. The waveforms for voltages and currents of the set1a and set2a SM sets have been demonstrated in Figure 8.12, and the waveforms for the set3a and set4a SM sets have been displayed in Figure 8.13.

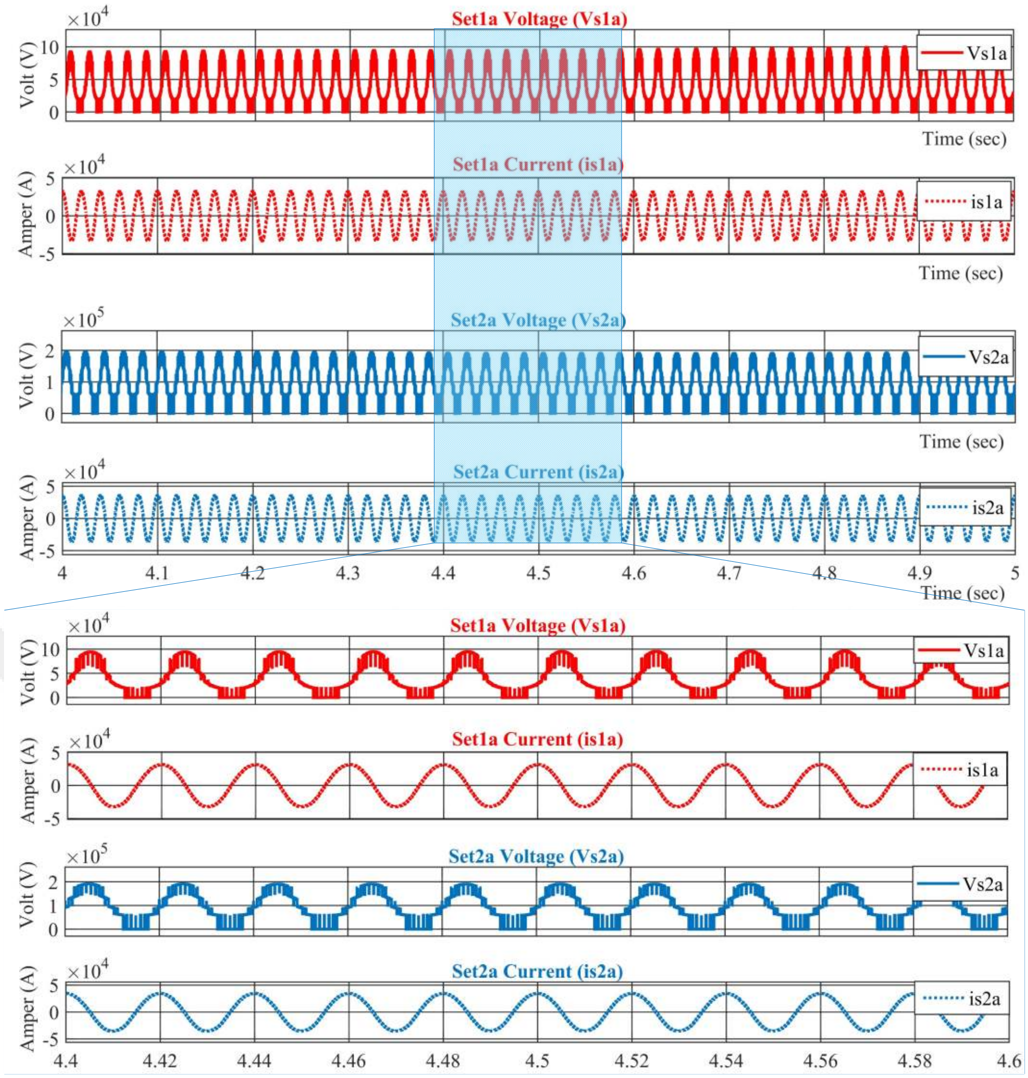

Figure 8. 12 Voltages and current waveforms of set1a and set2a.

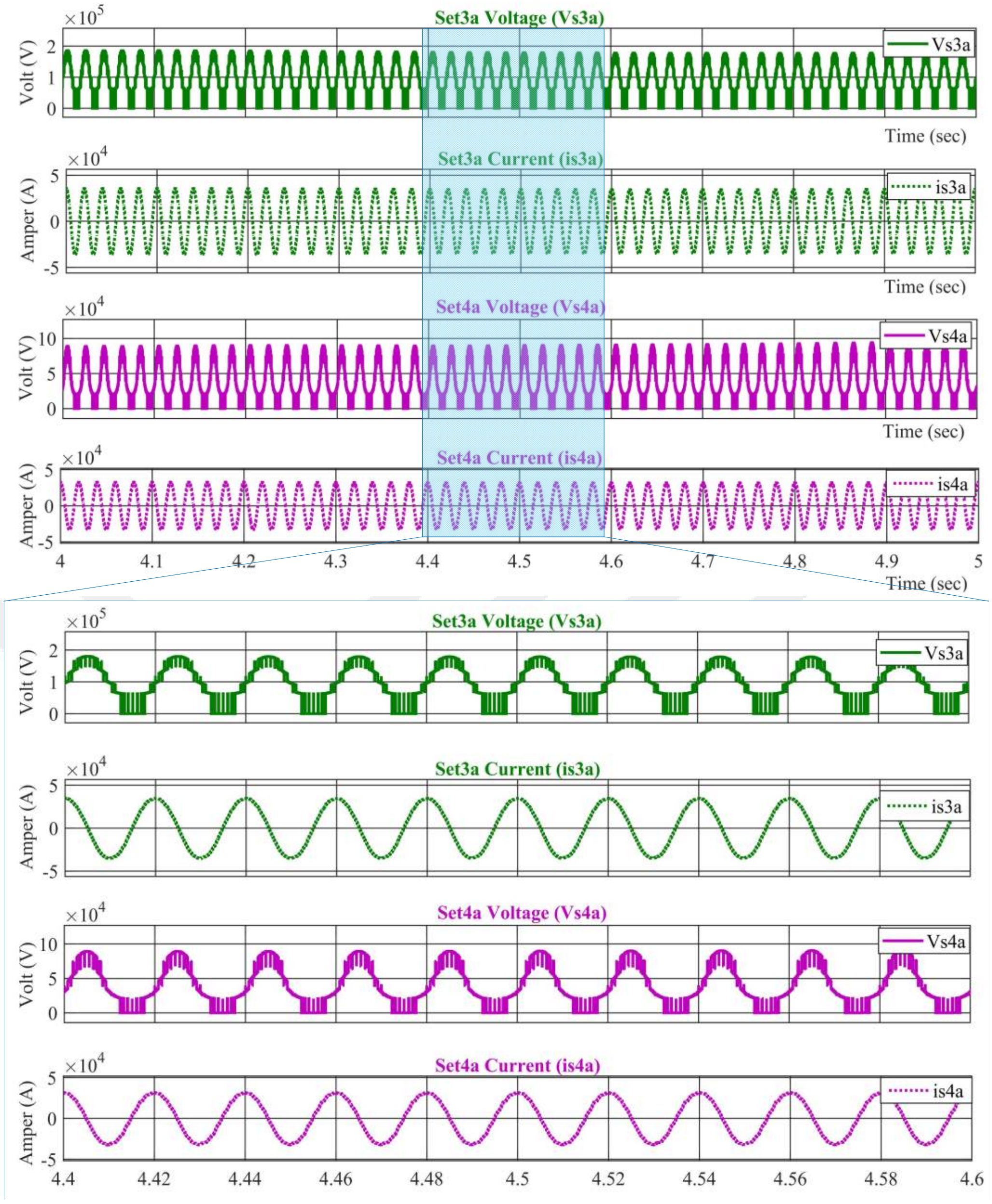

Figure 8. 13 Voltages and current waveforms of set3a and set4a.

Five distinguished voltage levels have been obtained since using four HBSMs in SM sets. As can be observed and predicted from the representation, the SM sets provide voltage values corresponding to different voltage levels, and the currents passing through them have the characteristics of a sinusoidal waveform. It is clear from examining the data produced by the pertinent voltage and current waveforms that the suggested architecture and associated control mechanisms operate admirably.

The waveforms of the capacitor voltages in the set1a SM set of the design's arm-a have been presented in Figure 8.14. It is readily apparent that an efficient capacitor voltage balancing has been accomplished when glancing at the waveforms of the capacitor voltages in Figure 8.14. In other words, it has been demonstrated that capacitor voltages are precisely regulated. The system's arm-a data illustrates that the innovative DC-DC MMC architecture that has been suggested successfully integrates two asynchronous power networks.

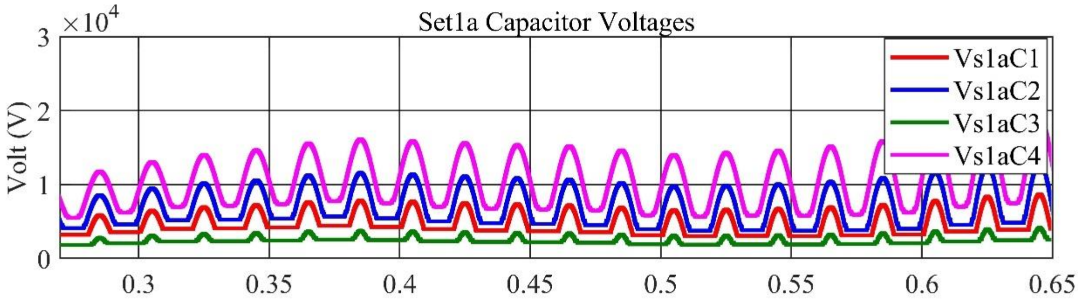

Figure 8. 14 Set1a capacitor voltages' waveforms of arm-a.

Each module set comprises four HBSMs, with each HBSM module incorporating a single capacitor. Consequently, four distinct waveforms corresponding to the voltage profiles of these capacitors are presented, as depicted in Figure 8.14. Specifically, the voltages denoted as $Vs1aC1, Vs1aC2, Vs1aC3, and\ Vs1aC4$ represent the voltages across the first, second, third, and fourth capacitors of the HBSM modules, respectively.

The Fast Fourier Transform (FFT) analysis of the SM sets of the a-arm and the current and voltage waveforms of the primary and secondary sides of the suggested DC-DC MMC converter architecture have been depicted in Figures 8.15-8.18. In cases where discrete impulses are transformed from the time domain to the frequency domain, the discrete Fourier transformation is implemented and improved upon with FFT. The phases, structure of the frequencies and additional characteristics of the electrical signal are all revealed by FFT estimations. The highest-performing FFT analyses, which were carried out using the fundamental grid frequency (50 Hz) for this scenario, are shown in Figures 8.15-8.18.

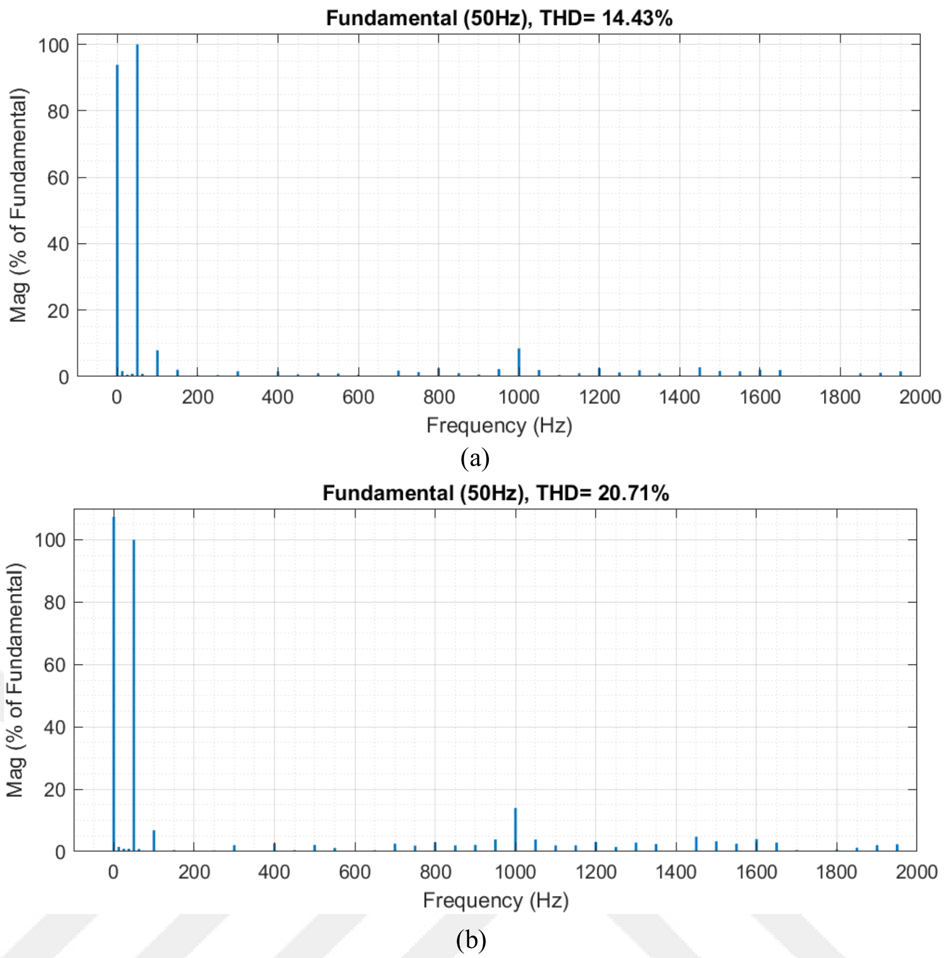

Figure 8. 15 FFT analysis of arm-a voltages waveform: (a) Set1a voltage FFT analysis; (b) Set2a voltage FFT analysis.

The FFT analysis of the voltage waveforms occurring on the Set1a and Set2a SM sets of the system's arm-a is illustrated in Figure 8.15. While the THD value of the voltage falling on set1a SM set in Figure 8.15(a) is 14.43%, the THD value of the voltage waveform of the se2a set in Figure 8.15(b) has been calculated as 20.71%. Furthermore, the FFT analysis of the voltage waveforms occurring on Set3a and Set4a SM sets of the system's arm-a is illustrated in Figure 8.16. While the THD value of the voltage falling on the set3a SM set in Figure 8.15(a) has been calculated as 19.46%, the THD value of the voltage waveform of the se4a set in Figure 8.16(b) has been measured as 14.08%.

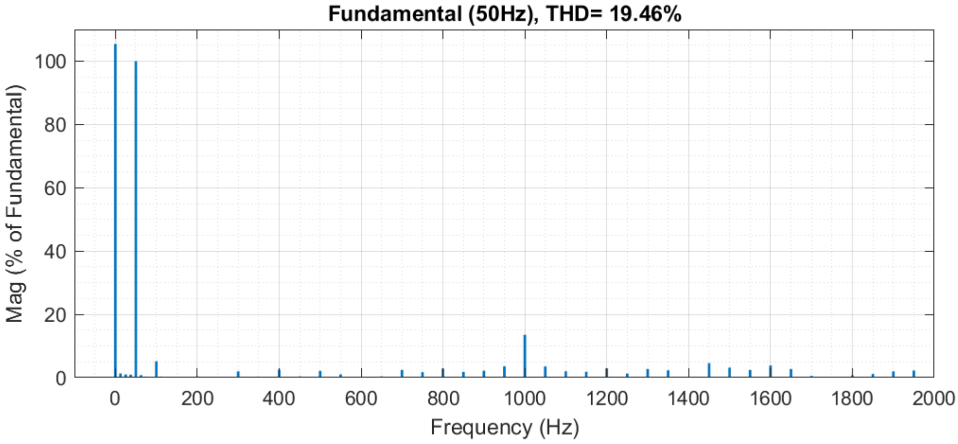

(a)

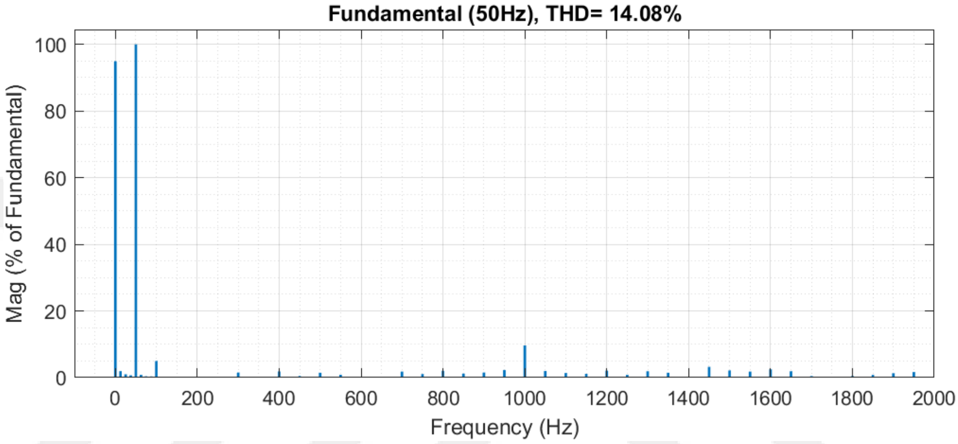

(b)

Figure 8. 16 FFT analysis of arm-a voltages waveform: (a) Set3a voltage FFT analysis; (b) Set4a voltage FFT analysis.

The FFT analysis of the current waveforms passing through set1a and set2a SM sets of the system's arm-a is illustrated in Figure 8.17. In addition to this, the FFT analysis of the current waveforms passing through the set3a and set4a SM sets of the system's arm-a is illustrated in Figure 8.18. While the THD value of the current passing through the set1a SM set in Figure 8.17(a) is 1.5%, the THD value of the current waveform of the se2a set in Figure 8.17(b) has been calculated as 1.79%. Similarly, while the THD value of the current passing through the set3a SM set in Figure 8.18(a) has been calculated as 2.08%, the THD value of the current waveform of the se4a set in Figure 8.18(b) has been measured as 1.97%. Considering the information above, it is unambiguous that the suggested DC-DC MMC structure integrates two asynchronous power networks while operating at maximal effectiveness, thanks to its innovative and modern construction. As can be provided, the THD statistics acquired by FFT analysis are exceedingly acceptable ranges.

In comparison to conventional power conversion systems, the suggested DC-DC MMC architecture is an innovative configuration intended to increase efficiency and lower harmonic distortion. THD is a metric that measures the degree to which a waveform deviates from its ideal sinusoidal shape as a result of harmonic levels. A high THD value in power systems is undesirable because it can degrade system productivity, boost power interruptions, and perhaps harm delicate equipment. Several parameters, such as the quantity of modules, the switching frequency, and the design of each individual SM, affect the degree of harmonic distortion in an MMC design. THD is often decreased by increasing the number of SMs since this produces a smoother output. These circumstances are taken into consideration when designing the suggested DC-DC MMC architecture. This is further supported by the acquired FFT data.

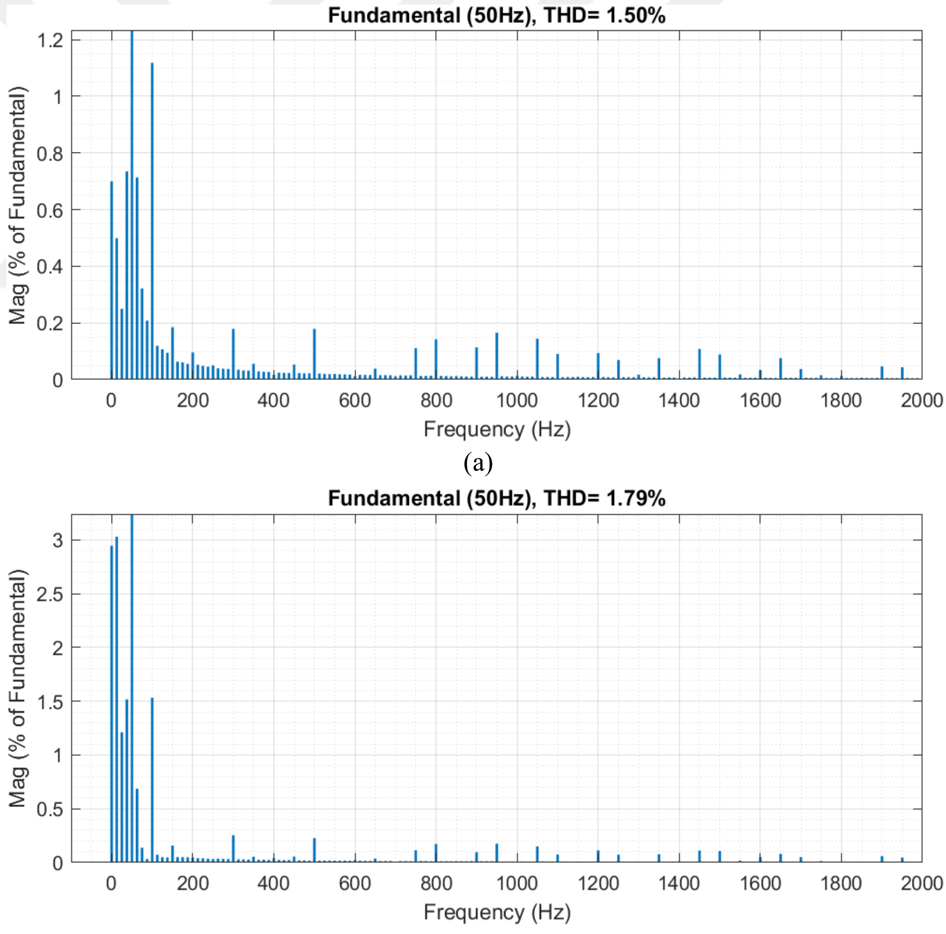

(b)

Figure 8. 17 FFT analysis of arm-a currents waveform: (a) Set1a current FFT analysis; (b) Set2a current FFT analysis.

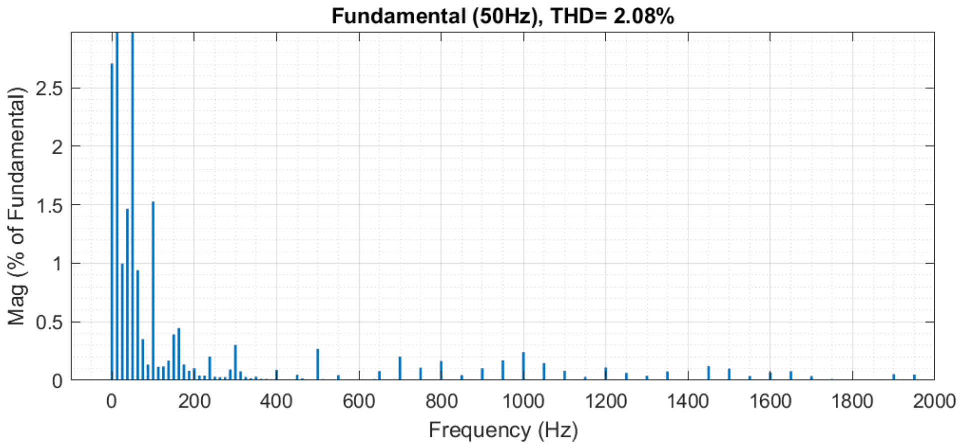

(a)

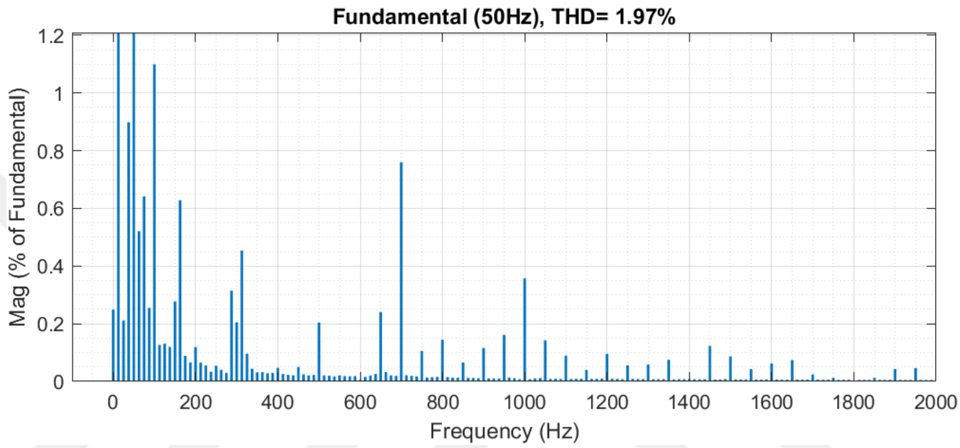

(b)

Figure 8. 18 FFT analysis of arm-a currents waveform: (a) Set3a current FFT analysis; (b) Set4a current FFT analysis.

The capability of the suggested DC-DC MMC design to produce minimal THD degrees, guaranteeing superior power effectiveness, is one of its main advantages. The modular architecture reduces harmonic distortion by assisting in smoothing the output voltage. The THD can be mitigated by meticulously reducing the number of modules and applying sophisticated modulation techniques, guaranteeing that the converter operates properly and doesn't add a lot of harmonic content to the system.

In Figures 8.12 and 8.13 the voltage and current waveforms correspond to the SM sets belonging to the arm-a branch of the proposed converter. Harmonic analysis (Figures 8.15-8.17) was performed for these arm-level signals to evaluate their spectral characteristics. The current waveforms exhibit nearly sinusoidal behavior, which results in relatively low harmonic distortion levels. In contrast, the arm voltages consist of stepped voltage levels generated by the series connection and switching operation of multiple SMs. Consequently, the voltage signals include high-frequency components inherent to the multilevel structure, leading to higher voltage THD values compared to the corresponding current THD levels. This behavior is a natural characteristic of modular multilevel converters, where the stepped voltage synthesis produces a multilevel sinusoidal waveform without affecting the overall AC-side power quality.

In the proposed non-isolated DC-DC MMC topology, circulating currents are minimized and the SM capacitor voltages are balanced. This is done using a control strategy that makes use of the arm and filtering inductors, and a way to control the capacitor voltages. The arm inductor L_a and the arm filter inductance L_f inserted in each arm are essential for the suppression of the short-term voltage oscillations that are generated by the SM switching. The arm inductors provide impedance to the arm paths and, therefore, limit the high-frequency circulating components. The model shown in Section 7.4 shows explicitly that the circulating currents' DC components are zero. As the simulation results (primary and secondary side voltages, currents, powers, and SM voltages etc.) show, the primary and secondary current waveforms show almost no distortion, and the circulating currents are reduced below 3% of the rated current amplitude even under step disturbances. Each SM capacitor is continuously monitored, and a balancing algorithm based on sorting and selective insertion ensures equalized voltage distribution. Figures 8.14, 8.24, and 8.32 illustrate capacitor voltage waveforms of arm-a under PD-PWM, POD-PWM, and APOD-PWM conditions, respectively. In all three cases, capacitor voltages remained tightly regulated, with deviations constrained within ±2% of nominal voltage, which is considered acceptable for MMC applications. The circulation current is minimized by the current limiter located in the control system. The system's performance is quantitatively evaluated through a set of simulation-based metrics that clearly demonstrate the effectiveness of the proposed control strategy and topology. The results indicate that the capacitor voltage ripple is consistently below 2% across all operating points, signifying effective voltage balancing. Furthermore, the current THD remains below 1.5% in PWM modes, confirming that the control strategy maintains high waveform quality. The system's dynamic response is evidenced by the achievement of stable balancing within 2 seconds following transient events. Lastly, the bidirectional operation has been successfully verified with minimal losses of balance, highlighting the converter's flexibility, which is crucial for modern HVDC applications. These results validate that the proposed control algorithm ensures both effective suppression of circulating currents and precise balancing of SM capacitor voltages, thereby maintaining converter stability, efficiency, and reliability across varying operating conditions.

The efficiency and loss characteristics of the suggested DC-DC MMC under PD-PWM modulation at various operating points are shown in Figure 8.19(a) and Figure 8.19(b). Efficiency greatly improves as the power level rises, surpassing 96%. The visualized data, represented by the loss curve, indicates that the system achieves a steady-state operational condition with a minimal loss rate remaining below 3%. The efficiency value given here is determined using the system's input and output power values. The sources of losses causing efficiency loss include switching losses, losses caused by internal resistances in inductors, diode losses, and conduction losses. The total losses occurring in the converter can be calculated as follows:

$$P_{Loss} = P_{swc} + P_{Lr} + P_{Lo} + P_{di} + P_{Cesr} \tag{8.1}$$

Here, P_{swc} represents the switching losses, P_{Lr} and P_{Lo} denote the losses originating from the internal resistance of the inductor inductance within the design, P_{di} signifies the diode losses, and P_{Cesr} indicates the losses arising from the capacitor's equivalent series resistance (ESR), which is primarily due to the dielectric/insulation resistance. The output power and efficiency were determined based on the equations provided below:

$$P_{out} = P_{in} - P_{Loss} \tag{8.2}$$

$$\eta = \frac{P_{out}}{P_{in}} x100) \tag{8.3}$$

The findings show that while the associated losses show a trend to decrease with power level, efficiency continuously rises. These two data are combined into a radar map in Figure 8.19(c), which amply illustrates the complementary connection between efficiency and losses across the operational range. These results show that the PD-PWM approach guarantees efficient converter operation with enhanced performance at greater power levels. According to this pattern, losses become less significant at greater power levels, allowing the system to function more effectively.

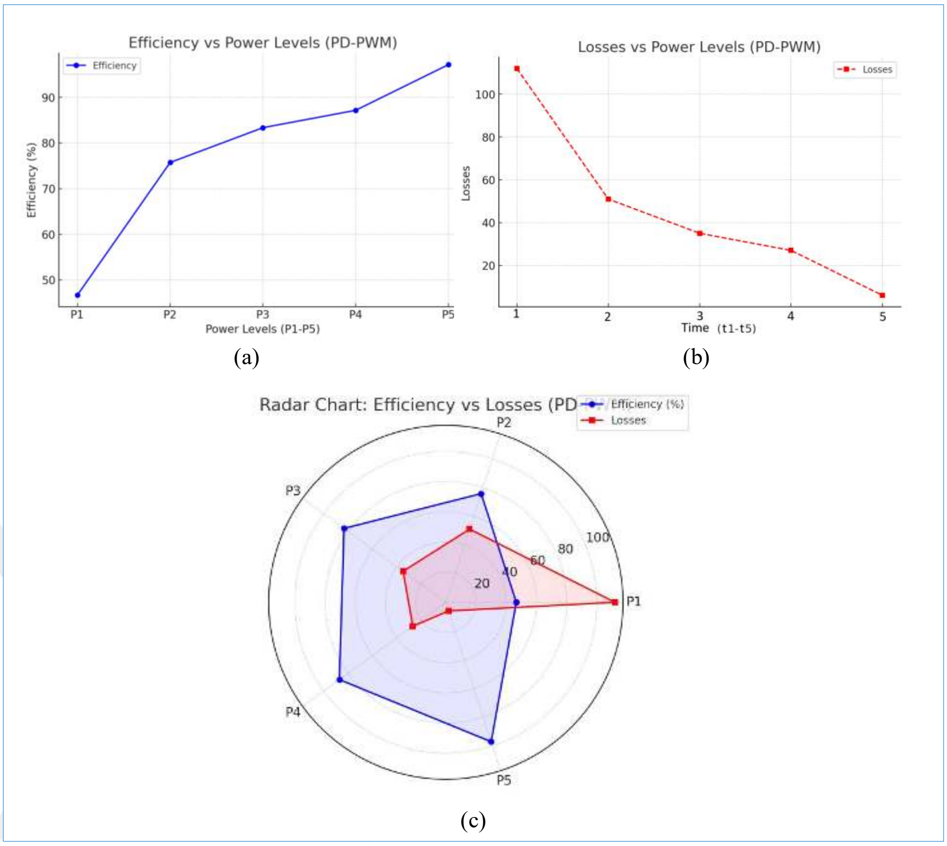

(a) (b) (c)

Figure 8. 19 The efficiency and losses waveforms of the proposed DC-DC MMC topology: (a) The efficiency waveform; (b) The losses waveform; (c) The efficiency and losses radar chart.

8.3.2 Case Study 2

In this section, the modulation technique in the control system is changed to POD-PWM, and the simulation findings obtained in the previous case study are re-evaluated. In line with the findings obtained, it is seen that the POD-PWM technique is as favorable as the PD-PWM technique. This proves that the designed topology adapts to different PWM techniques successfully. Figure 8.20 illustrates the primary side voltage, primary side current, secondary side voltage, and secondary side current waveforms of the proposed DC-DC MMC design, respectively. The results obtained for voltage and current are quite similar to those found in the initial case study.

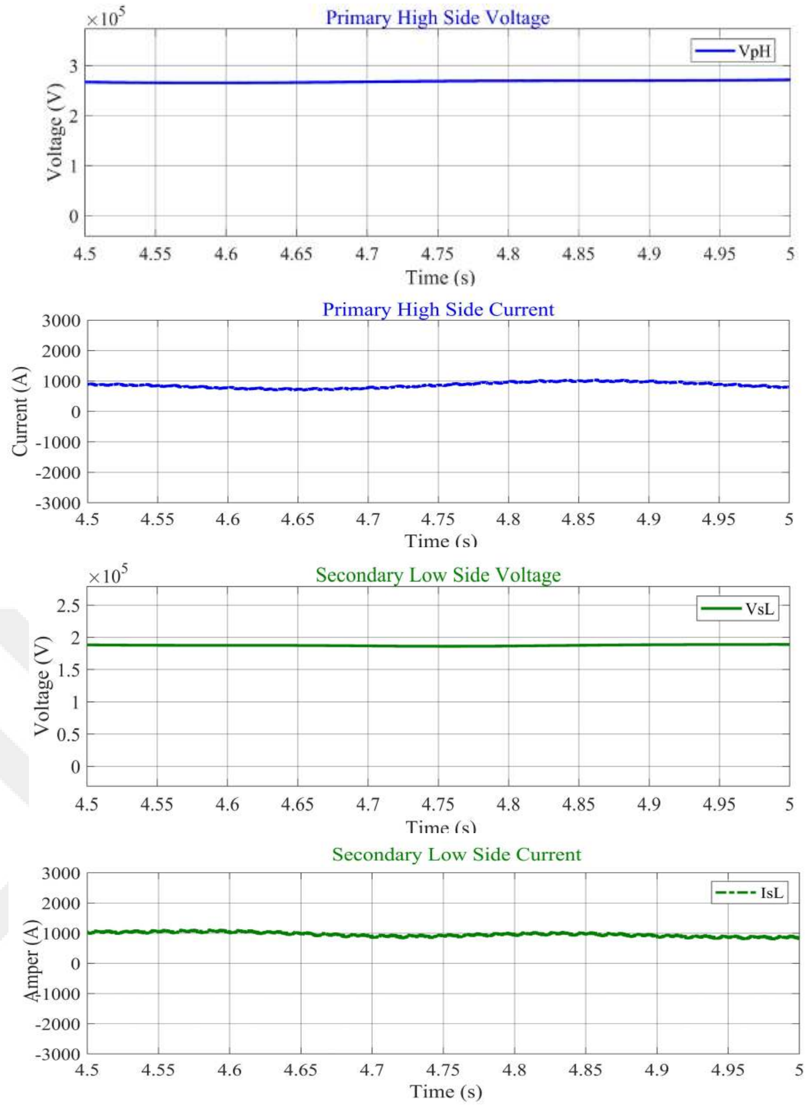

Figure 8. 20 Voltage and current waveforms of the primary and secondary sides of the proposed DC-DC MMC topology (POD-PWM based).

Figure 8.21, utilizing the POD-PWM technique, illustrates the power transfer between the primary and secondary terminals within the proposed DC-DC MMC configuration. As shown in Figures 8.21(a) and 8.21(b), power transfer from the primary to the secondary side and vice versa begins approximately 0.5 seconds after system initiation, triggered by a step command in the control system. The measured power waveforms accurately track the reference, demonstrating the controller's effectiveness in steady-state operation. Notably, the system exhibits a robust dynamic response to sudden variations in voltage and power at 2 and 3.14 seconds, maintaining stability and reference tracking post-disturbance. These results highlight the architecture's strong transient performance and its capacity to facilitate stable energy exchange between asynchronous HVDC networks. Additionally, the start-up process has been systematically assessed to ensure reliability and operational safety. The power ramp-up sequence, executed shortly after system activation, completes within 0.5 seconds, indicating effective control design. The well-coordinated start-up behavior mitigates risks associated with high-power transfers and enhances the system's resilience. Regular evaluation of the start-up dynamics and addressing any anomalies are essential for optimizing performance and ensuring long-term system stability. The proposed control strategy successfully supports both initial activation and dynamic power transfer between HVDC terminals.

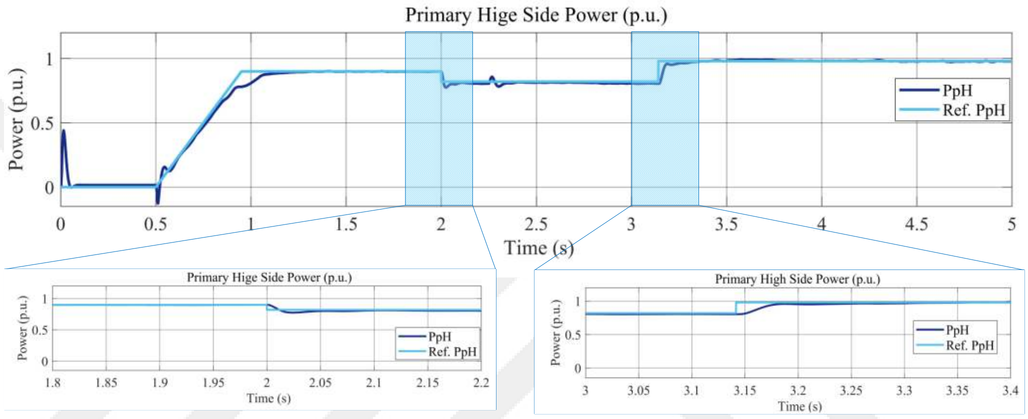

(a)

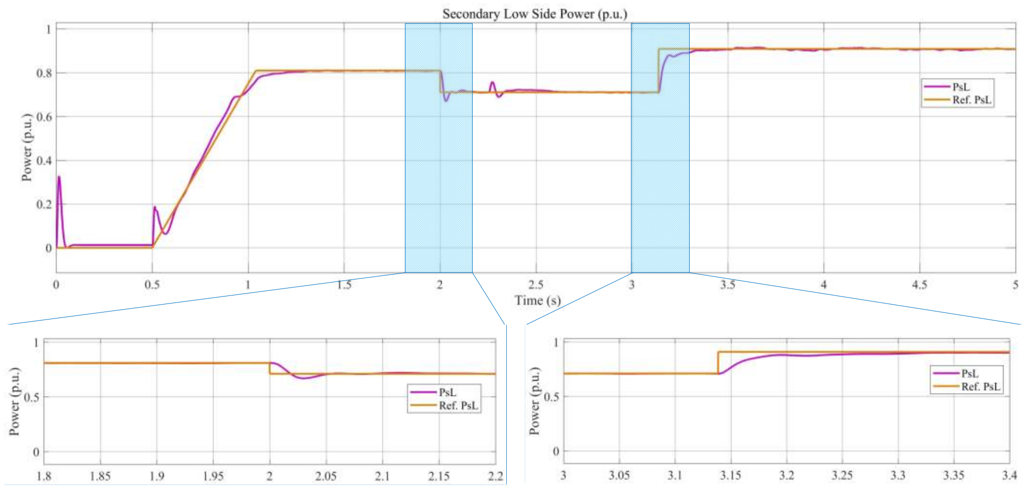

(b)

Figure 8. 21 Power waveforms of the primary and secondary sides of the proposed DC-DC MMC topology (POD-PWM based): (a) The power waveform transferred from the primary side to the secondary side; (b) The power waveform transferred from the secondary side to the primary side.

The voltage across the four SM sets in system arm-a and the currents flowing through the appropriate SM sets are shown in Figure 8.22 and Figure 8.23. The POD-PWM approach, which operates based on reference signals with a 120-degree phase difference between each arm, has been employed for switching the power switches. The voltage and current waveforms of the SM set on arm-a are given to keep the research from getting excessively extensive. Five distinguished voltage levels have been obtained since using four HBSMs in SM sets. As can be observed and predicted from the representation, the SM sets provide voltage values corresponding to different voltage levels, and the currents passing through them have the characteristics of a sinusoidal waveform. It is clear from examining the data produced by the pertinent voltage and current waveforms that the suggested architecture and associated control mechanisms operate admirably.

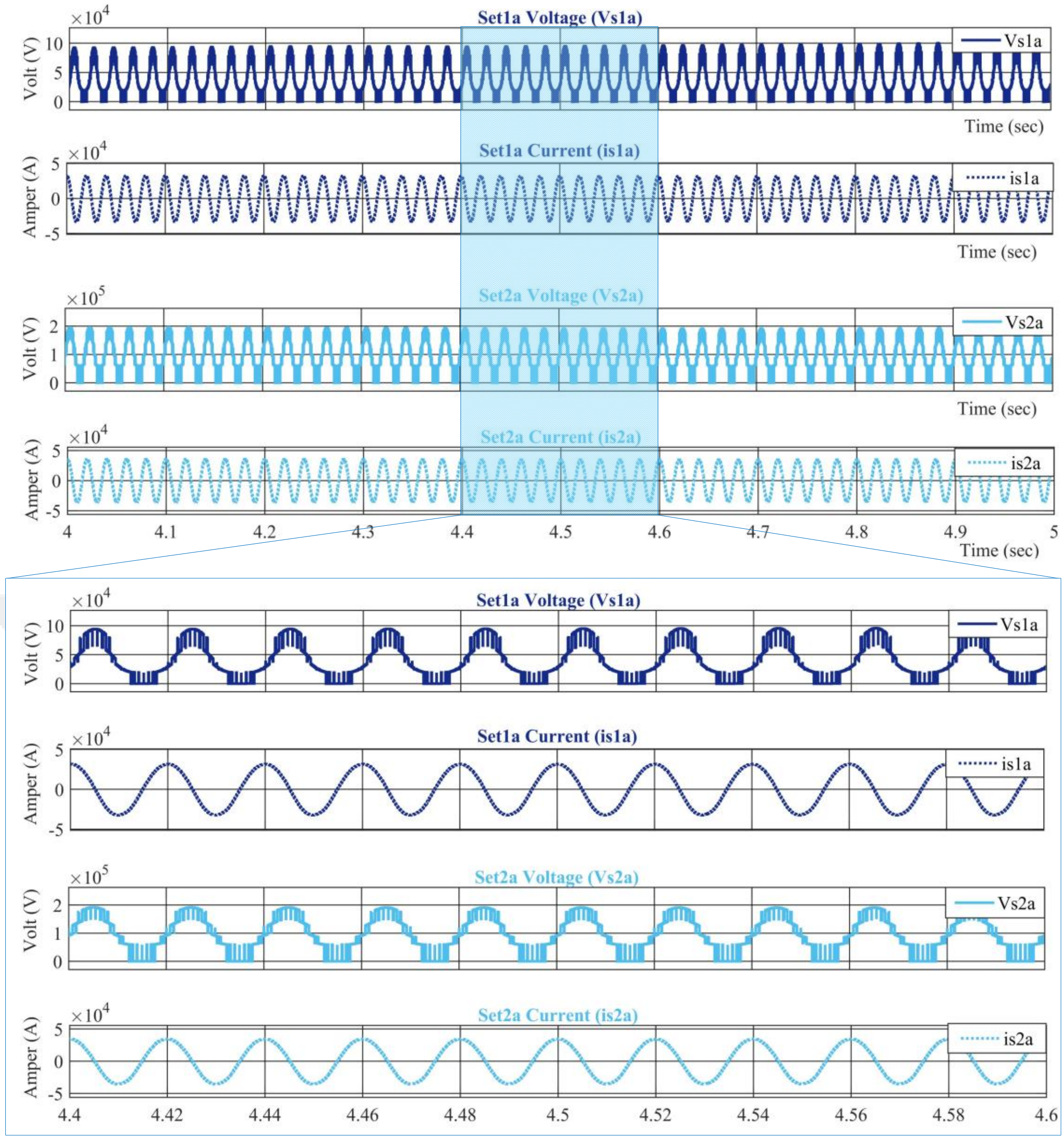

Figure 8. 22 Voltages and current waveforms of set1a and set2a (POD-PWM based).

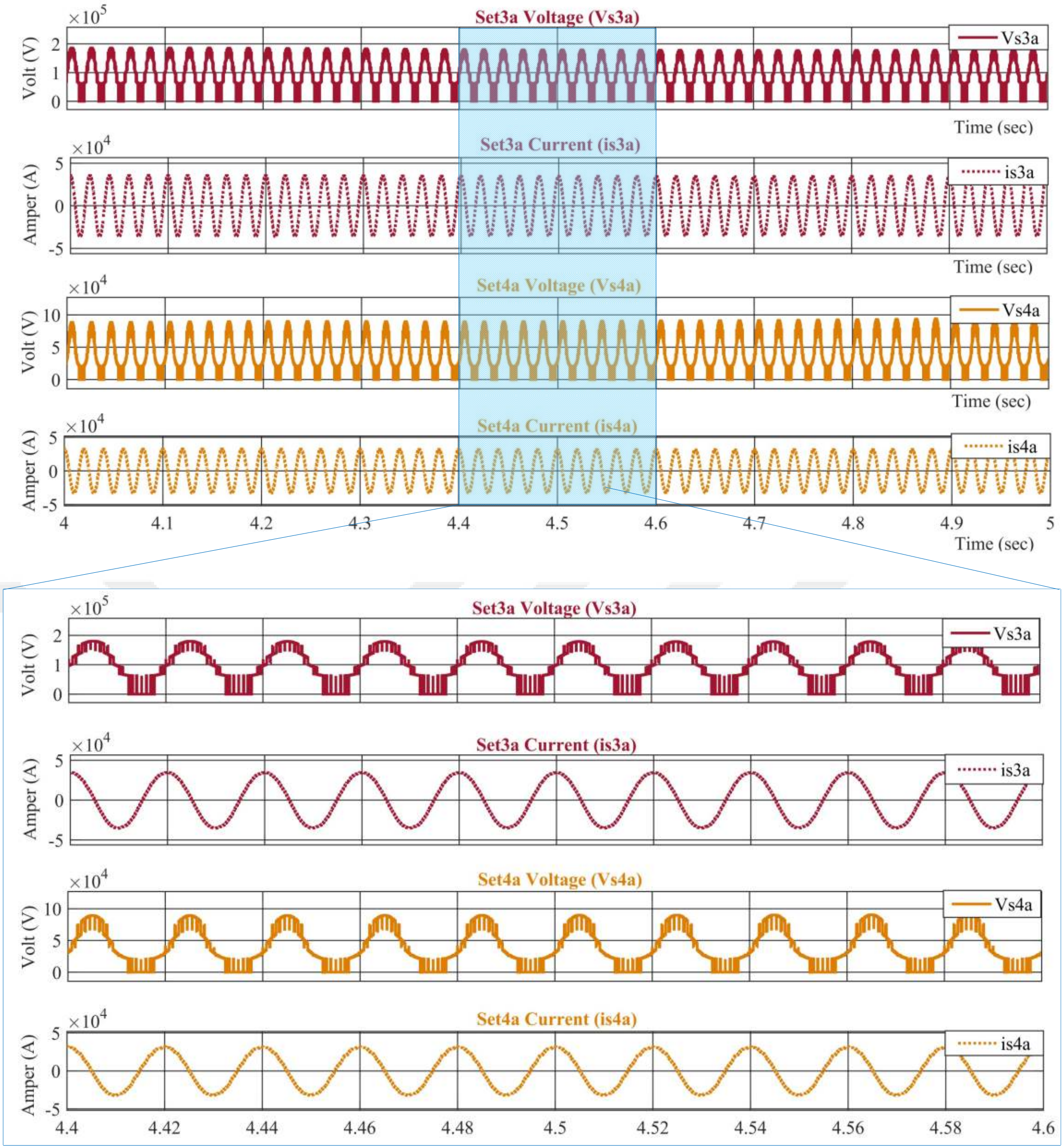

Figure 8. 23 Voltages and current waveforms of set3a and set4a (POD-PWM based).

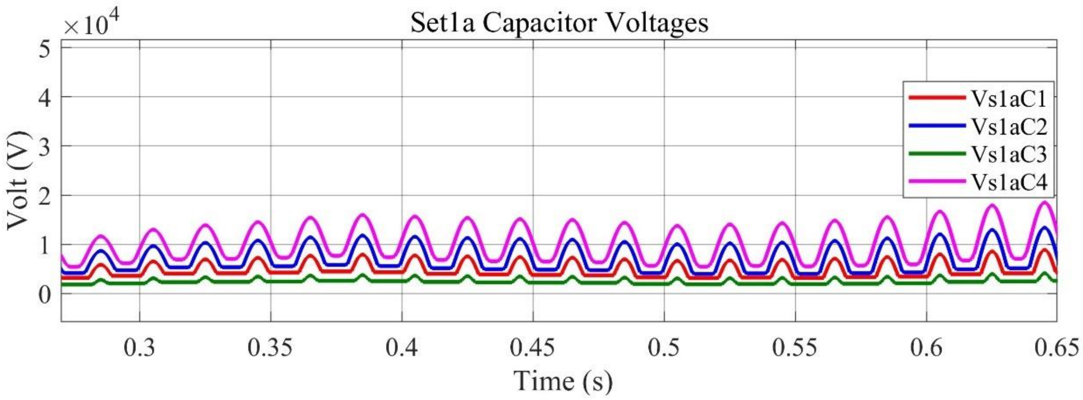

Figure 8. 24 Set1a capacitor voltages' waveforms of arm-a (POD-PWM).

The waveforms of the capacitor voltages in the set1a SM set of the design's arm-a have been presented in Figure 8.24. It is readily apparent that an efficient capacitor voltage balancing has been accomplished when glancing at the waveforms of the capacitor voltages in Figure 8.24. The system's arm-a data illustrates that the innovative DC-DC MMC architecture that has been suggested successfully integrates two asynchronous power networks. Each module set comprises four HBSMs, with each HBSM module incorporating a single capacitor. Consequently, four distinct waveforms corresponding to the voltage profiles of these capacitors are presented, as depicted in Figure 8.23. Specifically, the voltages denoted as Vs1aC1, Vs1aC2, Vs1aC3, and Vs1aC4 represent the voltages across the first, second, third, and fourth capacitors of the HBSM modules, respectively.

The POD-PWM-based FFT analysis for voltage and current waveforms of the SM sets of the a-arm and the current and voltage waveforms of the primary and secondary sides of the suggested DC-DC MMC converter architecture have been depicted in Figures 8.25-8.26. The findings from these FFT evaluations, which were conducted using 50 Hz as the basic grid frequency, show that the converter architecture that was created functions effectively.

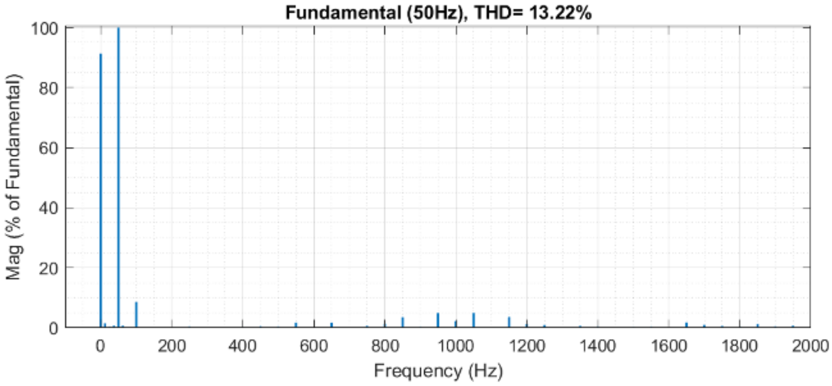

(a)

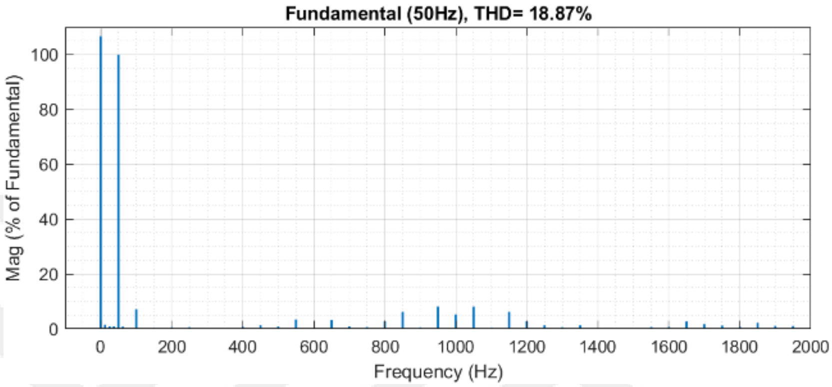

(b)

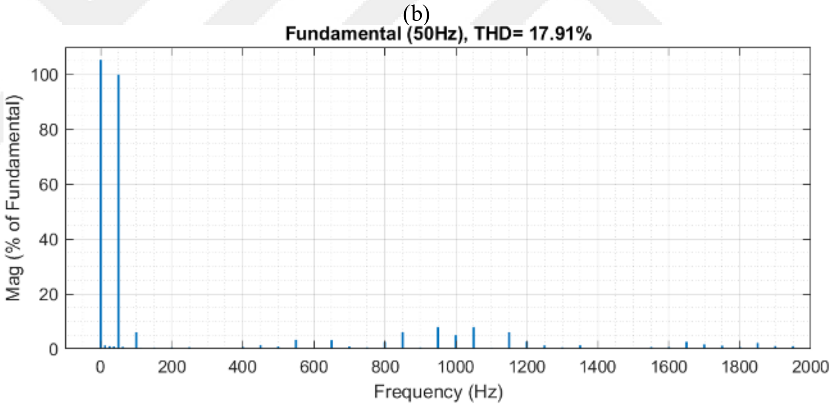

(c)

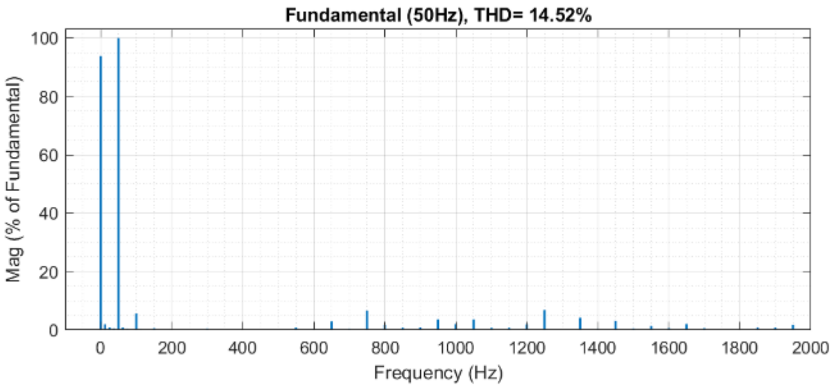

(d)

Figure 8. 25 FFT analysis of arm-a voltages waveform (POD-PWM based): (a) Set1a voltage FFT analysis; (b) Set2a voltage FFT analysis; (c) Set3a voltage FFT analysis; (d) Set4a voltage FFT analysis.

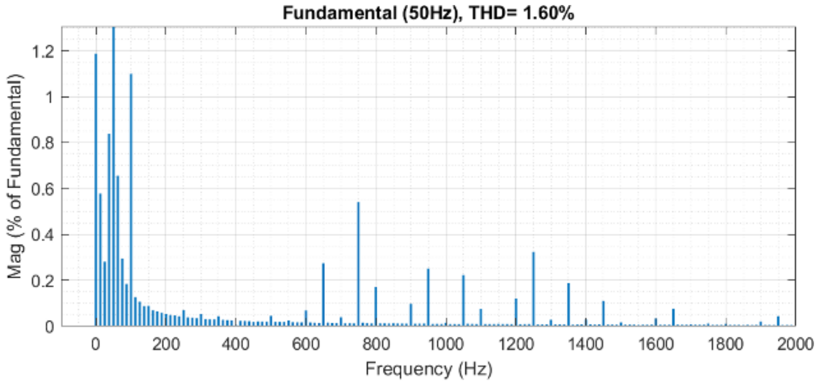

(a)

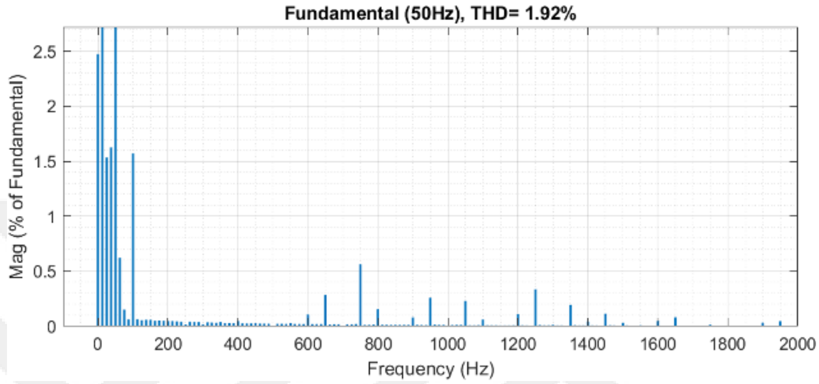

(b)

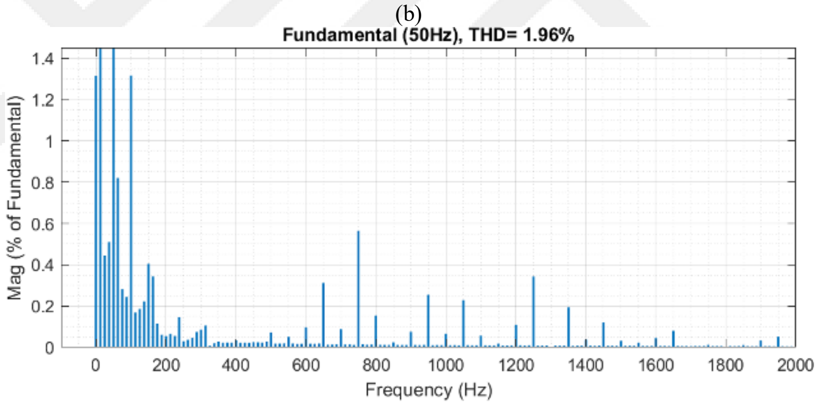

(c)

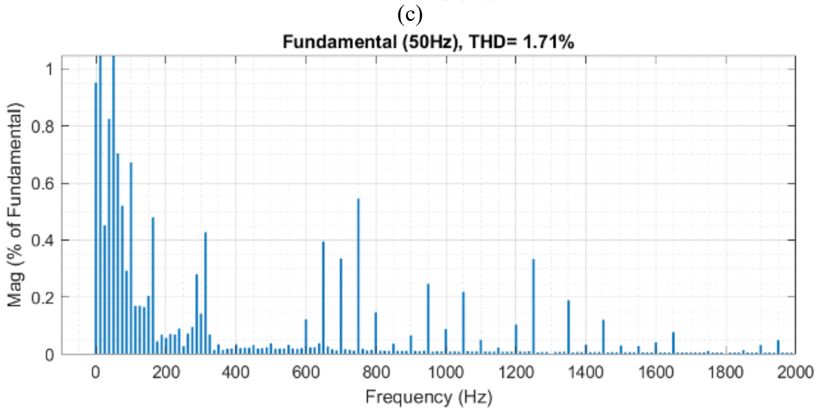

(d)

Figure 8. 26 FFT analysis of arm-a currents waveform (POD-PWM based): (a) Set1a current FFT analysis; (b) Set2a current FFT analysis; (c) Set3a current FFT analysis; (d) Set4a current FFT analysis.

The POD-PWM-based FFT analyses of the falling voltages on the SM sets on arm-a are displayed in Figure 8.25. FFT analysis of Set1a voltage, Set2a voltage, Set3a voltage, and Set4a voltage is demonstrated in Figure 8.25(a), Figure 8.25(b), Figure 8.25(c), and Figure 8.25(d), respectively. Figures 8.25(a)-8.25(d) present the harmonic spectra generated for the converter in each considered POD modulation configuration. The case represented in Figure 8.25(a) produces a THD of 13.22% and contains significant low order harmonics. Figure 8.25(b) provides the harmonic spectrum that incorporates the worst THD value of 18.87%. As previously mentioned, this case reflects the worst distortion including noticeable harmonic peaks. The case represented in Figure 8.25(c) offers a THD of 17.91%, with a harmonic distribution pattern similar to Figure 8.25(b). Finally, Figure 8.25(d) shows the best THD result at 14.52%- or less than any of the other cases in terms of distortion values and offers some improvement in the overall quality of the harmonic profile. However, despite improvements we see that the overall THD values are still somewhat high.

In a similar manner, the FFT analyses of the currents flowing throughout SM sets on arm-a, based on POD-PWM, are displayed in Figure 8.26. The FFT analysis of Set1a current, Set2a current, Set3a current, and Set4a current is displayed in Figures 8.26(a), 8.26(b), 8.26(c), and 8.26(d), correspondingly. In Figure 8.26(a), the THD for the converter is 1.60%, which is the least distortion achieved from the four possible outputs for the converter, and the energy spectral density is concentrated at the fundamental component (50 Hz), while the amplitude of higher order harmonics was heavily suppressed. The THD from Figure 8.26(b) was found to be 1.92%. The THD from Figure 8.26(c) was also found to be similar (1.96%), although each of these THD values is slightly higher than that of Figure 8.26(a); the harmonic contents were still within a reasonable range for quality power conversion. Figure 8.26(d) showed a THD of 1.71%, which revealed that the harmonics were more evenly distributed across the spectrum; however, they had relatively lower amplitudes, leading to a smoother and more balanced output waveform. Altogether, it can be seen that the harmonic distortion was less than 2% in all four instances, which is regarded as reasonable for practical uses, where Figure 8.26(a) and Figure 8.26(d) exhibited the best options in terms of spectral quality. Considering the FFT analysis was conducted at the fundamental frequency of 50 Hz, it is evident from Figures 25 to 26 that the total harmonic distortion (THD) is at low levels. The fundamental frequency components of these signals are displayed at the fundamental frequency (50 Hz). The THD parameter in power electronics systems indicates the strength of the signals' harmonic components, which are not the fundamental frequency. According to the THD values acquired for these signals, the signals are clean since they exhibit comparatively minimal distortions. As a result, it is obvious that the proposed DC-DC MMC topology and the adapted control approach are successful.

In the case study, the voltage and current waveforms presented in Figures 8.22 and 8.23 were used to perform harmonic analysis, and the resulting THD distributions are illustrated in Figures 8.25 and 8.26. The current waveform maintains a nearly sinusoidal profile, leading to low THD. In contrast, the voltage waveform exhibits a multilevel stepped structure formed by the sequential switching of SMs. Due to this stepped synthesis, the voltage signal inherently contains higher-frequency components, which results in higher voltage THD compared to the current. This characteristic behavior is typical of MMCs and does not indicate degraded power quality, as the multilevel structure ultimately produces a smooth current waveform and stable power transfer performance.

The efficiency and loss characteristics of the proposed DC-DC MMC design under POD-PWM modulation are shown in Figures 8.27(a) and 8.27(b). Efficiency rises as operational power levels do, while losses show a progressive decline throughout the periods under consideration. Using a radar diagram, Figure 8.27(c) highlights the complementary fluctuation of both parameters across the operational range and shows their comparative behavior. These findings suggest that at greater power levels, the POD-PWM approach offers steady operation and enhanced performance.

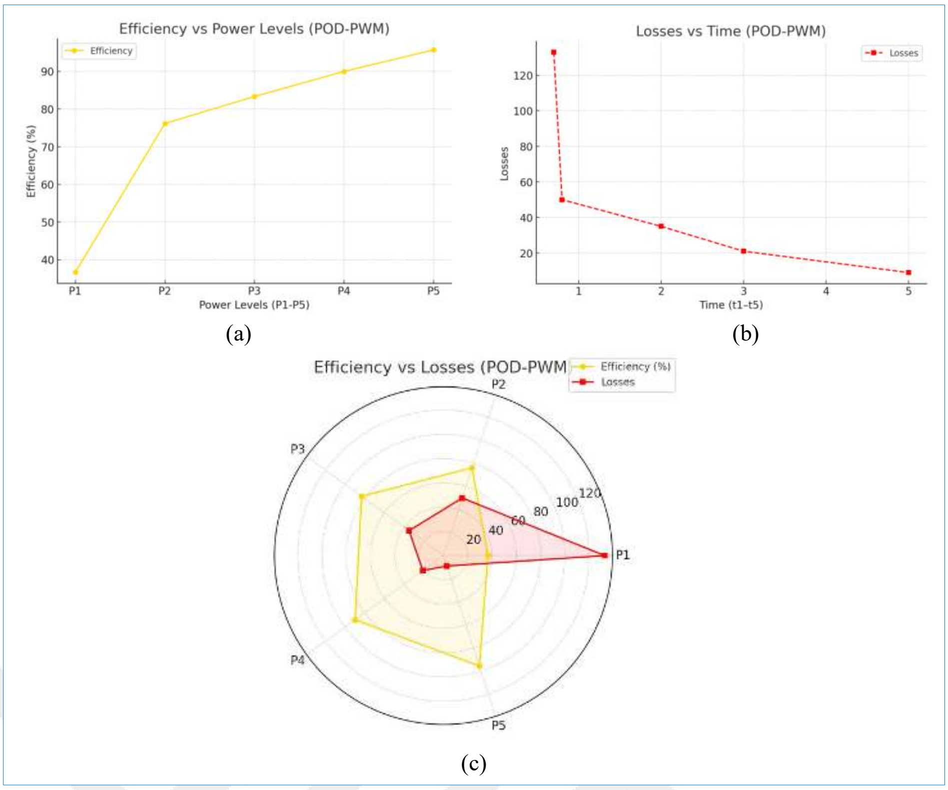

Figure 8. 27 The efficiency and losses waveforms of the proposed DC-DC MMC topology: (a) The efficiency waveform; (b) The losses waveform; (c) The efficiency and losses radar chart (POD-PWM).

8.3.3 Case Study 3

In this section, the modulation technique in the control system is changed to APOD-PWM, and the simulation findings obtained in Case Study 1 and Case Study 2 are re-evaluated. In line with the findings obtained in case study 2, it is apparent that the APOD-PWM approach is just as advantageous as the POD-PWM and PD-PWM procedures. This proves that the designed DC-DC MMC topology successfully adapts to different PWM techniques. Figure 8.28 illustrates the primary side voltage, primary side current, secondary side voltage, and secondary side current waveforms of the proposed DC-DC MMC design, respectively. The results obtained for voltage and current are quite similar to those found in the initial and second case studies.

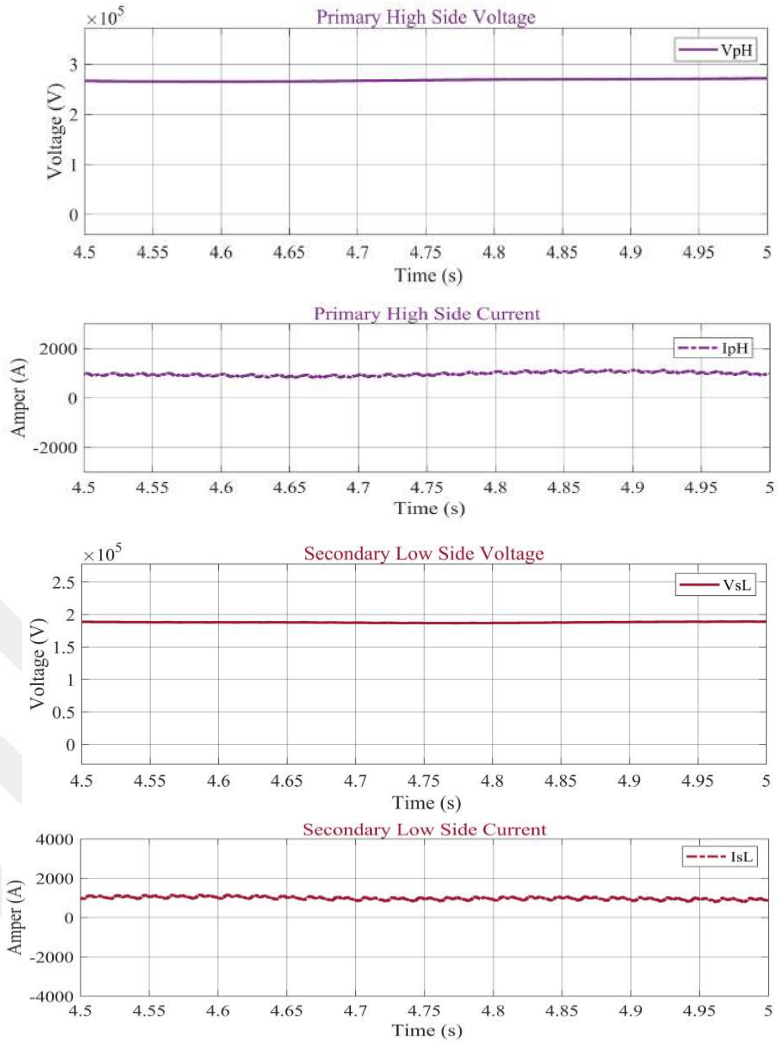

Figure 8. 28 Voltage and current waveforms of the primary and secondary sides of the proposed DC-DC MMC topology (APOD-PWM based).

Figure 8.29, utilizing the APOD-PWM technique, illustrates the power transfer between the primary and secondary terminals within the proposed DC-DC MMC configuration. The power transfer characteristics observed in both the initial and subsequent case studies are closely similar to those obtained through APOD-PWM-based power transmission. Specifically, Figure 8.29(a) depicts the power transfer from the primary to the secondary side, while Figure 8.29(b) presents the reciprocal transfer from the secondary to the primary side. Both figures demonstrate that power transfer initiates 0.5 seconds after system activation, following a step input by the control system. The power waveforms on both the primary and secondary sides exhibit a near-perfect correlation with the reference signal. Analyzing these waveforms reveals that the proposed converter design effectively manages abrupt fluctuations in system voltage and power, showcasing its exceptional performance. Furthermore, the observed power transfer responses between both sides of the system highlight the converter's outstanding transient characteristics, swiftly adjusting to sudden changes in system parameters.

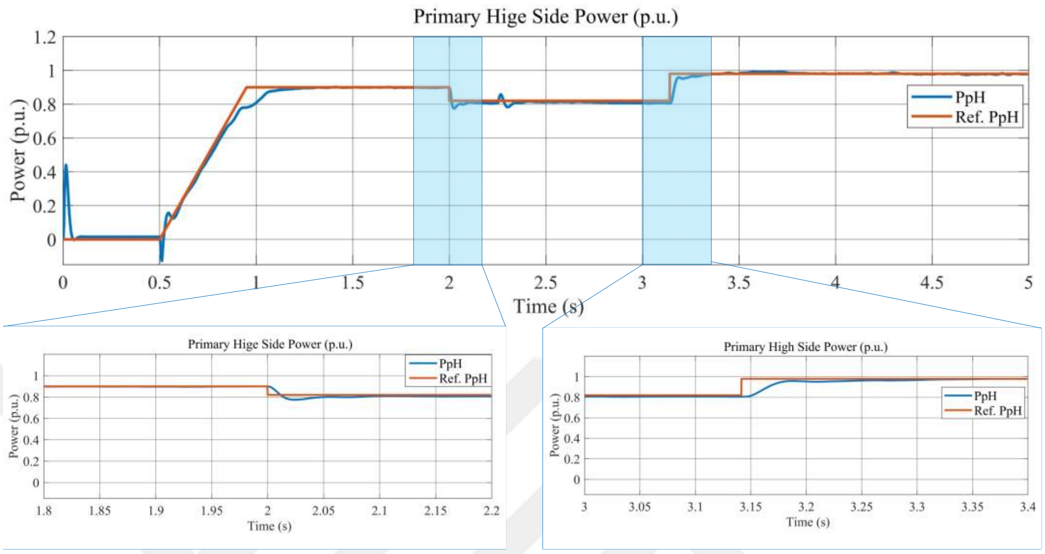

(a)

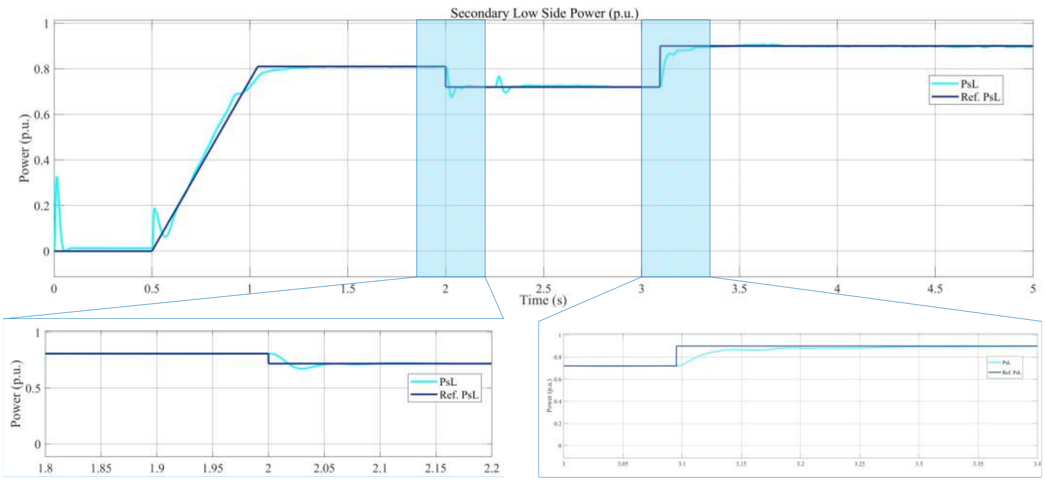

(b)

Figure 8. 29 Power waveforms of the primary and secondary sides of the proposed DC-DC MMC topology (APOD-PWM based): (a) the power waveform transferred from the primary side to the secondary side; (b) the power waveform transferred from the secondary side to the primary side.

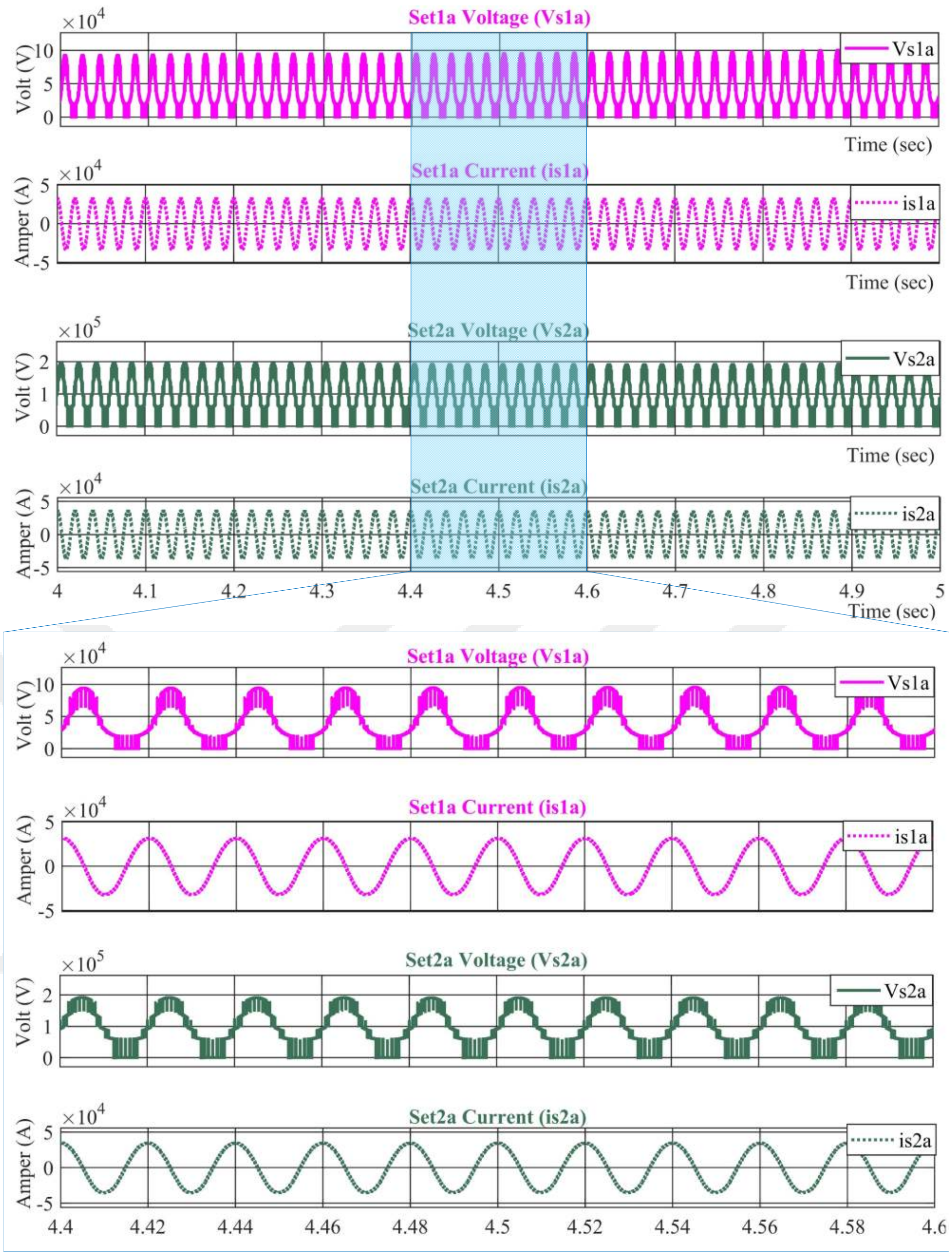

Figure 8. 30 Voltages and current waveforms of set1a and set2a (APOD-PWM based).

The voltage across the four SM sets in system arm-a and the currents flowing through the appropriate SM sets are shown in Figure 8.30 and Figure 8.31, which are obtained by the APOD-PWM technique. The APOD-PWM approach, which operates based on reference signals with a 120-degree phase difference between each arm, has been employed for switching the power switches such as PD-PWM and POD-PWM techniques.

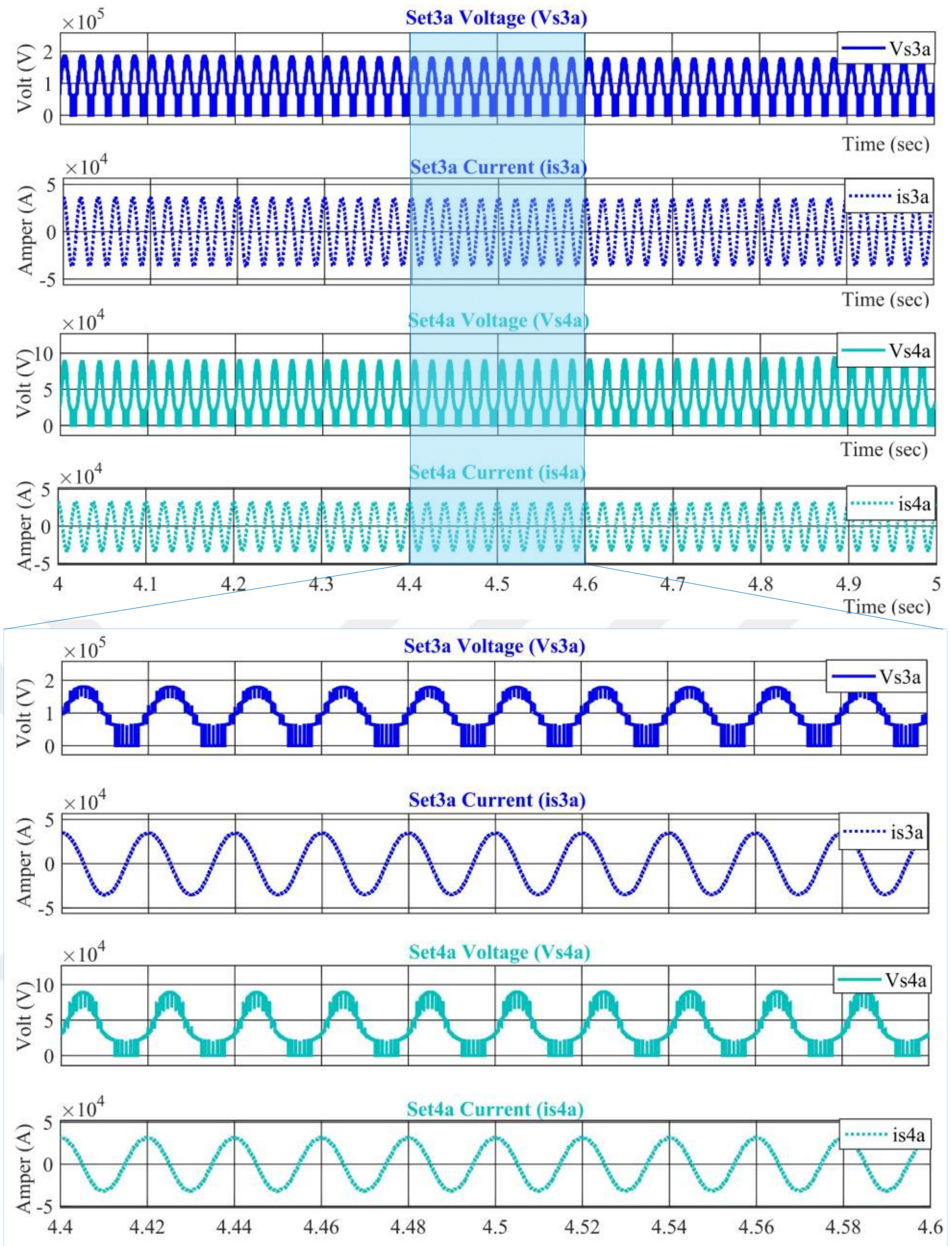

Figure 8. 31 Voltages and current waveforms of set3a and set4a (APOD-PWM based).

The voltage and current waveforms of the SM set on arm-a are given to keep the research from getting excessively extensive. Five distinguished voltage levels have been obtained since using four HBSMs in SM sets. As can be observed and predicted from the representation, the SM sets provide voltage values corresponding to different voltage levels, and the currents passing through them have the characteristics of a sinusoidal waveform. It is clear from examining the data produced by the pertinent voltage and current waveforms that the suggested architecture and associated control mechanisms operate admirably.

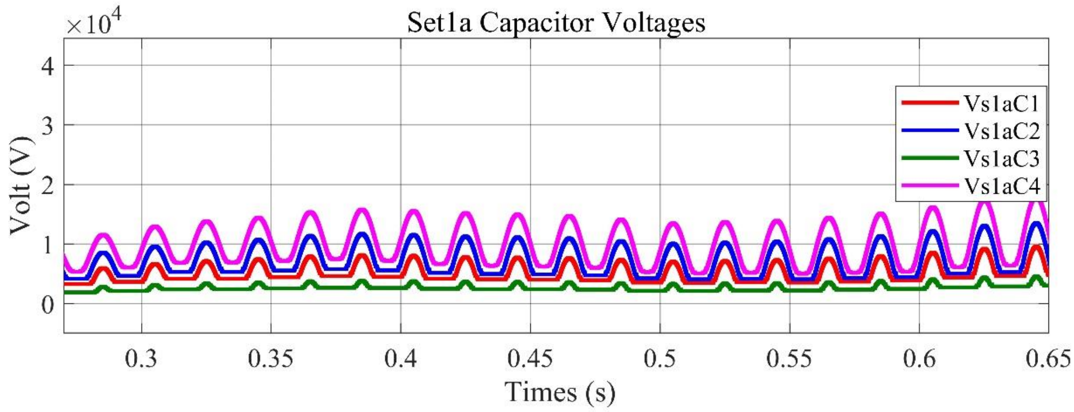

Figure 8. 32 Set1a capacitor voltages' waveforms of arm-a (APOD-PWM).

The waveforms of the capacitor voltages in the set1a SM set of the design's arm-a, which are obtained from the APOD-PWM technique, have been presented in Figure 8.32. Upon examining the capacitor voltage waveforms in Figure 8.32, it becomes immediately apparent that the system has achieved effective voltage balancing across the capacitors. The data from the arm-a section of the system further underscores the success of the proposed DC-DC MMC design in seamlessly integrating two asynchronous power networks. Each module set consists of four HBSMs, each housing a single capacitor. Accordingly, four distinct voltage waveforms corresponding to the individual capacitors within these submodules are presented in Figure 8.31. Specifically, the voltages labeled as $Vs1aC1$, $Vs1aC2$, $Vs1aC3$, and $Vs1aC4$ represent the voltage profiles of the first, second, third, and fourth capacitors across the respective HBSM modules, which are situated on the arm-a of the proposed DC-DC MMC design.

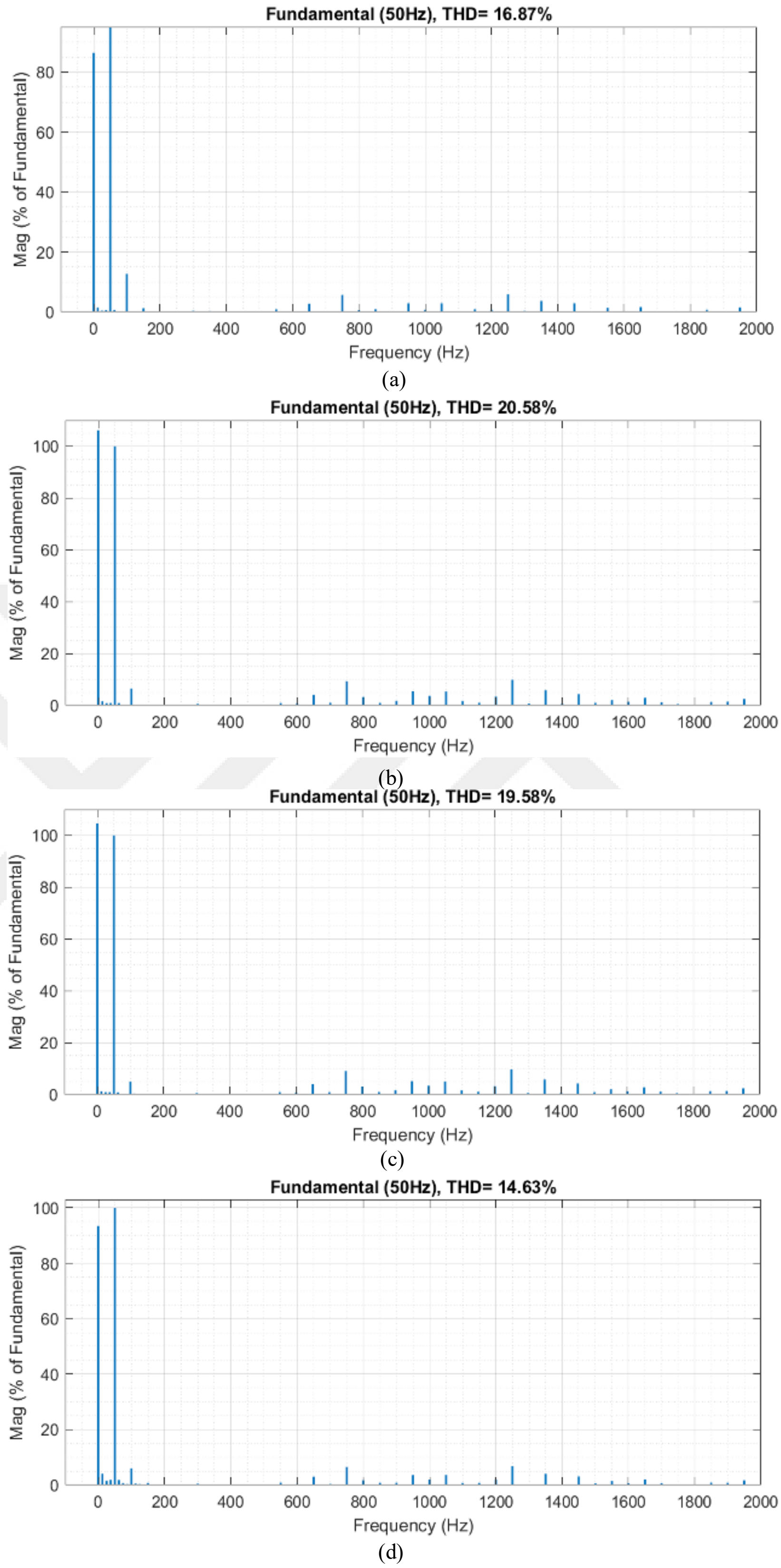

Figure 8. 33 FFT analysis of arm-a voltages waveform (APOD-PWM based): (a) Set1a voltage FFT analysis; (b) Set2a voltage FFT analysis; (c) Set3a voltage FFT analysis; (d) Set4a voltage FFT analysis.

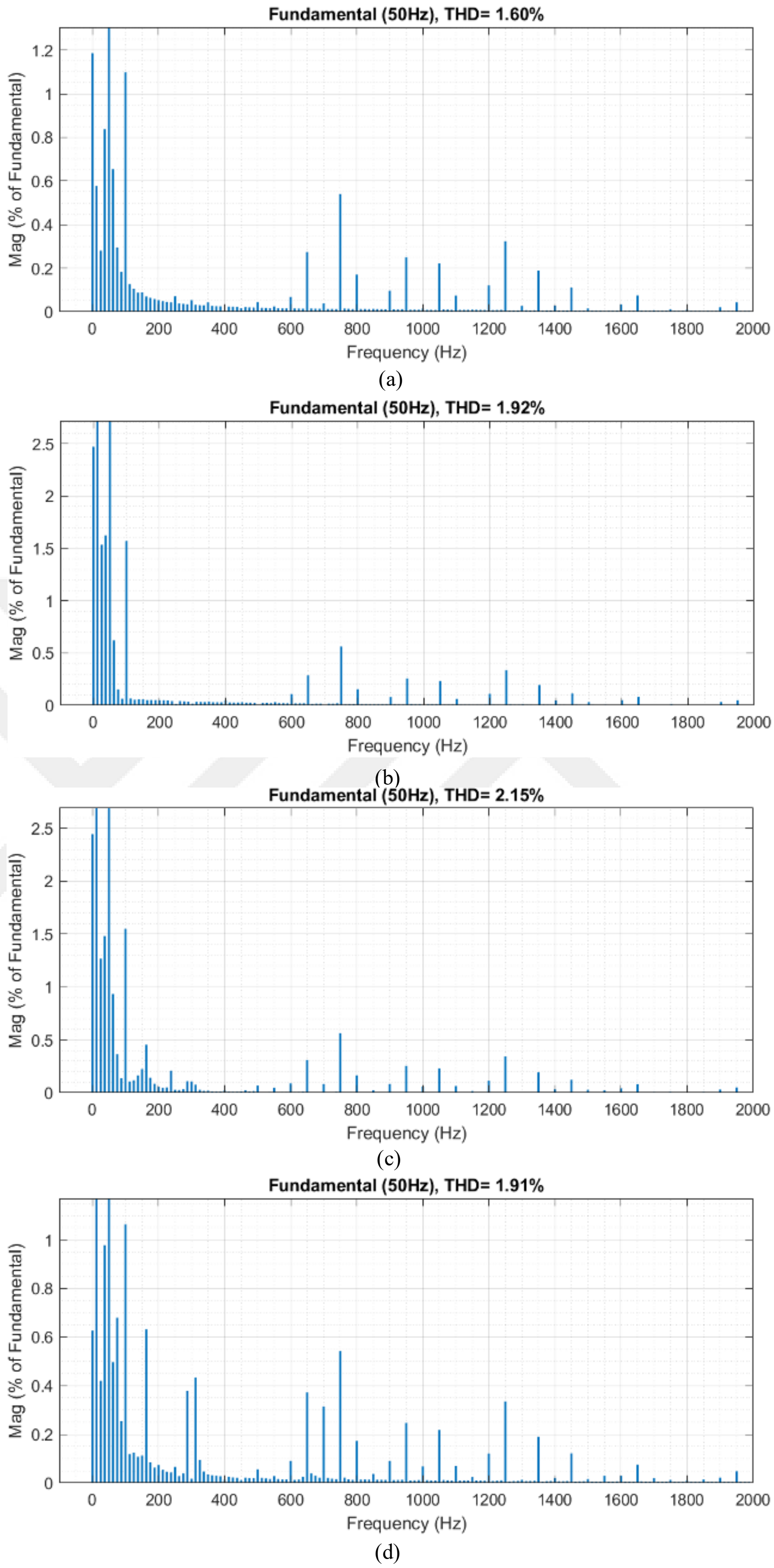

Figure 8. 34 FFT analysis of arm-a currents waveform (APOD-PWM based): (a) Set1a currents FFT analysis; (b) Set2a currents FFT analysis; (c) Set3a currents FFT analysis; (d) Set4a currents FFT analysis.

The FFT analyses of the SM voltage waveforms on arm-a, employing the APOD-PWM technique, are illustrated in Figure 8.33. Specifically, Figure 8.33(a) depicts the FFT analysis of the voltage across Set1a, Figure 8.33(b) presents the FFT analysis of the voltage across Set2a, Figure 8.33(c) illustrates the FFT analysis of the voltage across Set3a, and Figure 8.33(d) displays the FFT analysis of the voltage across Set4a. The THD shown in Figure 8.33(a) is calculated at 16.87%. In this case, varied harmonic components are among the lowest frequency regions. As shown in Figure 8.33(b), the highest amount of distortion, with a THD of 20.58%, showing that layer harmonics are the least effective in this condition. In Figure 8.33(c), it shows a THD of 19.58% with a harmonic spectral distribution pattern that is similar to Figure 8.33(b) with low-order harmonics predominating. Figure 8.33(d) has an average THD of 14.63%, which is the lowest of the cases presented, which shows harmonic performance is somewhat better even though harmonic performance still has significant distortion. Similarly, the FFT analyses of the currents flowing through the SM sets on arm-a, also based on the APOD-PWM technique, are shown in Figure 8.34. The FFT analyses of the currents for Set1a, Set2a, Set3a, and Set4a are presented in Figures 8.34(a), 8.34(b), 8.34(c), and 8.34(d), respectively. Figure 8.34(a) contains the THD of 1.60% in this case, the lowest distortion condition tested in these conditions, supporting the majority of the spectral energy at the fundamental frequencies and only small amounts of harmonic components at higher orders. Figure 8.34(b) shows a slightly increased THD of 1.92. The THD increases to 2.15% in Figure 8.34(c), which would represent the highest distortion case of this investigation. The final case in Figure 8.34(d) shows a THD of 1.91%, the closest result to Figure 8.34(b), which indicates relatively balanced spectral characteristics with harmonics being controlled in its amplitudes. Overall, these results show that the proposed APOD-PWM method maintains distortion below 2.2% in all cases, which provides a high quality of output waveform for practical applications.

In the third case study, the voltage and current waveforms shown in Figures 8.30 and 8.31 were analyzed to evaluate the harmonic content of the converter, and the corresponding THD results are presented in Figures 8.33 and 8.34. The current waveform demonstrates a nearly sinusoidal profile, resulting in a low THD $< 2.2\%$ and confirming the effectiveness of the implemented control and modulation strategies in minimizing current harmonics. The voltage waveform, on the other hand, exhibits a stepped multilevel structure that naturally contains higher-frequency components due to the switching sequence of submodules. As a result, the voltage THD appears higher than the current THD, which is a typical and expected outcome for modular multilevel converters. This condition does not indicate any degradation in the overall power quality, since the multilevel synthesis process produces a smooth current waveform and stable power transfer characteristics for the proposed converter.

The FFT analyses were conducted at the fundamental frequency of 50 Hz, and the results, as shown in Figures 8.33 to 8.34, reveal that the THD values remain at significantly low levels. The fundamental frequency components of these signals are prominently observed at 50 Hz, indicating a strong presence of the desired frequency with minimal interference from higher-order harmonics. In power electronics systems, the THD parameter serves as a critical metric for evaluating the purity of signals, quantifying the relative strength of harmonic components deviating from the fundamental frequency. The low THD values obtained for these signals suggest that the waveforms are of high quality, exhibiting negligible distortion. These findings underscore the effectiveness of the proposed DC-DC MMC topology and the associated control strategy. The ability to maintain low THD levels in both voltage and current waveforms demonstrates the robustness of the design and its suitability for applications requiring precise power conversion and minimal harmonic interference. Consequently, the results validate the proposed architecture's operational success and control methodology, highlighting its potential for implementation in advanced power electronic systems.

These analyses, conducted using a fundamental grid frequency of 50 Hz, demonstrate the effective functionality of the proposed converter architecture. The FFT analyses were performed to evaluate the converter's ability to manage harmonic components and its overall performance in energy conversion processes. These findings provide strong evidence that the proposed DC-DC MMC architecture is capable of operating with high efficiency and stability in power transmission and distribution systems. Furthermore, implementing the APOD-PWM strategy has effectively minimized harmonic content while optimizing the system's dynamic responses. This is particularly significant for applications requiring seamless grid integration and high-power quality, as the converter demonstrates superior performance in these areas. In conclusion, this study validates the theoretical and practical viability of the proposed architecture, establishing a robust foundation for future research in this domain.

FFT studies of the simulated voltage and current waveforms were performed to evaluate the harmonic effectiveness of the suggested DC-DC MMC architecture in more detail. As is customary in HVDC converter investigations, the FFT spectrum was assessed up to the 39th harmonic order in each of the three cases examined. The findings, which are displayed in Figures 8.15-8.18 (PD-PWM), 8.25-8.26 (POD-PWM), and 8.33-8.34 (APOD-PWM), reveal that higher-order components above the 25th order continue to be below 1% of the fundamental, while low-order harmonics continue to be restricted. The overall current THD is regularly low for all modulation techniques: <2.0% for POD-PWM, <2.2% for APOD-PWM, and around 1.8-2.0% for PD-PWM. The suggested converter naturally reduces distortion components, as seen by the constrained harmonic spectrum, which eliminates the need for large external filters. The suggested design not only meets harmonic performance criteria but also offers a high-quality power conversion solution appropriate for real-world HVDC connectivity applications, as demonstrated by the combination of reduced THD, restricted ripple, and balanced capacitor voltages.

Figure 8.35(a) demonstrates the proposed DC-DC MMC's efficiency at various power levels. Efficiency increases steadily as operating points rise, according to the information provided. In Figure 8.35(b), the comparable loss behavior over time is depicted, with values progressively declining as the procedure goes on. A radar chart combining both parameters is displayed in Figure 8.35(c), which illustrates how they vary in tandem under the operational circumstances under study. According to these findings, the APOD-PWM modulation technique promotes reliable and efficient converter performance, especially at high power levels.

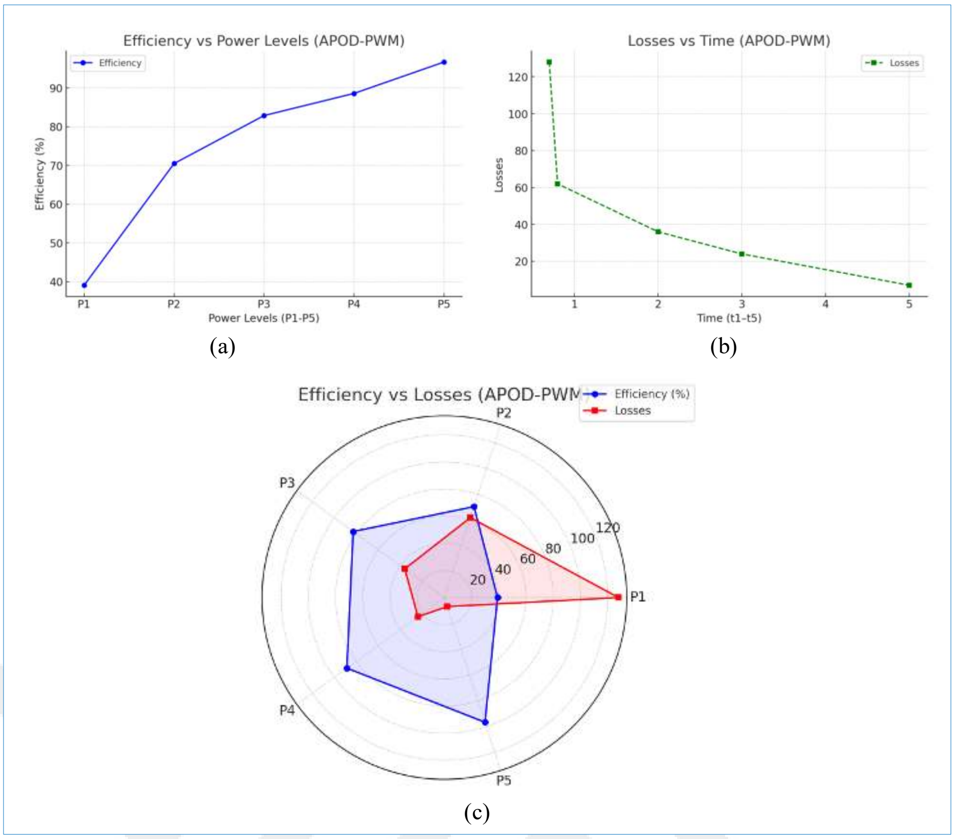

Figure 8. 35 The efficiency and losses waveforms of the proposed DC-DC MMC topology: (a) The efficiency waveform; (b) The losses waveform; (c) The efficiency and losses radar chart (APOD-PWM).

A crucial requirement for sophisticated power electronic systems is the capacity to transfer power in both directions, especially when grid-connected converters and renewable energy sources are involved. This section presents and examines simulation findings that demonstrate the proposed DC-DC MMC system's ability to flow power in both directions using three different PWM techniques: PD-PWM, POD-PWM, and APOD-PWM. Based on simulation diagrams showing power flow on both the primary and secondary sides under various operating circumstances, the study was carried out. The power flow diagrams of the left and right sides indicating the primary (high-voltage) and secondary (low-voltage) as well as the direction of power during forward and reverse operation modes are depicted in Figure 8.11, Figure 8.21, and Figure 8.29. Corresponding to the power profiles in all cases, the performance of the control system is highly efficient since the reference power commands are followed closely. The instantaneous change from primary side to secondary side and secondary side to primary side operation along with the minimal transient deviations observed at the mode-shifting instants is an indication for the stable dynamic behavior of the converter. In addition, similar results across the three PWM modulation methods provide a strong indication that the control strategies are capable of handling the bidirectional converter regardless of the PWM method used, thus representing broad applicability and the stability of the proposed control concept. The capacity for power flow in both directions of the proposed converter design has been checked beyond any doubt through the simulation results that were obtained applying APOD-PWM, POD-PWM, and PD-PWM modulation strategies. Figures 8.11, 8.21, and 8.29 show that the primary-side power follows the reference command very closely and reaches around 0.8-1.0 p.u. values for forward operation, respectively, when power is fed from the low-voltage side to the high-voltage side. In the APOD-PWM situation, the power is almost the reference with small oscillations; however, in the POD-PWM method, the measured and reference curves almost overlap, which is indicative of good tracking performance. The PD-PWM technique is the one that gives the closest result to the reference among all the cases demonstrating the best dynamic response. These findings show the proposed control system is capable of implementing the power accurately and keeping stable the bidirectional operation under various modulation strategies which is a prerequisite for applications like bidirectional chargers, vehicle-to-grid integration, and renewable energy systems.

Based on the results of the modeling procedure, this thesis study demonstrates the usefulness of the proposed DC-DC MMC design in linking HVDC power networks and its importance in ensuring successful electrical power transfer between these power networks. In the scope of this simulation-based research, an extensive control system has been built to allow the DC-DC MMC topology to fulfill its given role with high precision. To thoroughly evaluate the system, three case studies have been conducted, each relating to one of the three modulation methodologies examined in this work. The PD-PWM technique was used to achieve simulation results in the first case study. The performance of the converter under PD-PWM modulation is illustrated in Figures 8.8-8.14. While the corresponding currents are 780 A and 1040 A with ripple amplitudes of around 94 A and 102 A, respectively, the input and output voltages are closely monitored at 266 kV and 188 kV. The capacitor voltages are kept within ±3%, and the waveforms demonstrate steady and balanced functioning. During both forward and reverse transfer, power waveforms (Figure 8.11) show precise monitoring of reference values. Step shifts at 2.0 s and 3.14 s are followed by a quick transient recovery (<0.2 s). THD values for currents below 2% are confirmed by FFT analysis (Figures 8.15-8.18), confirming the converter's high-quality output performance.

The POD-PWM technique is used in the second case. The outcomes, which are displayed in Figures 8.20-8.27, attest to the suggested DC-DC MMC's ability to sustain steady power transfer and voltage control under this modulation approach. The reference is closely followed by the forward and reverse power flow waveforms (Figure 8.21), which exhibit high suppression of disturbances at 2.0 and 3.14 seconds. Figure 8.24 shows that the capacitor voltages are balanced within ±3%. The voltage THD values in the range of 13-19% and the current THD values below 2%, as shown by the FFT findings (Figures 8.25-8.26), are both within acceptable bounds for HVDC applications. As seen in Figure 8.27, efficiency is regularly above 96%, indicating strong performance.

The APOD-PWM approach is assessed in the third case. Consistent voltage and current patterns are shown throughout the converter arms in the simulation results (Figures 8.28-8.35), with the HBSM-based SM sets supplying five different voltage levels. Accurate bidirectional functioning with a steady dynamic response under perturbations is validated by the power transfer characteristics (Figure 8.29). While FFT tests (Figures 8.33–8.34) verify minimal harmonic distortion: current THD <2.2% across all SM sets, capacitor voltages (Figure 8.32) continue to be well balanced. As seen in Figure 8.35, efficiency increases with load and continuously exceeds 96%.

Several simulation situations outside of typical operating circumstances were examined in order to confirm the suggested DC-DC MMC topology's resilience. These situations include bidirectional (forward/reverse) power flow operation, fault circumstances, load fluctuation, and voltage sag occurrences. The outcomes demonstrate that the suggested converter continues to operate steadily, effectively, and dependably on a variety of real-world scenarios. The proposed converter controls voltages at 266 kV (primary) and 188 kV (secondary), with corresponding currents of 780 A and 1040 A, as seen by the primary and secondary waveforms (Figures 8.8-8.10). The primary side's ripple amplitude is around 94 A, whereas the secondary side's is approximately 102 A. Effective dynamic response is confirmed when step changes in powers, since power transfer tracks the new reference in around 0.5 seconds and current ripple stays below of rated values. The converter's robustness to voltage disturbance circumstances is illustrated by the transient occurrences shown in Figures 8.11, 8.21, and 8.29. Power waveforms precisely match the reference after a brief recovery of less than 200 ms when abrupt fluctuations take place at 2.0 s and 3.14 s. The suggested design maintains voltage stability and dependable power transfer even under sag-like operating circumstances, since overshoot is kept to less than 5% of rated transfer and capacitor voltages stay between ±2-5%. The converter's fault-handling capabilities are validated using step perturbations that simulate fault situations at 2.0 and 3.14 seconds. Power waveforms temporarily diverge during these occurrences but return to reference levels after 0.2 seconds. Currents stay below 3% of rated amplitude, and current waveforms don't exhibit any undue distortion. With capacitor voltages returned to within ±2-5% balance, post-disturbance functioning is steady, confirming the strength of the control and safety plan. Bidirectional functioning is expressly confirmed in Figures 8.11, 8.21, and 8.29. The converter converts 210 MW at 266 kV to 204 MW at 188 kV in forward operation (primary → secondary), and it exhibits about the same efficiency and precision for tracking in backwards operation (secondary → primary). Capacitor voltages are balanced within ±2-5%, efficiency is over 96% in both directions, and reference tracking error is less than 2%. Robustness for HVDC links is confirmed by the 0.5 s transition between forward and reverse power flow. These expanded case studies attest to the fact that the suggested non-isolated DC-DC MMC architecture not only performs well in ideal circumstances but also shows resilience in the face of actual operational difficulties. Its usefulness for large-scale HVDC interconnections and hybrid power network applications is established by its capacity to maintain steady power transmission despite load changes, voltage sags, and transient faults while guaranteeing dependable bidirectional operation.

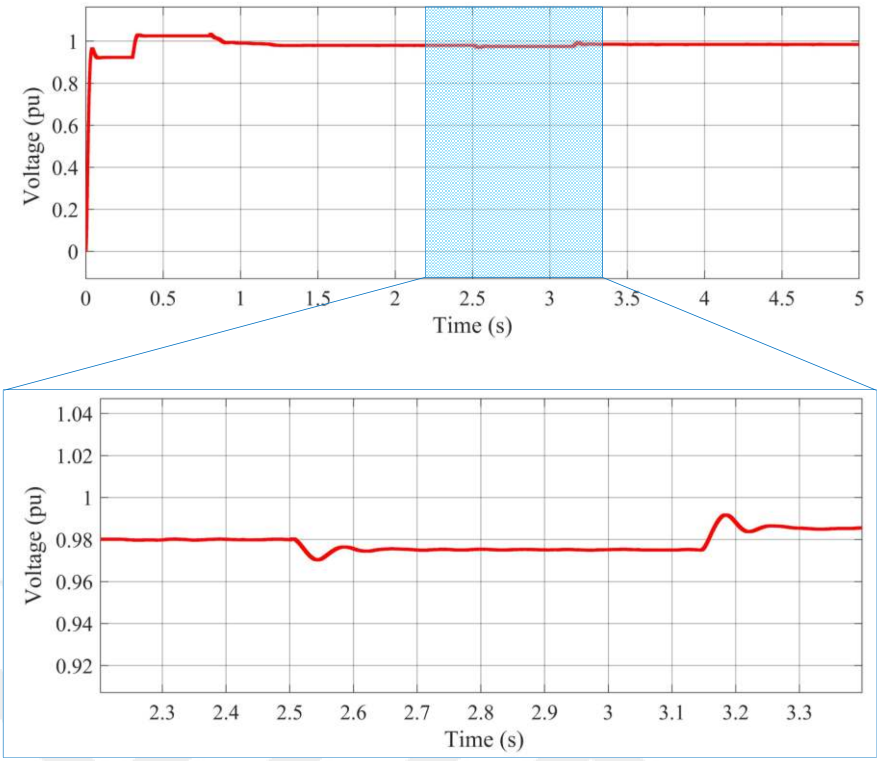

Figure 8. 36 Dynamic response of voltage under sudden variations

The dynamic response of the system to sudden variations in load is depicted in Figure 8.36. The suggested DC-DC MMC's voltage response under a load variation scenario is depicted in the provided figure. This scenario was created especially to evaluate the converter's dynamic stability and voltage regulation capabilities. The hatched area in the upper plot represents the step change in load that occurs when the system runs under nominal circumstances for around 2.5 seconds. In order to replicate an actual circumstance where the converter must instantly correct for a transitory disruption, this interval simulates a rapid load rise (also known as a voltage sag condition). A more detailed glance at the voltage waveform between 2.3 and 3.3 seconds is provided by the lower figure, which makes it easier to see the transient response features. The converter displays a transient voltage fluctuation of around 2-3% upon the applied load change, which is promptly followed by a quick return to normal voltage level. This illustrates the converter's strong control performance, especially its quick dynamic reaction and ability to regulate voltage effectively in the face of abrupt load fluctuations. System stability and seamless power transmission are ensured by the well-tuned internal current control and external voltage control loops, which are shown by the lack of persistent oscillations or overshoots. In conclusion, the simulation confirms that even in the presence of brief disruptions, the suggested DC–DC MMC design preserves voltage stability over time.

Figure 8.37 illustrates the circulating current waveforms of one arm string under three modulation strategies: (a) PD-PWM, (b) POD-PWM, and (c) APOD-PWM. In this study, the control and modulation approach was specifically designed to minimize the circulating current, thereby improving converter stability and efficiency. The results confirm that the proposed control successfully limits the arm circulating current to very small magnitudes. Although minor variations exist between modulation types, all three remain within a low-amplitude range, validating that the implemented circulating-current suppression control is effective. Overall, the measured results verify that the circulating current has been minimized in all modulation cases.

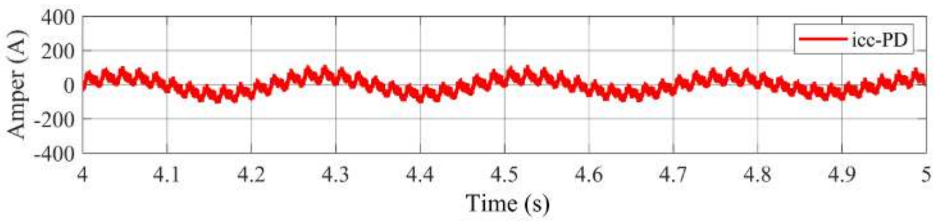

(a)

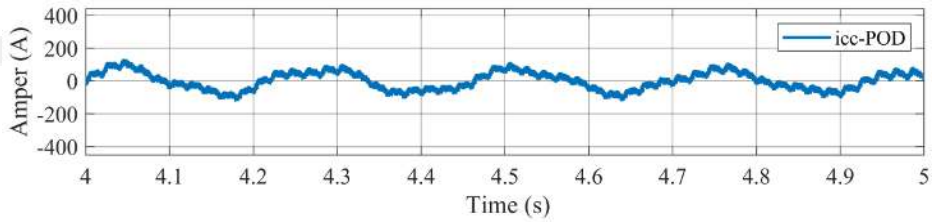

(b)

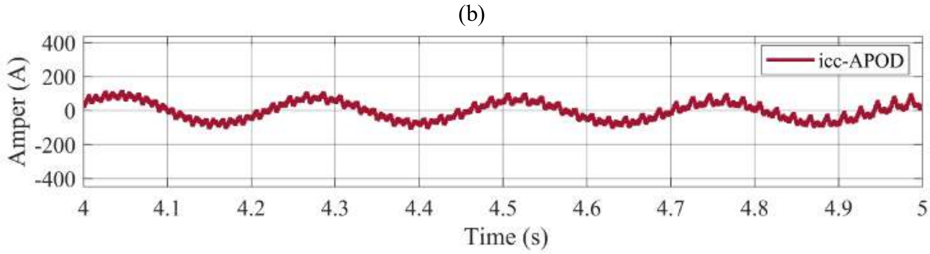

(c)

Figure 8. 37 Circulating currents for one arm string: (a) PD-PWM based, (b) POD-PWM based, (c) APOD-PWM based.

8.4 Quantitative Performance Evaluation

In the previous section, a general assessment regarding the performance evaluation of the proposed design was provided. In this section, this general assessment is further detailed by being more thoroughly examined and systematically organized. The quantitative performance of the proposed non-isolated DC-DC MMC topology has been thoroughly evaluated based on the simulation results obtained, including efficiency, harmonic distortion, ripple characteristics, voltage regulation, and overall system losses. The efficiency curves (Figures 8.19, 8.27, and 8.35) indicate that the efficiency of the converter is consistently above 96% through the operating range that has been tested, and maximum efficiency reaches approximately 97% at nominal load. Such performance is higher than isolated MMC-based DC-DC converters that typically remain in the range of 93-95%. Harmonic distortion assessments carried out on the simulated waveforms (Figures 8.15-8.18, 8.25-8.26, and 8.33-8.34) indicate that voltage THD is between 13% and 20%, based on the applied modulation scheme, while current THD was below 2.2%, indicating the quality of the waveforms produced by the proposed configuration. In addition, as described in the voltage and current waveforms (Figures 8.9-8.10), the amount of ripple was small, relative to the rated values, with the primary and secondary side voltage ripple in the range of 410 V and 448 V, respectively. The primary and secondary side current ripple was approximately 127 A and 260 A, respectively. The balancing performance of the SM capacitors demonstrates that for all operational scenarios, the voltage shifts are controlled within the range of ±2 to 5% and the voltage levels are tightly controlled, as illustrated in Figures 8.14, 8.24, and 8.32. When assessing the power losses from the simulations for the nominal load value, as illustrated in Figures 8.19(b), 8.27(b), and 8.35(b), the power losses are under 3% of the rated transferred power, primarily from semiconductor conduction and switching. All of the above indicate the low distortion, voltage-controlled, and loss performance efficiency of the system. This also indicates the suggested converter is qualified for reliable and extensive interconnections within the HVDC transmission framework.

Table 8.3 provides a comparative overview of PD-PWM, POD-PWM, and APOD-PWM strategies across important performance indices such as harmonic distortion, ripple levels, capacitor-voltage balance, efficiency, system losses, dynamic response, and power quality in order to synthesize the results of the three case studies.

Table 8. 3 Comparative Performance of PWM Strategies

Metric	PD-PWM (Case 1)	POD-PWM (Case 2)	APOD-PWM (Case 3)
Current THD (%)	1.8–2.0	<2.0	<2.2
Voltage THD (%)	13–18	13–19	14–20
Output voltage ripple	~448 V	~454 V	~451 V
Capacitor-voltage deviation	±2–5%	±2–5%	±2–5%
Efficiency (%)	96.5–97	≥96	≥96
System losses (% rated power)	~2.5	~3.0	~3.0
Transient recovery time	<0.2 s	<0.2 s	<0.2 s

The comparison findings demonstrate that all three modulation techniques provide incredibly dependable and effective performance. POD-PWM and APOD-PWM show similarly good ripple suppression and transient dynamics, but PD-PWM offers somewhat lower current THD (≈1.8%) and modestly decreased losses. In every scenario, the converter keeps the power factor close to unity, efficiency above 96%, transient recovery within 0.2 s, and capacitor-voltage balance under ±5%. These reliable results demonstrate that the suggested DC–DC MMC architecture is resilient to modulation selection and ensures outstanding dynamic stability, reduced ripple, and enhanced harmonic performance. This consistency across various PWM schemes not only confirms the suggested design's efficacy but also shows how flexible and adaptable it is to various control contexts, confirming its appropriateness for real-world HVDC interconnection and multi-terminal applications. Figure 8.36 presents efficiency and loss comparisons according to different PWM techniques used in the proposed control system. Figure 8.38 presents efficiency and loss comparisons based on different PWM techniques used.

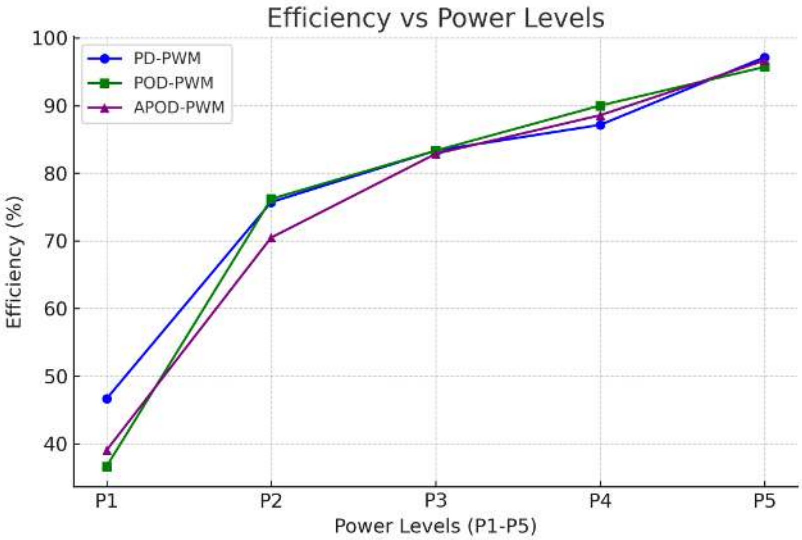

(a)

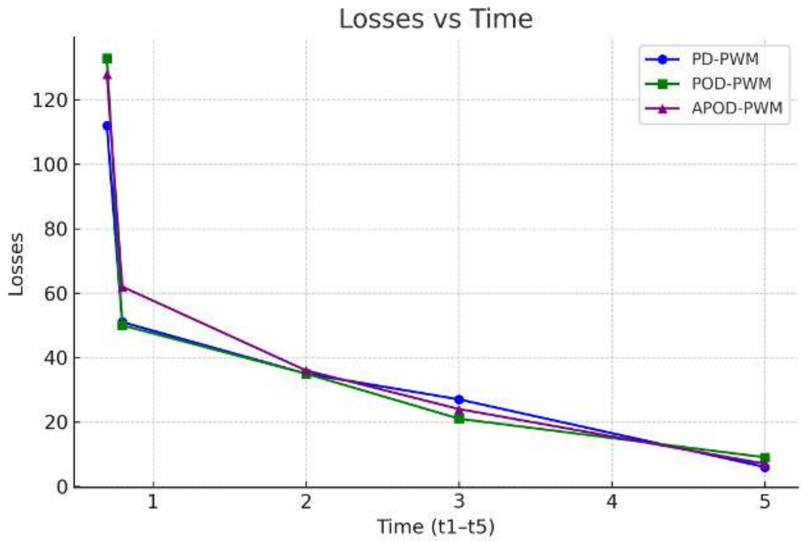

(b)

Figure 8. 38 Efficiency and loss comparisons based on different PWM techniques used.

8.5 Comparison with Existing Architectures

Comparing the suggested non-isolated DC-DC MMC topology especially to other DC-DC MMC topologies that have been documented in the literature reveals critical advantages. DC-DC MMC designs generally developed based on the traditional MMC design can generally be designed in two different ways: isolated and non-isolated. Isolated DC–DC MMCs offer adjustable voltage step-up or step-down capabilities and galvanic isolation by integrating high-frequency transformers between the primary and secondary converter sections. Nevertheless, the much greater structural bulk, electromagnetic losses, and higher circuit structure of such structures are intrinsic drawbacks. Efficiency and power density are reduced by the transformer and related magnetic components, which also create leakage inductance, insulation problems, and extra parasitic losses. These drawbacks are eliminated by developing this study in a transformerless framework. The suggested designs typically have one, two, or three legs; the more legs and the more SMs and other devices used, the higher the volume, weight, and cost of the developed designs; however, the modular structure and quantity of SMs used in this design promise that the design has a desirable volume, weight, and cost. Comparisons between certain designs from the literature and the suggested topology are shown in Table 1.1 in Chapter I and Table 7.1 in Chapter 7. The proposed transformerless architecture, requiring only 48 SMs, significantly distinguishes itself within literature as the topology with the lowest component count. This is particularly notable when contrasted with established configurations that necessitate hundreds of SMs, heavy-duty HV transformers, and complex, high-cost filter structures. Compared to existing models in the literature that utilize between 300 and 1600 SMs (e.g., 146 HBSMs, 680 HBSMs, or up to 1600 FBSMs), this design offers clear and substantial structural efficiency, leading to a dramatic reduction in both overall system cost and physical footprint. This substantial reduction in hardware not only minimizes converter size and weight but also decreases conduction paths, lowers switching stress, reduces control complexity, and diminishes installation and maintenance costs. From an efficiency perspective, isolated MMC converters typically operate within the 93–95% range, exhibiting power losses between 3% and 6%, whereas the proposed design consistently achieves efficiencies at or above 96% with total losses kept below 3%. Moreover, the capacitor voltage ripple has been limited to ±5% in the proposed converter, indicating improved energy balancing among SMs and enhanced system stability. Notably, the proposed converter attains low output ripple and low THD levels without resorting to the extremely high SM counts observed in other high-quality output designs, thereby achieving a more favorable trade-off between performance and hardware complexity. The transformer component is entirely eliminated in the suggested non-isolated DC–DC MMC while maintaining the MMC framework's scalability and modularity. Because of this architectural simplicity, there are fewer switches overall and a substantial reduction in gate-driver circuitry, which improves reliability, decreases control labor, and reduces system costs.

Furthermore, the suggested converter accomplishes a reduced size and lower overall weight than its isolated equivalents by doing away with large magnetic components and high-frequency transformer windings. Power density and thermal management, which are crucial in high-power and medium-voltage DC applications, are significantly improved by these physical advantages. Due to the lack of magnetic core losses and extra switching transitions brought on by transformer excitation, the suggested topology outperforms standalone DC–DC MMCs in terms of efficiency, achieving an efficiency exceeding 96%. All things considered, the suggested non-isolated configuration strikes the ideal mix between simplicity, scalability, and performance in the field of DC-DC MMC architectures, offering a small, affordable, and highly effective substitute for conventional transformer-based MMC systems.

8.6 Summary

This chapter examines the fundamental operational concepts of the proposed novel non-isolated DC-DC MMC architecture and provides a simulation-based assessment of performance. In this phase, a thorough simulation study is carried out to assess the topology's feasibility, efficacy, and productivity throughout different circumstances of operation. An efficient power transfer between two power grids of different voltage levels is achieved by designing an innovative control system specific to the proposed innovative converter design. PWM techniques, which are the main elements of the power transfer control system, were changed and realized for three different scenarios. The characteristic behavior of the proposed converter design for different switching states using PD-PWM, POD-PWM, and APOD-PWM techniques is investigated. In all three PWM tests, similar results and behaviors were observed. This shows that the proposed converter design and the related control system exhibit a stable characteristic. The analysis focuses on key parameters such as dynamic adaptability, entire system effectiveness, current circulation, and voltage control. This section examines potential improvements in voltage equilibrium, power loss removal, and other operational problems often encountered by traditional converter systems. The outcomes of these simulations are expected to provide valuable insights for enhancing the functionality and design of the suggested DC-DC MMC topology, promoting more reliable, viable, and effective power conversion techniques. The efficiency of the proposed converter design is evaluated by performing THD analysis for the input and output voltages and currents of the system and for the voltages and currents of some SM sets. One of the key features of the proposed DC-DC MMC architecture is its ability to generate low THD levels, ensuring excellent power efficiency. Harmonic distortion is decreased by the modular architecture's assistance in smoothing the output voltage. By carefully lowering the number of modules and using advanced modulation techniques, the THD levels are reduced, ensuring that the converter functions correctly and doesn't significantly increase the system's harmonic content. In summary, the DC–DC MMC has a good balance of fast operation and high efficiency. It can transfer power in less than 0.5 s, recover from disturbances in less than 200 ms, and has an efficiency of 96% when lightly loaded. These results show that it can work well in big HVDC systems that need quick response times and high energy efficiency.

CHAPTER IX
CONCLUSIONS

9.1 Summary of Contributions

A revolutionary DC-DC MMC design is presented in this study to interconnect power networks with different voltage levels. Compared to the existing DC-DC MMC configurations in the literature, the proposed DC-DC MMC design provides many innovations, remarkable achievements, and enhancements. First, a novel topology has been designed for the proposed DC-DC MMC architecture. The novel architecture that has been suggested is crucial for integrating modern HVDC power systems with already existing HVAC power systems as well as interconnecting asynchronous revolutionary HVDC power grids. With its symmetrical and modular structure, the novel design that has been suggested can achieve optimum efficiency in bi-directional power transmission across power grids. The converter's volume, weight, cost, and power losses have been considerably reduced since the suggested topology has been developed thanks to a transformerless and compact methodology. An efficiency examination and loss model have been used to observe that the recommended DC-DC architecture successfully achieves bi-directional power transfer. Even though DC-DC converter systems have losses from capacitors, inductors, switching, power transmission, etc., the proposed design provides bi-directional power transfer with high efficiency and low losses in comparison to conventional MMC designs because it settles on minimal SM structures (HBSM), utilizes a successful PWM technique, has a symmetrical and compact structure, and has an innovative control system. Whereas the majority of DC-DC MMC configurations in the literature offer solely DC-DC MMC analysis, the present investigation offers a significant analysis for both the integration of two asynchronous power systems that can occur in real life and the DC-DC MMC analysis of the recommended DC-DC MMC topology. According to the simulation data acquired, the control mechanism and architecture with such revolutionary flexibility, highly controllable capability, and unique characteristics have enabled the optimization of two asynchronous power networks to be accomplished effectively. The design's functioning concept, mathematical analysis, simulation analysis, FFT analysis, and detailed architectural structure have all been skillfully conveyed. Although it is a power electronics-based design, it is clear that it exhibits effective performance according to the simulation results and FFT analysis. With its adaptable multiset construction, the suggested DC-DC MMC can scale up to very high-power levels, requiring no need for any transformer. Transformers at the primary and secondary ports, passive components, and sophisticated filtering mechanisms are all eliminated in non-isolated converter topologies such as the suggested DC-DC MMC architecture. In addition to achieving outstanding conversion rates utilizing reduced semiconductor devices and small-scale passive components, this drastically decreases the volume and size of converter topologies. The suggested transformerless converter design provides an opportunity to reduce switching losses and prevent the issues experienced while constructing transformers, thus minimizing system volume and expense. Undoubtedly, nonetheless, as compared to isolated DC-DC MMC topologies, the suggested DC-DC MMC architecture has shortcomings such as the absence of electrical isolation between the primary and secondary side of the systems, limitations in secondary voltage adaptation, difficulty customizing to more considerable power demands, greater secondary side voltage the presence of harmonics, and sophisticated controller processes. With its unique architectural structure and effective control mechanism, the suggested DC-DC MMC topology significantly reduces these shortcomings. The suggested converter exhibits several characteristics, including a straightforward circuit design, innovative structure, acceptable swift dynamic reaction, controllability, bi-directional power flow, and customizable operation, as observed from the simulation outcomes. Time-domain simulation analyses carried out in the simulation environment confirmed the assessment that has been presented. The simulation analysis results confirm the suggested non-isolated DC-DC MMC and associated customized control arrangement's viability, efficiency, and functionality.

9.2 Future Trends

HVDC technologies are becoming increasingly important in today's shifting power circumstances, which are being propelled by the expanding demand for long-distance power transmission and the growing incorporation of renewable power sources. In this context, DC-DC MMCs present promising solutions for voltage level conversion, power flow control, and grid flexibility, particularly within MTDC systems. However, as a relatively nascent technology, DC-DC MMCs still face numerous challenges in both hardware design and control strategies, pointing to critical research gaps. Future developments in this field are expected to involve the integration of wide bandgap semiconductor devices such as SiC and GaN, enabling higher switching frequencies and lower losses. Moreover, the adoption of hybrid converter topologies, multi-port architectures, and direct integration of energy storage systems will provide increased flexibility and functionality in converter design. On the control side, the use of artificial intelligence-based algorithms, MPC, and distributed control architectures is anticipated to enhance real-time responsiveness and fault tolerance. Despite these advances, challenges related to system protection, fault detection, and recovery remain insufficiently addressed due to the inherent complexity of modular architecture. Key research gaps also include the lack of standardized design and testing methodologies, cost and complexity issues associated with large-scale implementation, limited interoperability with hybrid AC-DC networks, and scarcity of long-term operational data. Therefore, to enable the widespread and secure deployment of DC-DC MMCs in HVDC systems, it is essential to promote interdisciplinary research, develop digital twin and cyber-physical monitoring frameworks, and adopt advanced, integrated approaches to control and protection.

REFERENCES

[1] G. J. Kish, *A new class of modular multilevel DC/DC converters for HVDC systems*. University of Toronto (Canada), 2016.

[2] X. Xiang, "The modular multilevel DC converters for MVDC and HVDC applications," 2018.

[3] R. Razani and Y. A.-R. I. Mohamed, "Model Predictive Control of Non-Isolated DC/DC Modular Multilevel Converter Improving the Dynamic Response," *IEEE Open J. Power Electron.*, vol. 3, no. May, pp. 303–316, 2022, doi: 10.1109/OJPEL.2022.3176833.

[4] G. J. Kish, "On the Emerging Class of Non-Isolated Modular Multilevel DC–DC Converters for DC and Hybrid AC–DC Systems," *IEEE Trans. Smart Grid*, vol. 10, no. 2, pp. 1762–1771, Mar. 2019, doi: 10.1109/TSG.2017.2777473.

[5] M. A. Zama, "Modeling and control of modular multilevel converters (MMCs) for HVDC applications." Université Grenoble Alpes, 2017.

[6] M. Mehrabankhomartash, S. Yin, R. P. Kandula, D. Divan, and M. Saeedifard, "Analysis and Design Guidelines of the Isolated Modular Multilevel DC-DC Converter With the Impact of Magnetizing Inductance," *IEEE Trans. Ind. Electron.*, 2023.

[7] S. Kamakshaiah and V. Kamaraju, *HVDC transmission*. TATA McGraw-Hill, 2011.

[8] A. Alassi, S. Bañales, O. Ellabban, G. Adam, and C. MacIver, "HVDC transmission: Technology review, market trends and future outlook," *Renew. Sustain. Energy Rev.*, vol. 112, pp. 530–554, 2019.

[9] R. Ryndzionek and Ł. Sienkiewicz, "Evolution of the HVDC link connecting offshore wind farms to onshore power systems," *Energies*, vol. 13, no. 8, p. 1914, 2020.

[10] M. Cheah-Mane, J. Arevalo-Soler, E. Prieto-Araujo, and O. Gomis-Bellmunt, "Energy-based control of a DC modular multilevel converter for HVDC grids," *IEEE Trans. Power Deliv.*, vol. 35, no. 4, pp. 1823–1833, 2019.

[11] F. Qin, T. Hao, F. Gao, T. Xu, D. Niu, and Z. Ma, "A Multiport DC-DC Modular Multilevel Converter for HVDC Interconnection," in *2020 IEEE Applied Power*

Electronics Conference and Exposition (APEC), 2020, pp. 520–524. doi: 10.1109/APEC39645.2020.9124277.

[12] D. G. Acero, M. Cheah-Mane, J. D. Páez, F. Morel, O. Gomis-Bellmunt, and P. Dworakowski, “Dc-MMC for the interconnection of HVDC grids with different line topologies,” *IEEE Trans. Power Deliv.*, vol. 37, no. 3, pp. 1692–1703, 2021.

[13] S. Dey and T. Bhattacharya, “A Transformerless DC–DC Modular Multilevel Converter for Hybrid Interconnections in HVDC,” *IEEE Trans. Ind. Electron.*, vol. 68, no. 7, pp. 5527–5536, Jul. 2021, doi: 10.1109/TIE.2020.2994889.

[14] S. Song, R. A. McCann, and G. Jang, “Cost-Based Adaptive Droop Control Strategy for VSC-MTDC system,” *IEEE Trans. Power Syst.*, vol. 36, no. 1, pp. 659–669, Jan. 2021, doi: 10.1109/TPWRS.2020.3003589.

[15] R. H. Chandio *et al.*, “Control and protection of MMC-based HVDC systems: A review,” *Energy Reports*, vol. 9, pp. 1571–1588, 2023, doi: https://doi.org/10.1016/j.egyr.2022.12.056.

[16] R. Marquardt, “Stromrichterschaltungen mit verteilten energiespeichern,” *Ger. Pat. DE10103031A1*, vol. 24, p. 40, 2001.

[17] D. Ronanki and S. S. Williamson, “Modular Multilevel Converters for Transportation Electrification: Challenges and Opportunities,” *IEEE Trans. Transp. Electrif.*, vol. 4, no. 2, pp. 399–407, Jun. 2018, doi: 10.1109/TTE.2018.2792330.

[18] A. Dekka, B. Wu, R. L. Fuentes, M. Perez, and N. R. Zargari, “Evolution of Topologies, Modeling, Control Schemes, and Applications of Modular Multilevel Converters,” *IEEE J. Emerg. Sel. Top. Power Electron.*, vol. 5, no. 4, pp. 1631–1656, Dec. 2017, doi: 10.1109/JESTPE.2017.2742938.

[19] R. Razani and Y. A. I. Mohamed, “Operation Limits of the Hybrid DC/DC Modular Multilevel Converter for HVdc Grids Connections,” *IEEE J. Emerg. Sel. Top. Power Electron.*, vol. 9, no. 4, pp. 4459–4469, Aug. 2021, doi: 10.1109/JESTPE.2020.3017206.

[20] A. Lesnicar and R. Marquardt, “An innovative modular multilevel converter topology suitable for a wide power range,” in *2003 IEEE Bologna Power Tech Conference Proceedings,* 2003, vol. 3, pp. 6-pp.

[21] B. Xia *et al.*, “A modular multilevel DC/DC converter interconnecting HVDC systems,” in *IECON 2017 - 43rd Annual Conference of the IEEE Industrial*

Electronics Society, 2017, pp. 4477–4481. doi: 10.1109/IECON.2017.8216771.

[22] S. Du, B. Wu, D. Xu, and N. R. Zargari, "A Transformerless Bipolar Multistring DC–DC Converter Based on Series-Connected Modules," *IEEE Trans. Power Electron.*, vol. 32, no. 2, pp. 1006–1017, 2017, doi: 10.1109/TPEL.2016.2553450.

[23] G. Ning, B. Dai, M. Su, L. Shu, and W. Xiong, "Interleaved Buck-Integrated Modular Multilevel DC Transformer with Wide Voltage Range for DC Distribution Grids," *IEEE Trans. Power Electron.*, 2024.

[24] S. Du, B. Wu, and N. R. Zargari, "A Transformerless High-Voltage DC–DC Converter for DC Grid Interconnection," *IEEE Trans. Power Deliv.*, vol. 33, no. 1, pp. 282–290, 2018, doi: 10.1109/TPWRD.2017.2692480.

[25] Z. Lin *et al.*, "Small-signal stability analysis and design of the control system for modular multilevel DC-DC converter," *CSEE J. Power Energy Syst.*, pp. 1–12, 2025, doi: 10.17775/CSEEJPES.2024.07820.

[26] M. Ashraf, Y. Nazih, F. Alsokhiry, K. H. Ahmed, A. S. Abdel-Khalik, and Y. Al-Turki, "A New Hybrid Dual Active Bridge Modular Multilevel Based DC–DC Converter for HVDC Networks," *IEEE Access*, vol. 9, pp. 62055–62073, 2021, doi: 10.1109/ACCESS.2021.3074543.

[27] S. Sarkar and A. Das, "An Isolated Single Input-Multiple Output DC–DC Modular Multilevel Converter for Fast Electric Vehicle Charging," *IEEE J. Emerg. Sel. Top. Ind. Electron.*, vol. 4, no. 1, pp. 178–187, 2023, doi: 10.1109/JESTIE.2022.3221006.

[28] J. Lai, X. Yin, Y. Wang, L. Jiang, Z. Ullah, and X. Yin, "Isolated Bipolar Modular Multilevel DC-DC Converter with Self-balancing Capability for Interconnection of MVDC and LVDC Grids," *CSEE J. Power Energy Syst.*, vol. 9, no. 1, pp. 365–379, 2023, doi: 10.17775/CSEEJPES.2022.05460.

[29] G. Sha *et al.*, "Research on Multi-Port DC-DC Converter Based on Modular Multilevel Converter and Cascaded H Bridges for MVDC Applications," *IEEE Access*, vol. 9, pp. 95006–95022, 2021, doi: 10.1109/ACCESS.2021.3072161.

[30] Q. Zhou *et al.*, "A Step-Down Resonant Modular Multilevel DC/DC Converter With Extendable ZVS Range Based on Asymmetric Triangular Current," *IEEE Trans. Ind. Electron.*, vol. 69, no. 11, pp. 11088–11099, 2022, doi: 10.1109/TIE.2021.3125668.

[31] S. Dey and T. Bhattacharya, "A Hybrid Modular DC-DC Converter Topology

for Hybrid Interlink in HVDC," in *2021 IEEE Applied Power Electronics Conference and Exposition (APEC)*, Jun. 2021, pp. 1681–1687. doi: 10.1109/APEC42165.2021.9487421.

[32] D. G. Acero, M. Cheah-Mane, J. D. Paez, F. Morel, O. Gomis-Bellmunt, and P. Dworakowski, "Dc-MMC for the Interconnection of HVDC Grids With Different Line Topologies," *IEEE Trans. Power Deliv.*, vol. 37, no. 3, pp. 1692–1703, Jun. 2022, doi: 10.1109/TPWRD.2021.3095966.

[33] A. Elserougi, I. Abdelsalam, and A. Massoud, "A hybrid half-bridge submodule-based DC–DC modular multilevel converter with a single bidirectional high-voltage valve," *IET Gener. Transm. Distrib.*, vol. 17, no. 18, pp. 4146–4160, 2023.

[34] S. Zhao, Y. Chen, S. Cui, and J. Hu, "Modular multilevel DC-DC converter with inherent bipolar operation capability for resilient bipolar MVDC grids," *CPSS Trans. Power Electron. Appl.*, vol. 7, no. 1, pp. 37–48, 2022.

[35] X. Du, Y. Li, Z. Zhang, Z. Lin, and K. Ji, "Control Strategy and Main Parameter Design for Three-Phase Modular Multilevel DC-DC Transformer," in *2025 10th Asia Conference on Power and Electrical Engineering (ACPEE)*, 2025, pp. 835–841. doi: 10.1109/ACPEE64358.2025.11040943.

[36] X. He, J. Peng, P. Han, Z. Liu, S. Gao, and P. Wang, "A Novel Advanced Traction Power Supply System Based on Modular Multilevel Converter," *IEEE Access*, vol. 7, pp. 165018–165028, 2019, doi: 10.1109/ACCESS.2019.2949099.

[37] Y. N. Vijaykumar, V. Vemulapati, N. Visali, and K. Raju, "Railway Power Supply System using Modular Multilevel Converter with Droop Characteristics," in *2020 4th International Conference on Electronics, Communication and Aerospace Technology (ICECA)*, 2020, pp. 12–20. doi: 10.1109/ICECA49313.2020.9297599.

[38] V. Spudić and T. Geyer, "Model Predictive Control Based on Optimized Pulse Patterns for Modular Multilevel Converter STATCOM," *IEEE Trans. Ind. Appl.*, vol. 55, no. 6, pp. 6137–6149, 2019, doi: 10.1109/TIA.2019.2936797.

[39] Y. Jin *et al.*, "A Dual-Layer Back-Stepping Control Method for Lyapunov Stability in Modular Multilevel Converter Based STATCOM," *IEEE Trans. Ind. Electron.*, vol. 69, no. 3, pp. 2166–2179, 2022, doi: 10.1109/TIE.2021.3063973.

[40] Y. Pan, X. Sun, W. Zhao, X. Li, and Y. Cai, "Research on limits of uneven battery power in modular multilevel converter-based battery energy storage system," *CSEE J. Power Energy Syst.*, pp. 1–10, 2022, doi: 10.17775/CSEEJPES.2021.01510.

[41] K. Panuganti, R. S. Burye, and S. Figarado, "Variable Slope Trapezoidal Circulating Current Injection to Attenuate Capacitor Voltage Ripple in Modular Multilevel Converter Based Variable Speed Motor Drives Application," in *2022 IEEE International Conference on Industrial Technology (ICIT)*, 2022, pp. 1–6. doi: 10.1109/ICIT48603.2022.10002780.

[42] M. A. Tawfik, M. S. Irfan, C. Lee, A. Ahmed, and J.-H. Park, "Capacitor-less modular multilevel converter with sliding mode control for MV adjustable-speed motor drives," *J. Power Electron.*, vol. 22, no. 8, pp. 1265–1278, 2022, doi: 10.1007/s43236-022-00484-0.

[43] G. Jia, M. Chen, S. Tang, C. Zhang, and B. Zhao, "A Modular Multilevel Converter With Active Power Filter for Submodule Capacitor Voltage Ripples and Power Losses Reduction," *IEEE Trans. Power Electron.*, vol. 35, no. 11, pp. 11401–11417, Nov. 2020, doi: 10.1109/TPEL.2020.2982440.

[44] M. O. Badawy, M. Sharma, C. Hernandez, A. Elrayyah, S. Guerra, and J. Coe, "Model Predictive Control for Multi-Port Modular Multilevel Converters in Electric Vehicles Enabling HESDs," *IEEE Trans. Energy Convers.*, vol. 37, no. 1, pp. 10–23, 2022, doi: 10.1109/TEC.2021.3089668.

[45] S. Haq, S. P. Biswas, M. K. Hosain, M. A. Rahman, M. R. Islam, and S. Jahan, "A Modular Multilevel Converter with an Advanced PWM Control Technique for Grid-Tied Photovoltaic System," *Energies*, vol. 14, no. 2, p. 331, Jan. 2021, doi: 10.3390/en14020331.

[46] S. Khanal and V. Disfani, "Modular Multilevel Converter Design for Grid Integration of Solar Photovoltaic Systems," in *2020 IEEE Power & Energy Society General Meeting (PESGM)*, Aug. 2020, pp. 1–5. doi: 10.1109/PESGM41954.2020.9281607.

[47] H. Yang, M. Saeedifard, and A. Yazdani, "An Enhanced Closed-Loop Control Strategy With Capacitor Voltage Elevation for the DC–DC Modular Multilevel Converter," *IEEE Trans. Ind. Electron.*, vol. 66, no. 3, pp. 2366–2375, Mar. 2019, doi: 10.1109/TIE.2018.2850035.

[48] R. Razani and Y. Mohamed, "Augmented Design of DC/DC Modular

Multilevel Converter Improving Efficiency and Reducing Number of SMs," *IEEE Trans. Power Deliv.*, vol. 35, no. 6, pp. 1–1, 2020, doi: 10.1109/TPWRD.2020.2991894.

[49] R. Razani and Y. A.-R. I. Mohamed, "Fault-Tolerant Operation of the DC/DC Modular Multilevel Converter Under Submodule Failure," *IEEE J. Emerg. Sel. Top. Power Electron.*, vol. 9, no. 5, pp. 6139–6151, Oct. 2021, doi: 10.1109/JESTPE.2021.3050122.

[50] S. Dey and T. Bhattacharya, "A Transformerless DC–DC Modular Multilevel Converter for Hybrid Interconnections in HVDC," *IEEE Trans. Ind. Electron.*, vol. 68, no. 7, pp. 5527–5536, 2021, doi: 10.1109/TIE.2020.2994889.

[51] S. Kaler and A. Yazdani, "Modeling and Current-Mode Control of a DC–DC Modular Multilevel Converter," *IEEE Trans. Ind. Electron.*, vol. 68, no. 11, pp. 10826–10834, Nov. 2021, doi: 10.1109/TIE.2020.3034857.

[52] F. Gruson, Y. Li, P. Le Moigne, P. Delarue, F. Colas, and X. Guillaud, "Full State Regulation of the Modular Multilevel DC Converter (M2DC) Achieving Minimization of Circulating Currents," *IEEE Trans. Power Deliv.*, vol. 35, no. 1, pp. 301–309, Feb. 2020, doi: 10.1109/TPWRD.2019.2942527.

[53] M. Cheah-Mane, J. Arevalo-Soler, E. Prieto-Araujo, and O. Gomis-Bellmunt, "Energy-Based Control of a DC Modular Multilevel Converter for HVDC Grids," *IEEE Trans. Power Deliv.*, vol. 35, no. 4, pp. 1823–1833, Aug. 2020, doi: 10.1109/TPWRD.2019.2955007.

[54] J. D. Paez, F. Morel, S. Bacha, P. Dworakowski, and D. Frey, "Impact of DC fault blocking capability on the sizing of the DC-DC Modular Multilevel Converter," in *2020 22nd European Conference on Power Electronics and Applications (EPE'20 ECCE Europe)*, Sep. 2020, pp. 1–10. doi: 10.23919/EPE20ECCEEurope43536.2020.9215938.

[55] S. H. Kung and G. J. Kish, "Multiport Modular Multilevel Converter for DC Systems," *IEEE Trans. Power Deliv.*, vol. 34, no. 1, pp. 73–83, Feb. 2019, doi: 10.1109/TPWRD.2018.2846264.

[56] R. Mo, H. Li, and Y. Shi, "A Phase-Shifted Square Wave Modulation (PS-SWM) for Modular Multilevel Converter (MMC) and DC Transformer for Medium Voltage Applications," *IEEE Trans. Power Electron.*, vol. 34, no. 7, pp. 6004–6008, Jul. 2019, doi: 10.1109/TPEL.2018.2885278.

[57] X. Zhu, L. Jiang, B. Zhang, and K. Jin, "The Resonant Modular Multilevel DC–

DC Converter Adopting Switched-Inductor Cells for High Step-Up Ratio," *IEEE J. Emerg. Sel. Top. Power Electron.*, vol. 10, no. 6, pp. 6634–6647, Dec. 2022, doi: 10.1109/JESTPE.2022.3157618.

[58] F. Gruson, A. Tlemcani, Y. Li, P. Delarue, P. Le Moigne, and X. Guillaud, "Model and control of the DC–DC modular multilevel converter with DC fault tolerance," *EPE J.*, vol. 30, no. 4, pp. 153–164, Oct. 2020, doi: 10.1080/09398368.2020.1750847.

[59] P. A. Gray, P. W. Lehn, and N. Yakop, "A Modular Multilevel DC–DC Converter With Flying Capacitor Converter Like Properties," *IEEE Trans. Ind. Electron.*, vol. 69, no. 7, pp. 6774–6783, Jul. 2022, doi: 10.1109/TIE.2021.3099229.

[60] C. Pineda, J. Pereda, F. Rojas, G. Droguett, C. Burgos-Mellado, and A. J. Watson, "Optimal ZCS Modulation for Bidirectional High-Step-Ratio Modular Multilevel DC–DC Converter," *IEEE Trans. Power Electron.*, vol. 36, no. 11, pp. 12540–12550, Nov. 2021, doi: 10.1109/TPEL.2021.3078235.

[61] H. Saeedifard and A. Yazdani, "Modeling and Soft-Switching Operation of an Isolated Modular-Multilevel-Converter-Based DC-DC Converter," in *2022 IEEE Energy Conversion Congress and Exposition (ECCE)*, Oct. 2022, pp. 1–8. doi: 10.1109/ECCE50734.2022.9947871.

[62] S. M. Akbar, A. Hasan, A. Watson, P. Wheeler, and S. Odhano, "Finite Control Set Model Predictive Control of Isolated DC/DC Modular Multilevel Converter," in *IECON 2020 The 46th Annual Conference of the IEEE Industrial Electronics Society*, Oct. 2020, pp. 5282–5289. doi: 10.1109/IECON43393.2020.9254434.

[63] Z. Tian and F. Zhang, "A Hybrid Modular Multilevel DC-DC Converter with Minimized Circulating Current," in *2022 IEEE 5th International Electrical and Energy Conference (CIEEC)*, May 2022, pp. 4804–4810. doi: 10.1109/CIEEC54735.2022.9846155.

[64] S. Khattri and Y. Pal, "Modular Multilevel Dc Converter with Square Wave Phase Shift PWM," in *2022 1st International Conference on Sustainable Technology for Power and Energy Systems (STPES)*, Jul. 2022, pp. 1–4. doi: 10.1109/STPES54845.2022.10006616.

[65] M. Huang, "A Non-Isolated DC-DC Modular Multilevel Converter with Proposed Middle Cells," *Electronics*, vol. 11, no. 7, p. 1135, Apr. 2022, doi:

10.3390/electronics11071135.
[66] X. Xiang, X. Zhang, T. Luth, M. M. C. Merlin, and T. C. Green, "A Compact Modular Multilevel DC–DC Converter for High Step-Ratio MV and HV Use," *IEEE Trans. Ind. Electron.*, vol. 65, no. 9, pp. 7060–7071, Sep. 2018, doi: 10.1109/TIE.2018.2793249.
[67] N. Parida and A. Das, "Modular Multilevel DC–DC Power Converter Topology With Intermediate Medium Frequency AC Stage for HVDC Tapping," *IEEE Trans. Power Electron.*, vol. 36, no. 3, pp. 2783–2792, Mar. 2021, doi: 10.1109/TPEL.2020.3015708.
[68] C.-K. Kim, V. K. Sood, G.-S. Jang, S.-J. Lim, and S.-J. Lee, *HVDC transmission: power conversion applications in power systems*. John Wiley & Sons, 2009.
[69] A. Kalair, N. Abas, and N. Khan, "Comparative study of HVAC and HVDC transmission systems," *Renew. Sustain. Energy Rev.*, vol. 59, pp. 1653–1675, 2016, doi: https://doi.org/10.1016/j.rser.2015.12.288.
[70] K. Meah and S. Ula, "Comparative Evaluation of HVDC and HVAC Transmission Systems," in *2007 IEEE Power Engineering Society General Meeting*, 2007, pp. 1–5. doi: 10.1109/PES.2007.385993.
[71] N. Flourentzou, V. G. Agelidis, and G. D. Demetriades, "VSC-Based HVDC Power Transmission Systems: An Overview," *IEEE Trans. Power Electron.*, vol. 24, no. 3, pp. 592–602, 2009, doi: 10.1109/TPEL.2008.2008441.
[72] A. M. Vural, "Contribution of high voltage direct current transmission systems to inter-area oscillation damping: A review," *Renew. Sustain. Energy Rev.*, vol. 57, pp. 892–915, 2016.
[73] M. P. Bahrman and B. K. Johnson, "The ABCs of HVDC transmission technologies," *IEEE Power Energy Mag.*, vol. 5, no. 2, pp. 32–44, 2007, doi: 10.1109/MPAE.2007.329194.
[74] A. Erat and A. M. Vural, "DC/DC Modular Multilevel Converters for HVDC Interconnection: A Comprehensive Review.," *Int. Trans. Electr. Energy Syst.*, 2022.
[75] S. Ali, Z. Ling, K. Tian, and Z. Huang, "Recent Advancements in Submodule Topologies and Applications of MMC," *IEEE J. Emerg. Sel. Top. Power Electron.*, vol. 9, no. 3, pp. 3407–3435, 2021, doi: 10.1109/JESTPE.2020.2990689.

[76] M. Han and A. Gole, *Modeling and simulation of HVDC transmission*. Institution of Engineering and Technology, 2020.

[77] S. Ali, Z. Ling, K. Tian, and Z. Huang, “Recent advancements in submodule topologies and applications of MMC,” *IEEE J. Emerg. Sel. Top. Power Electron.*, vol. 9, no. 3, pp. 3407–3435, 2020.

[78] C. D. Barker, N. M. Kirby, N. M. MacLeod, and R. S. Whitehouse, “Widening the bottleneck: Increasing the utilisation of long distance AC transmission corridors,” in *IEEE PES T&D 2010*, 2010, pp. 1–6.

[79] J. Alcalá, V. Cardenas, J. Espinoza, and M. Durán, “Investigation on the limitation of the BTB-VSC converter to control the active and reactive power flow,” *Electr. Power Syst. Res.*, vol. 143, pp. 149–162, 2017.

[80] S. Dey and T. Bhattacharya, “A transformerless DC–DC modular multilevel converter for hybrid interconnections in HVDC,” *IEEE Trans. Ind. Electron.*, vol. 68, no. 7, pp. 5527–5536, 2020.

[81] R. Razani and Y. A.-R. I. Mohamed, “Operation limits of the hybrid DC/DC modular multilevel converter for HVDC grids connections,” *IEEE J. Emerg. Sel. Top. Power Electron.*, vol. 9, no. 4, pp. 4459–4469, 2020.

[82] M. A. Zama, “Modelling and control of modular multilevel converters dedicated to HVDC Grids.” Université Grenoble Alpes, 2017.

[83] G. Li, J. Liang, F. Ma, C. E. Ugalde-Loo, and H. Liang, “Analysis of single-phase-to-ground faults at the valve-side of HB-MMCs in HVDC systems,” *IEEE Trans. Ind. Electron.*, vol. 66, no. 3, pp. 2444–2453, 2018.

[84] J. Wei, “Review of current control strategies in modular multilevel converter.” NTNU, 2016.

[85] S. Le Blond, R. Bertho Jr, D. V. Coury, and J. C. M. Vieira, “Design of protection schemes for multi-terminal HVDC systems,” *Renew. Sustain. Energy Rev.*, vol. 56, pp. 965–974, 2016.

[86] L. M. Castro and E. Acha, “A unified modeling approach of multi-terminal VSC-HVDC links for dynamic simulations of large-scale power systems,” *IEEE Trans. Power Syst.*, vol. 31, no. 6, pp. 5051–5060, 2016.

[87] L. Zhang *et al.*, “Modeling, control, and protection of modular multilevel converter-based multi-terminal HVDC systems: A review,” *CSEE J. Power Energy Syst.*, vol. 3, no. 4, pp. 340–352, 2017.

[88] C. Gavriluta, I. Candela, C. Citro, A. Luna, and P. Rodriguez, “Design

considerations for primary control in multi-terminal VSC-HVDC grids," *Electr. Power Syst. Res.*, vol. 122, pp. 33–41, 2015.

[89] M. K. Bucher, R. Wiget, G. Andersson, and C. M. Franck, "Multiterminal HVDC networks—What is the preferred topology?," *IEEE Trans. Power Deliv.*, vol. 29, no. 1, pp. 406–413, 2013.

[90] M. Ndreko, A. Van der Meer, B. Rawn, and M. Gibescu, "Damping of power system oscillations by VSC-HVDC multi-terminal transmission networks," *TU Delft, Delft, Netherlands, Tech. Rep. WP*, vol. 6, 2013.

[91] P. Sun, "Modular Multilevel Converters in Hybrid Multi-Terminal HVDC Systems." UNSW Sydney, 2021.

[92] R. E. Torres-Olguin, M. Molinas, and T. Undeland, "A direct power control for hybrid HVDC transmission systems," in *2011 IEEE Trondheim PowerTech*, 2011, pp. 1–6.

[93] G. Li *et al.*, "Feasibility and reliability analysis of LCC DC grids and LCC/VSC hybrid DC grids," *Ieee Access*, vol. 7, pp. 22445–22456, 2019.

[94] Z. Li, Z. Wei, R. Zhan, Y. Li, and X.-P. Zhang, "System operational dispatching and scheduling strategy for hybrid cascaded multi-terminal HVDC," *Int. J. Electr. Power Energy Syst.*, vol. 122, p. 106195, 2020.

[95] Z. Xu, S. Wang, and H. Xiao, "Hybrid high-voltage direct current topology with line commutated converter and modular multilevel converter in series connection suitable for bulk power overhead line transmission," *IET Power Electron.*, vol. 9, no. 12, pp. 2307–2317, 2016.

[96] H. Ying, H. Weihuang, L. Ming, and L. Tao, "Steady-state control strategy of multi-terminal hybrid UHVDC," in *2017 19th European Conference on Power Electronics and Applications (EPE'17 ECCE Europe)*, 2017, p. P-1.

[97] H. Rao *et al.*, "Design aspects of hybrid HVDC system," *CSEE J. power energy Syst.*, vol. 7, no. 3, pp. 644–653, 2020.

[98] H. Xiao, K. Sun, J. Pan, Y. Li, and Y. Liu, "Review of hybrid HVDC systems combining line communicated converter and voltage source converter," *Int. J. Electr. Power Energy Syst.*, vol. 129, p. 106713, 2021.

[99] K. Yamashita, G. Tsukamoto, and S. Nishikata, "Steady-state characteristics of a line-commutated converter-based high-voltage direct current transmission system for series-connected wind power plants," *IEEE Trans. Ind. Appl.*, vol. 56, no. 4, pp. 3932–3939, 2020.

[100] H. Jiang, *Modeling and control of modular multilevel converter based on ordinary differential equations and its applications for HVDC system*. McGill University (Canada), 2019.

[101] D. Van Hertem, O. Gomis-Bellmunt, and J. Liang, *HVDC grids: for offshore and supergrid of the future*. John Wiley & Sons, 2016.

[102] O. Peake, "The history of high voltage direct current transmission," *Aust. J. Multi-Disciplinary Eng.*, vol. 8, no. 1, pp. 47–55, 2010.

[103] R. Rudervall, J. P. Charpentier, and R. Sharma, "High voltage direct current (HVDC) transmission systems technology review paper," *Energy week*, vol. 2000, pp. 1–19, 2000.

[104] D. Tiku, "DC power transmission: mercury-Arc to thyristor HVDC valves [history]," *IEEE power energy Mag.*, vol. 12, no. 2, pp. 76–96, 2014.

[105] S. J. Sutton, P. L. Lewin, and S. G. Swingler, "Review of global HVDC subsea cable projects and the application of sea electrodes," *Int. J. Electr. Power Energy Syst.*, vol. 87, pp. 121–135, 2017.

[106] D. A. M. Acevedo, "Implementation of control schemes on a dc-ac terminal based on a hvdc-mmc." Universidad Tecnológica de Pereira, 2022.

[107] H. Huang, M. Uder, R. Barthelmess, and J. Dorn, "Application of High Power Thyristors in HVDC and FACTS Systems".

[108] P. K. Steimer, H. E. Gruning, J. Werninger, E. Carroll, S. Klaka, and S. Linder, "IGCT-a new emerging technology for high power, low cost inverters," in *IAS'97. Conference Record of the 1997 IEEE Industry Applications Conference Thirty-Second IAS Annual Meeting*, 1997, vol. 2, pp. 1592–1599.

[109] M. Barnes and A. Beddard, "Voltage source converter HVDC links–the state of the art and issues going forward," *Energy Procedia*, vol. 24, pp. 108–122, 2012.

[110] U. Axelsson, "Gotland HVDC Light transmission-world's first commercial small scale DC transmission," in *Proc. of CIRED Conference in Nice, France, May*, 1999.

[111] G. Asplund, "HVDC Light-DC transmission based on voltage sourced converters," *ABB Rev.*, vol. 1, 1998.

[112] G. Asplund, K. Eriksson, and O. Tollerz, "HVDC light, a tool for electric power transmission to distant loads," in *VI SEPOPE Conference, Salvador, Brazil*, 1998.

[113] T. J. Hammons *et al.*, "Role of HVDC transmission in future energy

development," *IEEE Power Eng. Rev.*, vol. 20, no. 2, pp. 10–25, 2000.
[114] N. Serbia, "Modular multilevel converters for HVDC power stations." Institut National Polytechnique de Toulouse-INPT, 2014.
[115] H. K. Müller, S. S. Torbaghan, M. Gibescu, M. M. Roggenkamp, and M. Van Der Meijden, "The need for a common standard for voltage levels of HVDC VSC technology," *Energy Policy*, vol. 63, pp. 244–251, 2013.
[116] R. L. Sellick and M. Åkerberg, "Comparison of HVDC Light (VSC) and HVDC Classic (LCC) site aspects, for a 500MW 400kV HVDC transmission scheme," in *10th IET international conference on AC and DC power transmission (ACDC 2012)*, 2012, pp. 1–6.
[117] H. Alyami and Y. Mohamed, "Review and development of MMC employed in VSC-HVDC systems," in *2017 IEEE 30th Canadian Conference on Electrical and Computer Engineering (CCECE)*, 2017, pp. 1–6.
[118] M. Bahrman and P.-E. Bjorklund, "The new black start: System restoration with help from voltage-sourced converters," *IEEE Power Energy Mag.*, vol. 12, no. 1, pp. 44–53, 2013.
[119] M. Callavik, P. Lundberg, J. Häfner, H. Björklund, M. Rahimo, and F. Dugal, "Evolution of HVDC light®," *ABB Rev.*, no. 1, pp. 60–67, 2018, [Online]. Available: https://new.abb.com/news/detail/4224/evolution-of-hvdc-lightr
[120] S. Du, A. Dekka, B. Wu, and N. Zargari, *Modular multilevel converters: Analysis, control, and applications*. John Wiley & Sons, 2017.
[121] M. Priya, P. Ponnambalam, and K. Muralikumar, "Modular-multilevel converter topologies and applications–a review," *IET Power Electron.*, vol. 12, no. 2, pp. 170–183, 2019.
[122] J. Liu, D. Dong, and D. Zhang, "A Hybrid Modular Multilevel Converter Family With Higher Power Density and Efficiency," *IEEE Trans. Power Electron.*, vol. 36, no. 8, pp. 9001–9014, 2021, doi: 10.1109/TPEL.2021.3055690.
[123] F. Deng, Y. Lü, C. Liu, Q. Heng, Q. Yu, and J. Zhao, "Overview on submodule topologies, modeling, modulation, control schemes, fault diagnosis, and tolerant control strategies of modular multilevel converters," *Chinese J. Electr. Eng.*, vol. 6, no. 1, pp. 1–21, 2020, doi: 10.23919/CJEE.2020.000001.
[124] Y. Wang, A. Aksoz, T. Geury, S. B. Ozturk, O. C. Kivanc, and O. Hegazy, "A Review of Modular Multilevel Converters for Stationary Applications," *Applied*

Sciences, vol. 10, no. 21. 2020. doi: 10.3390/app10217719.

[125] M. N. Raju, J. Sreedevi, R. P Mandi, and K. S. Meera, “Modular multilevel converters technology: a comprehensive study on its topologies, modelling, control and applications,” *IET Power Electron.*, vol. 12, no. 2, pp. 149–169, Feb. 2019, doi: 10.1049/iet-pel.2018.5734.

[126] S. P. Teeuwsen, “Modeling the trans bay cable project as voltage-sourced converter with modular multilevel converter design,” in *2011 IEEE Power and Energy Society General Meeting*, 2011, pp. 1–8.

[127] P. Fairley, “New developments in high-voltage DC electronics could herald an epic shift in energy delivery,” *IEEE Spectr.*, vol. 29, 2013.

[128] M. O. M. E. Abdelsalam, “Capacitor voltage balancing, fault detection, and fault tolerant control techniques of modular multilevel converters.” Staffordshire University, 2016.

[129] G. Li *et al.*, “Power reversal strategies for hybrid LCC/MMC HVDC systems,” *CSEE J. Power Energy Syst.*, vol. 6, no. 1, pp. 203–212, 2020.

[130] Y. Zhou, D. Zhuojiang, and Y. Fenwang, “The development of HVDC transmission system,” in *2012 Third International Conference on Digital Manufacturing & Automation*, 2012, pp. 907–910.

[131] Y. Li, D. Liu, and G. J. Kish, “Generalized dc-dc-ac MMC structure for MVDC and HVDC applications,” in *2019 20th Workshop on Control and Modeling for Power Electronics (COMPEL)*, 2019, pp. 1–8.

[132] Z. Xing, X. Ruan, H. Xie, and X. Wang, “A modular bidirectional buck/boost dc/dc converter suitable for interconnecting HVDC grids,” in *2016 IEEE 8th International Power Electronics and Motion Control Conference (IPEMC-ECCE Asia)*, 2016, pp. 3348–3354.

[133] R. Zeng, L. Xu, and L. Yao, “DC/DC converters based on hybrid MMC for HVDC grid interconnection,” 2015.

[134] H. Liu, K. Ma, C. Wang, and F. Blaabjerg, “Fault diagnosis and fault-tolerant control of modular multi-level converter high-voltage DC system: a review,” *Electr. Power Components Syst.*, vol. 44, no. 16, pp. 1759–1785, 2016.

[135] J. D. Paez, D. Frey, J. Maneiro, S. Bacha, and P. Dworakowski, “Overview of DC–DC converters dedicated to HVdc grids,” *IEEE Trans. Power Deliv.*, vol. 34, no. 1, pp. 119–128, 2018.

[136] S. Cui, J. Hu, and R. W. De Doncker, “Control and experiment of a TLC-MMC

hybrid DC–DC converter for the interconnection of MVDC and HVDC grids," *IEEE Trans. Power Electron.*, vol. 35, no. 3, pp. 2353–2362, 2019.

[137] "Mitsubishi Electric-HVDC-Diamond® – Applications," 2024. https://www.mitsubishielectric.com/eig/energysystems/products/transmission/pss/hvdc/index_02.html

[138] "Hitachi Energy-High-Voltage Direct Current (HVDC)," 2024. https://www.hitachienergy.com/products-and-solutions/hvdc

[139] A. Stan, S. Costinaș, and G. Ion, "Overview and assessment of HVDC current applications and future trends," *Energies*, vol. 15, no. 3, p. 1193, 2022.

[140] X. Liang and M. Abbasipour, "HVDC transmission and its potential application in remote communities: Current practice and future trend," *IEEE Trans. Ind. Appl.*, vol. 58, no. 2, pp. 1706–1719, 2022.

[141] B. M. Saleh, F. D. Merlet, A. Costabeber, A. J. Watson, and J. C. Clare, "Trapezoidal operation of modular multilevel DC-DC converter for HVDC interconnections," in *IECON 2021–47th Annual Conference of the IEEE Industrial Electronics Society*, 2021, pp. 1–6.

[142] S. M. Muyeen, R. Takahashi, and J. Tamura, "Operation and control of HVDC-connected offshore wind farm," *IEEE Trans. Sustain. Energy*, vol. 1, no. 1, pp. 30–37, 2010.

[143] A. S. Ayobe and S. Gupta, "Comparative investigation on HVDC and HVAC for bulk power delivery," *Mater. Today Proc.*, vol. 48, pp. 958–964, 2022.

[144] N. R. Watson and J. D. Watson, "An Overview of HVDC Technology," *Energies*, vol. 13, no. 17. 2020. doi: 10.3390/en13174342.

[145] D. Van Hertem and M. Ghandhari, "Multi-terminal VSC HVDC for the European supergrid: Obstacles," *Renew. Sustain. energy Rev.*, vol. 14, no. 9, pp. 3156–3163, 2010.

[146] A. Shah Ayobe and S. Gupta, "Comparative investigation on HVDC and HVAC for bulk power delivery," *Mater. Today Proc.*, vol. 48, pp. 958–964, 2022, doi: https://doi.org/10.1016/j.matpr.2021.06.025.

[147] F. Mumtaz, N. Z. Yahaya, S. T. Meraj, B. Singh, R. Kannan, and O. Ibrahim, "Review on non-isolated DC-DC converters and their control techniques for renewable energy applications," *Ain Shams Eng. J.*, vol. 12, no. 4, pp. 3747–3763, 2021.

[148] A. Amir, A. Amir, H. S. Che, A. Elkhateb, and N. Abd Rahim, "Comparative

analysis of high voltage gain DC-DC converter topologies for photovoltaic systems," *Renew. energy*, vol. 136, pp. 1147–1163, 2019.

[149] S. Dahale, A. Das, N. M. Pindoriya, and S. Rajendran, "An overview of DC-DC converter topologies and controls in DC microgrid," in *2017 7th International Conference on Power Systems (ICPS)*, 2017, pp. 410–415.

[150] A. Lavanya, J. D. Navamani, K. Vijayakumar, and R. Rakesh, "Multi-input DC-DC converter topologies-a review," in *2016 International Conference on Electrical, Electronics, and Optimization Techniques (ICEEOT)*, 2016, pp. 2230–2233.

[151] M. Parvez, A. T. Pereira, N. Ertugrul, N. H. E. Weste, D. Abbott, and S. F. Al-Sarawi, "Wide bandgap DC–DC converter topologies for power applications," *Proc. IEEE*, vol. 109, no. 7, pp. 1253–1275, 2021.

[152] S. A. Gorji, H. G. Sahebi, M. Ektesabi, and A. B. Rad, "Topologies and control schemes of bidirectional DC–DC power converters: An overview," *IEEE Access*, vol. 7, pp. 117997–118019, 2019.

[153] F. L. Luo and H. Ye, *Advanced dc/dc converters*. crc Press, 2016.

[154] S. Ikeda and F. Kurokawa, "Isolated and wide input ranged boost full bridge DC-DC converter with low loss active snubber," in *2017 IEEE Energy Conversion Congress and Exposition (ECCE)*, 2017, pp. 2213–2218.

[155] F. Krismer and J. W. Kolar, "Efficiency-optimized high-current dual active bridge converter for automotive applications," *IEEE Trans. Ind. Electron.*, vol. 59, no. 7, pp. 2745–2760, 2011.

[156] A. Gnanasaravanan and M. Rajaram, "Dynamic response analysis and output voltage control of asymmetric half bridge DC–DC converter for low voltage applications," *Int. J. Electr. Power Energy Syst.*, vol. 43, no. 1, pp. 774–778, 2012.

[157] A. G. Saravanan and M. Rajaram, "Fuzzy controller for dynamic performance improvement of a half-bridge isolated DC–DC converter," *Neurocomputing*, vol. 140, pp. 283–290, 2014.

[158] R. W. A. A. De Doncker, D. M. Divan, and M. H. Kheraluwala, "A three-phase soft-switched high-power-density DC/DC converter for high-power applications," *IEEE Trans. Ind. Appl.*, vol. 27, no. 1, pp. 63–73, 1991.

[159] S. Shao, H. Chen, X. Wu, J. Zhang, and K. Sheng, "Circulating current and ZVS-on of a dual active bridge DC-DC converter: A review," *Ieee Access*, vol.

7, pp. 50561–50572, 2019.

[160] A. Kumar, A. H. Bhat, and P. Agarwal, "Review and comparative analysis of dual active bridge isolated DC to DC converter with different control techniques," *Int. J. Ind. Electron. Drives*, vol. 4, no. 2, pp. 69–84, 2018.

[161] Q. Bu, H. Wen, J. Wen, Y. Hu, and Y. Du, "Transient DC bias elimination of dual-active-bridge DC–DC converter with improved triple-phase-shift control," *IEEE Trans. Ind. Electron.*, vol. 67, no. 10, pp. 8587–8598, 2019.

[162] J.-Y. Lee, H.-S. Kim, and J.-H. Jung, "Enhanced dual-active-bridge DC–DC converter for balancing bipolar voltage level of DC distribution system," *IEEE Trans. Ind. Electron.*, vol. 67, no. 12, pp. 10399–10409, 2019.

[163] L. Chen, S. Shao, Q. Xiao, L. Tarisciotti, P. W. Wheeler, and T. Dragičević, "Model predictive control for dual-active-bridge converters supplying pulsed power loads in naval DC micro-grids," *IEEE Trans. Power Electron.*, vol. 35, no. 2, pp. 1957–1966, 2019.

[164] S. Zengin and M. Boztepe, "A novel current modulation method to eliminate low-frequency harmonics in single-stage dual active bridge AC–DC converter," *IEEE Trans. Ind. Electron.*, vol. 67, no. 2, pp. 1048–1058, 2019.

[165] H. Qin and J. W. Kimball, "Generalized Average Modeling of Dual Active Bridge DC–DC Converter," *IEEE Trans. Power Electron.*, vol. 27, no. 4, pp. 2078–2084, 2012, doi: 10.1109/TPEL.2011.2165734.

[166] R. Jha, M. Forato, S. Prakash, H. Dashora, and G. Buja, "An analysis-supported design of a single active bridge (SAB) converter," *Energies*, vol. 15, no. 2, p. 666, 2022.

[167] D. Vinnikov, A. Chub, E. Liivik, F. Blaabjerg, and Y. Siwakoti, "Boost half-bridge DC-DC converter with reconfigurable rectifier for ultra-wide input voltage range applications," in *2018 IEEE Applied Power Electronics Conference and Exposition (APEC)*, 2018, pp. 1528–1532.

[168] H.-S. Lee, B. Kang, W.-S. Kim, and S.-J. Yoon, "Reduction of input voltage/current ripples of boost half-bridge DC-DC converter for photovoltaic micro-inverter," *Sol. Energy*, vol. 188, pp. 1084–1101, 2019.

[169] C.-E. Kim, G.-W. Moon, and S.-K. Han, "Voltage Doubler Rectified Boost-Integrated Half Bridge (VDRBHB) Converter for Digital Car Audio Amplifiers," *IEEE Trans. Power Electron.*, vol. 22, no. 6, pp. 2321–2330, 2007, doi: 10.1109/TPEL.2007.904222.

[170] H.-S. Lee, H.-J. Choe, and J.-J. Yun, “Improved Boost Half-Bridge DC–DC Converter for DC Distribution Networks,” *J. Electr. Eng. Technol.*, vol. 17, no. 5, pp. 2889–2898, 2022, doi: 10.1007/s42835-022-01107-1.

[171] C. Yoon, J. Kim, and S. Choi, “Multiphase DC–DC Converters Using a Boost-Half-Bridge Cell for High-Voltage and High-Power Applications,” *IEEE Trans. Power Electron.*, vol. 26, no. 2, pp. 381–388, 2011, doi: 10.1109/TPEL.2010.2060498.

[172] H.-S. Lee and J.-J. Yun, “Quasi-Resonant Voltage Doubler With Snubber Capacitor for Boost Half-Bridge DC–DC Converter in Photovoltaic Micro-Inverter,” *IEEE Trans. Power Electron.*, vol. 34, no. 9, pp. 8377–8388, 2019, doi: 10.1109/TPEL.2018.2883535.

[173] K. Fathy, H. W. Lee, T. Mishima, and M. Nakaoka, “Boost-half bridge single power stage PWM DC-DC converter for small scale fuel cell stack,” in *2006 IEEE International Power and Energy Conference*, 2006, pp. 426–431.

[174] V. A. G. Cunha, A. O. C. Neto, G. B. Lima, and L. C. G. Freitas, “A Bridgeless Boost Half Bridge DC-DC Converter for Electrical and Hybrid Vehicle Applications,” in *2019 IEEE PES Innovative Smart Grid Technologies Conference - Latin America (ISGT Latin America)*, 2019, pp. 1–6. doi: 10.1109/ISGT-LA.2019.8895388.

[175] C. Yoon, J. Kim, and S. Choi, “Multiphase DC–DC converters using a boost-half-bridge cell for high-voltage and high-power applications,” *IEEE Trans. Power Electron.*, vol. 26, no. 2, pp. 381–388, 2010.

[176] B. Su, T. Yang, Z. Lu, and D. Xu, “Soft-switching dual forward DC/DC converters employing secondary side control,” in *2009 IEEE Energy Conversion Congress and Exposition*, 2009, pp. 1855–1859.

[177] K.-H. Cheng, C.-F. Hsu, C.-M. Lin, T.-T. Lee, and C. Li, “Fuzzy–neural sliding-mode control for DC–DC converters using asymmetric Gaussian membership functions,” *IEEE Trans. Ind. Electron.*, vol. 54, no. 3, pp. 1528–1536, 2007.

[178] R. Kanthimathi and J. Kamala, “Analysis of different flyback converter topologies,” in *2015 international conference on industrial instrumentation and control (ICIC)*, 2015, pp. 1248–1252.

[179] M. C. Taneri, N. Genc, and A. Mamizadeh, “Analyzing and comparing of variable and constant switching frequency flyback DC-DC Converter,” in *2019 4th International Conference on Power Electronics and their Applications*

(ICPEA), 2019, pp. 1–5.

[180] J.-W. Yang and H.-L. Do, "Soft-switching dual-flyback DC–DC converter with improved efficiency and reduced output ripple current," *IEEE Trans. Ind. Electron.*, vol. 64, no. 5, pp. 3587–3594, 2017.

[181] Z. Zhang, M. Liao, D. Jiang, X. Yang, and S. Li, "High step-up isolated forward-flyback DC/DC converter based on resonance with pulse frequency modulation," *J. Power Electron.*, vol. 21, no. 2, pp. 483–493, 2021, doi: 10.1007/s43236-020-00186-5.

[182] R. W. Erickson, "DC–DC power converters," *Wiley Encycl. Electr. Electron. Eng.*, 2001.

[183] K.-H. Chen and T.-J. Liang, "Design of Quasi-resonant flyback converter control IC with DCM and CCM operation," in *2014 International Power Electronics Conference (IPEC-Hiroshima 2014-ECCE ASIA)*, 2014, pp. 2750–2753.

[184] V. Parkash, P. Kumar, P. Sharma, and G. Sapra, "Design and implementation of flyback converter as high voltage power supply for nanofibers production," *Mater. Today Proc.*, vol. 45, pp. 5285–5291, 2021.

[185] Y. Wu, Y. Huangfu, R. Ma, A. Ravey, and D. Chrenko, "A strong robust DC-DC converter of all-digital high-order sliding mode control for fuel cell power applications," *J. Power Sources*, vol. 413, pp. 222–232, 2019.

[186] M. Salem *et al.*, "Three-phase series resonant DC-DC boost converter with double LLC resonant tanks and variable frequency control," *IEEE Access*, vol. 8, pp. 22386–22399, 2020.

[187] M. Salem, A. Jusoh, N. R. N. Idris, H. S. Das, and I. Alhamrouni, "Resonant power converters with respect to passive storage (LC) elements and control techniques–An overview," *Renew. Sustain. Energy Rev.*, vol. 91, pp. 504–520, 2018.

[188] F. Alaql and I. Batarseh, "Review and comparison of resonant DC-DC converters for wide-output voltage range applications," in *2020 IEEE Energy Conversion Congress and Exposition (ECCE)*, 2020, pp. 1197–1203.

[189] X. Zhao *et al.*, "A high-efficiency hybrid series resonant DC-DC converter with boost converter as secondary for photovoltaic applications," in *2015 IEEE Energy Conversion Congress and Exposition (ECCE)*, 2015, pp. 5462–5467. doi: 10.1109/ECCE.2015.7310428.

[190] X. Zhao, L. Zhang, R. Born, and J.-S. Lai, "A High-Efficiency Hybrid Resonant Converter With Wide-Input Regulation for Photovoltaic Applications," *IEEE Trans. Ind. Electron.*, vol. 64, no. 5, pp. 3684–3695, 2017, doi: 10.1109/TIE.2017.2652340.

[191] G. I. Vacheva, K. Genev, and N. L. Hinov, "Modeling and Simulation of DC-DC Push-Pull Converter," in *2022 57th International Scientific Conference on Information, Communication and Energy Systems and Technologies (ICEST)*, 2022, pp. 1–4. doi: 10.1109/ICEST55168.2022.9828584.

[192] Q. Wu, Q. Wang, J. Xu, and L. Xiao, "A wide load range ZVS push–pull DC/DC converter with active clamped," *IEEE Trans. Power Electron.*, vol. 32, no. 4, pp. 2865–2875, 2016.

[193] S. Musumeci and S. Di Mauro, "Low voltage single fuel cell interface by Push-Pull converter: A case of study," in *2017 6th International Conference on Clean Electrical Power (ICCEP)*, 2017, pp. 541–548.

[194] S. Bal, A. K. Rathore, and D. Srinivasan, "Naturally clamped snubberless soft-switching bidirectional current-fed three-phase push–pull DC/DC converter for DC microgrid application," *IEEE Trans. Ind. Appl.*, vol. 52, no. 2, pp. 1577–1587, 2015.

[195] R. Kalpana, "Configurations of modular push-pull buck dc-dc converters for 12KW telecom SMPS and its design," in *2016 Biennial International Conference on Power and Energy Systems: Towards Sustainable Energy (PESTSE)*, 2016, pp. 1–7.

[196] H. Zenk, "Comparison of the Performance of Photovoltaic Power Generation-Consumption System with Push-Pull Converter under the Effect of Five Different Types of Controllers," *Int. J. Photoenergy*, vol. 2019, no. 1, p. 3810970, 2019.

[197] H. Givi, E. Farjah, and T. Ghanbari, "A comprehensive monitoring system for online fault diagnosis and aging detection of non-isolated DC–DC converters' components," *IEEE Trans. Power Electron.*, vol. 34, no. 7, pp. 6858–6875, 2018.

[198] S. N. Singh, "Selection of non-isolated DC-DC converters for solar photovoltaic system," *Renew. Sustain. Energy Rev.*, vol. 76, pp. 1230–1247, 2017.

[199] T. K. Nizami and C. Mahanta, "An intelligent adaptive control of DC–DC buck converters," *J. Franklin Inst.*, vol. 353, no. 12, pp. 2588–2613, 2016.

[200] B. B. Naik and A. J. Mehta, "Sliding mode controller with modified sliding function for DC-DC Buck Converter," *ISA Trans.*, vol. 70, pp. 279–287, 2017.

[201] C. Nan, R. Ayyanar, and Y. Xi, "A 2.2-MHz active-clamp buck converter for automotive applications," *IEEE Trans. Power Electron.*, vol. 33, no. 1, pp. 460–472, 2017.

[202] J. Wang, J. Rong, and L. Yu, "Dynamic prescribed performance sliding mode control for DC–DC buck converter system with mismatched time-varying disturbances," *ISA Trans.*, vol. 129, pp. 546–557, 2022.

[203] W. Chen, Z. Ge, Y. Cheng, H. Du, Q. Du, and M. Yu, "Current-constrained finite-time control algorithm for DC-DC buck converter," *J. Franklin Inst.*, vol. 358, no. 18, pp. 9467–9482, 2021.

[204] T. K. Nizami, A. Chakravarty, and C. Mahanta, "Time bound online uncertainty estimation based adaptive control design for DC–DC buck converters with experimental validation," *IFAC J. Syst. Control*, vol. 15, p. 100127, 2021.

[205] İ. Yazici, "Robust voltage-mode controller for DC–DC boost converter," *IET Power Electron.*, vol. 8, no. 3, pp. 342–349, 2015.

[206] F. L. Tofoli, D. de C. Pereira, W. Josias de Paula, and D. de S. Oliveira Junior, "Survey on non-isolated high-voltage step-up dc–dc topologies based on the boost converter," *IET power Electron.*, vol. 8, no. 10, pp. 2044–2057, 2015.

[207] T. K. Nizami and A. Chakravarty, "Neural network integrated adaptive backstepping control of DC-DC boost converter," *IFAC-PapersOnLine*, vol. 53, no. 1, pp. 549–554, 2020.

[208] S. Vadi, F. B. Gurbuz, S. Sagiroglu, and R. Bayindir, "Optimization of pi based buck-boost converter by particle swarm optimization algorithm," in *2021 9th International Conference on Smart Grid (icSmartGrid)*, 2021, pp. 295–301.

[209] K. Prag, M. Woolway, and T. Celik, "Data-driven model predictive control of DC-to-DC buck-boost converter," *IEEE Access*, vol. 9, pp. 101902–101915, 2021.

[210] E. Babaei, M. E. S. Mahmoodieh, and H. M. Mahery, "Operational modes and output-voltage-ripple analysis and design considerations of buck–boost DC–DC converters," *IEEE Trans. Ind. Electron.*, vol. 59, no. 1, pp. 381–391, 2011.

[211] K. Wang, D. Liu, and L. Wang, "The implementation of synergetic control for a DC-DC buck-boost converter," *Procedia Comput. Sci.*, vol. 199, pp. 900–907, 2022.

[212] M. Martinez-Lopez, J. Moreno-Valenzuela, and W. He, “A robust nonlinear PI-type controller for the DC–DC buck–boost power converter,” *ISA Trans.*, vol. 129, pp. 687–700, 2022.

[213] S. Kumar, R. Kumar, and N. Singh, “Performance of closed loop SEPIC converter with DC-DC converter for solar energy system,” in *2017 4th International Conference on Power, Control & Embedded Systems (ICPCES)*, 2017, pp. 1–6.

[214] L. Kathi, A. Ayachit, D. K. Saini, A. Chadha, and M. K. Kazimierczuk, “Open-loop small-signal modeling of Cuk DC-DC converter in CCM by circuit-averaging technique,” in *2018 IEEE Texas Power and Energy Conference (TPEC)*, 2018, pp. 1–6.

[215] B. P. Mokal and K. Vadirajacharya, “Extensive modeling of DC-DC Cuk converter operating in continuous conduction mode,” in *2017 International Conference on Circuit, Power and Computing Technologies (ICCPCT)*, 2017, pp. 1–5.

[216] S. Sivakumar, M. J. Sathik, P. S. Manoj, and G. Sundararajan, “An assessment on performance of DC–DC converters for renewable energy applications,” *Renew. Sustain. Energy Rev.*, vol. 58, pp. 1475–1485, 2016.

[217] M. B. Ferrera, S. P. Litran, E. D. Aranda, and J. M. A. Marquez, “A converter for bipolar DC link based on SEPIC-Cuk combination,” *IEEE Trans. Power Electron.*, vol. 30, no. 12, pp. 6483–6487, 2015.

[218] J. Marjani, A. Imani, A. Hekmati, and E. Afjei, “A new dual output DC-DC converter based on SEPIC and Cuk converters,” in *2016 International Symposium on Power Electronics, Electrical Drives, Automation and Motion (SPEEDAM)*, 2016, pp. 946–950.

[219] A. H. R. Rosa, L. M. F. Morais, G. O. Fortes, and S. I. S. Júnior, “Practical considerations of nonlinear control techniques applied to static power converters: A survey and comparative study,” *Int. J. Electr. Power Energy Syst.*, vol. 127, p. 106545, 2021.

[220] M. Verma and S. S. Kumar, “Hardware design of sepic converter and its analysis,” in *2018 International Conference on Current Trends towards Converging Technologies (ICCTCT)*, 2018, pp. 1–4.

[221] A. Cordeiro *et al.*, “Hybrid Sepic-Cuk DC-DC converter associated to a SRM drive for a solar PV powered water pumping system,” in *2019 8th International*

Conference on Renewable Energy Research and Applications (ICRERA), 2019, pp. 169–174.

[222] R. K. Pachauri and Y. K. Chauhan, "Modeling and simulation analysis of PV fed Cuk, Sepic, Zeta and Luo DC-DC converter," in *2016 IEEE 1st international conference on power electronics, intelligent control and energy systems (ICPEICES)*, 2016, pp. 1–6.

[223] K. Manikandan, A. Sivabalan, R. Sundar, and P. Surya, "A study of landsman, sepic and zeta converter by particle swarm optimization technique," in *2020 6th international conference on advanced computing and communication systems (ICACCS)*, 2020, pp. 1035–1038.

[224] M. Kaouane, A. Boukhelifa, and A. Cheriti, "Implementation of incremental-conductance MPPT algorithm in a photovoltaic conversion system based on DC-DC ZETA converter," in *2016 8th International Conference on Modelling, Identification and Control (ICMIC)*, 2016, pp. 612–617.

[225] J. S. Alagesan, J. Gnanavadivel, N. S. Kumar, and K. S. K. Veni, "Design and Simulation of Fuzzybased DC-DC Interleaved Zeta Converter for Photovoltaic Applications," in *2018 2nd International Conference on Trends in Electronics and Informatics (ICOEI)*, 2018, pp. 704–709.

[226] M. M. Nishat, M. R. K. Shagor, H. Akter, S. A. Mim, and F. Faisal, "An optimal design of PID controller for DC-DC zeta converter using particle swarm optimization," in *2020 23rd International Conference on Computer and Information Technology (ICCIT)*, 2020, pp. 1–6.

[227] M. Bindi *et al.*, "Failure prevention in DC–DC converters: Theoretical approach and experimental application on a zeta converter," *IEEE Trans. Ind. Electron.*, vol. 70, no. 1, pp. 930–939, 2022.

[228] A. M. S. S. Andrade and M. L. da Silva Martins, "Quadratic-boost with stacked zeta converter for high voltage gain applications," *IEEE J. Emerg. Sel. Top. Power Electron.*, vol. 5, no. 4, pp. 1787–1796, 2017.

[229] A. Raj, S. R. Arya, and J. Gupta, "Solar PV array-based DC–DC converter with MPPT for low power applications," *Renew. Energy Focus*, vol. 34, pp. 109–119, 2020.

[230] V. Jonnalagadda, K. R. Sugavanam, K. Mohanasundaram, C. L. Kuppuswamy, R. Bhukya, and K. S. Kadali, "Modified zeta converter based on ANFIS controller using MPPT PV system," in *Journal of Physics: Conference Series*,

2021, vol. 1916, no. 1, p. 12126.

[231] A. Jha and B. Singh, "Bridgeless ZETA PFC converter for low voltage high current LED driver," in *2017 6th International Conference on Computer Applications In Electrical Engineering-Recent Advances (CERA)*, 2017, pp. 539–544.

[232] M. Ashari, O. Penangsang, and I. Mahmudi, "Fuzzy based wide range voltage control of dc step-up ZETA converter for energy management system," in *2021 4th International Seminar on Research of Information Technology and Intelligent Systems (ISRITI)*, 2021, pp. 423–428.

[233] G. G. Gadhave and S. B. Patil, "Implementation on PF improvement of brushless DC motor drives using zeta converter," in *2020 International Conference on Communication and Signal Processing (ICCSP)*, 2020, pp. 1006–1010.

[234] H. Sarkawi, Y. Ohta, and P. Rapisarda, "On the switching control of the DC–DC zeta converter operating in continuous conduction mode," *IET Control Theory Appl.*, vol. 15, no. 9, pp. 1185–1198, 2021.

[235] N. Vosoughi, M. Abbasi, E. Abbasi, and M. Sabahi, "A Zeta-based switched-capacitor DC-DC converter topology," *Int. J. Circuit Theory Appl.*, vol. 47, no. 8, pp. 1302–1322, 2019.

[236] R. F. Rajakumari and M. S. Ramkumar, "Design considerations and performance analysis based on ripple factors and switching loss for converter techniques," *Mater. Today Proc.*, vol. 37, pp. 2681–2686, 2021.

[237] S. Du, B. Wu, N. R. Zargari, and Z. Cheng, "A flying-capacitor modular multilevel converter for medium-voltage motor drive," *IEEE Trans. Power Electron.*, vol. 32, no. 3, pp. 2081–2089, 2016.

[238] S. Qin, Y. Lei, Z. Ye, D. Chou, and R. C. N. Pilawa-Podgurski, "A high-power-density power factor correction front end based on seven-level flying capacitor multilevel converter," *IEEE J. Emerg. Sel. Top. Power Electron.*, vol. 7, no. 3, pp. 1883–1898, 2018.

[239] C. B. Barth *et al.*, "Design and control of a GaN-based, 13-level, flying capacitor multilevel inverter," *IEEE J. Emerg. Sel. Top. Power Electron.*, vol. 8, no. 3, pp. 2179–2191, 2019.

[240] N. Ghasemi, F. Zare, C. Langton, and A. Ghosh, "A new unequal DC link voltage configuration for a single phase multilevel converter to reduce low order

harmonics," in *Proceedings of the 2011 14th European Conference on Power Electronics and Applications*, 2011, pp. 1–9.

[241] A. Marquez *et al.*, "Discontinuous-PWM method for multilevel N-cell cascaded H-bridge converters," *IEEE Trans. Ind. Electron.*, vol. 68, no. 9, pp. 7996–8005, 2020.

[242] A. M. Alcaide *et al.*, "Variable-angle PS-PWM technique for multilevel cascaded H-bridge converters with large number of power cells," *IEEE Trans. Ind. Electron.*, vol. 68, no. 8, pp. 6773–6783, 2020.

[243] Y. Koyama, Y. Nakazawa, H. Mochikawa, A. Kuzumaki, K. Sano, and N. Okada, "A transformerless 6.6-kV STATCOM based on a hybrid cascade multilevel converter using SiC devices," *IEEE Trans. Power Electron.*, vol. 33, no. 9, pp. 7411–7423, 2017.

[244] H. D. Tafti, A. I. Maswood, G. Konstantinou, C. D. Townsend, P. Acuna, and J. Pou, "Flexible control of photovoltaic grid-connected cascaded H-bridge converters during unbalanced voltage sags," *IEEE Trans. Ind. Electron.*, vol. 65, no. 8, pp. 6229–6238, 2017.

[245] M. Glinka and R. Marquardt, "A new AC/AC-multilevel converter family applied to a single-phase converter," in *The Fifth International Conference on Power Electronics and Drive Systems, 2003. PEDS 2003.*, 2003, vol. 1, pp. 16–23.

[246] M. Glinka and R. Marquardt, "A new AC/AC multilevel converter family," *IEEE Trans. Ind. Electron.*, vol. 52, no. 3, pp. 662–669, 2005.

[247] R. Marquardt, "A new modular voltage source inverter topology," in *Conf. Rec. EPE 2003*, 2003.

[248] M. A. Perez, S. Ceballos, G. Konstantinou, J. Pou, and R. P. Aguilera, "Modular Multilevel Converters: Recent Achievements and Challenges," *IEEE Open J. Ind. Electron. Soc.*, vol. 2, pp. 224–239, 2021, doi: 10.1109/OJIES.2021.3060791.

[249] G. A. Reddy, N. R. Karaka, and A. Shukla, "Constant overlap-time based sms capacitor voltage balancing scheme for alternate arm converter," in *2021 IEEE Energy Conversion Congress and Exposition (ECCE)*, 2021, pp. 2595–2600.

[250] H. R. Wickramasinghe, G. Konstantinou, Z. Li, and J. Pou, "Alternate arm converters-based HVDC model compatible with the CIGRE B4 DC grid test system," *IEEE Trans. Power Deliv.*, vol. 34, no. 1, pp. 149–159, 2018.

[251] H. R. Wickramasinghe, P. Sun, and G. Konstantinou, "Interoperability of modular multilevel and alternate arm converters in hybrid HVDC systems," *Energies*, vol. 14, no. 5, p. 1363, 2021.

[252] D. Vozikis, G. Adam, D. Holliday, and S. Finney, "An improved alternate arm converter for HVDC applications," in *IECON 2018-44th Annual Conference of the IEEE Industrial Electronics Society*, 2018, pp. 3921–3925.

[253] X. Liu, P. Sun, F. Arraño-Vargas, and G. Konstantinou, "Provision of synthetic inertia by alternate arm converters in VSC-HVDC systems," in *2021 31st Australasian Universities Power Engineering Conference (AUPEC)*, 2021, pp. 1–5.

[254] M. Kaya, A. Costabeber, A. J. Watson, F. Tardelli, and J. C. Clare, "A push–pull series connected modular multilevel converter for HVdc applications," *IEEE Trans. Power Electron.*, vol. 37, no. 3, pp. 3111–3129, 2021.

[255] P. A. Gray, P. W. Lehn, and N. Yakop, "A modular multilevel DC–DC converter with flying capacitor converter like properties," *IEEE Trans. Ind. Electron.*, vol. 69, no. 7, pp. 6774–6783, 2021.

[256] S. Du, B. Wu, K. Tian, N. R. Zargari, and Z. Cheng, "An active cross-connected modular multilevel converter (AC-MMC) for a medium-voltage motor drive," *IEEE Trans. Ind. Electron.*, vol. 63, no. 8, pp. 4707–4717, 2016.

[257] P. A. Gray, Z. C. Ma, and P. W. Lehn, "A high-frequency MMC for DC–DC applications using a three-winding transformer with DC flux cancellation," *IEEE J. Emerg. Sel. Top. Ind. Electron.*, vol. 3, no. 3, pp. 647–657, 2021.

[258] H. Yang, M. Saeedifard, and A. Yazdani, "An enhanced closed-loop control strategy with capacitor voltage elevation for the DC–DC modular multilevel converter," *IEEE Trans. Ind. Electron.*, vol. 66, no. 3, pp. 2366–2375, 2018.

[259] F. Zhang, W. Li, and G. Joós, "A Transformerless Hybrid Modular Multilevel DC–DC Converter With DC Fault Ride-Through Capability," *IEEE Trans. Ind. Electron.*, vol. 66, no. 3, pp. 2217–2226, 2019, doi: 10.1109/TIE.2018.2869355.

[260] N. Parida and A. Das, "A reduced arm DC–AC modular multilevel converter topology," *IETE Tech. Rev.*, vol. 39, no. 3, pp. 613–622, 2022.

[261] M. Kurtoğlu, F. Eroğlu, A. O. Arslan, and A. M. Vural, "Recent contributions and future prospects of the modular multilevel converters: A comprehensive review," *Int. Trans. Electr. Energy Syst.*, vol. 29, no. 3, p. e2763, 2019.

[262] S. Norrga, L. Ängquist, K. Ilves, L. Harnefors, and H.-P. Nee, "Decoupled

steady-state model of the modular multilevel converter with half-bridge cells," in *6th IET International Conference on Power Electronics, Machines and Drives (PEMD 2012)*, 2012, pp. 1–6.

[263] C. Sun, J. Zhang, X. Cai, and G. Shi, "Analysis and arm voltage control of isolated modular multilevel DC–DC converter with asymmetric branch impedance," *IEEE Trans. Power Electron.*, vol. 32, no. 8, pp. 5978–5990, 2016.

[264] M. Mehrasa, E. Pouresmaeil, S. Zabihi, I. Vechiu, and J. P. S. Catalão, "A multi-loop control technique for the stable operation of modular multilevel converters in HVDC transmission systems," *Int. J. Electr. Power Energy Syst.*, vol. 96, pp. 194–207, 2018.

[265] S. Safaee, A. Ketabi, M. Farshadnia, and M. Shahidehpour, "A multi-port MMC topology with reduced capacitor size for use in grid-connected PV systems," *Energy Sci. Eng.*, vol. 9, no. 11, pp. 2019–2035, 2021.

[266] M. Ayari, M. M. Belhaouane, X. Guillaud, and N. B. Braiek, "Global advanced control strategy for modular multilevel converter integrated in a HVDC link," *Int. Trans. Electr. Energy Syst.*, vol. 28, no. 4, p. e2511, 2018.

[267] E. N. Abildgaard and M. Molinas, "Modelling and control of the modular multilevel converter (MMC)," *Energy procedia*, vol. 20, pp. 227–236, 2012.

[268] Y. Wang, Z. Yuan, J. Fu, Y. Li, and Y. Zhao, "A feasible coordination protection strategy for MMC-MTDC systems under DC faults," *Int. J. Electr. Power Energy Syst.*, vol. 90, pp. 103–111, 2017.

[269] C. M. Diez, A. Costabeber, F. Tardelli, D. Trainer, and J. Clare, "Control and experimental validation of the series bridge modular multilevel converter for HVDC applications," *IEEE Trans. Power Electron.*, vol. 35, no. 3, pp. 2389–2401, 2019.

[270] D. Ronanki, S. A. Singh, and S. S. Williamson, "Comprehensive topological overview of rolling stock architectures and recent trends in electric railway traction systems," *IEEE Trans. Transp. Electrif.*, vol. 3, no. 3, pp. 724–738, 2017.

[271] P. Guo *et al.*, "Analysis and control of modular multilevel converter with split energy storage for railway traction power conditioner," *IEEE Trans. Power Electron.*, vol. 35, no. 2, pp. 1239–1255, 2019.

[272] F. Ma *et al.*, "A railway traction power conditioner using modular multilevel converter and its control strategy for high-speed railway system," *IEEE Trans.*

Transp. Electrif., vol. 2, no. 1, pp. 96–109, 2016.

[273] Q. Xu *et al.*, "Analysis and comparison of modular railway power conditioner for high-speed railway traction system," *IEEE Trans. Power Electron.*, vol. 32, no. 8, pp. 6031–6048, 2016.

[274] S. N. Duarte, P. M. de Almeida, and P. G. Barbosa, "A novel energizing strategy for a grid-connected modular multilevel converter operating as static synchronous compensator," *Int. J. Electr. Power Energy Syst.*, vol. 109, pp. 672–684, 2019.

[275] M. Vasiladiotis and A. Rufer, "Analysis and control of modular multilevel converters with integrated battery energy storage," *IEEE Trans. Power Electron.*, vol. 30, no. 1, pp. 163–175, 2014.

[276] Y. Chen, S. Zhao, Z. Li, X. Wei, and Y. Kang, "Modeling and control of the isolated DC–DC modular multilevel converter for electric ship medium voltage direct current power system," *IEEE J. Emerg. Sel. Top. Power Electron.*, vol. 5, no. 1, pp. 124–139, 2016.

[277] Y. Chen, Z. Li, S. Zhao, X. Wei, and Y. Kang, "Design and implementation of a modular multilevel converter with hierarchical redundancy ability for electric ship MVDC system," *IEEE J. Emerg. Sel. Top. Power Electron.*, vol. 5, no. 1, pp. 189–202, 2016.

[278] S. Du, B. Wu, and N. Zargari, "Delta-channel modular multilevel converter for a variable-speed motor drive application," *IEEE Trans. Ind. Electron.*, vol. 65, no. 8, pp. 6131–6139, 2018.

[279] S. Sau and B. G. Fernandes, "Modular multilevel converter based variable speed drive with reduced capacitor ripple voltage," *IEEE Trans. Ind. Electron.*, vol. 66, no. 5, pp. 3412–3421, 2018.

[280] Q. Chen, R. Li, and X. Cai, "Analysis and fault control of hybrid modular multilevel converter with integrated battery energy storage system," *IEEE J. Emerg. Sel. Top. Power Electron.*, vol. 5, no. 1, pp. 64–78, 2016.

[281] M. Luh, T. Blank, and M. Weber, "Comparison and evaluation of modular multilevel converter topologies for li-ion battery systems," in *PCIM Europe 2017; International Exhibition and Conference for Power Electronics, Intelligent Motion, Renewable Energy and Energy Management*, 2017, pp. 1–8.

[282] R. Hariri, F. Sebaaly, and H. Y. Kanaan, "A review on modular multilevel

converters in electric vehicles," in *IECON 2020 The 46th Annual Conference of the IEEE Industrial Electronics Society*, 2020, pp. 1993–4987.

[283] X. Wang, G. Tang, Z. He, X. Wei, H. Pang, and X. Xiao, "Modeling and control of an isolated module multilevel DC/DC converter for DC grid," *CSEE J. Power Energy Syst.*, vol. 3, no. 2, pp. 150–159, 2017.

[284] S. Kedia and H. J. Bahirat, "DC-DC converter for HVDC grid application," in *2017 National Power Electronics Conference (NPEC)*, 2017, pp. 346–351.

[285] M. A. Perez, S. Bernet, J. Rodriguez, S. Kouro, and R. Lizana, "Circuit topologies, modeling, control schemes, and applications of modular multilevel converters," *IEEE Trans. power Electron.*, vol. 30, no. 1, pp. 4–17, 2014.

[286] M. A. Perez, S. Bernet, J. Rodriguez, S. Kouro, and R. Lizana, "Circuit Topologies, Modeling, Control Schemes, and Applications of Modular Multilevel Converters," *IEEE Trans. Power Electron.*, vol. 30, no. 1, pp. 4–17, 2015, doi: 10.1109/TPEL.2014.2310127.

[287] A. E. Leon and S. J. Amodeo, "Energy balancing improvement of modular multilevel converters under unbalanced grid conditions," *IEEE Trans. Power Electron.*, vol. 32, no. 8, pp. 6628–6637, 2016.

[288] M. Tayyab and A. Sarwar, "Submodule capacitor voltage balancing of modular multilevel converter," in *2019 International Conference on Electrical, Electronics and Computer Engineering (UPCON)*, 2019, pp. 1–5.

[289] J.-H. Lee, J.-J. Jung, and S.-K. Sul, "Balancing of submodule capacitor voltage of hybrid modular multilevel converter under DC-bus voltage variation of HVDC system," *IEEE Trans. power Electron.*, vol. 34, no. 11, pp. 10458–10470, 2019.

[290] H. M. Ismail and S. Kaliyaperumal, "Enhanced voltage sorting algorithm for balancing the capacitor voltage in modular multilevel converter," *IEEE Access*, vol. 9, pp. 167489–167502, 2021.

[291] Z. Geng, M. Han, C. Xia, and L. Kou, "A switching times reassignment-based voltage balancing strategy for submodule capacitors in modular multilevel HVDC converters," *IEEE Trans. Power Deliv.*, vol. 37, no. 2, pp. 1215–1225, 2021.

[292] H. M. Ismail, S. Kaliyaperumal, and R. A. Bhuhari, "A simplified logical method (SLM) based capacitor balancing technique for modular multilevel converter," *IEEE Access*, vol. 9, pp. 35452–35463, 2021.

[293] S. S. Hussain, R. Raina, H. M. Ismail, and S. Kaliyaperumal, “Voltage balancing strategy for mitigating capacitor ripple voltage in modular multilevel converter,” in *2022 Advances in Science and Engineering Technology International Conferences (ASET)*, 2022, pp. 1–5.

[294] D. Tebaldi and R. Zanasi, “Model-based cascade control of single-phase Modular Multilevel Converters using ideal capacitor voltages reference,” *Control Eng. Pract.*, vol. 151, p. 106031, 2024, doi: https://doi.org/10.1016/j.conengprac.2024.106031.

[295] J. Lyu, M. Molinas, and X. Cai, “Harmonic state space modeling of a three-phase modular multilevel converter,” *arXiv Prepr. arXiv1706.09925*, 2017.

[296] M. Ayari, M. M. Belhaouane, X. Guillaud, and N. B. Braiek, “Multivariable optimal PID control design for modular multilevel converter,” in *Proceedings of the Conférence Internationale en Sciences et Technologies Electriques, Marrakech, Maroc*, 2016, pp. 25–28.

[297] A. R. Kumar, M. S. Bhaskar, U. Subramaniam, D. Almakhles, S. Padmanaban, and J. B.-H. Nielsen, “An Improved Harmonics Mitigation Scheme for a Modular Multilevel Converter,” *IEEE Access*, vol. 7, pp. 147244–147255, 2019, doi: 10.1109/ACCESS.2019.2946617.

[298] H. Kadhum, A. J. Watson, M. Rivera, P. Zanchetta, and P. Wheeler, “Model Predictive Control of a Modular Multilevel Converter with Reduced Computational Burden,” *Energies*, vol. 17, no. 11. 2024. doi: 10.3390/en17112519.

[299] J. Mei, Y. Ji, X. Du, T. Ma, C. Huang, and Q. Hu, “Quasi-fixed-frequency hysteresis current tracking control strategy for modular multilevel converters,” *J. power Electron.*, vol. 14, no. 6, pp. 1147–1156, 2014.

[300] Y. Sun, Z. Li, and Z. Zhang, “Hybrid predictive control with simple linear control based circulating current suppression for modular multilevel converters,” *CES Trans. Electr. Mach. Syst.*, vol. 3, no. 4, pp. 335–341, 2019.

[301] R. Darus, J. Pou, G. Konstantinou, S. Ceballos, and V. G. Agelidis, “Controllers for eliminating the ac components in the circulating current of modular multilevel converters,” *IET Power Electron.*, vol. 9, no. 1, pp. 1–8, 2016.

[302] J. Wang, X. Han, H. Ma, and Z. Bai, “Analysis and injection control of circulating current for modular multilevel converters,” *IEEE Trans. Ind. Electron.*, vol. 66, no. 3, pp. 2280–2290, 2018.

[303] G. A. Reddy and A. Shukla, "Circulating current optimization control of MMC," *IEEE Trans. Ind. Electron.*, vol. 68, no. 4, pp. 2798–2811, 2020.

[304] M. Xiang, J. Hu, and Y. Qiu, "Coordinated control of power loss and capacitor voltage ripple reduction for AC voltage boosted FBSM MMC with second harmonic circulating current injection," *High Volt.*, vol. 3, no. 4, pp. 272–278, 2018.

[305] S. Isik, M. Alharbi, and S. Bhattacharya, "An optimized circulating current control method based on PR and PI controller for MMC applications," *IEEE Trans. Ind. Appl.*, vol. 57, no. 5, pp. 5074–5085, 2021.

[306] F. Deng *et al.*, "Circulating current suppression for MMC-HVDC systems with asymmetric arm impedance," *CSEE J. Power Energy Syst.*, vol. 7, no. 3, pp. 530–540, 2020.

[307] G. A. Reddy and A. Shukla, "Optimized circulating current injection control scheme for modular multilevel converters," in *2021 IEEE Energy Conversion Congress and Exposition (ECCE)*, 2021, pp. 2444–2450.

[308] M. Huang, Z. Kang, W. Li, J. Zou, X. Ma, and J. Li, "Modified modular multilevel converter with third-order harmonic voltage injection to reduce submodule capacitor voltage ripples," *IEEE Trans. Power Electron.*, vol. 36, no. 6, pp. 7074–7086, 2020.

[309] M. Huang, J. Zou, and X. Ma, "An improved phase-shifted carrier modulation for modular multilevel converter to suppress the influence of fluctuation of capacitor voltage," *IEEE Trans. Power Electron.*, vol. 31, no. 10, pp. 7404–7416, 2016.

[310] M. Huang, J. Zou, X. Ma, Y. Li, and M. Han, "Modified modular multilevel converter to reduce submodule capacitor voltage ripples without common-mode voltage injected," *IEEE Trans. Ind. Electron.*, vol. 66, no. 3, pp. 2236–2246, 2018.

[311] D. Ronanki, N. A. Azeez, L. Patnaik, and S. S. Williamson, "Hybrid multi-carrier PWM technique with computationally efficient voltage balancing algorithm for modular multilevel converter," in *2018 IEEE International Conference on Industrial Electronics for Sustainable Energy Systems (IESES)*, 2018, pp. 224–229. doi: 10.1109/IESES.2018.8349878.

[312] H. Yang and M. Saeedifard, "A capacitor voltage balancing strategy with minimized AC circulating current for the DC–DC modular multilevel

converter," *IEEE Trans. Ind. Electron.*, vol. 64, no. 2, pp. 956–965, 2016.

[313] S. Shi, F. Wang, Y. Zhu, T. Zhu, F. Zhuo, and H. Zhai, "An improved control method applied to the DC/DC converter based on MMC," in *2017 IEEE 3rd International Future Energy Electronics Conference and ECCE Asia (IFEEC 2017-ECCE Asia)*, 2017, pp. 1822–1826.

[314] D. Jovcic and H. Zhang, "Dual channel control with DC fault ride through for MMC-based, isolated DC/DC converter," *IEEE Trans. Power Deliv.*, vol. 32, no. 3, pp. 1574–1582, 2017.

[315] S. Fan, L. M. Tolbert, X. Xiang, and W. Li, "Submodule Voltage Balancing Methods in Modular Multilevel Converters – A Review," in *2024 IEEE Energy Conversion Congress and Exposition (ECCE)*, 2024, pp. 2775–2782. doi: 10.1109/ECCE55643.2024.10861740.

[316] L. A. M. Barros, A. P. Martins, and J. G. Pinto, "A Comprehensive Review on Modular Multilevel Converters, Submodule Topologies, and Modulation Techniques," *Energies*, vol. 15, no. 3. 2022. doi: 10.3390/en15031078.

[317] S. P. Martin, H. Li, and O. M. Anubi, "Modulated MPC for Arm Inductor-Less MVDC MMC With Reduced Computational Burden," *IEEE Trans. Energy Convers.*, vol. 36, no. 3, pp. 1776–1786, 2021, doi: 10.1109/TEC.2021.3069150.

[318] S. M. Akbar and A. Hasan, "Review of high voltage DC/DC modular multilevel converters," in *2018 15th International Conference on Smart Cities: Improving Quality of Life Using ICT & IoT (HONET-ICT)*, 2018, pp. 46–50.

[319] H. Liu, M. S. A. Dahidah, J. Yu, R. T. Naayagi, and M. Armstrong, "Design and control of unidirectional DC–DC modular multilevel converter for offshore DC collection point: Theoretical analysis and experimental validation," *IEEE Trans. Power Electron.*, vol. 34, no. 6, pp. 5191–5208, 2018.

[320] B. Li, X. Zhao, D. Cheng, S. Zhang, and D. Xu, "Novel hybrid DC/DC converter topology for HVDC interconnections," *IEEE Trans. Power Electron.*, vol. 34, no. 6, pp. 5131–5146, 2018.

[321] S. Martin and H. Li, "Model predictive control of an arm inductor-less MMC-based DC SST," in *2021 IEEE Applied Power Electronics Conference and Exposition (APEC)*, 2021, pp. 2113–2119.

[322] R. Razani and Y. A.-R. I. Mohamed, "Model Predictive Control of Non-Isolated DC/DC Modular Multilevel Converter Improving the Dynamic Response,"

IEEE Open J. Power Electron., vol. 3, pp. 303–316, 2022, doi: 10.1109/OJPEL.2022.3176833.

[323] S. Du, A. Dekka, B. Wu, and N. Zargari, *Modular multilevel converters: analysis, control, and applications*. John Wiley & Sons, 2018.

[324] H. D. Tafti and A. I. Maswood, "Advanced multilevel converters and applications in grid integration," 2018.

[325] L. Franquelo, J. Rodriguez, J. Leon, S. Kouro, R. Portillo, and M. Prats, "The age of multilevel converters arrives," *IEEE Ind. Electron. Mag.*, vol. 2, no. 2, pp. 28–39, Jun. 2008, doi: 10.1109/MIE.2008.923519.

[326] ALİ OSMAN ARSLAN, "MODULAR MULTILEVEL CONVERTER DESIGN Ph.D.," gaziantep, 2021.

[327] B. ÇİFTÇİ, "Selection of Suitable Pwm Switching and Control Methods," no. December, pp. 1–261, 2014.

[328] B. Zhao, Q. Song, J. Li, Y. Wang, and W. Liu, "Modular Multilevel High-Frequency-Link DC Transformer Based on Dual Active Phase-Shift Principle for Medium-Voltage DC Power Distribution Application," *IEEE Trans. Power Electron.*, vol. 32, no. 3, pp. 1779–1791, 2017, doi: 10.1109/TPEL.2016.2558660.

[329] L. Zhang, Z. Zhao, and J. Qin, "Efficiency optimization design of DC-DC solid state transformer based on modular multilevel converters," in *2017 IEEE Energy Conversion Congress and Exposition (ECCE)*, 2017, pp. 3508–3513. doi: 10.1109/ECCE.2017.8096626.

[330] S. Sarkar and A. Das, "An isolated single input-multiple output DC–DC modular multilevel converter for fast electric vehicle charging," *IEEE J. Emerg. Sel. Top. Ind. Electron.*, vol. 4, no. 1, pp. 178–187, 2022.

[331] S. Zhao, Y. Chen, S. Cui, B. J. Mortimer, and R. W. De Doncker, "Three-port bidirectional operation scheme of modular-multilevel DC–DC converters interconnecting MVDC and LVDC grids," *IEEE Trans. Power Electron.*, vol. 36, no. 7, pp. 7342–7348, 2020.

[332] M. S. Ansari, A. Shukla, and H. J. Bahirat, "A Novel Hybrid Multilevel DC–DC Converter Employing Trapezoidal Modulation," *IEEE Trans. Power Electron.*, vol. 38, no. 10, pp. 12679–12691, 2023.

CURRICULUM VITAE

Name, Surname: Abdurrahim ERAT

EDUCATION

Degree	Institution	Graduation Year
MSc	Necmettin Erbakan University	2018
BSc	Niğde Ömer Halisdemir University	2013

WORK EXPERIENCE

Year	Place	Position
2013-2018	Private Sector	Electrical and Electronics Engineer
2019-Present	Şırnak University	Lecturer

PUBLICATIONS

SCI/SCI-Expanded Journal Papers:

1) Erat Abdurrahim, Vural Ahmet Mete (2022). DC/DC Modular Multilevel Converters for HVDC Interconnection: A Comprehensive Review, International Transactions on Electrical Energy Systems, 2687243, 49 pages. DOI: https://doi.org/10.1155/2022/2687243

2) Erat Abdurrahim, Vural Ahmet Mete (2025). Design and Analysis of a Novel Non-isolated DC-DC MMC Architecture for HVDC Power Networks Interconnections, Tehnicki Vjesnik/Technical Gazette, (page 1954-1967). DOI: https://doi.org/10.17559/TV-20250207002344

Conference Papers:

1) Erat Abdurrahim, Vural Ahmet Mete (2023). An Innovative DC-DC Modular Multilevel Converter Topology for Interconnection Asynchronous High Voltage Direct Current Power Grids, 14th International Conference on Electrical and Electronics Engineering (ELECO), DOI: 10.1109/ELECO60389.2023.10416055.

2) Erat Abdurrahim, Vural Ahmet Mete (2023). Design And Control of Nonisolated DC-DC Modular Multilevel Converter for Interconnection of High Voltage Direct Current Grids, The 5th International Conference of Materials and Engineering Technology (TICMET'23), ISBN: E-ISBN: 978-625-00-8185-3.

3) Erat Abdurrahim, Vural Ahmet Mete (2023). An Assessment of Pulse Width Modulation Methods For DC-DC Modular Multilevel Converters, 1st International Future Engineering Conference (1st IFEC 2023), ISBN:978-625-367-594-3.

4) Erat Abdurrahim, Vural Ahmet Mete (2022). Yüksek Gerilim Doğru Akım Güç Şebekelerinin Ara Bağlantıları İçin DA/DA Modüler Çok Seviyeli Dönüştürücüler, 12. Elektrik-Elektronik ve Biyomedikal Mühendisliği Konferansı, ISBN:978-605-01-1437-9.